One-Loop Effects on the T Parameter in the Universal Custodial Randall-Sundrum Model

A thesis submitted to the University of Manchester for the degree of

Doctor of Philosophy

in the Faculty of Engineering and Physical Sciences

2011

Luke McDermott

School of Physics and Astronomy

Contents

wordcount: 27234

List of Tables

List of Figures

Absract

In this thesis we investigate the fermionic one-loop contributions to the Peskin and Takeuchi oblique parameter T within the framework of the Universal Custodial Randall-Sundrum (UCRS) model. Specifically we investigate in detail those diagrams containing mixing between SM and Kaluza-Klein (KK) gauge bosons. We find that, contrary to an assumption made widely in the literature, the individual 4D contributions to T are UV divergent, while the sum over all such contributions is also divergent. Without performing a full renormalisation, we conduct a numerical analysis of these contributions to T and find that the constraint they impose on the KK scale of the theory, M_{KK}, is potentially significantly stronger than that imposed by the tree-level contributions to the S parameter, S_{tree}. We subsequently repeat this analysis in the framework of a "Little RS" (LRS) variant of the UCRS model and find that, although weaker than in the standard UCRS model case, the constraint on M_{KK} is still stronger than that from S_{tree}. We conclude that the T parameter does not receive custodial protection at the quantum level in the UCRS model.

In addition to the above we have derived approximate analytical expressions for the tree-level contributions to S and T, correctly quantised the UCRS model and derived the mass matrices and Feynman rules for all scalar degrees of freedom in the model.

Declaration

No portion of the work referred to in this thesis has been submitted in support of an application for another degree or qualification of this or any other university or other institution of learning.

Luke McDermott
School of Physics and Astronomy
University of Manchester
Oxford Road
Manchester
M13 9PL
September 2011

Copyright

The Author

The author was educated at Calderstones Comprehensive School, Liverpool, between 1995 and 2003, before obtaining a first class Bsc (Hons) degree at the University of Manchester. The work presented in this thesis was undertaken at the University of Manchester, under the supervision of Prof. Apostolos Pilaftsis.

Acknowledgements

I would firstly like to thank my wife Rachel for all the love, support and belief she has given me in the last four years and particularly in the last 6 months; they would have been a lot harder without her.

I would also like to thank my family, and in particular my mum, for being a constant source of support (and amusement) and always being supportive of any decision I have made.

A big thank you goes to all my friends throughout my 7 years in Manchester but in particular Rahma, Stevie Ronson, Ben and RCS Huxley who have made the experience particularly enjoyable and memorable.

A great number of people within the particle physics group deserve thanks but particularly Sabah (for the interesting conversations and IT support), Fred (for his stories and sage advice) and all those who have contributed in any way to the completion of this work. I would also like to thank my supervisor Prof. Apostolos Pilaftsis for the help he provided during the completion of this thesis.

Finally, I would like to thank Mr Caine from Calderstones School whose enthusiasm for physics and skilled use of keys to demonstrate fundamental concepts played a big part in me choosing to study physics in the first place.

Chapter 1

Introduction

One of the major challenges facing modern particle physics is the explanation of the observed 10^{16} order of magnitude difference between the scale at which the weak, $\mathcal{O}(TeV)$, and gravitational, $\mathcal{O}(M_{Planck})$, interactions become non-negligible in particle physics processes. This conundrum is generally refered to as the *gauge-hierarchy problem* (HP). As it does not include a description of quantum gravitation, it can be assumed that the Standard Model (SM) is an effective theory, valid up to M_{Pl}. In the absence of some protective symmetry, however, such a high cut-off leads to equally large quantum corrections to the Higgs mass and consequently to the weak scale. The effect of such corrections is to make the observed electroweak symmetry breaking (EWSB) scale achievable only through an extreme fine tuning of the Higgs potential parameters, a very unnatural (and therefore unappealing) solution to the problem of matching theory to observation. A more palatable alternative to this scenario is for New Physics (NP) to appear at some intermediate scale (preferably $\mathcal{O}(1\,TeV)$ so as not to result in a *little hierarchy problem* [1]) thereby lowering the SM cut-off and removing the need to fine-tune the SM Higgs mass.

There have been a multitude of diverse suggestions as to exactly what form this NP will take, ranging from the introduction of a new symmetry of the Higgs sector which protects the SM Higgs mass from the problematic M_{Pl} scale corrections (the famous Supersymmetry [2]) to the introduction of *large*, *flat* extra-dimensions (EXDs) throughout which a low scale ($\sim$ TeV) higher dimensional gravitational force is diluted, resulting in a weak effective 4D gravity [3]. A further interesting extra-dimensional solution was suggested by Randall and Sundrum (RS) [4] and consists of a *small* and exponentially *warped* EXD bounded by two 3-branes, on one of which all SM fields (though not gravity) were originally confined. A single, Planckian, fundamental mass scale is *warped down* by the non-factorisable geometry of the EXD, resulting in a 4D effective mass scale which varies exponentially along the EXD. At one end of the EXD (known as the UV brane) the effective scale is Planckian and is where 4D gravity is *localised*, while at the opposite end the effective scale is $\mathcal{O}(TeV)$ and is where the SM fields were confined.

It was quickly realised however that the original RS setup, though providing a possible solution to the HP, suffered from some severe phenomenological constraints associated with TeV scale supression of the non-renormalisable operators which cause such phenomena as proton decay, Majorana neutrino masses, flavour changing neutral currents (FCNC) [5, 6] and excessive contributions to the Peskin-Takeuchi [7] S and T parameters [8–11]. The simplest way to relax such constraints was to remove the matter fields from their confinement on the IR brane and allow them to propagate throughout the entire bulk of the EXD [5, 8, 12–16], thereby making the suppression scale of non-renormalisable operators dependent upon the localisation of its constituent fermionic fields in the EXD. Simultaneously it was realised that RS models with bulk fermionic fields held greater model building potential than those with TeV confined fields; the exponential nature of the fermionic zero modes and

their sensitivity to $\mathcal{O}(1)$ changes in the bulk fermionic mass parameters allowing for a solution to the fermionic flavour hierarchy problem based on 5D geography to be proposed [5, 6, 14, 17, 18].

RS models with bulk matter and gauge fields are not, however, without their own phenomenological issues, in particular excessive contributions to the T parameter [9, 15, 16, 19] and anomolous contributions to $Zb_L\bar{b}_L$ couplings [20]. It has been noted in the literature that these further phenomenological issues can be ameliorated through an expansion of the EW sector gauge group of the model to include both an additional, *right-handed*, $SU(2)$ symmetry and a discrete symmetry interchanging this with the $SU(2)_L$ group of the SM. The well known effect of the gauged custodial symmetry group being to protect the T parameter from large contributions while the additional discrete symmetry, in combination with the custodial symmetry, protects the $Zd^i_L\bar{d}^j_L$ couplings of the model from large anomolous contributions [21]. The potential problems with FCNC experienced by RS type models with bulk fermionic fields are, to a large extent, controlled by the RS-GIM mechanism [18]. A more detailed discussion of their effect on the constraints present on the fundamental parameters of the model can be found in references [11, 17, 22].

An alternative method of weakening the phenomenological constraints on the RS model from these sources which was suggested in reference [23] is know as the "Little RS" (LRS) model and is an RS variation of "Little Higgs" models well known in the literature [24] . In the LRS model the aim of solving the HP is relinquished for that of solving the smaller *flavour* problem, i.e. the difference between the weak scale and the scale required to adequately suppress flavour violating higher-dimensional operators, $\mathcal{O}(10^3\,TeV)$. Such a change of priorities requires that the 5D mass scale of the model be reduced thereby allowing for other fundamental parameters, on which some of the most phenenomenologically stringent observables (such as S and

T) depend, to be simultaneously reduced in size.

In light of the fermionic, gauge and gravitational fields all being allowed to propagate in the bulk it might appear slightly anomalous that in the majority of the literature the Higgs field remains confined to the IR brane [1]. Initially this reluctance to remove the Higgs field from the brane stemmed from the difficulty in reproducing, without fine tuning, the masses of the SM gauge bosons using a 5D spontaneous symmetry breaking (SSB) procedure [15,28]. There has since been a small number of papers which have addressed the problems associated with combining a fundamental Higgs with a warped extra-dimensional background [29,30], the model of Davoudiasl et al [29] which utilises the tachyonic nature of the lightest Higgs mode in certain regions of parameter space to induce SSB at a 4D level being of particular interest in the current context.

In this thesis we investigate a *universal* (all fields propagating in the bulk) variant of the custodial RS model presented in references [26,31,32], the Higgs sector of which is a custodial version of that proposed in reference [29]. We refer to this model throughout as the Universal Custodial RS model (UCRS). In chapter 2 we repeat the derivation of the original RS model, explicitly work through its solution to the HP and discuss the details of embedding the different varieties of bulk field into a RS framework. In chapter 3 we discuss in detail the UCRS model with particular attention paid to the gauge fixing and scalar sector. As part of this discussion we derive the mass matrices of both physical and non-physical scalar modes in addition to the Feynman rules for all interactions between scalar degrees of freedom (DOFs) and vector or fermionic fields. In chapter 4 we then repeat the well known calculation

[1] This does not include that portion of the literature concerned with gauge-Higgs unification models in which a bulk Higgs is a fixture due to its origin as a component of a higher-dimensional gauge field [25–27]

of the tree-level contributions to the S and T parameters for the case of the UCRS model, deriving approximate analytical expressions for each; we assume that the U parameter is zero throughout. In chapter 5 we subsequently calculate the contributions to the T parameter from those fermionic one-loop diagrams containing mixing between left and right-handed gauge bosons and no Yukawa mass insertions. After initially determining the finiteness of the individual 4D KK contributions from such diagrams we assess the convergence of the KK sum over such contributions before deriving approximate analytical expressions for those contributions containing $n = 1$ modes and lighter. Finally, the KK scale and fermionic bulk mass parameter dependence of the set of contributions with $n \leq 2$ is investigated for both standard and LRS variants of the UCRS model and the compatability of these contributions with the current 95% confidence level limit of T and a KK scale $\mathcal{O}(TeV)$ commented upon. In chapter 6 we summarise our results, while in the appendices are collected some technical details which may be useful to the reader.

Chapter 2

The Randall-Sundrum Model

2.1 Model Motivation and Geometry

2.1.1 Derivation of Geometry

In the majority of the literature the term Randall-Sundrum (RS) model is a convenient shorthand for a model based upon the RS1 setup, i.e. a model with an additional, compact, spatial dimension [1] whose geometry is generally non-factorisable and specifically described by a variation of the RS metric [4]

$$ds^2 = e^{-2ky}\eta_{\mu\nu}dx^\mu dx^\nu - dy^2, \tag{2.1}$$

where $0 \leq y \leq L$ is the coordinate associated with the extra spatial dimension, k is a constant associated with the curvature of the EXD (henceforth the curvature

[1] Not all "RS" models are of this form as there are many examples in the literature in which a model with more than one additional dimension has an RS-like geometry and is referred to as an "RS" model (see for example [33]). There is also the case of the RS2 model [34] which contains an EXD which is infinite.

scale), typically of the order of the Planck scale and $\eta_{\mu\nu}$ is the standard Minkowskian metric which throughout this thesis has the signature $\eta_{\mu\nu} = diag\,(1, -1, -1, -1)$. The exact form of the metric appearing in the literature is dependent on the type of compactification which has been used in the particular work, the above example being associated with an EXD compactified on an interval of length L. The most frequently used compactification used for RS type models initially (including in the original paper) was an $S_1/\mathcal{Z}_2$ orbifold.

The original derivation of the RS metric, from which ultimately all of the interesting phenomenological properties of RS models are derived, was based upon the solving of Einstein's equations of gravitation in 5D given the following assumptions:

- At both ends of the EXD are 3-branes on which we are able to localise 4D fields
- The bulk (our 5D space not including the two 3-branes) and 3-branes each contain separate cosmological constants
- The overall geometry of our 5D space is non-factorisable
- The spacetime respects 4D Poincare symmetry

Ignoring the backreaction of any fields we might later want to add, the gravitational action for such a setup is

$$S = S_{grav} + S_{UV} + S_{IR}, \tag{2.2}$$

where the constituent actions are defined as

$$S_{grav} = \int d^4x \int_0^L dy \sqrt{G} \left\{ -\Lambda + 2M_*^3 R^{(5)} \right\},$$

$$S_{UV} = \int d^4x \int_0^L dy \sqrt{G} \left\{ V_{UV} \right\} \delta\left(y\right),$$

$$S_{IR} = \int d^4x \int_0^L dy \sqrt{G} \left\{ V_{IR} \right\} \delta\left(y - L\right) \tag{2.3}$$

and where $R^{(5)}$ is the 5D Ricci scalar, M_* is the fundamental mass scale of the 5D theory (taken to be the of the same order as the curvature constant k to maintain the naturalness of the model), Λ is the *bulk* cosmological constant and V_{UV} and V_{IR} are energy densities associated with the branes at $y = 0$ (UV brane) and $y = L$ (IR brane) respectively. The final non-standard quantity which needs defining is the determinant of the 5D metric g_{MN}, G, where $N, M = 0, 1, 2, 3, 5$. We note that throughout this thesis we use the standard convention that upper case Latin characters are used for 5D indices, and as such take the aforementioned values, while lower case Greek letters are retained in their standard role for four-dimensional indices.

Solving Einstein's equations for the above action we find that we obtain the RS metric if the following two conditions are met:

- $V_{UV} = -V_{IR} = 24M_*^3 k$
- $\Lambda = -24M_*^3 k^2$

We note that the bulk cosmological constant must be negative in order to obtain the RS metric, meaning that the bulk of the RS model is a 5D Anti-de-Sitter space (AdS_5). This fact has allowed holographic principles [35] to be used in the building

and phenomenological interpretation of RS type models throughout the literature (see for example [36]).

2.1.2 The Hierarchy Problem

It is fair to say that the original motivation of the RS model was to reproduce the large hierarchy in the effective 4D weak and Planck scale from a compact EXD model containing a single fundamental, Planckian, mass scale. This approach being in contrast to that taken by Arkani-Hamed, Dimopolous and Dvali (ADD) which relied upon *large*, flat EXDs with sizes $\mathcal{O}(1mm)$.

The capacity of the RS setup to solve the HP can be clearly demonstrated using a toy model containing only gravity and an IR-brane-confined Higgs field. We first investigate whether the model predicts the weak scale, or equivalently the Higgs VEV, to be $\mathcal{O}(TeV)$. The action for the Higgs field in our toy model is

$$S_{Higgs} = \int d^4x \int_0^L dy \sqrt{G} \left\{ \partial_\mu H^\dagger \partial^\mu H - \lambda \left(H^\dagger H - v_0^2 \right)^2 \right\} \delta(y - L), \tag{2.4}$$

where $G = \det G_{MN} = e^{-8ky}$, λ is the dimensionless quartic coupling constant and, in keeping with the previously stated philosophy of the RS setup, the term of mass dimensions v_0 is $\mathcal{O}(M_*)$. Now, lowering the Lorentz index of the second partial derivative using the 4D part of the RS metric tensor $G^{\mu\nu} = e^{2ky}\eta^{\mu\nu}$ and integrating over the extra-dimensional coordinate y we obtain the expression

$$S_{Higgs} = \int d^4x\, e^{-4kL} \left\{ e^{2kL} \eta^{\mu\nu} \partial_\mu H^\dagger \partial_\nu H - \lambda \left(H^\dagger H - v_0^2 \right)^2 \right\}. \tag{2.5}$$

If we now return the Higgs action to canonical normalisation through the field redefinition $H \to e^{kL} H$ the action finally becomes

$$S_{Higgs} = \int d^4x \left\{ \partial_\mu H^\dagger \partial^\mu H - \lambda \left(H^\dagger H - e^{-2kL} v_0^2 \right)^2 \right\}. \tag{2.6}$$

We therefore observe that there is a rescaling in 4D of the original Higgs 5D VEV, v_0^2, by an exponential factor originating from the RS metric. Such exponential factors are referred to as *warp factors* and the Higgs VEV is said to have been warped down,

$$v \equiv e^{-kL} v_0. \tag{2.7}$$

From this relationship we are able to determine that in order to obtain the weak scale of the SM we must have the relationship in our fundamental parameters

$$kL \sim 36. \tag{2.8}$$

This small hierarchy in the required values for the curvature scale and the length of the EXD is generally considered to be not too large and as such is compatible with our aim of removing *severe* hierarchies from our model. In the case of any concerns regarding the stability of this relationship, given the dynamic nature of the background space time, Goldberger and Wise have shown that it is indeed possible to generate such a stable hierarchy dynamically using additional scalar fields [37].

If we were to repeat the above analysis but now with the Higgs situated on the UV brane we would find that its VEV would receive no warping down at all and would therefore remain at the Planck scale. We are therefore able to infer the key principle of the RS model: the effective 4D mass scale depends exponentially on the distance along the EXD,

$$\Lambda_{eff}(y) = \Lambda e^{-ky} = M_* e^{-ky}. \tag{2.9}$$

It is clear that the branes which bookend the EXD are the extremities of this sliding mass scale. The UV brane having a 4D effective mass scale of the order the Planck scale ($\Lambda_{eff}(0) = M_*$) while on the IR brane the effective mass scale is

$$\Lambda_{eff}(L) \sim k e^{-kL} = M_{KK}, \tag{2.10}$$

where M_{KK} is known as the Kaluza-Klein (KK) scale. Comparing equations (2.10) and (2.7), and remembering that there is a single mass scale in the 5D theory, we see that in order for the RS model to indeed offer a solution to the HP the KK scale must therefore be close to the weak scale. Exactly how far away from $1\,TeV$ is a matter for debate but it is usually assumed that $M_{KK} \gtrsim 10\,TeV$ introduces a *little hierarchy problem* into the model. It is for this reason that fully IR confined RS models are not considered in the literature (the non-renormalisable operators associated with proton decay, Majorana neutrinos and FCNCs are only suppressed by M_{KK} meaning that the KK scale must be approaching the Planck scale) and, as we shall discuss in detail, why suppression of excessive contributions to the T parameter is important.

It remains for us to check that the prediction for the strength of gravitational interactions predicted from such a setup agree with observation and are not also warped down to a phenomenologically problematic scale. The strength of gravitational interactions in 4D are determined by the coefficient of the term containing the Ricci scalar in the gravitational action (the Planck mass squared)

$$S_{4D\,grav} \supset -M_{Pl}^2 \int d^4x \sqrt{-G^{(4)}} R, \tag{2.11}$$

where $G^{(4)}$ is the determinant of the 4D metric tensor and R is the 4D Ricci scalar. It is therefore necessary for us to derive an expression for the Planck mass in terms of the fundamental parameters of the RS model starting from the part of the 5D gravitational action related to curvature

$$S_{5D\,grav} \supset -M_*^3 \int d^4x \int_0^L dy\, \sqrt{G} R^{(5)}. \tag{2.12}$$

As it is only the $\mu\nu$ components of the Ricci tensor in which we are interested ($R = \eta^{\mu\nu} R_{\mu\nu}$) we ignore its 55 components and use the fact that the Ricci tensor is

invariant under a constant rescaling of the metric to rewrite our expression in the form

$$S_{5D\,grav} \supset -M_*^3 \int d^4x \int_0^L dy\, e^{-4ky} \sqrt{-G^{(4)}} e^{2ky} \eta^{\mu\nu} R_{\mu\nu}, \tag{2.13}$$

where we have exploited the relationship between the 5D and 4D metrics in the RS model. Finally, integrating (2.13) over y and comparing with (2.11) we find that the relationship between the fundamental mass scale of the theory and the scale which sets the strength of gravitational interactions is

$$M_{Pl}^2 = \frac{M_*^3}{k} \left(1 - e^{-2kL}\right). \tag{2.14}$$

Given the smallness of the exponential term for a value of kL which solves the HP, this expression tells us that in order to agree with observation the fundamental mass scale of the RS model must be of the order of the 4D Planck scale, as was assumed in the derivation of the weak scale above. We are therefore able to declare that the RS setup provides a possible solution to the HP. In terms of the y dependence of effective mass scales, the weakness of 4D gravity can be understood as an extreme UV brane localisation of the massless graviton.

2.2 Bulk Fields and Boundary Conditions

As RS type models are necessarily formulated in terms of 5D fields, during the calculations which form the core of this thesis we have used the dimensional reduction techniques know as KK reduction, [38], in order to a obtain a 4D effective theory. The following section will therefore mainly be a summary of the (important) results pertinent to this thesis. We will also include some more detailed discussion of topics not so widely covered in the literature, such as the boundary conditions (BCs) of fields in RS models and the process through which a weak scale Higgs VEV is obtained.

2.2.1 General Procedure

We will now illustrate the general procedure used to obtain a 4D effective theory from a RS type model, using as an example a theory containing only a non-interacting scalar field, $\Phi(x, y)$ [39]. We start by writing down the 5D action for the scalar field (dropping the coordinate dependence of the field for convenience),

$$S_\Phi = \int d^4x \int_0^L dy \sqrt{G} \left\{ \partial_M \Phi \partial^M \Phi - m^2 \Phi^2 \right\}. \tag{2.15}$$

The 5D field is then replaced in the above action by an infinite tower of 4D fields, $\phi^{(n)}(x)$, and associated extra-dimensional wavefunctions (known as bulk profiles), $f_\phi^{(n)}(y)$ [2],

$$\Phi(x, y) = \frac{1}{\sqrt{L}} \sum_{n=0}^{\infty} \phi^{(n)}(x) f_\phi^{(n)}(y). \tag{2.16}$$

This stage is known as KK decomposition. These 4D modes are assumed to be eigenstates of the mass obtained as a result of integrating over the EXD (the KK masses), a fact which allows us to determine the properties of their associated bulk profiles. Substituting into (2.15) the explicit form of the RS metric and requiring that the after integration over the extra-dimensional coordinate the action of the effective theory be of the form

$$S_\Phi = \sum_{n=0}^{\infty} \int d^4x \, \left\{ \partial_\mu \phi^{(n)} \partial^\mu \phi^{(n)} - m_\phi^{(n)\,2} \phi^{(n)\,2} \right\}, \tag{2.17}$$

we find that the orthogonality condition of the bulk profiles is

$$\frac{1}{L} \int_0^L dy \, e^{-2ky} f_\phi^{(n)}(y) f_\phi^{(m)}(y), \tag{2.18}$$

[2] We have stated the form of the KK decomposition specific to an interval compactification. For the case of an orbifold compactification only the normalisation prefactor will change.

and that they must also obey the additional condition

$$\partial_5 \left(e^{-4ky} \partial_5 f_\phi^{(n)}(y) \right) + m^2 e^{-4ky} f_\phi^{(n)}(y) = m_\phi^{(n)\,2} e^{-2ky} f_\phi^{(n)}(y), \tag{2.19}$$

which we will refer to as the mass equation/condition.

In order to find the profile of the KK modes in the EXD we need to solve equation (2.19). To this end we first investigate whether the KK decomposition of the scalar field contains a *zero mode*, a massless mode usually associated with a SM particle and labelled by the index $n = 0$. We therefore set the KK mass to zero and look for a solution to the resulting equation. For the case of a scalar field we see that unless the bulk mass, m, is equal to zero (in which case the zero mode has a flat profile in the EXD) the KK decomposition of the field does not contain a zero mode. We next consider the profiles of the massive (heavy) KK modes ($n > 0$). We therefore solve the second order differential equation in its full form for the region of the EXD between the two branes, obtaining the well known, general result that the extra-dimensional profiles of heavy KK modes are Bessel function like,

$$f_\phi^{(n)}(y) = \frac{e^{2ky}}{N_\phi^{(n)}} \left[J_{\alpha^\phi} \left(\frac{m_\phi^{(n)} e^{ky}}{k} \right) + b_\phi^{(n)} Y_{\alpha^\phi} \left(\frac{m_\phi^{(n)} e^{ky}}{k} \right) \right], \tag{2.20}$$

where $\alpha^\phi = \sqrt{4 + \frac{m^2}{k^2}}$ and the normalisation constant, $N_\phi^{(n)}$, is found by applying the orthogonality condition, (2.18). We have decided that, due to the limited validity of some of the approximate expressions for normalisation constants given in the literature, e.g. [40]

$$N^{(n)} \simeq \frac{e^{kL/2}}{\sqrt{\pi L m^{(n)}}}, \tag{2.21}$$

we prefer to evaluate these expressions numerically in our subsequent investigation. We note that (2.21) is independent of the type of field.

Finally, we must use the boundary conditions (BCs) of the 5D fields on the UV and IR branes to determine the so far undetermined constant $b_\phi^{(n)}$ and subsequently the mass spectrum of the heavy KK modes, $m_\phi^{(n)\,2}$. Throughout this thesis we consistently apply BCs which ensure the variation of the action of the relevant field vanishes on the boundaries of our EXD [41, 42], of which there are generally two types

- A *Dirichlet* condition (represented by the shorthand (-)) where the relevant field is zero on the boundary. In the case of the scalar field

$$f_\phi^{(n)}(y)\,|_{brane} = 0. \tag{2.22}$$

- A *Neumann-like* condition (represented by the shorthand (+)) where some expression containing the derivative of the field is zero on the boundary. In the case of the scalar field this condition is in fact a pure Neumann condition and therefore of the form

$$\partial_5 f_\phi^{(n)}(y)\,|_{brane} = 0. \tag{2.23}$$

To illustrate the process through which we find the KK mass spectrum of a field we consider the example of a scalar field subject to (-,+) BCs. Applying these BCs to (2.20) we find the following expressions for the so far undetermined constant b_n^ϕ,

$$b_\phi^{(n)} = -\frac{J_{\alpha^\phi}\left(\frac{m_\phi^{(n)}}{k}\right)}{Y_{\alpha^\phi}\left(\frac{m_\phi^{(n)}}{k}\right)} = -\frac{2J_{\alpha^\phi}\left(\frac{m_\phi^{(n)}e^{kL}}{k}\right) + \frac{m_\phi^{(n)}e^{kL}}{k}J'_{\alpha^\phi}\left(\frac{m_\phi^{(n)}e^{kL}}{k}\right)}{2Y_{\alpha^\phi}\left(\frac{m_\phi^{(n)}e^{kL}}{k}\right) + \frac{m_\phi^{(n)}e^{kL}}{k}Y'_{\alpha^\phi}\left(\frac{m_\phi^{(n)}e^{kL}}{k}\right)}. \tag{2.24}$$

The mass spectrum is then found from the second equality in the above expression. Practically, after making the change of variables $x_\phi^{(n)} = m_\phi^{(n)}e^{kL}/k$, the mass spectrum

of the scalar field is of the form

$$m_{\phi}^{(n)} = x_{\phi}^{(n)} k e^{-kL} = x_{\phi}^{(n)} M_{KK}, \tag{2.25}$$

where $x_{\phi}^{(n)}$ is the n^{th} root of the mass equation

$$J_{\alpha^{\phi}}\left(xe^{-kL}\right)\left[2Y_{\alpha^{\phi}}\left(x\right)+xY'_{\alpha^{\phi}}\left(x\right)\right]-Y_{\alpha^{\phi}}\left(xe^{-kL}\right)\left[2J_{\alpha^{\phi}}\left(x\right)+xJ'_{\alpha^{\phi}}\left(x\right)\right]=0. \tag{2.26}$$

The first of these roots usually being $\mathcal{O}\left(1\right)$ and with all subsequent roots approximately separated by π. As was the case with the normalisation constants of the bulk profiles, we find it inconvenient to give approximate expressions for the values of these roots in terms of the 5D parameters of the theory as they are generally found numerically and the approximate relationships given in the literature are usually only valid for a very small region of parameter space. We note that although the form of the mass equation is dependent upon the type of field being considered, expression (2.25) is completely general, meaning the first KK mode of all fields are $\mathcal{O}(M_{KK})$.

As it stands there is an amount of ambiguity in our notation for the bulk profiles and mass spectra of the 5D fields. This arises from the fact that clearly the mass spectrum, and therefore the bulk profiles, are dependent upon the BCs of the 5D field. The set of BCs that a given profile obeys could be included explicitly amongst its arguments, for example $f_{\phi}^{(n)}\left(y,BC\right)$, however this could be misleading as well as being overly bulky when dealing with overlap integrals involving many different profiles (as will be the case once we begin to discuss the Feynman rules of the UCRS model). We therefore extend the notation introduced in [40]

$$f_{\phi}^{(n)}\left(y,(+,+)\right)=f_{\phi}^{(n)}\left(y\right),$$

$$f_{\phi}^{(n)}\left(y,(-,+)\right)=\tilde{f}_{\phi}^{(n)}\left(y\right), \tag{2.27}$$

to incorporate all four possible combinations of BCs, using a bar to indicate a reversal of BCs,

$$f_\phi^{(n)}(y,(-,-)) = \bar{f}_\phi^{(n)}(y)\,,$$

$$f_\phi^{(n)}(y,(+,-)) = \bar{\tilde{f}}_\phi^{(n)}(y)\,. \tag{2.28}$$

This notation can also be applied directly to the mass terms in order to indicate which set of BCs has been used in its calculation, i.e.

$$\begin{aligned} (+,+) \quad &\rightarrow \quad m_\phi^{(n)\,2}, & (-,+) \quad &\rightarrow \quad \widetilde{m}_\phi^{(n)\,2}, \\ (-,-) \quad &\rightarrow \quad \bar{m}_\phi^{(n)\,2}, & (+,-) \quad &\rightarrow \quad \bar{\widetilde{m}}_\phi^{(n)\,2}. \end{aligned} \tag{2.29}$$

For the remainder of this section we will consider the KK reduction of the fields which will feature in the UCRS model which will be the focus this work. Particular attention will be paid to the Higgs field due to the non-standard requirement that the lightest Higgs mode be tachyonic in order to generate the 4D SSB process required of it.

2.2.2 Gauge Fields

The action of a 5D Abelian gauge field $A_M(x,y)$ in the RS setup is

$$S_{gauge} = \int d^4x \int_0^L dy\, \sqrt{G} \left\{ -\frac{1}{4} F^{MN} F_{MN} \right\}, \tag{2.30}$$

where $F_{MN} = \partial_M A_N - \partial_N A_M$ and our gauge field now has five components

$$A_M(x,y) = \begin{pmatrix} A_\mu(x,y) \\ A_5(x,y) \end{pmatrix}. \tag{2.31}$$

Writing the 5 components of the 5D gauge field in this way highlights their respective roles in the 4D effective theory, with the vector components clearly corresponding to 4D vector boson modes after decomposition and the 5th component corresponding to an additional (relative to the SM) set of scalar degrees of freedom (DOFs). Due to their different 4D interpretations it is sensible to decompose the vector and scalar components of the 5D gauge field separately,

$$A_\mu(x,y) = \frac{1}{\sqrt{L}} \sum_{n=0}^{\infty} A_\mu(x) f_V^{(n)}(y), \tag{2.32}$$

$$A_5(x,y) = \frac{1}{\sqrt{L}} \sum_{n=0}^{\infty} A_5(x) f_S^{(n)}(y). \tag{2.33}$$

Substituting these decompositions into the action of the 5D gauge field and requiring that after integration the action is of the form

$$S_{gauge} = \sum_{n=0}^{\infty} \int d^4x \, \left(\mathcal{L}^{(n)}_{vector} + \mathcal{L}^{(n)}_{scalar} + \mathcal{L}^{(n)}_{mixing} \right), \tag{2.34}$$

where, as the name suggests, the mixing Lagrangian contains terms which mix the vector and scalar fields. The form of these mixing terms, the details of their subsequent removal and their connection to the massive vector modes will be discussed in detail in section 3.1.5

Completing the reduction procedure we find that the orthonormality conditions

for the two sets of extra-dimensional profiles are

$$\frac{1}{L}\int_0^L dy\, f_V^{(n)}(y) f_V^{(m)}(y) = \delta_{nm},$$

$$\frac{1}{L}\int_0^L dy\, e^{-2ky} f_S^{(n)}(y) f_S^{(m)}(y) = \delta_{nm}. \tag{2.35}$$

The well known bulk profiles of the vector fields are

$$f_V^{(0)}(y) = 1,$$

$$f_V^{(n)}(y) = \frac{e^{ky}}{N_V^{(n)}}\left[J_1\left(\frac{m_V^{(n)} e^{ky}}{k}\right) + b_V^{(n)} Y_1\left(\frac{m_V^{(n)} e^{ky}}{k}\right)\right], \qquad (n = 1, 2, \dots), \tag{2.36}$$

while those of the gauge scalar modes are

$$f_S^{(0)}(y) = \sqrt{\frac{2kL}{e^{2kL}-1}} e^{2ky},$$

$$f_S^{(n)}(y) = \frac{e^{2ky}}{N_S^{(n)}}\left[J_0\left(\frac{m_S^{(n)} e^{ky}}{k}\right) + b_S^{(n)} Y_0\left(\frac{m_S^{(n)} e^{ky}}{k}\right)\right], \qquad (n = 1, 2, \dots). \tag{2.37}$$

Notice that the zero modes of both fields only exist if the associated 5D field has Neumann-like BCs at both ends of the extra dimension which for the gauge vector and scalar fields take the specific forms

$$\partial_5 f_V^{(n)}(y)\,|_{brane} = 0,$$

$$\partial_5\left(e^{-2ky} f_S^{(n)}(y)\right)|_{brane} = 0. \tag{2.38}$$

However, due to the coupling of their respective equations of motion (EOM) the BCs of the vector and scalar components of the 5D gauge field must be the opposite of each other [41] making it impossible for gauge scalar and vector boson zero modes to exist simultaneously.

Another consequence of the coupled nature of their EOMs is that the mass spectra of the vector and scalar components of the same 5D gauge fields are in fact identical. This can be seen by considering the case of a 5D gauge field whose vector components have $(+,+)$ BCs (and consequently has a scalar component with BCs of $(-,-)$). Applying the BCs of the vector field to the bulk profiles of its heavy KK modes $(n>0)$ we find that the mass spectrum of the vector modes can be found from the equality

$$b_V^{(n)} = -\frac{J_1(x_n) + x_n J_1'(x_n)}{Y_1(x_n) + x_n Y_1'(x_n)} = -\frac{J_1\left(x_n e^{kL}\right) + x_n e^{kL} J_1'\left(x_n e^{kL}\right)}{Y_1(x_n e^{kL}) + x_n e^{kL} Y_1'(x_n e^{kL})}, \tag{2.39}$$

which,using the Bessel function identity

$$J_p'(x) = -\frac{p}{x} J_p(x) + J_{p-1}(x) \tag{2.40}$$

we are able to rewrite as

$$b_V^{(n)} = -\frac{J_0(x_n)}{Y_0(x_n)} = -\frac{J_0\left(x_n e^{kL}\right)}{Y_0(x_n e^{kL})}. \tag{2.41}$$

This is exactly the same condition which we obtain from application of the $(-,-)$ condition to the gauge *scalar* bulk profiles and therefore we are able to conclude that the two fields will have identical mass spectra for their heavy KK modes. Using the same approach we are also able to show the equivalence of the vector Dirichlet and scalar Neumann-like conditions. From these equivalences we are able to conclude that *in general* the mass spectra of the vector and scalar components of a 5D gauge field are identical. Making use of this identity, we dispense with a separate notation

for the mass spectrum of the gauge scalar modes, using instead the notation for the equivalent gauge vector mass, e.g.

$$\bar{m}_S^{(n)} \quad \rightarrow \quad m_V^{(n)}. \tag{2.42}$$

We finally observe that, although not exactly the same, the mass spectra associated with the four different BC combinations are similar. An example being that the mass of the $n = 1$ mode of a vector boson with BCs of (+,+) differs from that of a vector boson with BCs of (-,+) by approximately 2%. The remaining two combinations of BC do not appear in our investigation and as such are not relevant to the current discussion.

2.2.3 Fermionic Fields

The action of a free 5D fermionic field, $\Psi(x, y)$, in the RS setup is

$$S_\psi = \int d^4x \int_0^L dy \sqrt{G} \left\{ \bar{\Psi} \Big(i\Gamma^M \left(\partial_M + \omega_M \right) - c^\psi k \Big) \Psi \right\}, \tag{2.43}$$

where c^ψ is the bulk mass parameter and $\mathcal{O}(1)$, the curved space gamma matrices are defined as $\Gamma^M = E_a^M \gamma^a$ [3], the inverse vielbein for the RS metric is $E_a^M = diag\left(e^{ky}, \ e^{ky}, \ e^{ky}, \ e^{ky}, \ 1\right)$ and ω_M is the spin connection, which in the RS model takes the form

$$\omega_M = \begin{cases} \dfrac{i}{2} k e^{-ky} \gamma_\mu \gamma^5 & \text{for } M = \mu \\ 0 & \text{for } M = 5. \end{cases} \tag{2.44}$$

Due to the required chirality of the low energy effective theory, it is sensible to

[3] $\gamma^a = \left(\gamma^\mu, -i\gamma^5\right)$, γ^5 is defined in the standard fashion and all lower case gammas refer to the 4D, flat space gamma matrices.

decompose the chiral fermionic fields separately,

$$\Psi_{L,R}(x,y) = \frac{e^{2ky}}{\sqrt{L}} \sum_{n=0}^{\infty} \psi_{L,R}^{(n)}(x) f_{L,R}^{(n)}(y) \tag{2.45}$$

and following through with the general decomposition procedure we find that the orthogonality conditions for the fermionic bulk profiles are

$$\frac{1}{L}\int_0^L dy\, e^{ky} f_{L,R}^{(n)}(y) f_{L,R}^{(m)}(y) = \delta_{nm}, \tag{2.46}$$

while their functional forms are

$$f_{L,R}^{(0)}(y) = \sqrt{\frac{\left(1 \mp 2c^{\psi}\right) kL}{e^{\left(1\mp 2c^{\psi}\right)kL} - 1}} e^{\mp c^{\psi} ky} \tag{2.47}$$

$$f_{L,R}^{(n)}(y) = \frac{e^{ky/2}}{N_{\psi}^{(n)}} \left[J_{\alpha_{L(R)}^{\psi}}\left(\frac{m_{\psi}^{(n)} e^{ky}}{k}\right) + b_{\psi}^{(n)} Y_{\alpha_{L(R)}^{\psi}}\left(\frac{m_{\psi}^{(n)} e^{ky}}{k}\right)\right], \qquad (\text{n} = 1,2,\dots), \tag{2.48}$$

where $\alpha^{\psi} = 1/2 \pm c^{\psi}$ and the left (right) chirality takes the upper (lower) sign choice where there is ambiguity [4]. The form of the Neumann-like condition (+) which is applied to these profiles is

$$\left(\partial_5 \pm c^{\psi} k\right) f_{L,R}^{(n)}(y)\,|_{brane} = 0, \tag{2.49}$$

while the Dirichlet condition is the same as that given for the previously considered fields.

As was the case with the vector and scalar components of the same 5D gauge field, the coupling of the EOM for the left and right-handed fermionic components

[4]It is necessary to note that our expression for $\alpha_{L(R)}^{\psi}$ does not agree with the majority of the literature (with the exception of [12]) . In order for the masses of the left and right-handed modes of the same 5D field to be identical α^{ψ} must be of the form stated here

leads to them having exactly *opposite* BCs. If we now calculate the mass spectra of the two components of the 5D fermionic field we find (again making use of the Bessel identity (2.40)) that they are identical. Following our approach with the masses of the vector and scalar gauge modes, we therefore represent the fermionic masses of both left and right-handed modes using a single notation, $m_{\psi}^{(n)}$, the BC symbols ,(2.29), refer to the BCs which must be applied to a *left-handed* field in order to obtain the mass of the relevant mode, e.g.

$$\widetilde{m}_{L}^{(n)} \quad = \quad \widetilde{\bar{m}}_{R}^{(n)} \quad \equiv \quad \widetilde{m}_{\psi}^{(n)}. \tag{2.50}$$

A few comments are in order regarding the general properties of the fermionic mass spectra which will be of use in our later discussions:

- Although there is a dependence on the bulk mass parameter of the field, for the c^{ψ} values required to reproduce the SM fermionic masses (see for example reference [6]) the differences between the $x_{\psi}^{(1)}$ values are smaller than 1.
- The difference between the $x_{\psi}^{(1)}$ values for the different BC combinations is smaller than the equivalent differences for gauge fields. The case which will be of particular interest is the difference between the $(-,+)$ and $(+,+)$ BCs. Our investigations have shown that this difference is typically less than 0.1%.

A further consequence of the left and right-handed fermionic fields respecting opposite BCs is that, as was the case with the gauge vector and scalar fields, it is not possible for the spectra of both components to simultaneously contain a zero mode. It is this property which provides a solution to the chirality problem (the production of a chiral low energy effective theory from the non-chiral fundamental) common to all 5D models.

Finally, a key element of model building in RS type models is the variation in fermionic zero mode localisation which can be achieved through changes $\mathcal{O}(1)$ in the bulk mass parameter c (see figure 2.1). This property can be seen by simply considering the form of (2.47) for values of c^{ψ} either side of the value for which the LH profile is flat, $c^{\psi} = 1/2$,

$$e^{ky/2} f_L^{(0)}(y) \sim \begin{cases} e^{\left(1/2-c^{\psi}\right)ky}\sqrt{\left(c^{\psi}-1/2\right)2kL} & \text{for } c^{\psi} > 1/2 \quad \text{UV localisation} \\ 1 & \text{for } c^{\psi} = 1/2 \quad \text{non-localised} \\ e^{k\left(1/2-c^{\psi}\right)(y-L)}\sqrt{\left(1/2-c^{\psi}\right)2kL} & \text{for } c^{\psi} < 1/2 \quad \text{IR localisation.} \end{cases} \tag{2.51}$$

It was quickly realised that this property allowed for the explanation of the fermionic mass hierarchy through a higher-dimensional geography [5, 6, 17] similar to the split fermion framework suggested in references [43, 44]. Furthermore, the small masses of the majority of fermions means that they are necessarily UV localised with the result that the effective cut-off scale associated with any higher-dimensional operator involving light fermions is Planckian. This prevents phenomenological problems with any of the potentially troublesome higher-dimensional operators mentioned in the Introduction.

A potential drawback for such a model of fermionic masses is the well known issue with large FCNCs experienced by models with split fermions [43, 45]. Here again the lightness of the SM fermions allows a potentially serious phenomenological issue be avoided, the UV localisation of the light fermions greatly lessening the degree of non-universal gauge-fermion couplings largely responsible for such effects [18]. Once again this mechanism via which the phenomenological ills of the RS model are cured due

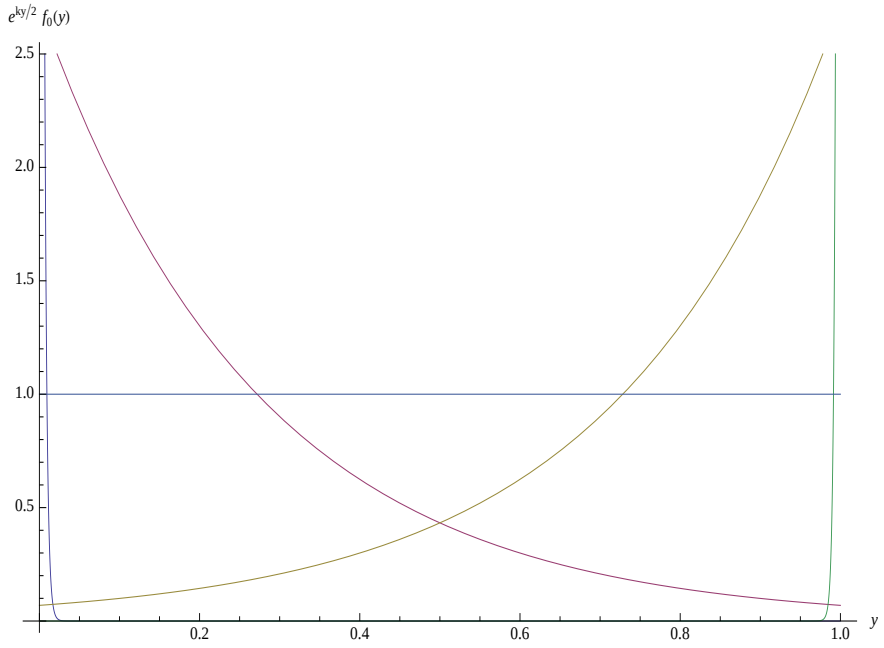

Figure 2.1: In the above figure we demonstrate the possibility of varying the bulk localisation of left-handed zero mode fermions through $\mathcal{O}(1)$ *changes in the bulk mass parameter* c^{ψ}*. In the above the* c^{ψ} *values shown are: 10 (curved blue), 0.6 (pink), 0.5 (flat blue), 0.4 (yellow) and -10 (green). The distance along the EXD is measured in units of L.*

to the lightness, and associated UV localisation, of the majority of the SM fermions is termed the RS-GIM mechanism in reference to the obvious similarities with the SM GIM mechanism [46].

2.2.4 Higgs Field

When considering the KK reduction of the Higgs field there is the additional complication that we require that in order to replicate the SSB of the SM without introducing additional light scalars the mass spectrum should have the following two

characteristics:

- The lightest KK mode of the Higgs should be both *tachyonic* and $\mathcal{O}(v)$,
- The remaining modes should be non-tachyonic and the lightest of these should be $\mathcal{O}(TeV)$.

As was shown in reference [29] such a KK spectrum can be obtained through a judicious choice of the 5D Higgs potential parameters, the precise details of which are not required for the current discussion. For the remainder of this section we will therefore outline the KK reduction procedure in much the same way as has been done for the previous field types, all the time assuming that we have chosen the Higgs potential parameters such that a KK spectrum with the above characteristics has been obtained.

The most general action up to and including quartic self-couplings for a complex 5D scalar field (which we suggestively label H and refer to as the Higgs) [5] is of the form

$$S_{Higgs} = \int d^4x \int_0^L dy \sqrt{G} \left\{ \left(\partial_M H^\dagger \right) \partial^M H - V(H) \right\}, \tag{2.52}$$

where the Higgs potential is given by the expression

$$\begin{aligned} V(H) =& m^2 H^\dagger H + \frac{\lambda_B}{k} |H^\dagger H|^2 + \left[\frac{\mu_{IR}^2}{k} H^\dagger H + \frac{\lambda_{IR}}{k^2} |H^\dagger H|^2 \right] \delta(y - L) \\ & - \left[\frac{\mu_{UV}^2}{k} H^\dagger H + \frac{\lambda_{UV}}{k^2} |H^\dagger H|^2 \right] \delta(y). \end{aligned} \tag{2.53}$$

Jumping ahead somewhat, we are able to simplify this general form by considering the relative sizes of the effective 4D couplings resulting from the KK reduction of

[5] This procedure is not dependent upon the exact form of the Higgs field and therefore we wait until the next chapter to define the Higgs field of the UCRS model

the three original quartic couplings. Our investigations have shown that even in the most sympathetic region of parameter space the effective coupling resulting from the reduction of the IR confined quartic term is two orders of magnitude smaller than the couplings originating from the bulk quartic term. The coupling originating from the UV confined quartic term is suppressed by two powers of the Planck scale relative to the bulk term. We are therefore able to ignore the two brane confined quartic terms and will relabel the bulk quartic coupling as simply λ_{5D}, thereby allowing the Higgs potential to be simplified to

$$V(H) = \frac{1}{k}\Big[m^2\, k + \mu_{IR}^2\, \delta(y-L) - \mu_{UV}^2\, \delta(y) + \lambda_{5D}\, H^\dagger H\Big] H^\dagger H. \tag{2.54}$$

Sticking with the conventions of reference [29], we rewrite the above mass parameters in terms of the curvature constant of the theory and a set of dimensionless parameters,

$$m^2 = 20k^2\xi \qquad\qquad \mu_{UV,IR}^2 = 16k^2\xi\beta_{UV,IR}. \tag{2.55}$$

As μ_{UV} will receive a Planck scale suppression in 4D it will be the values of ξ and β_{IR} which will determine the mass spectrum of the Higgs, the details of which will be given alongside the specifics of the Higgs field within the framework of the UCRS model in the next chapter.

The Higgs field is now decomposed in the usual manner,

$$H(x,y) = \frac{1}{\sqrt{L}} \sum_{n=1}^{\infty} H^{(n)}(x)\, f_H^{(n)}(y)\,. \tag{2.56}$$

The orthogonality condition for the bulk profiles is

$$\frac{1}{L}\int_0^L dy\, e^{-2ky} f_H^{(n)}(y)\, f_H^{(m)}(y) = \delta_{nm}. \tag{2.57}$$

The explicit forms of the Higgs bulk profiles are

$$f_H^{(1)}(y) = \frac{e^{2ky}}{N_H^{(1)}} \left[I_\nu \left(\frac{m_H^{(1)} e^{ky}}{k} \right) + b_H^{(1)} K_\nu \left(\frac{m_H^{(1)} e^{ky}}{k} \right) \right], \tag{2.58}$$

$$f_H^{(n)}(y) = \frac{e^{2ky}}{N_H^{(n)}} \left[J_\nu \left(\frac{m_H^{(n)} e^{ky}}{k} \right) + b_H^{(n)} Y_\nu \left(\frac{m_H^{(n)} e^{ky}}{k} \right) \right], \qquad (n = 1, 2, \ldots), \tag{2.59}$$

where $\nu = \sqrt{4 + 20\xi}$, I_ν and K_ν are the hyperbolic Bessel functions and $m_H^{(1)}$ is the absolute value of the tachyonic mass. Figure 2.2 shows the bulk profile of the tachyonic Higgs mode for a particular choice of Higgs potential parameters. The values of the specific parameters used to generate this plot are in fact irrelevant as it is a feature common to all tachyonic modes that they are exponentially IR brane-localised.

For completeness we note that in order to obtain the required KK mass spectrum the bulk profiles of the Higgs field must obey $(+,+)$ BCs, where in the case of a Higgs field with the potential shown in (2.54) the Neumann-like conditions on the two branes take the form

$$\left(\partial_5 + \frac{\mu_{UV}^2}{k} \right) f_H^{(n)}(y)\,|_{y=0} = 0,$$

$$\left(\partial_5 + \frac{\mu_{IR}^2}{k} \right) f_H^{(n)}(y)\,|_{y=L} = 0. \tag{2.60}$$

After completing the KK reduction process the 4D effective action of the Higgs field contains the terms

$$S_{\text{Higgs}} \supset \int d^4x \left\{ \partial_\mu H^{(1)\dagger} \partial^\mu H^{(1)} + m_H^{(1)\,2} H^{(1)\dagger} H^{(1)} - \lambda_{SM} |H^{(1)\dagger} H^{(1)}|^2 + \ldots \right\}, \tag{2.61}$$

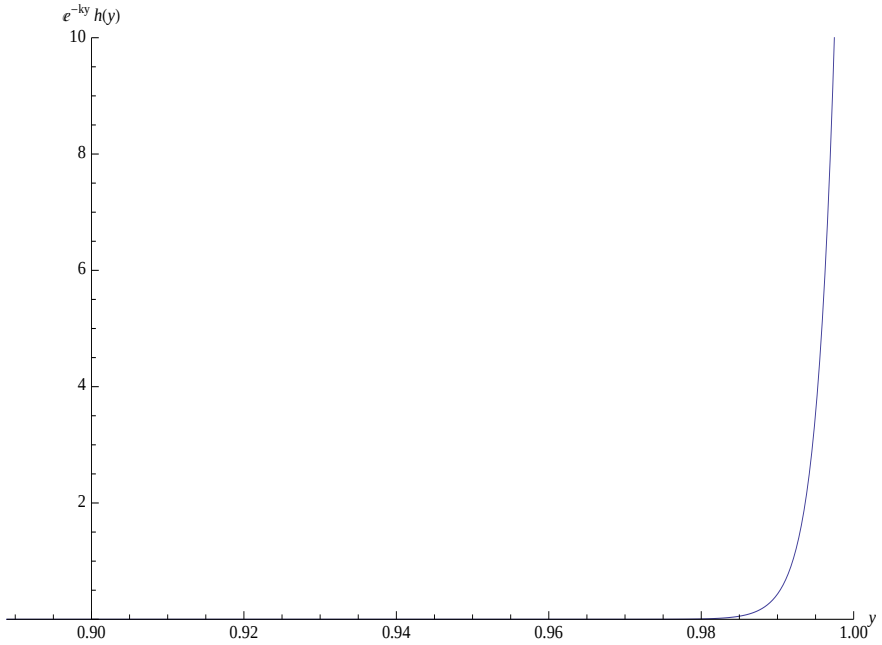

Figure 2.2: The above figure shows the normalised profile of the tachyonic Higgs mode over the last 9th of the length of the EXD. As can be seen, the main feature of the VEV profile is its high degree of IR localisation, closely mimicking the previous case of the IR brane confined Higgs.

where the ellipsis represent terms containing at least one heavy Higgs mode and we define the effective coupling

$$\lambda_{SM} = \frac{\lambda_{5D}}{kL^2} \int_0^L dy\, e^{-4ky} \left[f_H^{(1)}(y) \right]^4 . \tag{2.62}$$

As was the original aim, we see that the 4D effective action of our fundamental Higgs field contains a single field with a non-zero VEV, $v = \sqrt{m_H^{(1)\,2}/\lambda_{SM}}$, suitable for a role in a SM like SSB process at the weak scale.

Chapter 3

The Universal Custodial RS Model

In this chapter we will discuss the specific details of the UCRS model, within which framework we will eventually calculate the fermionic loop contributions to the T parameter. The full action of the model is

$$S_{UCRS} = \int d^4x \int_0^L dy \sqrt{G} \left(\mathcal{L}_{\text{Gauge}} + \mathcal{L}_{\text{Higgs}} + \mathcal{L}_{\text{fermion}} + \mathcal{L}_{\text{Yukawa}} + \mathcal{L}_{\text{Gauge Fixing}} \right), \tag{3.1}$$

where the precise form of each constituent Lagrangian will be the focus of a subsequent subsection of this chapter. The gauge symmetry of the EW sector of the model is the extended (compared to the SM) group

$$G_{\text{EW}} = SU(2)_L \times SU(2)_R \times U(1)_X \times P_{LR}, \tag{3.2}$$

where P_{LR} is a discrete symmetry exchanging the left and right-handed $SU(2)$ groups. Our model also contains the usual $SU(3)_C$ colour gauge symmetry but as QCD effects do not feature in our calculation of S and T we suppress all quark colour indices during the remainder of our discussion.

3.1 Model Details

3.1.1 Gauge Sector

The EW gauge sector of our model is described by the Lagrangian

$$\mathcal{L}_{\text{Gauge}} = \left[-\frac{1}{4} L^a_{MN} L^{MNa} - \frac{1}{4} R^\alpha_{MN} R^{MN\alpha} - \frac{1}{4} X_{MN} X^{MN} \right] \tag{3.3}$$

and the field strength tensors of the Abelian and non-Abelian fields take their usual forms

$$L_{MN} = \partial_M W^a_{LN} - \partial_N W^a_{LM} - g_5 \epsilon^{abc} W^b_{LM} W^c_{LN} \tag{3.4}$$

$$R_{MN} = \partial_M W^\alpha_{RN} - \partial_N W^\alpha_{RM} - g_5 \epsilon^{\alpha\beta\gamma} W^\beta_{RM} W^\gamma_{RN}, \tag{3.5}$$

$$X_{MN} = \partial_M X_N - \partial_N X_M. \tag{3.6}$$

We note that our convention is for all Latin gauge indices to be associated with the left-handed $SU(2)$ gauge group while all Greek indices are associated with the right-handed group. We also draw attention to the fact that the P_{LR} symmetry demands that the couplings of the two $SU(2)$ gauge fields be equal; in general this is not the case [1].

Clearly, for phenomenological reasons this extended gauge group must ultimately be broken down to the $U(1)_{\text{EM}}$ group in the low energy 4D effective theory. From Goldstone's theorem, however, we see that we may not simply use an extended version of the SM Higgs mechanism to break all of the necessary gauge generators without introducing three new, phenomenologically problematic, EW scale gauge bosons into

[1] For an example of a similar discussion without this right-left symmetry see reference [26]

the 4D effective theory. In order to circumvent this problem we split the process of symmetry breaking into two distinct stages:

1. The extended gauge symmetry is broken down to the SM EW gauge group on the UV brane using the BCs of the gauge fields [2],

$$SU(2)_L \times SU(2)_R \times U(1)_X \to SU(2)_L \times U(1)_Y. \tag{3.7}$$

2. The two $SU(2)$ groups are spontaneously broken down to their diagonal subgroup through the Higgs sector,

$$SU\left(2\right)_L \times SU\left(2\right)_R \to SU\left(2\right)_{L+R}. \tag{3.8}$$

The combined effect of these two stages is to break the original extended gauge group down to the standard electromagnetic $U\left(1\right)$ gauge group [3]. We delay a detailed discussion of the second stage of this procedure until section 3.1.2.

The gauge BC assignments necessary to achieve the symmetry breaking shown in (3.7) are as follows [31],

$$W^{1,2}_{R\,\mu}\left(-,+\right), \qquad Z_{X\,\mu}(-,+), \tag{3.9}$$

$$W^{1,2,3}_{L\,\mu}\left(+,+\right), \qquad B_{\mu}\left(+,+\right). \tag{3.10}$$

The two 'new' fields arise from orthogonal combinations of the $W^3_{R\,M}$ and X_M fields

[2] For a detailed discussion of symmetry breaking via BCs in extra-dimensions see references [42, 47]

[3] A group theoretic explanation of this can be found in reference [48]

defined, in analogy with the SM, as

$$Z_{X\,M} = \cos\phi\, W^3_{R\,M} - \sin\phi\, X_M, \tag{3.11}$$

$$B_M = \sin\phi\, W^3_{R\,M} + \cos\phi\, X_M \tag{3.12}$$

and the mixing angles by the expressions

$$\cos\phi = \frac{g_5}{\sqrt{g_5^2 + g_X^2}}, \qquad \sin\phi = \frac{g_X}{\sqrt{g_5^2 + g_X^2}}, \tag{3.13}$$

where g_X is the coupling constant associated with the $U(1)_X$ gauge symmetry.

During the course of this discussion it will also be useful to define the following field combinations

$$W_L^{\pm} = \frac{W_L^1 \mp i W_L^2}{\sqrt{2}}, \qquad W_R^{\pm} = \frac{W_R^1 \mp i W_R^2}{\sqrt{2}}, \tag{3.14}$$

$$Z_M = \cos\psi\, W^3_{L\,M} - \sin\psi\, B_M, \tag{3.15}$$

$$A_M = \cos\psi\, B_M + \sin\psi\, W^3_{L\,M}, \tag{3.16}$$

where we define the mixing angles

$$\cos\psi = \frac{1}{\sqrt{1 + \sin^2\phi}}, \qquad \sin\psi = \frac{\sin\phi}{\sqrt{1 + \sin^2\phi}}. \tag{3.17}$$

It should be noted that due to the mixing between the different gauge KK modes induced by the SSB procedure the above mixing angle is not same as the SM weak mixing angle, $\sin\theta_W = s_W$. As the mixing between KK modes is an effect $\mathcal{O}\left(v^2/M_{KK}^2\right)$ the difference between the two mixing angles is small and will actually be negligible

when we come to calculate the one-loop contributions to the T parameter in chapter 5.

As could be inferred from the similarity which the BC symmetry breaking procedure bears to the SM Higgs mechanism, such a set of BCs can be obtained dynamically using a UV confined, Higgs-like scalar transforming as a singlet under the left-handed $SU(2)$ group, a doublet under the right-handed $SU(2)$ group and with a $U(1)_X$ charge of $1/2$, or for convenience $(\mathbf{1},\mathbf{2})_{1/2}$. The only difference between the SM Higgs mechanism and this BC generating process is the need for the VEV of the UV brane localised scalar to be taken to infinity in order that the associated particles decouple from the low energy effective theory. Taking such a limit enforces Dirichlet BCs for the relevant fields on the UV boundary. For more details of this process see references [41, 42]

3.1.2 Higgs Sector

The Higgs field required to complete the SSB part of the symmetry breaking procedure outlined above is a bidoublet of the two $SU(2)$ groups and has zero $U(1)_X$ charge, i.e. transforms as $(\mathbf{2},\mathbf{2})_0$. For the purposes of this thesis we find it convenient to parameterise such a field as

$$H(x,y) = \frac{1}{2}\begin{pmatrix} -(\phi^2 + i\phi^1) & -(h - i\phi^3) \\ (h + i\phi^3) & -(\phi^2 - i\phi^1) \end{pmatrix}, \qquad H \to U_L H U_R^T, \tag{3.18}$$

where ϕ^i are the Would be Goldstone Bosons (WGBs) of the theory and h is the *physical* Higgs field. In the name of clarity we have shown the transformation properties of the Higgs bidoublet with the $SU(2)_L$ group acting vertically (as in the SM) and $SU(2)_R$ acting horizontally. These transformation properties are shared with the fermionic bidoublets which we will encounter in the fermionic sector of the

model. We will also find it convenient to define, in analogy with the gauge sector, the charged WGBs

$$\phi^{\pm} = \frac{\phi^1 \mp i\phi^2}{\sqrt{2}}. \tag{3.19}$$

Adapting the Higgs Lagrangian already discussed in detail in section 2.2.4 to the case of a bidoublet Higgs, we find that the Lagrangian of the Higgs sector of our model is

$$\mathcal{L}_{\text{Higgs}} = Tr\left[\left(D_M H^{\dagger}\right) D^M H\right] - V(H), \tag{3.20}$$

where the covariant derivative is

$$(D_M H) = \partial_M H + ig_5 \tau^c W^c_{L\,M} H + ig_5 H\,\left(\tau^{\gamma} W^{\gamma}_{R\,M}\right)^T, \tag{3.21}$$

$\tau^{a\,(\alpha)} = \sigma^{a\,(\alpha)}/2$ are the generators of the left-handed (right-handed) $SU\,(2)$ group and the adapted Higgs potential is

$$V(H) = \frac{1}{k}\Big[m^2\,k + \mu^2_{IR}\,\delta(y-L) - \mu^2_{UV}\,\delta(y) + \lambda_{5D}\,TrH^{\dagger}H\Big]TrH^{\dagger}H. \tag{3.22}$$

We note that we have used the fact that for the Higgs appearing in our model $Tr|H^{\dagger}H|^2 = Tr^2|H^{\dagger}H|$ to simplify the most general Higgs potential.

Choosing the dimensionless Higgs potential parameters to be

$$\xi = 5.2, \qquad\qquad \beta_{IR} = -0.3, \tag{3.23}$$

we obtain a KK mass spectrum which meets the criteria set out in section 2.2.4 and therefore a Higgs mode which acquires a VEV $\mathcal{O}\,(TeV)$ as required by the symmetry breaking procedure previously discussed.

3.1.3 Fermionic Sector

We now consider how to embed the SM fermions into representations of our extended gauge group. Although there are clearly a number of possible formulations (see [31] for a possible alternative) we will make use of the assignment which has almost become the standard for analyses such as ours due to its compatibility with the $SO(5)$ group of gauge-Higgs unification models [26, 27, 32, 40].

The fermionic action can obviously be split into quark and leptonic sectors

$$\mathcal{L}_{\text{fermionic}} = \mathcal{L}_{\text{Quark}} + \mathcal{L}_{\text{Lepton}}. \tag{3.24}$$

Below we present a detailed discussion of the quark sector and then use the minimality of our model to state the representation structure of the leptonic sector.

Quark Sector

The general form of the quark sector utilised in our model is

$$\xi_1^q = \begin{pmatrix} \chi^u(-,+)_{5/3} & q^u(+,+)_{2/3} \\ \chi^d(-,+)_{2/3} & q^d(+,+)_{-1/3} \end{pmatrix}, \qquad \xi_2^q = u(-,-)_{2/3}, \tag{3.25}$$

$$\xi_3^q = T_3^q \oplus T_4^q = \begin{pmatrix} \psi'(+,-)_{5/3} \\ U'(+,-)_{2/3} \\ D'(+,-)_{-1/3} \end{pmatrix} \oplus \begin{pmatrix} \psi''(+,-)_{5/3} \\ U''(+,-)_{2/3} \\ D(-,-)_{-1/3} \end{pmatrix}, \tag{3.26}$$

where the bidoublet containing the fields from which the left-handed SM quarks will originate, ξ_1^q, transforms as $(\mathbf{2},\mathbf{2})_{2/3}$, the custodial singlet identified with the right-handed SM up type quarks, ξ_2^q, as $(\mathbf{1},\mathbf{1})_{2/3}$ and the right-handed triplet containing the field to be identified with right-handed SM down type quark, T_4^q, as $(\mathbf{1},\mathbf{3})_{2/3}$. Due

to the presence of the discrete symmetry P_{LR} in the gauge group of the model in order to correctly form an irreducible representation including T_4^q we must combine it with a left-handed equivalent, T_3^q, transforming as $(\mathbf{3},\mathbf{1})_{2/3}$. ξ_3^q is therefore analogous to the Dirac spinor which is a reducible representation of the Lorentz group but irreducible when an additional parity transformation is added to the theory.

Some further notes are required to fully explain the complicated looking notation used in the above representations:

- All fields are 5D and therefore *non-chiral*. The BCs accompanying each field is the BC of the *left-handed* component of the 5D field. As has been discussed in section 2.2.3, the BCs of the right-handed component can be obtained by simply taking the opposite BC on each brane.

- We remind the reader that only fermionic fields with $(+,+)$ BCs contain a zero-mode in their KK spectrum. A field accompanied by $(-,-)$ above therefore contains a *right-handed* zero-mode in its KK spectrum.

- The subscript to each field indicates the EM charge of that field, $Q_{EM} = T_L^3 + T_R^3 + Q_X$.

The Lagrangian of the quark sector is therefore

$$\begin{aligned}\mathcal{L}_{\text{Quark}} \supset \Big[& Tr\,\bar{\xi}_1^q\, i\Gamma^M D_M^1\, \xi_1^q - Tr\,\bar{\xi}_1^q\, c_1^q\, k\, \xi_1^q \\ & + \bar{\xi}_2^q\, i\Gamma^M D_M^2\, \xi_2^q - \bar{\xi}_2^q\, c_2^q\, k\, \xi_2^q \\ & + \bar{T}_3^q\, i\Gamma^M D_M^3\, T_3^q - \bar{T}_3^q\, c_3^q\, k\, T_3^q \\ & + \qquad\qquad 3 \leftrightarrow 4 \qquad\qquad \Big] \end{aligned} \tag{3.27}$$

and the EW part of the covariant derivatives are defined as

$$D_M^1 \xi_1^q \supset \left(\partial_M + \omega_M + i\frac{2}{3} g_X X_M\right) \xi_1^q + i g_5 \left(\tau^c W_{L\,M}^c\right) \xi_1^q + i g_5\, \xi_1^q \left(\tau^\gamma W_{R\,M}^\gamma\right)^T, \tag{3.28}$$

$$D_M^2 \xi_2^q \supset \left(\partial_M + \omega_M + i\frac{2}{3} g_X X_M\right) \xi_2^q, \tag{3.29}$$

$$D_M^3 T_3^q \supset \left(\partial_M + \omega_M + i\frac{2}{3} g_X X_M\right) T_3^q + g_5 \epsilon^{abc} W_{L\,M}^c T_3^q, \tag{3.30}$$

$$D_M^4 T_4^q \supset \left(\partial_M + \omega_M + i\frac{2}{3} g_X X_M\right) T_4^q + g_5 \epsilon^{\alpha\beta\gamma} W_{R\,M}^\gamma T_4^q. \tag{3.31}$$

At this point we note that due to a change of basis the form of the triplet representations when appearing in the covariant derivative is not the same as that given

in (3.26), but is instead

$$T_3^q = \begin{pmatrix} \frac{1}{\sqrt{2}}\left(\psi' + D'\right) \\ \frac{i}{\sqrt{2}}\left(\psi' - D'\right) \\ U' \end{pmatrix}, \qquad T_4^q = \begin{pmatrix} \frac{1}{\sqrt{2}}\left(\psi'' + D\right) \\ \frac{i}{\sqrt{2}}\left(\psi'' - D\right) \\ U'' \end{pmatrix}. \tag{3.32}$$

Such a change of basis is necessary so as to prevent our covariant derivative containing a mixed set of $SU(2)_{L,R}$ bases, the gauge boson triplets already appearing in the above basis.

Leptonic Sector

The leptonic sector, in analogy with the quark sector, contains the representations

$$\xi_1^l = \begin{pmatrix} \chi^\nu(-,+)_1 & \nu(+,+)_0 \\ \chi^l(-,+)_0 & l(+,+)_{-1} \end{pmatrix}, \qquad \xi_2^l = N(-,-)_0, \tag{3.33}$$

$$\xi_3^l = T_3^l \oplus T_4^l = \begin{pmatrix} \lambda'(+,-)_1 \\ N'(+,-)_0 \\ L'(+,-)_{-1} \end{pmatrix} \oplus \begin{pmatrix} \lambda''(+,-)_1 \\ N''(+,-)_0 \\ E(-,-)_{-1} \end{pmatrix}, \tag{3.34}$$

where the above multiplets have the same transformation properties as their quark analogues under the $SU(2)_L \times SU(2)_R$ group but, in order to obtain the correct EM charge for the SM leptons, have zero charge under the $U(1)_X$ group. The Lagrangian of the leptonic sector can therefore be obtained from that of the quark sector (3.27)

by simply making the replacement $q \to l$ and using the following covariant derivatives

$$D^1_M \xi^l_1 = (\partial_M + \omega_M)\xi^l_1 + ig_5 \left(\tau^c W^c_{L\,M}\right) \xi^l_1 + ig_5\, \xi^l_1 \left(\tau^\gamma W^\gamma_{R\,M}\right)^T, \tag{3.35}$$

$$D^2_M \xi^l_2 = (\partial_M + \omega_M)\, \xi^l_2, \tag{3.36}$$

$$D^3_M T^l_3 = (\partial_M + \omega_M)\, T^l_3 + g_5 \epsilon^{abc} W^c_{L\,M} T^l_3, \tag{3.37}$$

$$D^4_M T^l_4 = (\partial_M + \omega_M)\, T^l_4 + g_5 \epsilon^{\alpha\beta\gamma} W^\gamma_{R\,M} T^l_4. \tag{3.38}$$

3.1.4 The Yukawa Sector

Again, we simply state the form of the quark Yukawa couplings and provide the replacements necessary to obtain the leptonic equivalents,

$$\mathcal{L}_{\text{Yukawa}} \supset 2\left[Y^u_{5D}\, Tr\, \bar{\xi}^q_1 H \xi^q_2 - \sqrt{2} Y^d_{5D} \Big[Tr\left\{\bar{\xi}^q_1 \tau^c H\right\} (T^q_3)^c + Tr\left\{\bar{\xi}^q_1 H (\tau^\gamma)^T\right\} (T^q_4)^\gamma \Big] \right], \tag{3.39}$$

where $Y^{u,\,d}_{5D}$ are the 5D, flavour non-diagonal [4] Yukawa couplings for the up and down type quarks respectively.

We make the following observations about the exact form of the Yukawa sector of our model:

- The 5D Yukawa couplings have mass dimensions $[Y^{u,\,d}_{5D}] = -1/2$. It is therefore natural for $\sqrt{k}\, Y^{u,\,d}_{5D}$ to be $\mathcal{O}(1)$.

[4] As the flavour structure of the model is beyond the scope of this work we have dropped the flavour indices from all fermionic fields and their associated couplings

- The factors of 2 and $\sqrt{2}$ have been chosen such that the masses of SM fermions are of their canonical form.
- The choice of sign for the Yukawa couplings also comes from the fact that we wish the SM particles to have masses of the "correct" sign, namely $-$.
- The triplets appearing are again of the form shown in (3.32).

The leptonic Yukawa couplings are obtained from (3.39) by the making the trivial substitutions

$$\begin{aligned} u &\to \nu, \\ d &\to l, \\ q &\to l, \end{aligned} \tag{3.40}$$

where d (u) is the label given to the Yukawa couplings providing the down (up) type SM quarks with their masses, l (ν) labels those couplings providing the SM charged leptons (neutrinos) with their masses and q (l) labels the quark (lepton) multiplets.

3.1.5 Gauge Fixing Sector

In this section we will extend to the case of the UCRS model the work on extra-dimensional gauge fixing originally done in flat space in reference [49] and subsequently applied to the Standard RS model in papers such as [11, 50, 51]. Apart from the greater number of vector bosons to consider, the main point of difference between our discussion and that of the previous works listed is the fact that our model is compactified on an interval rather than an orbifold. The result of this is that our gauge-fixing sector is not simply a trivial extension of that found in [11, 51].

In order to correctly define the analogue of the SM R_ξ gauges within the framework of extra-dimensional models it is necessary to remove all terms which mix 4D vector DOFs with 4D scalar DOFs. Unlike in the SM, in the UCRS model (and more generally in minimal extra-dimensional extensions of the SM) there are typically two sources for such mixing terms:

- Mixing between gauge vector and gauge scalar modes originating from the higher-dimensional field-strength tensor.
- SM like mixing between gauge vector modes and those of the WGBs.

We first wish to consider those terms originating from the gauge sector of our model and to this end rewrite the action of our general Abelian gauge field from section 2.2.2 by separating the purely vector terms from those mixing vector and scalar DOFs,

$$S_{\text{gauge}} = \int d^4x \int_0^L dy \left\{ -\frac{1}{4} F_{\mu\nu} F^{\mu\nu} + \frac{e^{-2ky}}{2} \left(\partial_\mu A_5 \partial^\mu A_5 + \partial_5 A_\mu \partial_5 A^\mu - 2 \partial_\mu A_5 \partial_5 A^\mu \right) \right\}, \tag{3.41}$$

where we have substituted in the explicit form of the RS metric. In order to connect with the gauge-fixing sectors stated in the aforementioned references, we rewrite the above mixing terms using integration by parts,

$$S_{\text{gauge}} \supset \int d^4x \int_0^L dy \Big\{ -\partial_5 \left(e^{-2ky} A_5 \right) \partial_\mu A^\mu + \left[e^{-2ky} A_5 \partial_\mu A^\mu \right] \delta(y - L) - \left[e^{-2ky} A_5 \partial_\mu A^\mu \right] \delta(0) \Big\}. \tag{3.42}$$

We can see from the above expression that in addition to the bulk mixing terms which are present in an orbifold compactification we also obtain boundary confined terms. The actions of each of the seven gauge fields present in our model will contain a set of analogous mixing terms, all of which must be removed separately.

The form of the terms mixing gauge vector and WGB scalar DOFs are found by expanding the covariant derivatives of the Higgs sector (3.21) in much the same way as in the SM. The difference between the two cases is that in the case at hand we must remember that it is only the $n = 1$ mode of the Higgs field which will obtain a VEV. As a result it is convenient to perform the expansion of the Higgs covariant derivative *after* performing the KK decomposition of the Higgs field while leaving the gauge fields in their 5D form. The terms which, after SBB, will produce vector/scalar mixing terms are

$$\mathcal{L}_{\text{Higgs}} \supset \frac{1}{L}\sum_{n=1}^{\infty} e^{-2ky}\Bigg[ig_5\, Tr\left\{\partial_\mu H^{(n)\,\dagger}\left(\tau^c W_L^{c\,\mu}\right) H^{(1)}\right\} + ig_5\, Tr\left\{\partial_\mu H^{(n)\,\dagger} H^{(1)}\left(\tau^\gamma W_R^{\gamma\,\mu}\right)^T\right\}$$

$$+ H.c.\Bigg] f_H^{(1)}(y) f_H^{(n)}(y). \tag{3.43}$$

We are now in a position to be able to write down the gauge-fixing Lagrangian which will remove all vector/scalar mixing terms from the UCRS model, thereby

defining the R_ξ gauges,

$$\mathcal{L}_{\text{Gauge Fixing}} = -\frac{1}{2\xi_\gamma}\left(\partial_\mu A^\mu - \xi_\gamma \partial_5(e^{-2ky}A_5)\right)^2$$

$$-\frac{1}{2\xi_Z}\left(\partial_\mu Z^\mu - \xi_Z\left[\partial_5(e^{-2ky}Z_5) - \frac{e^{-2ky}v(y)g}{2\cos\psi}\phi^0\right]\right)^2$$

$$-\frac{1}{2\xi_{Z_X}}\left(\partial_\mu Z_X^\mu - \xi_{Z_X}\left[\partial_5(e^{-2ky}Z_{X5}) + \frac{e^{-2ky}v(y)g\cos\phi}{2}\phi^0\right]\right)^2$$

$$-\frac{1}{\xi_{W_{L,R}}}\left(\partial_\mu W_{L,R}^{+\mu} - \xi_{W_{L,R}}\left[\partial_5(e^{-2ky}W_{5\,L,R}^{+}) \mp \frac{e^{-2ky}v(y)g}{2}\phi^+\right]\right)$$
$$\times\left(\partial_\mu W_{L,R}^{\mu-} - \xi_{W_{L,R}}\left[\partial_5(e^{-2ky}W_{5\,L,R}^{-}) \mp \frac{e^{-2ky}v(y)g}{2}\phi^-\right]\right)$$

$$-\frac{1}{2\xi_{\gamma\,0}}\left(\partial_\mu A^\mu - \xi_{\gamma\,0}e^{-2ky}A_5\right)^2\delta(0) - \frac{1}{2\xi_{\gamma\,L}}\left(\partial_\mu A^\mu + \xi_{\gamma\,L}e^{-2ky}A_5\right)^2\delta(y-L)$$

$$+ \quad \text{analogous boundary terms for each gauge field} \tag{3.44}$$

where we have introduced the shorthands $v\,(y) = v f_H^{(1)}\,(y)$ and $g = g_5/\sqrt{L}$

3.2 Scalar Mass Matrices

Although the mass matrices of the fermionic and gauge modes present in the UCRS model have been considered in detail in reference [40] those mass matrices associated with the scalar DOFs of the model have not. The mass matrices of scalar DOFs have previously been calculated for RS type models but only within the context

of a *non-universal* model. In this section therefore we discuss the difference between the scalar sector of a non-universal RS type model and that of the UCRS model.

3.2.1 The Geometric Higgs Mechanism

Before addressing the specific form of the scalar sector in the UCRS model we first wish to outline the argument which allows us to predict that the scalar sector of an universal extra-dimensional model will, in addition to containing the usual set of *unphysical* scalar modes, contain an additional set of *physical* scalar modes.

The geometric Higgs mechanism is the name given to the process through which the heavy vector modes of a 5D gauge field obtain their KK masses, and therefore additional DOFs, by "eating" the associated gauge scalar mode. As we saw in section 2.2.2 it is not possible for a gauge vector and gauge scalar zero mode to exist simultaneously, explaining why gauge zero modes remain massless after dimensional reduction. This also explains why a 5D gauge symmetry translates into a single, low energy, gauge symmetry in 4D rather than an infinite number of separate 4D symmetries at each KK level. In non-universal models, therefore, there are no *physical* scalar DOFs at all, the WGBs of the IR confined 4D Higgs are eaten by the gauge vector zero modes as part of the SSB procedure just as occurs in the SM. The case of universal extra-dimensional models is quite different however, as there are now *two* infinite towers of scalar modes which can be "eaten" by the heavy vector modes, those of the gauge scalars and, due to the SSB procedure, those of the 5D WGBs. The final result is that one linear combination of the gauge and WGB scalar DOFs are eaten by the gauge vector modes while the orthogonal combination forms a tower of heavy (the lightest WGB modes are still absorbed by the vector boson zero modes) physical scalar modes capable of contributing to EW precision observables

(EWPOs).

In the remainder of this section we consider the form of the mass matrices associated with these additional scalar modes, as well as, for completeness, giving the form of the mass matrix associated with the physical Higgs modes and the unphysical scalar DOFs of the theory.

3.2.2 Additional Physical Scalar Modes

The mass terms of the physical scalars all originate from the Higgs sector of our model and come in three varieties: those mixing different gauge scalar modes, those mixing different WGB modes and finally those mixing gauge scalar modes *with* WGB modes. The first of these varieties originates from the covariant derivative of the Higgs sector and, like the masses of their equivalent vector modes, can be written in the succinct form

$$\mathcal{L}_{\text{Higgs}} \supset -\sum_{n,m=1}^{\infty} \frac{g^2 v^2}{2} \left(FF^T\right)^{ab} W_5^{a\,(n)} W_5^{b\,(m)\,\dagger} \mathcal{I}_{11nm}^{\phi\phi SS}, \tag{3.45}$$

where there is an implied sum over $a, b = W_L^+, W_L^-, Z, W_R^+, W_R^-, Z_X$ and we define the matrix

$$gF_i^a = \frac{1}{2} \begin{pmatrix} -g & 0 & 0 \\ 0 & -g & 0 \\ 0 & 0 & -g/\cos\psi \\ g & 0 & 0 \\ 0 & g & 0 \\ 0 & 0 & g\cos\theta \end{pmatrix}. \tag{3.46}$$

The overlap integral appearing in (3.45) is defined using the conventions presented in appendix A and the indices of which will be labelled according to the BCs of

the particular gauge field appearing using the bar/tilde conventions defined in the previous chapter.

The mass terms mixing the KK modes of the WGBs originate from the quartic coupling present in the Higgs potential (3.22) and are of the form

$$\mathcal{L}_{\text{Higgs}} \supset -v^2\lambda_{SM}\sum_{n,m=2}^{\infty}\Bigg\{\mathcal{I}^{\phi\phi\phi\phi}_{111n}\left[\phi^{0\,(1)}\phi^{0\,(n)}+\phi^{+\,(n)}\phi^{-\,(1)}+\phi^{+\,(1)}\phi^{-\,(n)}\right]$$

$$+\,\mathcal{I}^{\phi\phi\phi\phi}_{11nm}\left[\frac{1}{2}\,\phi^{0\,(n)}\phi^{0\,(m)}+\phi^{+\,(n)}\phi^{-\,(m)}\right]\Bigg\}. \tag{3.47}$$

Finally we have the mass terms, also originating from the covariant derivative of the Higgs sector, which mix the two types of scalar fields

$$\mathcal{L}_{Higgs} \supset \sum_{n=1}^{\infty}\left[gv\left(\mathcal{I}^{\phi\phi' S^a}_{n1m}-\mathcal{I}^{\phi\phi' S^a}_{1nm}\right)F^a_i\phi^{(n)i}W_5^{a\,(m)\,\dagger}\right], \tag{3.48}$$

where a sum over the WGB index, i, and the gauge scalar index, a, is assumed and the primed field appearing in the superscript indicates that the bulk profile of that field is differentiated with respect to y. It is also necessary to note that the differentiated Higgs profile comes with an additional factor of the RS warp factor relative to the normalised bulk profile i.e.

$$\mathcal{I}^{\phi\phi' S^a}_{1nm} = \frac{1}{L}\int_0^L dy\, e^{-4ky}\left(\partial_5 f_H^{(1)}(y)\right) f_H^{(n)}(y)\, f_S^{a\,(m)}(y)\,. \tag{3.49}$$

We note that due to the presence of the derivative term this integral has mass dimension of one. Although this is not desirable it was not possible to find a clear alternative notation with which to express such an integral. Evaluating (3.49) numerically we have found that, as we would naively expect from comparisons with the integral in B.12, it is $\mathcal{O}(M_{KK})$.

In order to express the physical (not proportional to ξ_a) scalar mass terms in an efficient manner we group all scalar DOFs into the following infinite dimensional vectors

$$\Phi^{\pm} = \left(\phi^{\pm\,(1)},\ \ \phi^{\pm\,(2)},\ \ W_{L\,5}^{\pm\,(1)},\ \ W_{R\,5}^{\pm\,(1)},\ \ \ldots\right)^T, \tag{3.50}$$

$$\Phi^{0} = \left(\phi^{0\,(1)},\ \ \phi^{0\,(2)},\ \ Z_{5}^{(1)},\ \ Z_{X\,5}^{(1)},\ \ \ldots\right)^T. \tag{3.51}$$

In terms of these vectors the physical masses can be written as

$$\mathcal{L}_{\text{Higgs}} \supset -\Phi^{+\,T} M^2_{\Phi^{\pm}} \Phi^{-} - \frac{1}{2}\Phi^{0\,T} M^2_{\Phi^{0}} \Phi^{0}, \tag{3.52}$$

where the mass matrices are of the form

$$M^2_{\Phi^{\pm}} = \begin{pmatrix} 0 & \lambda_{SM} v^2 \mathcal{I}^{\phi\phi\phi\phi}_{1112} & 0 & 0 & \ldots \\ \lambda_{SM} v^2 \mathcal{I}^{\phi\phi\phi\phi}_{1121} & m_H^{(2)\,2} + \lambda_{SM} v^2 \mathcal{I}^{\phi\phi\phi\phi}_{1122} & \frac{gv}{2}\left(\mathcal{I}^{\phi\phi' S}_{12\bar{1}} - \mathcal{I}^{\phi\phi' S}_{21\bar{1}}\right) & -\frac{gv}{2}\left(\mathcal{I}^{\phi\phi' S}_{12\bar{\bar{1}}} - \mathcal{I}^{\phi\phi' S}_{21\bar{\bar{1}}}\right) & \ldots \\ 0 & \frac{gv}{2}\left(\mathcal{I}^{\phi\phi' S}_{12\bar{1}} - \mathcal{I}^{\phi\phi' S}_{21\bar{1}}\right) & \frac{g^2v^2}{4}\mathcal{I}^{\phi\phi SS}_{11\bar{1}\bar{1}} & -\frac{g^2v^2}{4}\mathcal{I}^{\phi\phi SS}_{11\bar{1}\bar{\bar{1}}} & \ldots \\ 0 & -\frac{gv}{2}\left(\mathcal{I}^{\phi\phi' S}_{12\bar{\bar{1}}} - \mathcal{I}^{\phi\phi' S}_{21\bar{\bar{1}}}\right) & -\frac{g^2v^2}{4}\mathcal{I}^{\phi\phi SS}_{11\bar{\bar{1}}\bar{1}} & \frac{g^2v^2}{4}\mathcal{I}^{\phi\phi SS}_{11\bar{\bar{1}}\bar{\bar{1}}} & \ldots \\ \vdots & \vdots & \vdots & \vdots & \ddots \end{pmatrix}, \tag{3.53}$$

$$M^2_{\Phi^{0}} = \begin{pmatrix} 0 & \lambda_{SM} v^2 \mathcal{I}^{\phi\phi\phi\phi}_{1112} & 0 & 0 & \ldots \\ \lambda_{SM} v^2 \mathcal{I}^{\phi\phi\phi\phi}_{1121} & m_H^{(2)\,2} + \lambda_{SM} v^2 \mathcal{I}^{\phi\phi\phi\phi}_{1122} & \frac{gv}{2c^{\psi}}\left(\mathcal{I}^{\phi\phi' S}_{12\bar{1}} - \mathcal{I}^{\phi\phi' S}_{21\bar{1}}\right) & -\frac{gv}{2}c^{\theta}\left(\mathcal{I}^{\phi\phi' S}_{12\bar{\bar{1}}} - \mathcal{I}^{\phi\phi' S}_{21\bar{\bar{1}}}\right) & \ldots \\ 0 & \frac{gv}{2c^{\psi}}\left(\mathcal{I}^{\phi\phi' S}_{12\bar{1}} - \mathcal{I}^{\phi\phi' S}_{21\bar{1}}\right) & \frac{g^2v^2}{4c^{\psi\,2}}\mathcal{I}^{\phi\phi SS}_{11\bar{1}\bar{1}} & -\frac{g^2v^2c^{\theta}}{4c^{\psi}}\mathcal{I}^{\phi\phi SS}_{11\bar{1}\bar{\bar{1}}} & \ldots \\ 0 & -\frac{gv}{2}c^{\theta}\left(\mathcal{I}^{\phi\phi' S}_{12\bar{\bar{1}}} - \mathcal{I}^{\phi\phi' S}_{21\bar{\bar{1}}}\right) & -\frac{g^2v^2c^{\theta}}{4c^{\psi}}\mathcal{I}^{\phi\phi SS}_{11\bar{\bar{1}}\bar{1}} & \frac{g^2v^2}{4}c^{\theta\,2}\mathcal{I}^{\phi\phi SS}_{11\bar{\bar{1}}\bar{\bar{1}}} & \ldots \\ \vdots & \vdots & \vdots & \vdots & \ddots \end{pmatrix} \tag{3.54}$$

and we have introduced the shorthands

$$\cos\psi(\phi) \equiv c^{\psi(\phi)},$$
$$\sin\psi(\phi) \equiv s^{\psi(\phi)}. \tag{3.55}$$

Although we do not explicitly diagonalise these matrices we note that, due to the mixing between the gauge scalars of the left and right-handed sectors, diagonalisation of each of the above matrices will give *two* distinct towers of mass eigenstates with a small mass splitting between the two at each KK level [5].

3.2.3 Unphysical Scalars

As discussed in section 3.2.1, in an universal extra-dimensional model the scalar DOFs "eaten" by the heavy vector modes are no longer simply the modes of the corresponding gauge scalar mode, but are in fact an admixture of the full tower of gauge scalar and WGB modes. In order to find this unphysical admixture we must diagonalise the mass matrices containing mass terms proportional to the gauge fixing parameters ξ_a, i.e. the unphysical scalar masses of the theory. By definition all of these unphysical mass terms originate from the gauge fixing sector of our model,

$$\mathcal{L}_{\text{Gauge Fixing}} \supset \sum_{n,m=1}^{\infty} -\frac{\xi_a}{2}\Big(m_V^{a\,(n)\,2} W_5^{(n)\,a} W_5^{(n)\,a\,\dagger} + g^2 v^2 \mathcal{I}^{\phi\phi\phi\phi}_{11nm} \left(F^T F\right)_{ij} \phi^{i\,(n)} \phi^{j\,(m)\,\dagger}$$
$$+ 2\, g v\, m_V^{a\,(n)} \mathcal{I}^{\phi\phi V^a}_{1nm} F_i^a \phi^{i\,(n)} W_5^{a\,(m)\,\dagger} \Big) - \frac{\xi_\gamma}{2}\left(m_V^{(n)\,2} A_5^{(n)} A_5^{(n)} \right), \tag{3.56}$$

where again there is an implied sum over the indices a and i.

[5] See reference [40] for the equivalent analysis of the corresponding vector modes

We note the apparently anomalous appearance of the gauge KK mass and vector mode bulk profile in the term mixing the gauge scalar and WGB modes. This is due to the rewriting of the overlap integral appearing in the original form of the term, using the identity

$$\partial_5 \left(e^{-2ky} f_S^{(n)}(y) \right) = m_V^{(n)} f_\mu^{(n)}(y). \tag{3.57}$$

We now define the unphysical analogues of $\Phi^\pm$ and Φ^0

$$\mathcal{W}_5^\pm = \left(\phi^{\pm\,(1)}, \quad \phi^{\pm\,(2)}, \quad W_{L\,5}^{\pm\,(1)}, \quad W_{R\,5}^{\pm\,(1)}, \quad \ldots \right)^T, \tag{3.58}$$

$$\mathcal{Z}_5 = \left(\phi^{0\,(1)}, \quad \phi^{0\,(2)}, \quad Z_5^{(1)}, \quad Z_{X\,5}^{(1)}, \quad \ldots \right)^T, \tag{3.59}$$

$$\mathcal{A}_5 = \left(A_5^{(1)}, \quad A_5^{(2)}, \quad A_5^{(3)}, \quad \ldots \right)^T, \tag{3.60}$$

in terms of which the mass terms of (3.56) can be expressed succinctly as

$$\mathcal{L}_{\text{Gauge Fixing}} \supset -\frac{\xi_Z}{2} \mathcal{Z}_5^T M_{\xi_Z}^2 \mathcal{Z}_5 - \frac{\xi_\gamma}{2} \mathcal{A}_5^T M_{\xi_\gamma}^2 \mathcal{A}_5 - \xi_W W_5^{+\,T} M_{\xi_W}^2 W_5^- \tag{3.61}$$

and where the mass matrices are of the form

$$M_{\xi_W}^2 = \begin{pmatrix} \frac{g^2v^2}{2}\mathcal{I}_{1111}^{\phi\phi\phi\phi} & \frac{g^2v^2}{2}\mathcal{I}_{1121}^{\phi\phi\phi\phi} & -m_V^{(1)}\frac{gv}{2}\mathcal{I}_{11\bar{1}}^{\phi\phi S} & \tilde{m}_V^{(1)}\frac{gv}{2}\mathcal{I}_{11\bar{\tilde{1}}}^{\phi\phi S} & \ldots \\ \frac{g^2v^2}{2}\mathcal{I}_{1121}^{\phi\phi\phi\phi} & \frac{g^2v^2}{2}\mathcal{I}_{1122}^{\phi\phi\phi\phi} & -m_V^{(1)}\frac{gv}{2}\mathcal{I}_{12\bar{1}}^{\phi\phi S} & \tilde{m}_V^{(1)}\frac{gv}{2}\mathcal{I}_{12\bar{\tilde{1}}}^{\phi\phi S} & \ldots \\ -m_V^{(1)}\frac{gv}{2}\mathcal{I}_{11\bar{1}}^{\phi\phi S} & -m_V^{(1)}\frac{gv}{2}\mathcal{I}_{12\bar{1}}^{\phi\phi S} & m_V^{(1)\,2} & 0 & \ldots \\ \tilde{m}_V^{(1)}\frac{gv}{2}\mathcal{I}_{11\bar{\tilde{1}}}^{\phi\phi S} & \tilde{m}_V^{(1)}\frac{gv}{2}\mathcal{I}_{12\bar{\tilde{1}}}^{\phi\phi S} & 0 & \tilde{m}_V^{(1)\,2} & \ldots \\ \vdots & \vdots & \vdots & \vdots & \ddots \end{pmatrix}, \tag{3.62}$$

$$M^2_{\xi_z} = \begin{pmatrix} \frac{g^2v^2}{4}\left(1/c^{\psi\,2}+c^{\phi\,2}\right)\mathcal{I}^{\phi\phi\phi\phi}_{1111} & \frac{g^2v^2}{4}\left(1/c^{\psi\,2}+c^{\phi\,2}\right)\mathcal{I}^{\phi\phi\phi\phi}_{1121} & -m_V^{(1)}\frac{gv}{2c^\psi}\mathcal{I}^{\phi\phi S}_{11\bar{1}} & \tilde{m}_1\frac{gv}{2}c^\theta\mathcal{I}^{\phi\phi S}_{11\bar{\tilde{1}}} & \\ \frac{g^2v^2}{4}\left(1/c^{\psi\,2}+c^{\phi\,2}\right)\mathcal{I}^{\phi\phi\phi\phi}_{1121} & \frac{g^2v^2}{4}\left(1/c^{\psi\,2}+c^{\phi\,2}\right)\mathcal{I}^{\phi\phi\phi\phi}_{1122} & -m_V^{(1)}\frac{gv}{2c^\psi}\mathcal{I}^{\phi\phi S}_{12\bar{1}} & \tilde{m}_V^{(1)}\frac{gv}{2}c^\theta\mathcal{I}^{\phi\phi S}_{12\bar{\tilde{1}}} & \dots \\ -m_V^{(1)}\frac{gv}{2c^\psi}\mathcal{I}^{\phi\phi S}_{11\bar{1}} & -m_V^{(1)}\frac{gv}{2c^\psi}\mathcal{I}^{\phi\phi S}_{12\bar{1}} & m_V^{(1)\,2} & 0 & \dots \\ \tilde{m}_V^{(1)}\frac{gv}{2}c^\theta\mathcal{I}^{\phi\phi S}_{11\bar{\tilde{1}}} & \tilde{m}_V^{(1)}\frac{gv}{2}c^\theta\mathcal{I}^{\phi\phi S}_{12\bar{\tilde{1}}} & 0 & \tilde{m}_V^{(1)\,2} & \dots \\ \vdots & \vdots & \vdots & \vdots & \ddots \end{pmatrix}. \tag{3.63}$$

Due to the unbroken nature of the $U(1)_{EM}$ gauge symmetry, the mass matrix of the scalar photon modes is diagonal,

$$M^2_{\xi_\gamma} = diag\left(m_V^{(1)\,2},\ \ m_V^{(2)\,2},\ \ m_V^{(3)\,2},\ \ \ldots\right). \tag{3.64}$$

3.2.4 The Physical Higgs

For completeness we also give the mass matrix associated with the modes of the physical Higgs field $h(x,y)$. The mass terms which make up this matrix arise from three sources: the $n=1$ mode obtains the analogue of the SM Higgs mass as a result of SSB, the KK decomposition of the Higgs provides all modes with the usual TeV scale KK masses and quadratic couplings in which two modes are tachyonic provide additional mass terms which mix the higher KK modes,

$$\mathcal{L}_{\text{Higgs}} \supset -\lambda_{SM}\frac{3v^2}{2}\left[h^{(n)}h^{(m)}\mathcal{I}^{\phi\phi\phi\phi}_{11nm}\right], \tag{3.65}$$

where the index combination $n=m=1$ is not included in the above summation.

Again we are able to write these three sets of mass terms in the succinct form

$$\mathcal{L}_{\text{Higgs}} \supset -\frac{1}{2}\mathcal{H}^T M_H^2 \mathcal{H}, \tag{3.66}$$

where the infinite matrix is simply

$$\mathcal{H} = \left(h^{(1)}, \quad h^{(2)}, \quad h^{(3)}, \quad \ldots \right)^T \tag{3.67}$$

and the mass matrix is

$$M_H^2 = \begin{pmatrix} m_h^2 & 3\lambda_{SM} v^2 \mathcal{I}_{1121}^{\phi\phi\phi\phi} & 3\lambda_{SM} v^2 \mathcal{I}_{1131}^{\phi\phi\phi\phi} & \ldots \\ 3\lambda_{SM} v^2 \mathcal{I}_{1121}^{\phi\phi\phi\phi} & \left(m_H^{(2)} \right)^2 + 3\lambda_{SM} v^2 \mathcal{I}_{1122}^{\phi\phi\phi\phi} & 3\lambda_{SM} v^2 \mathcal{I}_{1132}^{\phi\phi\phi\phi} & \ldots \\ 3\lambda_{SM} v^2 \mathcal{I}_{1131}^{\phi\phi\phi\phi} & 3\lambda_{SM} v^2 \mathcal{I}_{1132}^{\phi\phi\phi\phi} & \left(m_H^{(3)} \right)^2 + 3\lambda_{SM} v^2 \mathcal{I}_{1133}^{\phi\phi\phi\phi} & \ldots \\ \vdots & \vdots & \vdots & \ddots \end{pmatrix} \tag{3.68}$$

The analogue of the SM Higgs mass is defined as $m_h = \sqrt{2} m_H^{(1)}$.

3.3 Feynman Rules

In appendix B we give a complete list of the vertex factors for interactions between scalar DOFs and vector or fermionic modes within the UCRS model. Some notes on the conventions used in deriving the vertex factors and also some general simplifications required to express the large number of couplings in an efficient manner are necessary:

- Due to the complicated nature of the scalar mass matrices listed in the previous section it is sensible to use a semi-mass-insertion approximation, whereby we treat the weak scale masses originating from the SSB procedure as perturbations of the KK reduced theory. Practically this means that the propagator associated with any internal line will simply have a KK mass in the denominator. In the name of consistency we have adopted this approach for all of the fields which appear in our model.

- The vector nature of the higher fermionic KK modes means that for interactions involving two heavy fermionic fields there are two possible chiral combinations the vertex factors of which differ only in the overlap integral which appears. To halve the number of Feynman rules we simply give one of the chiral combinations plus the replacements which must be made in the overlap integrals in order to obtain the alternative combination. Those replacements are:
  - Exchange all right-handed fermionic profiles for left-handed ones and vice versa ($L \leftrightarrow R$)
  - Unbar any associated fermionic index which is initially bared and bar any which is initially unbarred ($n \leftrightarrow \bar{n}$)
- We have stated the vertex factors for the quark sector of our model only. The equivalent couplings of the leptonic sector can be found by making the following substitutions in the vertex factors stated

$$\begin{aligned} u &\rightarrow \nu, \\ d &\rightarrow l. \end{aligned} \tag{3.69}$$

- In order to remove any ambiguity over the range of the indices appearing in the stated Feynman rules, we have chosen to state the interactions of zero modes separately from those of heavy KK modes modes. This allows us to state that all indices appearing in appendix B start from $n = 1$.
- We have reduced the degree of unnecessary repetition of vertex factors by only listing one of the two possible zero/heavy mode interactions arising from couplings containing two fields with $(+,+)$ BCs. The vertex factors for these 'missing' couplings can be found from the corresponding stated vertex factor

by making the obvious index change in the associated overlap integral. We give as an example of this procedure

$$\begin{aligned} &\text{Stated} && \bar{q}_L^{u\,(n)} u_R^{(0)} \phi^{0\,(k)} : && -Y^u \times \mathcal{I}_{n0k}^{L^1 R^2 \phi}, \\ &\text{Unstated} && \bar{q}_L^{u\,(0)} u_R^{(m)} \phi^{0\,(k)} : && -Y^u \times \mathcal{I}_{0mk}^{L^1 R^2 \phi}. \end{aligned} \tag{3.70}$$

Chapter 4

Tree-level Contributions to S and T

4.1 Preliminaries

Given that the original motivation for the RS model was to provide a solution to the HP it could be argued that the most important parameter of the theory to constrain is M_{KK}. As has already been mentioned, two of the most stringent constraints on this parameter come from the EW oblique parameters S and T ($U = 0$ in both the standard RS and UCRS models [9] and will therefore be discussed no further in this thesis), which in terms of SM vacuum polarisations are defined as [7]

$$\alpha T = \frac{e^2}{s_W^2 c_W^2 m_Z^2} \left[\Pi_{11}(0) - \Pi_{33}(0)\right], \tag{4.1}$$

$$\alpha S = 4e^2 \left[\Pi'_{33}(0) - \Pi'_{3Q}(0)\right], \tag{4.2}$$

where $\alpha = e^2/4\pi$ is the electromagnetic fine structure constant, m_Z^2 is the mass of the SM Z boson, the primes indicate differentiation with respect to q^2 and $\Pi_{XY}\left(q^2\right)$ is the part of the vacuum polarisation proportional to the metric tensor,

$$\Pi_{XY}^{\mu\nu}\left(q^2\right) = g^{\mu\nu}\Pi_{XY}\left(q^2\right) + q^\mu q^\nu \Delta_{XY}\left(q^2\right), \tag{4.3}$$

where $XY = \{11, 22, 33, 3Q, QQ\}$. We also remind the reader that the mixing angle appearing in the above expression, $\sin\theta_W (s_W)$, is that between the neutral SM gauge bosons in the *physical basis* and is therefore not equal to the previously defined mixing angle, $\sin\psi$.

As is well known [9,26,31], within RS type models the leading order contributions to the S and T parameters appear at tree-level and arise from two distinct sources:

- *Oblique contributions*: from the standard corrections to the SM gauge boson propagators.

- *Universal non-oblique contributions*: from *universal* (independent of the fermion flavour) corrections to SM vector boson-fermion vertices

The presence of two distinct sources of tree-level contributions to the S and T parameters is due to our analysis being performed within the KK basis of the theory and the subsequent mixing between zero and heavy gauge modes induced by SSB. If we were to work within the mass basis of the theory both of these contributions would be included within the deviation of the masses of the lightest gauge boson modes and their SM equivalents (see references [9,52] for this alternative treatment). In order to avoid any confusion during the following calculation of S and T, a superscript of S will be used to indicate contributions arising from the standard oblique corrections while a superscript of U will be used to indicate contributions arising

from the universal non-oblique corrections,

$$T_{tree} = T^S + T^U, \qquad S_{tree} = S^S + S^U. \tag{4.4}$$

The calculations of the total tree-level contributions to S and T have previously been done for the case of the standard RS model [9–11, 19],

$$S_{standard} = \frac{2\pi v^2}{M_{KK}^2}\left(1 - \frac{1}{kL}\right), \qquad T_{standard} = \frac{\pi v^2}{2c_W^2 M_{KK}^2}\left(kL - \frac{1}{2kL}\right) \tag{4.5}$$

and also a non-universal custodial RS model (IR confined Higgs) [10, 31, 52],

$$S_{custodial} = \frac{2\pi v^2}{M_{KK}^2}\left(1 - \frac{1}{kL}\right), \qquad T_{custodial} = -\frac{\pi v^2}{4c_W^2 M_{KK}^2}\frac{1}{kL}, \tag{4.6}$$

from which the suppressive effect of the custodial symmetry on the contributions to the T parameter are clear. In reference [11] it has been shown that associated with such a suppression is a reduction in the predicted KK scale of the theory from $M_{KK} > 4\,TeV$ to $M_{KK} > 2.4\,TeV$ and where now the main constraint on M_{KK} comes from contributions to the S parameter.

In this chapter we will repeat the analysis of these papers for the case of the UCRS model with the aim of confirming that the custodial gauge symmetry has the same suppressive effect on contributions to the T parameter as in the non-universal case.

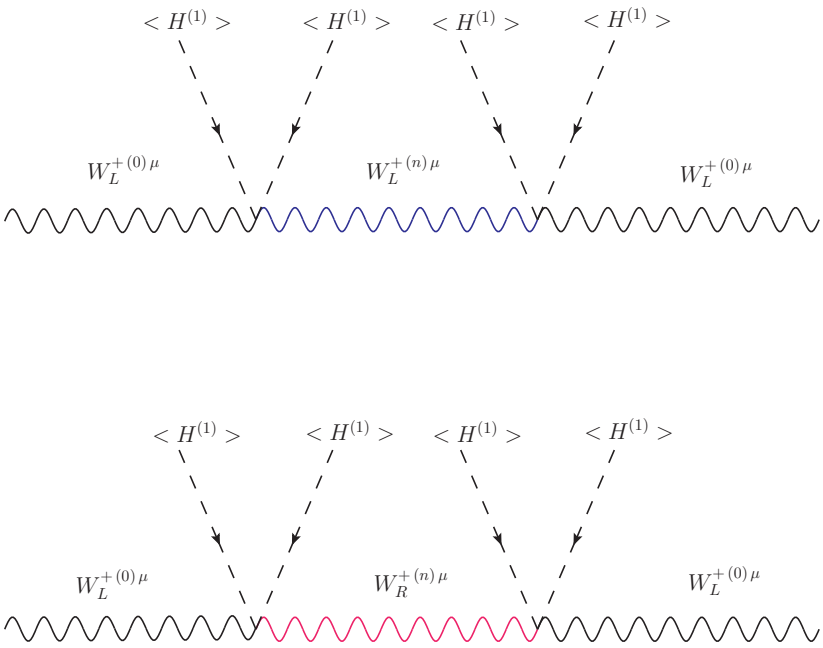

Figure 4.1: The leading order diagrams in ε which contribute at tree-level to the self-energy of the $W_L^{+\,(0)\,\mu}$ field.

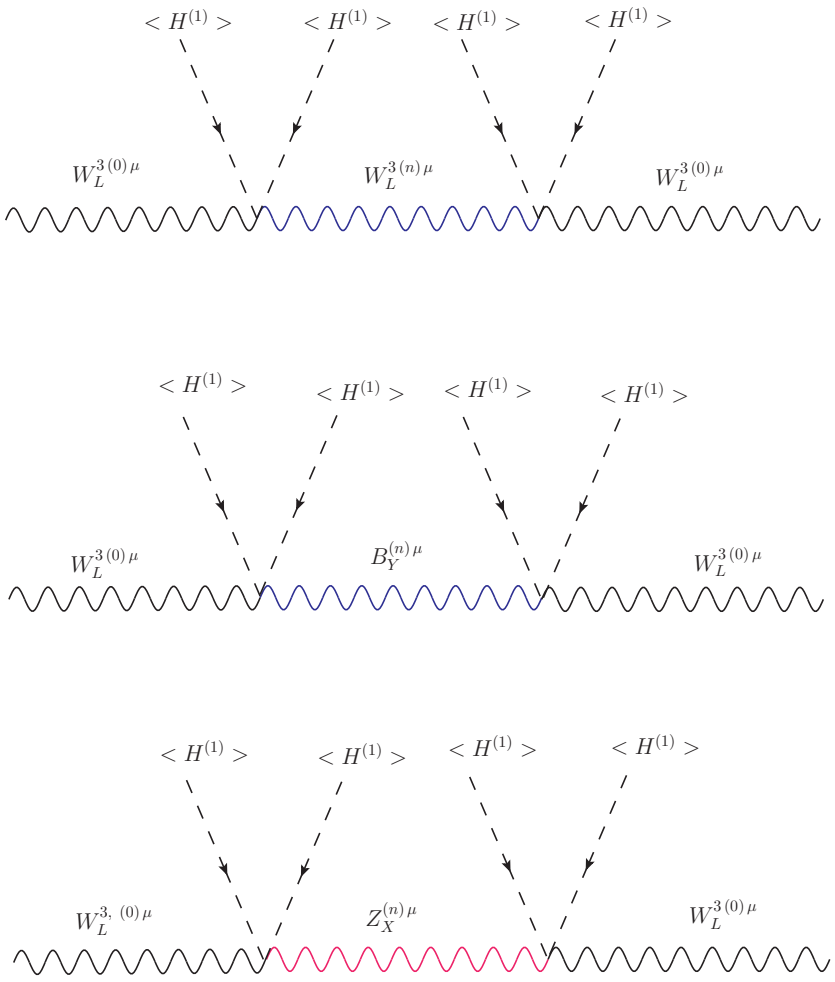

Figure 4.2: The leading order diagrams in ε which contribute at tree-level to the self-energy of the $W_L^{3\,(0)\,\mu}$ field. We note that we have written $W_R^{3\,(n)\,\mu}$ in terms of its admixture of fields with definite BCs.

4.2 Standard Oblique Contributions

4.2.1 T parameter

We now work through in detail the calculation of the oblique contributions of the T parameter. As we have chosen to work in the KK basis during our calculations the tree-level contributions we calculate are actually the *leading order* terms in an expansion in the small parameter $\varepsilon = v/M_{KK}$, or equivalently the number of mass insertions. These leading order contributions can themselves be written in terms of an expansion in powers of kL. During the calculations to follow we will also generally work to leading order in powers of kL, though in cases where cancellations occur between different contributions it may be necessary to include higher order terms in intermediate expressions.

The diagrams to be calculated are shown in figure 4.1 and 4.2, where we have used the identity

$$\Pi_{WW}(q^2) = \frac{e^2}{s_W^2}\Pi_{11}\left(q^2\right) \tag{4.7}$$

to work in terms of the charged vector boson's one-particle irreducible self-energy rather than the vacuum polarisations and have used (3.12) to write the W_R^3 field in terms of fields with definite BCs. This substitution allows us to properly define the two-particle gauge boson couplings, as well as more clearly illustrating the origins of the cancellations which occur in the contributions to the T parameter.

Feynman rules for vector boson mass insertions	
$\langle H^{(1)}\rangle\langle H^{(1)}\rangle\, W_L^{+\,(0)\,\mu} W_L^{-\,(n)\,\nu}$	$i\dfrac{g^2v^2}{4}\mathcal{I}_{110n}^{\phi\phi VV}\, g_{\mu\nu}$
$\langle H^{(1)}\rangle\langle H^{(1)}\rangle\, W_L^{+\,(0)\,\mu} W_R^{-\,(n)\,\nu}$	$-i\dfrac{g^2v^2}{4}\mathcal{I}_{110\widetilde{n}}^{\phi\phi VV}\, g_{\mu\nu}$
$\langle H^{(1)}\rangle\langle H^{(1)}\rangle\, W_R^{+\,(n)\,\mu} W_L^{-\,(0)\,\nu}$	$-i\dfrac{g^2v^2}{4}\mathcal{I}_{11\widetilde{n}0}^{\phi\phi VV}\, g_{\mu\nu}$
$\langle H^{(1)}\rangle\langle H^{(1)}\rangle\, W_L^{3\,(0)\,\mu} W_L^{3\,(n)\,\nu}$	$i\dfrac{g^2v^2}{4}\mathcal{I}_{110n}^{\phi\phi VV}\, g_{\mu\nu}$
$\langle H^{(1)}\rangle\langle H^{(1)}\rangle\, W_L^{3\,(0)\,\mu} B_Y^{(n)\,\nu}$	$-i\sin\phi\,\dfrac{g^2v^2}{4}\mathcal{I}_{110n}^{\phi\phi VV}\, g_{\mu\nu}$
$\langle H^{(1)}\rangle\langle H^{(1)}\rangle\, W_L^{3\,(0)\,\mu} Z_X^{(n)\,\nu}$	$-i\cos\phi\,\dfrac{g^2v^2}{4}\mathcal{I}_{110\widetilde{n}}^{\phi\phi VV}\, g_{\mu\nu}$

Table 4.1: A list of the Feynman rules associated with SSB induced vector boson mass insertions relevant to the calculation of the S and T parameters

Using the vertex factors for the two-particle gauge boson couplings shown in table

4.1 we are able to write down the amplitude of the diagrams shown in figure 4.1

$$
\begin{aligned}
i\Pi^{S}_{WW}\left(q^2\right) =& i\left(\frac{g^2v^2}{4}\right)^2 \frac{1}{L}\int_0^L dydy'\, e^{-2k(y+y')}\left(f_H^{(1)}\left(y\right)\right)^2\left(\frac{1}{L}\sum_{n=1}^{\infty}\frac{f_V^{(n)}(y)f_V^{(n)}(y')}{q^2-m_V^{(n)\,2}}\right) \\
& \times\left(f_H^{(1)}\left(y'\right)\right)^2 \\
& + i\left(\frac{g^2v^2}{4}\right)^2 \frac{1}{L}\int_0^L dydy'\, e^{-2k(y+y')}\left(f_H^{(1)}\left(y\right)\right)^2\left(\frac{1}{L}\sum_{n=1}^{\infty}\frac{\widetilde{f}_V^{(n)}(y)\widetilde{f}_V^{(n)}(y')}{q^2-\widetilde{m}_V^{(n)\,2}}\right) \\
& \times\left(f_H^{(1)}\left(y'\right)\right)^2, \qquad (4.8)
\end{aligned}
$$

where we have written explicitly the overlap integrals from the two-particle vertices and have substituted in the well known form of the zero mode vector bulk profile, $f_V^{(0)}\left(y\right)=1$. We note that, despite the KK spectrum of the W_L^+ field containing a zero mode the summation over the intermediate KK modes in the upper diagram of figure 4.1 starts at $n=1$ rather than $n=0$. This is due to the fact that the all orders sum of diagrams containing only zero mode vector bosons provide the propagators of the zero mode vector bosons with their SM masses and are therefore not relevant to our discussion of NP contributions to the SM gauge boson self-energies.

At first sight the above expression looks daunting, containing as it does two infinite sums over the KK modes of the right and left-handed charged vector boson fields. However, as can be guessed from the suggestive positioning of the summation signs, we are actually able to convert the summations above into a more readily evaluated form by identifying the terms in parenthesis as eigenvalue expansions of mixed coordinate position/momentum space 5D propagators [31]. In the case of the right-handed gauge field the summation above is equal to the full mixed space 5D

propagator, $\bar{G}_q^{-+}(y,y')$, while for the left-handed field, due to the absence of the $n=0$ term, the summation is equal to the full 5D propagator, $G_q^{++}(y,y')$, minus the propagator of the y independent zero mode propagator, $G_q^{(0)}$. Such a term is referred to as the subtracted 5D propagator and the absence of a zero mode is denoted using a bar, $\bar{G}_q^{++}(y,y')$.

Using these mixed coordinate propagators and equation (4.7) we are able to write the (11) vacuum polarisation as

$$\Pi_{11}^S(q^2) = \left(\frac{e^2v^2}{4s_W^2}\right)\left(\frac{v^2}{4}\right)\left(\delta_q^{(++)} + \delta_q^{(-+)}\right), \tag{4.9}$$

where we have introduced the following shorthand for the convolutions over the EXD

$$\delta_q^{(BC)} = \frac{1}{L}\int_0^L dydy' e^{-2k(y+y')}\left(f_H^{(1)}(y)\right)^2 \bar{G}_q^{(BC)}(y,y')\left(f_H^{(1)}(y')\right)^2. \tag{4.10}$$

Written in the same notation the (33) vacuum polarisation is of the form

$$\Pi_{33}^S\left(q^2\right) = \left(\frac{e^2v^2}{4s_W^2}\right)\left(\frac{v^2}{4}\right)\left\{\left(1+\sin^2\phi\right)\,\delta_q^{(+,+)} + \cos^2\phi\,\delta_q^{(-,+)}\right\}. \tag{4.11}$$

Substituting (4.9) and (4.11) into the definition for the T parameter above we find that the expression which we must evaluate is

$$T^S = -\frac{\pi}{c_W^2}\left(\delta_{q=0}^{(+,+)} - \delta_{q=0}^{(-,+)}\right). \tag{4.12}$$

In order to evaluate the convolution integrals appearing in (4.12) we first simplify the complicated combinations of Bessel functions which make up the general expressions for the mixed coordinate propagators (the derivation of which are shown in appendix C) by expanding around their arguments for small external momenta, retaining those terms independent of the small parameter q/k. The expanded 5D propagators which are used in the numerical evaluation of the convolution integral

are of the form

$$\bar{G}^{++}_{q=0}(y,y') = \frac{1}{4k\,(kL)}\left\{\frac{1-e^{2kL}}{kL} + e^{2ky_<}\,(1-2ky_<) + e^{2ky_>}\,[1+2k\,(L-y_>)]\right\}, \tag{4.13}$$

$$\bar{G}^{-+}_{q=0}(y,y') = -\frac{1}{2k}\left[e^{2ky_<}-1\right], \tag{4.14}$$

where $y_<(y_>)$ indicates the smaller (larger) of the two extra-dimensional coordinates appearing in expression (4.8).

In order to be able to compare (4.12) with the equivalent contributions derived in a non-universal custodial model it is necessary to derive an analytical form containing the dependence of T on M_{KK} and kL. Due to the Bessel function-like nature of the tachyonic Higgs profile this might not appear to be possible, however, if we make the phenomenologically backed assumption that the KK scale of the UCRS model is larger than the weak scale (and therefore $x_H^{(1)} < 1$) we find that even at its largest (at the point $y = L$) the argument of the tachyonic profile is less than one. As a result we are able to Taylor expand the tachyonic profile thereby obtaining an expression with a simple exponential dependence on the extra-dimensional coordinate, y, and allowing us to evaluate the convolution integrals appearing in (4.12) analytically. To first order in its argument the hyperbolic Bessel function $I_\nu\left(m_H^{(1)}e^{ky}/k\right)$ is

$$I_\nu \sim \frac{1}{2^{-\nu}\gamma_E\,(1+\nu)}\left(x_H^{(1)}e^{-kL}e^{ky}\right)^\nu. \tag{4.15}$$

where γ_E is the usual Euler-Mascheroni constant and ν is the the Bessel function order of the tachyonic Higgs profile defined below (2.59). Setting the bulk profile of the tachyonic Higgs mode to be (4.15) and substituting it into the orthonormality condition (2.57) we find that, given our initial assumption about the size of the KK

scale, the *normalised* bulk profile of the tachyonic Higgs mode can be approximated by the expression

$$e^{-ky}\chi_T(y) \sim \sqrt{2kL\,(1+\nu)}e^{-kL(1+\nu)}e^{ky(1+\nu)}. \tag{4.16}$$

Finally, substituting this expression into (4.12) and integrating over the extra-dimensional coordinates we obtain the following approximate expression for the T parameter

$$T^S \simeq -\frac{\pi}{2c_W^2}\frac{v^2}{M_{KK}^2}\left[\frac{(1+\nu)}{(2+\nu)}\left[1+\frac{1}{(2+\nu)}\right]-\frac{1}{2kL}+\mathcal{O}\left(1/\left(kL\right)^2\right)\right], \tag{4.17}$$

where the approximate equality signifies the fact that we have dropped from the expression those terms of the same order in kL which are exponentially suppressed relative to those stated.

4.2.2 S Parameter

As at tree-level $\Pi_{3Q}\left(0\right)=0$ the standard oblique contributions to the S parameter take the form,

$$S^S = 16\pi\left(\frac{e^2v^2}{4s_W^2}\right)\left(\frac{v^2}{4}\right)\left\{\left(1+\sin^2\phi\right)\delta_{q=0}^{(+,+)\prime}+\cos^2\phi\,\delta_{q=0}^{(-,+)\prime}\right\} \tag{4.18}$$

In order to evaluate this expression we must once more expand the general solutions of the 5D mixed coordinate propagators for the case of small external momentum squared, this time keeping all terms up to order $\left(q/k\right)^2$.

Performing the aforementioned expansion, again using our approximate expression for the Higgs profile to integrate over the two extra-dimensional coordinates and removing all exponentially suppressed terms we find that the oblique contribution to the S parameter are

$$S^S \simeq \frac{e^2}{c_W^2 s_W^2}\frac{v^4}{M_{KK}^4}\left\{\left(c_W^2\left[\left(\frac{1+\nu}{2+\nu}\right)^2-\frac{1}{2}\left(\frac{1+\nu}{3+\nu}\right)\right]+s_W^2\left[\frac{(1+\nu)^2}{(2+\nu)^3}\right]\right)kL+\mathcal{O}\left(1\right)\right\}. \tag{4.19}$$

The key feature of these contributions to S is that their leading term is $\mathcal{O}(\varepsilon^4)$. As we shall see such contributions are highly subdominant to those originating from the non-oblique sources discussed in the next section.

4.3 Universal Non-oblique Contributions

In this section we calculate the contributions to the S and T parameters originating from corrections to SM gauge-fermion vertices caused by mixing between vector boson KK modes (for example figure 4.3). Due to the different localisations of the fermionic zero modes in the EXD these corrections are generally dependent upon the flavour of fermion taking part in the interaction and are therefore by definition non-oblique in nature (and as such should not contribute to the oblique parameters). It can be shown, however, that although the full corrections to the couplings are dependent upon the flavour of fermion, every correction contains an *universal* correction which we are able to absorb into the oblique parameters [9, 31, 53, 54]. Due to the exponential UV localisation of the light fermion zero modes the bulk mass parameter dependent parts of their effective couplings to heavy gauge boson modes are exponentially suppressed relative to the universal contributions discussed above. This justifies our so far implicit assumption that the dominant NP contributions to the EWPOs are oblique (universal) in nature and means that in the remainder of this chapter we are able to ignore all non-universal contributions.

4.3.1 The Effective Action

For maximum transparency we have decided to make use of an effective action approach while discussing these non-oblique contributions to the S and T parameter.

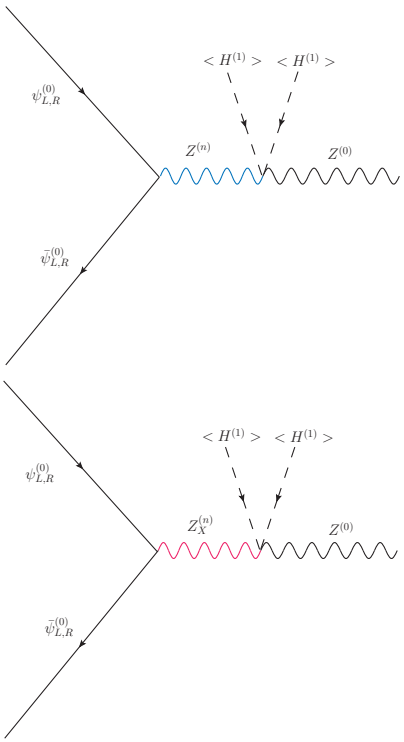

Figure 4.3: Corrections to the SM Z boson-fermion interactions resulting from the mixing induced by SSB. Here ψ stands for any of the SM fermions which can take part in such an interaction

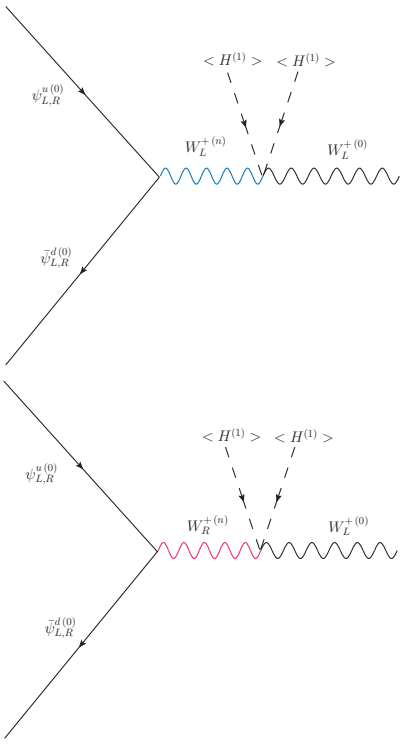

Figure 4.4: Corrections to the SM W^+ boson-fermion interactions resulting from the mixing induced by SSB. Here $\psi^{u,d}$ stands for any of the SM fermions which can take part in such an interaction

This approach parameterises the oblique corrections to the EWPOs in terms of a generic set of 'additional' (relative to the SM) operators [55]

$$\mathcal{L} = -\frac{(1+A)}{4}\hat{F}^{\mu\nu}\hat{F}_{\mu\nu} - \frac{(1+B)}{4}\hat{W}^{\mu\nu}\hat{W}_{\mu\nu} - \frac{(1+C)}{4}\hat{Z}^{\mu\nu}\hat{Z}_{\mu\nu} + \frac{(1+G)}{4}\hat{F}^{\mu\nu}\hat{Z}_{\mu\nu}$$

$$-(1+w)\tilde{m}_W^2\hat{W}_\mu^+\hat{W}^{\mu-} - \frac{(1+z)}{2}\tilde{m}_Z^2\hat{Z}_\mu\hat{Z}^\mu, \tag{4.20}$$

where the hats above the fields indicates that they are *not* canonically normalised and the tildes over the masses indicates that these are bare Lagrangian parameters. We note that as we are using the formalism of a low energy effective theory we work in terms of the vector bosons present in the SM *after* electroweak SSB and will therefore be calculating diagrams containing the Z boson rather than W_L^3.

In terms of the above coefficients the S and T parameters are defined as

$$\alpha S = 4s_W^2 c_W^2 \left(A - C - \frac{c_W^2 - s_W^2}{c_W s_W} G \right), \tag{4.21}$$

$$\alpha T = w - z. \tag{4.22}$$

The task is now to match the generic effective Lagrangian above to the low energy effective Lagrangian of the UCRS model.

4.3.2 Coefficient Calculation

The ultimate aim of this section is to absorb the universal part of the non-oblique corrections into a redefinition of the gauge boson fields and to calculate the contributions to the effective Lagrangian coefficients resulting from this redefinition.

Including the tree-level corrections to gauge-fermion vertices from zero-KK gauge

boson mixing, the neutral and charged current sector of our model looks like

$$\mathcal{L}_{NC} = \frac{e}{s_W c_W} Z_\mu \sum_{\psi^{(0)}_{L,R}} \left\{ \bar{\psi}^{(0)}_L \gamma^\mu \left(T^3_L - s^2_W Q \right) \psi^{(0)}_L \left[1 + \frac{e^2 v^2}{4 s^2_W c^2_W} \mathcal{G}^{(00)_L}_{q=0} \right] \right.$$

$$\left. - \frac{e^2 v^2}{4 s^2_W c^2_W} \bar{\psi}^{(0)}_L \gamma^\mu \left(c^2_W T^3_R + s^2_W T^3_L - s^2_W Q \right) \psi^{(0)} \widetilde{\mathcal{G}}^{(00)_L}_{q=0} \right\} + L \to R, \tag{4.23}$$

$$\mathcal{L}_{CC} = \frac{e}{\sqrt{2} s_W} W^+_\mu \sum_{\psi^{(0)}_L} \left\{ \bar{\psi}^{(0)}_L \gamma^\mu T^+_L \psi^{(0)}_L \left[1 + \frac{e^2 v^2}{4 s^2_W} \mathcal{G}^{(00)_L}_{q=0} \right] \right\} + \text{H.c.}, \tag{4.24}$$

where the summations are over all relevant fermionic zero modes present in our model and the left-right exchange in the neutral current indicates the right-handed equivalents to the left-handed terms stated (only the fermionic profile in the convolution integral will distinguish the couplings of the two chiralities). The new convolution shorthand [1] is defined as

$$\mathcal{G}^{(nm)_{L(R)}}_q = \frac{1}{L} \int_0^L dy dy' \, e^{ky} f^{(n)}_{L(R)}(y) f^{(m)}_{L(R)}(y) \; \bar{G}^{BC}_q(y, y') e^{-2ky'} \left(f^{(1)}_H(y') \right)^2 \tag{4.25}$$

and we have used the now familiar tilde notation to indicate the BC obeyed by the 5D mixed propagator appearing in the integral. We also note that the above integral is not symmetric in the two extra-dimensional coordinates. After numerical investigations we found that the difference between the two choices is small and so have, based upon the relative localisations of the fermionic and Higgs fields, chosen

[1] We note the differences between the definition of the convolution shorthands used above and those used in reference [26]. As earlier in our discussions the differences arise due to the different KK decompositions used, particularly in this case the absorption of a factor of e^{ky} into the fermion zero-mode. See the appendix in the aforementioned paper for details

to take the coordinate associated with the fermionic field to be the smaller of the two appearing in (4.25).

We now use the explicit forms of the fermionic zero modes, (2.47), and the mixed propagators, (C.18,C.20), as well as the orthonormality condition of the Higgs field, (2.57), to separate the universal part of the convolution integrals from the c dependent parts

$$\mathcal{G}_{q=0}^{(00)_{L(R)}} = \mathcal{G}_{universal} + \frac{1}{4k^2}\frac{e^{2kL}}{(1-e^{(2c^\psi \mp 1)kL})}\frac{(1\mp 2c^\psi)}{(3\mp 2c^\psi)}\left[-2kL + \frac{(5\mp 2c^\psi)}{(3\mp 2c^\psi)}\right], \quad (4.26)$$

$$\widetilde{\mathcal{G}}_{q=0}^{(00)_{L(R)}} = -\frac{1}{2k^2}\frac{(1\mp 2c^\psi)kL}{\left(1-e^{(2c^\psi \mp 1)kL}\right)(3\mp 2c^\psi)}, \quad (4.27)$$

where the left-handed (right-handed) integral is associated with the upper (lower) sign choices and the universal contribution is of the form

$$\mathcal{G}_{universal} = \frac{1}{4k(kL)}\int_0^L dy'\, e^{-2ky'}\left(f_H^{(1)}(y')\right)^2\left\{\frac{1-e^{2kL}}{kL} + e^{2ky'}(1+(L-y'))\right\}. \quad (4.28)$$

The field redefinitions necessary to restore the canonical form of the SM gauge-fermion interactions (assuming, for the reasons previously stated, that the non-universal contributions are negligible) are therefore

$$Z_\mu \to Z_\mu\left(1 - \frac{e^2v^2}{4s_W^2c_W^2}\mathcal{G}_{universal}\right), \quad (4.29)$$

$$W_\mu^+ \to W_\mu^+\left(1 - \frac{e^2v^2}{4s_W^2}\mathcal{G}_{universal}\right). \quad (4.30)$$

Substituting these field redefinitions into our low energy effective action the mass

terms of the electroweak gauge bosons now take the form

$$\mathcal{L}_{gauge} \supset m_W^2 \left(1 + \frac{\Pi_{WW}^S(0)}{m_W^2}\right)\left(1 - \frac{e^2v^2}{2s_W^2}\mathcal{G}_{universal}\right) W_\mu^+ W^{-\,\mu} \\ + m_Z^2 \left(1 + \frac{\Pi_{ZZ}^S(0)}{m_Z^2}\right)\left(1 - \frac{e^2v^2}{2s_W^2c_W^2}\mathcal{G}_{universal}\right) Z_\mu Z^\mu, \tag{4.31}$$

where of course the first set of parentheses contain the standard oblique corrections to the SM W and Z propagators previously calculated. Again making use of the fact that all NP corrections to EWPO must be small, we are able to read off the coefficients

$$w = \frac{\Pi_{WW}^S(0)}{m_W^2} - \frac{e^2v^2}{2s_W^2}\mathcal{G}_{universal}, \tag{4.32}$$

$$z = \frac{\Pi_{ZZ}^S(0)}{m_Z^2} - \frac{e^2v^2}{2s_W^2c_W^2}\mathcal{G}_{universal} \tag{4.33}$$

and therefore the T parameter

$$T^U = 2\pi\frac{v^2\mathcal{G}_{universal}}{c_W^2}. \tag{4.34}$$

Using the same approach as was taken for the oblique contributions we derive the approximate analytical expression,

$$T^U \simeq \frac{\pi}{2c_W^2}\frac{v^2}{M_{KK}^2}\left\{\frac{(1+\nu)}{(2+\nu)}\left[1 + \frac{1}{(2+\nu)}\right] - \frac{1}{kL} + \mathcal{O}\left(1/(kL)^2\right)\right\} \tag{4.35}$$

To leading order this expression is equal and opposite to the equivalent expression for the standard oblique contributions. Combining (4.35) with (4.17) we obtain the following expression for the total tree-level contribution to the T parameter

$$T_{tree} \simeq -\frac{\pi v^2}{4c_W^2 M_{KK}^2}\left\{\frac{1}{kL} + \mathcal{O}\left(1/\left(kL\right)^2\right)\right\}. \tag{4.36}$$

We note that to leading order this expression is identical to that derived within the framework of the non-universal custodial RS model, (4.6).

We finally plot the M_{KK} dependence of T_{tree} on the same axes as the current experimental limit on T at the 95% confidence level,

$$-0.09 < T_{exp} < 0.23, \tag{4.37}$$

which we have obtained from the values of T calculated from the experimentally measured electroweak observables assuming a Higgs mass of $m_h = 117\,GeV$ [56]

$$T_{exp} = 0.07 \pm 0.08. \tag{4.38}$$

We find the resulting plot, figure 4.5, in agreement with the literature, showing as it does the weakness of the constraint placed on M_{KK} by the tree-level contributions to the T parameter.

We now finally look at the contributions to the S parameter from this non-oblique source. Making the field redefinitions shown in (4.30) in the kinetic terms of our effective Lagrangian we find that that the operator coefficient required to calculate the S parameter is

$$C = -\frac{e^2 v^2}{2 c_W^2 s_W^2} \mathcal{G}_{universal}. \tag{4.39}$$

Meaning that the S parameter is given by the expression

$$S^U = 8\pi v^2 \mathcal{G}_{universal}, \tag{4.40}$$

or approximately

$$S^U \simeq 2\pi \frac{v^2}{M_{KK}^2} \left\{ \frac{(1+\nu)}{(2+\nu)} \left[1 + \frac{1}{(2+\nu)} \right] - \frac{1}{kL} + \mathcal{O}\left(1/\left(kL\right)^2\right) \right\}. \tag{4.41}$$

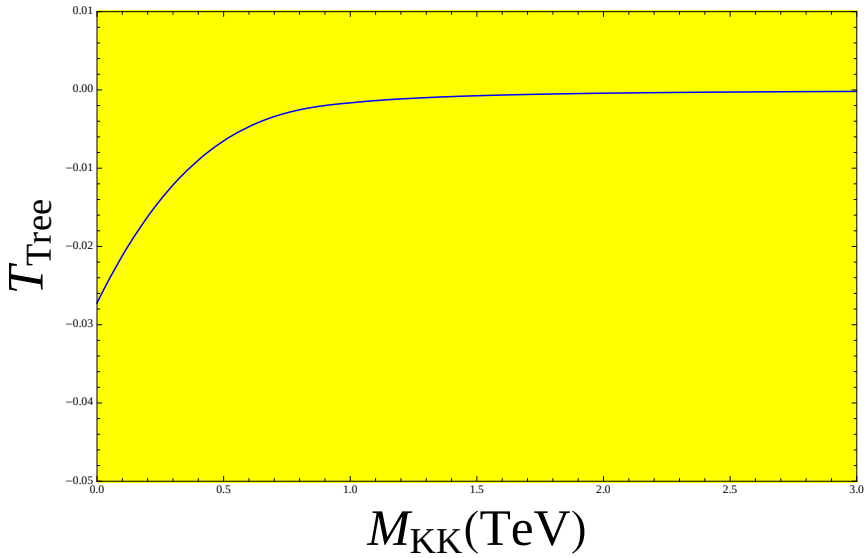

Figure 4.5: The M_{KK} dependence of the tree-level contributions to T in the UCRS model. The yellow band is the current experimental limit on T at 95% confidence level obtained using a Higgs mass of $m_h = 117\,GeV$ [56].

As noted below (4.19), this term is only $\mathcal{O}(\varepsilon^2)$ and is therefore extremely dominant over the oblique contributions. As a result we simply state that to leading order in ε

$$S_{tree} \simeq S^U. \tag{4.42}$$

Although this expression is not identical to the non-universal case we observe that the contributions to S in the UCRS model and non-universal models occur at the same order in the kL expansion. Using the values for the Higgs potential parameters stated in (3.23), we find that the tree-level contributions to S are predicted to differ between the universal and non-universal cases by a factor of ~ 0.9.

We finally wish to compare these tree-level contributions with the current experimental limit on S at the 95% confidence level

$$-0.06 < S_{exp} < 0.12 \tag{4.43}$$

which we have again calculated from the current value of S calculated from experimentally measured electroweak observables [56]

$$S = 0.03 \pm 0.09, \tag{4.44}$$

where of course the assumed value of the Higgs mass was the same as that used in the calculation of the T parameter, $m_h = 117\,GeV$. The resulting plot is shown in figure 4.6.

From figures 4.5 and 4.6 we can conclude that at tree-level the S parameter places a constraint on the M_{KK} of the UCRS model many times stronger than that resulting from the tree-level contributions to T. This is in line with the well known results from considerations of the non-universal custodial RS model, (4.6), and is evidence of the effectiveness of the gauged custodial symmetry in suppressing the tree-level contributions to T.

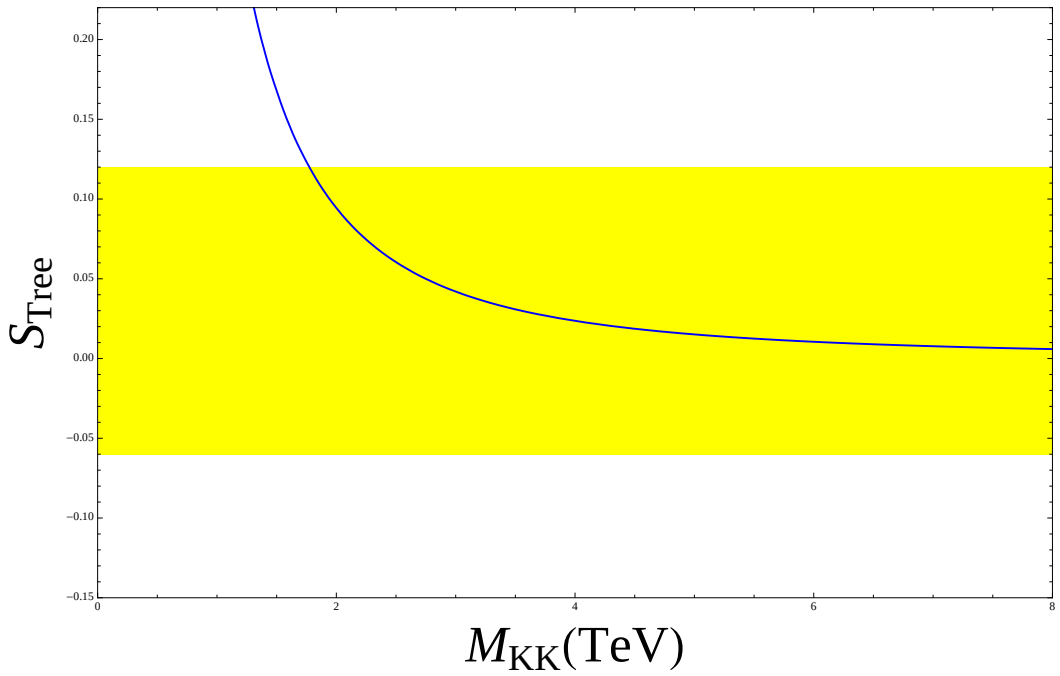

Figure 4.6: The M_{KK} dependence of the tree-level contributions to S in the UCRS model. The yellow band is the current experimental limit on S at 95% confidence level obtained using a Higgs mass of $m_h = 117\,GeV$ [56]

Chapter 5

Fermionic Loop Contributions to T

We now consider the contributions to T from loops containing fermionic modes. Given that the T parameter is effectively a measure of custodial symmetry breaking, we recognise that of all the fermionic one-loop contributions to the SM vacuum polarisations possible within the UCRS framework contributions to T will arise only from diagrams containing at least one of two sources of custodial symmetry breaking:

1. Yukawa mass insertions on the fermionic propagators present in the loop.
2. Mixing between the SM gauge bosons and the heavy modes of their $SU(2)_R$ analogues, accompanied by *right-handed* (as in $SU(2)_R$) fermionic currents.

To lowest order in ε the diagrams contributing to T contain only one of the two aforementioned sources of custodial symmetry breaking allowing us to unambiguously refer to Yukawa and gauge boson-mixing (GBM) contributions to T. Examples of these two distinct contributions are shown in figure 5.3 and figures 5.1 and 5.2 respectively.

In references [31] and [26] the leading order contributions to T from both of these sources were considered. In these papers it was argued that as the unbroken *bulk* cus-

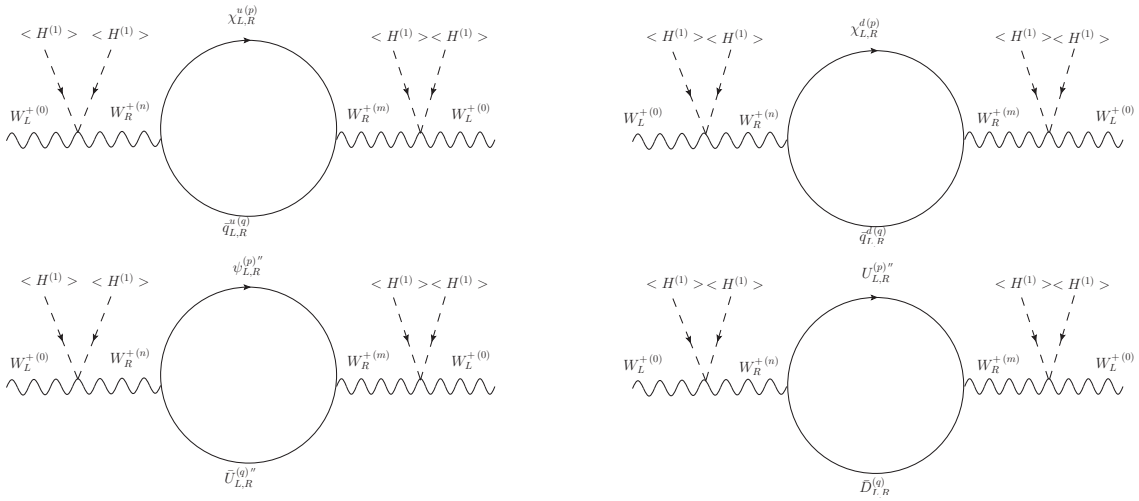

Figure 5.1: The contributions to $\Pi_{WW}\left(q^2\right)$ *from diagrams containing mixing between right and left-handed gauge bosons and a loop containing two quark KK modes with no Yukawa insertions. In addition to these diagrams the equivalent set of diagrams containing leptons also make contributions to the T parameter. Note that for loops containing fermionic zero modes only one of the two stated chiralities is possible.*

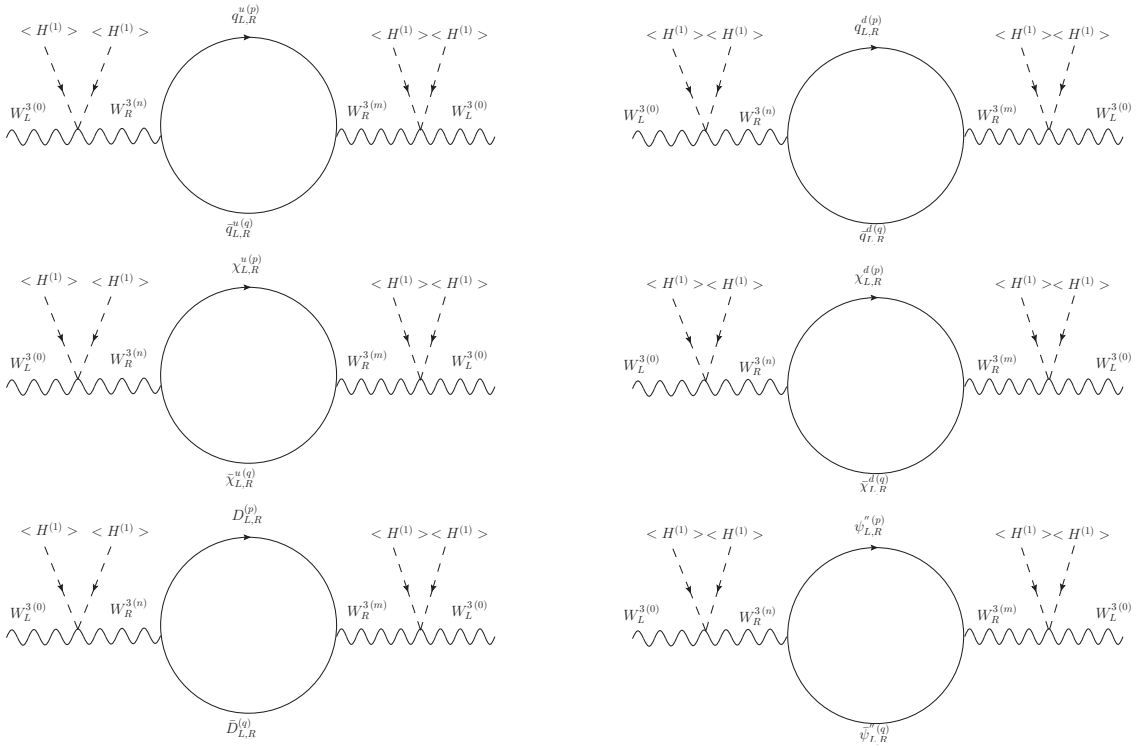

Figure 5.2: The contributions to $\Pi_{33}(q^2)$ from diagrams containing mixing between right and left-handed gauge bosons and a loop containing two quark KK modes with no Yukawa insertions. In addition to these diagrams, the equivalent set of diagrams containing leptons also make contributions to the T parameter. Note that for loops containing a fermionic zero mode only one of the two stated chiralities is possible.

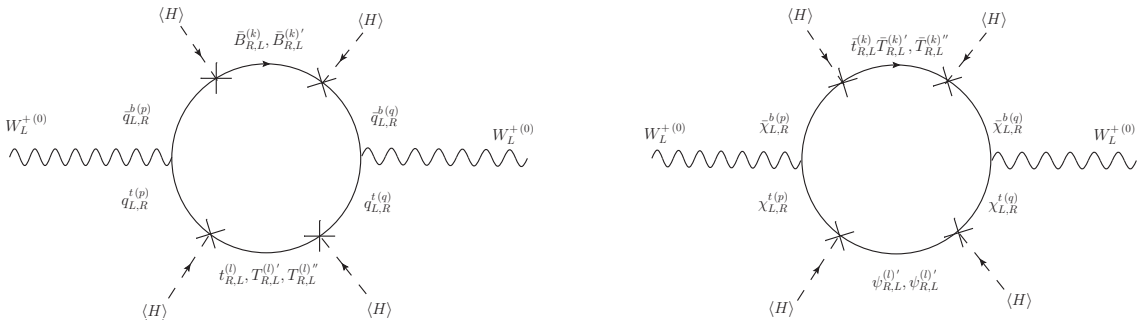

Figure 5.3: The contributions to $\Pi_{WW}\left(q^2\right)$ *from loop diagrams containing the third generation of quarks and four Yukawa mass insertions. We note that for diagrams containing fermionic zero modes there is only a single combination of quark chiralities possible (rather than the two possible for a diagram containing only heavy fermionic modes).*

todial symmetry of the UCRS model forbids any non-Planck scale suppressed counter terms with which to remove unwanted infinities, all individual KK loop contributions (contributions from 4D diagrams containing KK modes) to the T parameter must be UV finite and the sum over these contributions convergent. Following a simple estimation of the relative sizes of the two contributions, the Yukawa contributions were assumed to be dominant and were calculated in full, while the GBM contributions were considered no further. In this section, therefore, we will complete the detailed discussion of the contributions to T arising from fermionic loop diagrams by first attempting to directly verify the finiteness (or not) of the GBM contributions before subsequently providing a numerical analysis of the contributions arising from both fermionic bidoublets, $\xi_1^{q,l}$, and the *right-handed* triplets, $T_4^{q,l}$ (cf. (3.25) and (3.26)).

In order to simplify the following discussion it is useful to define shorthands for the two distinct GBM contributions,

$$T_B^{\psi} = \sum_{n,m=0}^{\infty} T_B^{(nm)}, \qquad T_T^{\psi} = \sum_{n,m=0}^{\infty} T_T^{(nm)}, \tag{5.1}$$

where the sum is over the KK modes of the two fermions which take part in the GBM diagrams and the subscript $B(T)$ refers to bidoublet (triplet).

Before starting the detailed discussion of the calculation of these contributions we note that although GBM diagrams containing all generations of quark and lepton can contribute to T we have found it convenient to explicitly calculate the GBM contributions to T from diagrams involving the third generation of quark only. All expressions appearing in the remainder of this chapter therefore refer to the contributions from these fields while all remaining contributions can be found from those expressions explicitly stated through simple substitution for the quantum numbers (QNs), masses and bulk fermionic mass parameters of the relevant fermionic field.

5.1 Bidoublet Contributions

In order to calculate the contribution to T_B^{ψ} from the third generation of quark we will need, in addition to the gauge boson two-particle interaction vertex factors given in table 4.1, the Feynman rules associated with vector-fermion interactions. Although we have not derived these rules as part of this thesis we can obtain the relevant vertex factors from the corresponding gauge scalar-fermion Feynman rules,

given in section B.2, by making the following replacements:

$$\begin{aligned} -i\gamma^5 \quad &\to \quad \gamma^\mu, \\ \bar{f}_S^{(n)}(y) \quad &\to \quad f_V^{(n)}(y), \\ \bar{\tilde{f}}_S^{(n)}(y) \quad &\to \quad \tilde{f}_V^{(n)}(y). \end{aligned} \tag{5.2}$$

Using these rules we are now able to write down the total contribution to the one-particle irreducible self-energy of the charged SM vector boson from diagrams of the type shown in the upper half of figure 5.1,

$$i\Big(\Pi_{WW}^{\mu\nu}\Big)_B^{\psi}(q^2) \supset 2 \sum_{\substack{n,m,p,q=1 \\ l=0}}^{\infty} \left(-i\frac{g^2v^2}{4}\right)^2 \left(\frac{g}{\sqrt{2}}\right)^2 \mathcal{I}^{\phi\phi VV}_{110\tilde{n}} \mathcal{I}^{\phi\phi VV}_{11\tilde{m}0} \left(\frac{-i}{q^2 - \widetilde{m}_V^{(n)\,2}}\right)$$

$$\times \left(\frac{-i}{q^2 - \widetilde{m}_V^{(m)\,2}}\right) \Bigg[\left(\mathcal{I}^{L^1L^1V}_{\tilde{p}l\tilde{n}} \mathcal{I}^{L^1L^1V}_{\tilde{p}l\tilde{m}}\right) \left(L^{\tilde{p}l}_{L^1L^1}\right)^{\mu\nu} + \left(\mathcal{I}^{R^1R^1V}_{\tilde{\bar{p}}\tilde{q}\tilde{n}} \mathcal{I}^{R^1R^1V}_{\tilde{\bar{p}}\tilde{q}\tilde{m}}\right) \left(L^{\tilde{p}q}_{R^1R^1}\right)^{\mu\nu}$$

$$+ \left(\mathcal{I}^{L^1L^1V}_{\tilde{p}q\tilde{n}} \mathcal{I}^{R^1R^1V}_{\tilde{\bar{p}}\tilde{q}\tilde{m}}\right) \left(L^{\tilde{p}q}_{L^1R^1}\right)^{\mu\nu} + \left(\mathcal{I}^{R^1R^1V}_{\tilde{\bar{p}}\tilde{q}\tilde{n}} \mathcal{I}^{L^1L^1V}_{\tilde{p}q\tilde{m}}\right) \left(L^{\tilde{p}q}_{R^1L^1}\right)^{\mu\nu} \Bigg], \tag{5.3}$$

where we have adopted the same notation to label the contributions to the self-energy as we have used for contributions to the T parameter, (5.1), and we have defined the loop-momentum integral shorthand

$$\left(L^{\tilde{p}q}_{L^a(R^a)L^a(R^a)}\right)^{\mu\nu} = -\int \frac{d^4k}{(2\pi)^4} Tr\left\{ i\gamma^\mu P_{L(R)} \frac{i}{\not{k} + \not{q} - \widetilde{m}^{(p)}_{\psi^a}} i\gamma^\nu P_{L(R)} \frac{i}{\not{k} - m^{(q)}_{\psi^a}} \right\} \tag{5.4}$$

with $P_{L,R}$ being the 4D fermionic projection operators,

$$P_{L,R} = \left(\frac{1 \pm \gamma_5}{2}\right). \tag{5.5}$$

We also draw the reader's attention to the fact that the mass spectrum of the q^t and q^b fields contain left-handed zero modes. We have therefore used different KK indices (l and q) for the right-handed and left-handed chiral modes of these fields to account for this difference in spectrum. We also note that due to the identical KK mass spectra of the up and down components of the two *left-handed* $SU(2)$ doublets, their separate contributions to the above expression can be combined into a single term.

It is also important to clarify the difference between the use of our tilde/bar notation in the loop integral shorthand defined in (5.4) and the previously defined overlap integrals. In the case of the loop momentum integral shorthand the tilde/bar above a given index indicates the BCs obeyed by the *left-handed* modes of the related fermionic field even if the mode appearing in the diagram associated with the integral is in fact *right-handed*. The reason for this slightly counterintuitive notation is to indicate clearly the fermionic masses appearing in a given loop integral, these being independent of the chirality of the mode appearing but instead determined (in our convention) by BCs of the *left-handed* modes.

The above form of the self-energy can immediately be simplified greatly by again making use of the 5D mixed coordinate propagator technique to evaluate the two sums over the vector boson KK modes. Applying this to both of the sums over gauge KK modes appearing in (5.3) enables us to obtain the following expression for the

(11) vacuum polarisation amplitude

$$i\Big(\Pi_{11}^{\mu\nu}(q^2)\Big)_B^{\psi} \supset \left(\frac{g^2v^2}{4}\right)^2 \sum_{\substack{p,q=1\\ l=0}}^{\infty} \Bigg[\left(\widetilde{\mathcal{G}}_q^{(\widetilde{p}l)_L}\widetilde{\mathcal{G}}_q^{(\widetilde{p}l)_L}\right)\left(L_{L^1L^1}^{\widetilde{p}l}\right)^{\mu\nu} + \left(\widetilde{\mathcal{G}}_q^{(\widetilde{\bar{p}}\bar{q})_R}\widetilde{\mathcal{G}}_q^{(\widetilde{\bar{p}}\bar{q})_R}\right)\left(L_{R^1R^1}^{\widetilde{p}q}\right)^{\mu\nu}$$

$$+ \left(\widetilde{\mathcal{G}}_q^{(\widetilde{p}q)_L}\widetilde{\mathcal{G}}_q^{(\widetilde{\bar{p}}\bar{q})_R}\right)\left(L_{L^1R^1}^{\widetilde{p}q}\right)^{\mu\nu} + \left(\widetilde{\mathcal{G}}_q^{(\widetilde{\bar{p}}\bar{q})_R}\widetilde{\mathcal{G}}_q^{(\widetilde{p}q)_L}\right)\left(L_{R^1L^1}^{\widetilde{p}q}\right)^{\mu\nu} \Bigg]. \tag{5.6}$$

In order to write down the contributions to $\Pi_{33}^{\mu\nu}(q^2)$ from the class of diagram shown in figure 5.2 it is convenient to again exchange the modes of the W_R^3 field for those of the B_Y and Z_X fields. Decomposing the total vacuum polarisation into the contributions involving different combinations of heavy B_Y (the diagram containing zero mode B_Y fields is a SM diagram and therefore can not contribute to T) and Z_X modes,

$$i\Big(\Pi_{33}^{\mu\nu}(q^2)\Big)_B^{\psi} = i\Bigg[\Big(\Pi_{Z_XZ_X}^{\mu\nu}(q^2)\Big)_B^{\psi} + \Big(\Pi_{B_YB_Y}^{\mu\nu}(q^2)\Big)_B^{\psi} + \Big(\Pi_{B_YZ_X}^{\mu\nu}(q^2)\Big)_B^{\psi}$$

$$+ \Big(\Pi_{Z_XB_Y}^{\mu\nu}(q^2)\Big)_B^{\psi}\Bigg], \tag{5.7}$$

where the individual expressions are of the form

$$i\Big(\Pi^{\mu\nu}_{Z_X Z_X}(q^2)\Big)^{\psi}_{B} \supset\ 2\sum_{\substack{p,q=1\\ l,k=0}}^{\infty}\left(\cos\phi\frac{g^2v^2}{4}\right)^2\left\{\left(\frac{1}{\cos\phi}\left[\frac{1}{2}-\frac{7}{6}\sin^2\phi\right]\right)^2\right.$$

$$\times\left[\left(\widetilde{\mathcal{G}}_q^{(\widetilde{p}\widetilde{q})_L}\widetilde{\mathcal{G}}_q^{(\widetilde{p}\widetilde{q})_L}\right)\left(L^{\widetilde{p}\widetilde{q}}_{L^1L^1}\right)^{\mu\nu}+\left(\widetilde{\mathcal{G}}_q^{(\bar{\widetilde{p}}\bar{\widetilde{q}})_R}\widetilde{\mathcal{G}}_q^{(\bar{\widetilde{p}}\bar{\widetilde{q}})_R}\right)\left(L^{\widetilde{p}\widetilde{q}}_{R^1R^1}\right)^{\mu\nu}\right.$$

$$\left.+\,2\left(\widetilde{\mathcal{G}}_q^{(\widetilde{p}\widetilde{q})_L}\widetilde{\mathcal{G}}_q^{(\bar{\widetilde{p}}\bar{\widetilde{q}})_R}\right)\left(L^{\widetilde{p}\widetilde{q}}_{L^1R^1}\right)^{\mu\nu}\right]$$

$$+\left(\frac{1}{\cos\phi}\left[-\frac{1}{2}-\frac{1}{6}\sin^2\phi\right]\right)^2\left[\left(\widetilde{\mathcal{G}}_q^{(lk)_L}\widetilde{\mathcal{G}}_q^{(lk)_L}\right)\left(L^{lk}_{L^1L^1}\right)^{\mu\nu}+\left(\widetilde{\mathcal{G}}_q^{(\bar{p}\bar{q})_R}\widetilde{\mathcal{G}}_q^{(\bar{p}\bar{q})_R}\right)\left(L^{pq}_{R^1R^1}\right)^{\mu\nu}\right.$$

$$\left.\left.+\,2\left(\widetilde{\mathcal{G}}_q^{(pq)_L}\widetilde{\mathcal{G}}_q^{(\bar{p}\bar{q})_R}\right)\left(L^{pq}_{L^1R^1}\right)^{\mu\nu}\right]\right\}, \tag{5.8}$$

$$i\Big(\Pi^{\mu\nu}_{B_Y B_Y}(q^2)\Big)^{\psi}_{B} \supset\ 2\sum_{\substack{p,q=1\\ l,k=0}}^{\infty}\left(\sin\phi\frac{g^2v^2}{4}\right)^2\Bigg\{\left(\frac{7}{6}\sin\phi\right)^2\Bigg[\left(\mathcal{G}_q^{(\widetilde{pq})_L}\mathcal{G}_q^{(\widetilde{pq})_L}\right)\left(L^{\widetilde{pq}}_{L^1L^1}\right)^{\mu\nu}$$

$$+\left(\mathcal{G}_q^{(\bar{\widetilde{pq}})_R}\mathcal{G}_q^{(\bar{\widetilde{pq}})_R}\right)\left(L^{\widetilde{pq}}_{R^1R^1}\right)^{\mu\nu}+2\left(\mathcal{G}_q^{(\widetilde{pq})_L}\mathcal{G}_q^{(\bar{\widetilde{pq}})_R}\right)\left(L^{\widetilde{pq}}_{L^1R^1}\right)^{\mu\nu}\Bigg]$$

$$+\left(\frac{1}{6}\sin\phi\right)^2\Bigg[\left(\mathcal{G}_q^{(lk)_L}\mathcal{G}_q^{(lk)_L}\right)\left(L^{lk}_{L^1L^1}\right)^{\mu\nu}+\left(\mathcal{G}_q^{(\bar{pq})_R}\mathcal{G}_q^{(\bar{pq})_R}\right)\left(L^{pq}_{R^1R^1}\right)^{\mu\nu}$$

$$+2\left(\mathcal{G}_q^{(pq)_L}\mathcal{G}_q^{(\bar{pq})_R}\right)\left(L^{pq}_{L^1R^1}\right)^{\mu\nu}\Bigg]\Bigg\}, \tag{5.9}$$

$$i\Big(\Pi^{\mu\nu}_{B_Y Z_X}(q^2)\Big)^{\psi}_{B} \supset 2\sum_{\substack{p,q=1\\ l,k=0}}^{\infty}\left(\sin\phi\frac{g^2v^2}{4}\right)\left(\cos\phi\frac{g^2v^2}{4}\right)\Bigg\{\left(\frac{7}{6}\sin\phi\right)$$

$$\times\left(\frac{1}{\cos\phi}\left[\frac{1}{2}-\frac{7}{6}\sin^2\phi\right]\right)\Bigg[\left(\mathcal{G}_q^{(\widetilde{pq})_L}\widetilde{\mathcal{G}}_q^{(\widetilde{pq})_L}\right)\left(L^{\widetilde{pq}}_{L^1L^1}\right)^{\mu\nu}+\left(\mathcal{G}_q^{(\widetilde{\bar{p}\bar{q}})_R}\widetilde{\mathcal{G}}_q^{(\widetilde{\bar{p}\bar{q}})_R}\right)\left(L^{\widetilde{pq}}_{R^1R^1}\right)^{\mu\nu}$$

$$+\left(\mathcal{G}_q^{(\widetilde{pq})_L}\widetilde{\mathcal{G}}_q^{(\widetilde{\bar{p}\bar{q}})_R}\right)\left(L^{\widetilde{pq}}_{L^1R^1}\right)^{\mu\nu}+\left(\mathcal{G}_q^{(\widetilde{\bar{p}\bar{q}})_R}\widetilde{\mathcal{G}}_q^{(\widetilde{pq})_L}\right)\left(L^{\widetilde{pq}}_{R^1L^1}\right)^{\mu\nu}\Bigg]$$

$$+\left(\frac{1}{6}\sin\phi\right)\left(\frac{1}{\cos\phi}\Big[-\frac{1}{2}-\frac{1}{6}\sin^2\phi\Big]\right)\Bigg[\left(\mathcal{G}_q^{(lk)_L}\widetilde{\mathcal{G}}_q^{(lk)_L}\right)\left(L^{lk}_{L^1L^1}\right)^{\mu\nu}$$

$$+\left(\mathcal{G}_q^{(\bar{p}\bar{q})_R}\widetilde{\mathcal{G}}_q^{(\bar{p}\bar{q})_R}\right)\left(L^{pq}_{R^1R^1}\right)^{\mu\nu}+\left(\mathcal{G}_q^{(pq)_L}\widetilde{\mathcal{G}}_q^{(\bar{p}\bar{q})_R}\right)\left(L^{pq}_{L^1R^1}\right)^{\mu\nu}$$

$$+\left(\mathcal{G}_q^{(\bar{p}\bar{q})_R}\widetilde{\mathcal{G}}_q^{(pq)_L}\right)\left(L^{pq}_{R^1L^1}\right)^{\mu\nu}\Bigg]\Bigg\}, \tag{5.10}$$

$$i\Big(\Pi^{\mu\nu}_{Z_X B_Y}(q^2)\Big)^{\psi}_{B} = i\Big(\Pi^{\mu\nu}_{B_Y Z_X}(q^2)\Big)^{\psi}_{B}, \tag{5.11}$$

where we have used the identities

$$(L^{nm}_{L^aL^a})^{\mu\nu} = (L^{nm}_{R^aR^a})^{\mu\nu}\,,$$

$$(L^{nm}_{L^aR^a})^{\mu\nu} = (L^{nm}_{R^aL^a})^{\mu\nu}\,. \tag{5.12}$$

Considering the above expressions it should be noted that as the BC breaking of the $SU(2)_R$ symmetry occurs simultaneously in the gauge *and* fermionic sectors the contributions to T_B^ψ are not simply proportional to the mixing angle $\sin\phi$ (as would be the case if the breaking were confined to the gauge sector), but also to $(T_R^1)^2$ and $(T_R^3)^2$.

5.1.1 UV Behaviour

Before we are able to numerically evaluate the contributions to T_B^ψ we must first consider the assumption made in the literature that each individual 4D KK contribution is UV finite. This task first requires us to evaluate the loop momentum integrals which appear in the above expressions using the standard dimensional regularisation approach. Performing the necessary integrals we find that the relevant terms (those proportional to the metric tensor) are

$$L^{pq}_{L^aL^b(R^aR^b)}\left(q^2\right) = -\frac{i}{8\pi^2}\Big[2B_{22}(q^2, m_{\psi_a}^{(p)\,2}, m_{\psi_b}^{(q)\,2}) - q^2 B_1(q^2, m_{\psi_a}^{(p)\,2}, m_{\psi_b}^{(q)\,2}) - A_0(m_{\psi_b}^{(q)\,2})$$

$$+ B_0(q^2, m_{\psi_a}^{(p)\,2}, m_{\psi_b}^{(q)\,2})\Big],$$

$$L^{pq}_{L^aR^b(R^aL^b)}\left(q^2\right) = -\frac{i}{8\pi^2}\, m_{\psi_a}^{(p)} m_{\psi_b}^{(q)}\, B_0(q^2, m_{\psi_a}^{(p)\,2}, m_{\psi_b}^{(q)\,2}), \tag{5.13}$$

where the Veltman-Passarino functions [57] appearing above are defined in appendix D. In the context of the current discussion we are particularly interested in the parts of the loop integrals proportional to the divergent quantity $\Delta_{\rm UV}$,

$$\Delta_{\rm UV} = \frac{2}{\epsilon} - \gamma_E + \ln 4\pi, \tag{5.14}$$

which are of the form,

$$\left(L^{pq}_{L^aL^b(R^aR^b)}\left(q^2\right)\right)^{\rm UV} = -\frac{i}{8\pi^2}\left[-\frac{1}{2}\left(m^{(p)\,2}_{\psi_a}+m^{(q)\,2}_{\psi_b}\right)+\frac{q^2}{3}\right]\Delta_{\rm UV},$$

$$\left(L^{pq}_{L^aR^b(R^aL^b)}\left(q^2\right)\right)^{\rm UV} = -\frac{i}{8\pi^2}\left[m^{(p)}_{\psi_a}m^{(q)}_{\psi_b}\right]\Delta_{\rm UV}. \tag{5.15}$$

At zero external momentum, the UV divergent parts of the relevant vacuum polarisations are therefore

$$i\Big(\Pi^{\rm UV}_{11}(0)\Big)^{\psi}_{B} \supset \left(\frac{g^2v^2}{4}\right)^2\left(-\frac{i}{8\pi^2}\right)\sum_{\substack{p,q=1\\ l=0}}^{\infty}\Bigg\{-\frac{1}{2}\widetilde{\mathcal{G}}^{(\tilde{p}l)_L}_{q=0}\widetilde{\mathcal{G}}^{(\tilde{p}l)_L}_{q=0}\left(\widetilde{m}^{(p)\,2}_{\psi_1}+m^{(l)\,2}_{\psi_1}\right)$$

$$-\frac{1}{2}\widetilde{\mathcal{G}}^{(\tilde{\bar{p}}\bar{q})_R}_{q=0}\widetilde{\mathcal{G}}^{(\tilde{\bar{p}}\bar{q})_R}_{q=0}\left(\widetilde{m}^{(p)\,2}_{\psi_1}+m^{(q)\,2}_{\psi_1}\right)+2\widetilde{\mathcal{G}}^{(\tilde{p}q)_L}_{q=0}\widetilde{\mathcal{G}}^{(\tilde{\bar{p}}\bar{q})_R}_{q=0}\left(\widetilde{m}^{(p)}_{\psi_1}m^{(q)}_{\psi_1}\right)\Bigg\}\Delta_{\rm UV}, \tag{5.16}$$

$$i\Big(\Pi^{\rm UV}_{Z_XZ_X}(0)\Big)^{\psi}_{B} \supset 2\left(\frac{g^2v^2}{4}\right)^2\left(-\frac{i}{8\pi^2}\right)\sum_{\substack{p,q=1\\ l,k=0}}^{\infty}\Bigg\{\left[\frac{1}{2}-\frac{7}{6}\sin^2\phi\right]^2$$

$$\times\Bigg[-\frac{1}{2}\left(\widetilde{\mathcal{G}}^{(\tilde{p}\bar{q})_L}_{q=0}\widetilde{\mathcal{G}}^{(\tilde{p}\bar{q})_L}_{q=0}+\widetilde{\mathcal{G}}^{(\tilde{\bar{p}}\tilde{\bar{q}})_R}_{q=0}\widetilde{\mathcal{G}}^{(\tilde{\bar{p}}\tilde{\bar{q}})_R}_{q=0}\right)\left(\widetilde{m}^{(p)\,2}_{\psi_1}+\widetilde{m}^{(q)\,2}_{\psi_1}\right)+2\widetilde{\mathcal{G}}^{(\tilde{p}\bar{q})_L}_{q=0}\widetilde{\mathcal{G}}^{(\tilde{\bar{p}}\tilde{\bar{q}})_R}_{q=0}\left(\widetilde{m}^{(p)}_{\psi_1}\widetilde{m}^{(q)}_{\psi_1}\right)\Bigg]$$

$$+\left[-\frac{1}{2}-\frac{1}{6}\sin^2\phi\right]^2\Bigg[-\frac{1}{2}\widetilde{\mathcal{G}}^{(lk)_L}_{q=0}\widetilde{\mathcal{G}}^{(lk)_L}_{q=0}\left(m^{(l)\,2}_{\psi_1}+m^{(k)\,2}_{\psi_1}\right)$$

$$-\frac{1}{2}\widetilde{\mathcal{G}}^{(\bar{p}\bar{q})_R}_{q=0}\widetilde{\mathcal{G}}^{(\bar{p}\bar{q})_R}_{q=0}\left(m^{(p)\,2}_{\psi_1}+m^{(q)\,2}_{\psi_1}\right)+2\widetilde{\mathcal{G}}^{(pq)_L}_{q=0}\widetilde{\mathcal{G}}^{(\bar{p}\bar{q})_R}_{q=0}\left(m^{(p)}_{\psi_1}m^{(q)}_{\psi_1}\right)\Bigg]\Bigg\}\Delta_{\rm UV}, \tag{5.17}$$

$$i\Big(\Pi^{\rm UV}_{B_Y B_Y}\Big)^{\psi}_{B}(0) \supset\ 2\sin^4\phi\left(\frac{g^2v^2}{4}\right)^2\left(-\frac{i}{8\pi^2}\right)\sum_{\substack{p,q=1\\ l,k=0}}^{\infty}\Bigg\{\left(\frac{7}{6}\right)^2$$

$$\times\Big[-\frac{1}{2}\left(\mathcal{G}^{(\widetilde{p}\widetilde{q})_L}_{q=0}\mathcal{G}^{(\widetilde{p}\widetilde{q})_L}_{q=0}+\mathcal{G}^{(\bar{\widetilde{p}}\bar{\widetilde{q}})_R}_{q=0}\mathcal{G}^{(\bar{\widetilde{p}}\bar{\widetilde{q}})_R}_{q=0}\right)\left(\widetilde{m}^{(p)\,2}_{\psi_1}+\widetilde{m}^{(q)\,2}_{\psi_1}\right)+2\mathcal{G}^{(\widetilde{p}\widetilde{q})_L}_{q}\mathcal{G}^{(\bar{\widetilde{p}}\bar{\widetilde{q}})_R}_{q}\left(\widetilde{m}^{(p)}_{\psi_1}\widetilde{m}^{(q)}_{\psi_1}\right)\Big]$$

$$+\left(\frac{1}{6}\right)^2\Bigg[-\frac{1}{2}\widetilde{\mathcal{G}}^{(lk)_L}_{q=0}\widetilde{\mathcal{G}}^{(lk)_L}_{q=0}\left(m^{(l)\,2}_{\psi_1}+m^{(k)\,2}_{\psi_1}\right)$$

$$-\frac{1}{2}\widetilde{\mathcal{G}}^{(\bar{p}\bar{q})_R}_{q=0}\widetilde{\mathcal{G}}^{(\bar{p}\bar{q})_R}_{q=0}\left(m^{(p)\,2}_{\psi_1}+m^{(q)\,2}_{\psi_1}\right)+2\mathcal{G}^{(pq)_L}_{q=0}\mathcal{G}^{(\bar{p}\bar{q})_R}_{q=0}\left(m^{(p)}_{\psi_1}m^{(q)}_{\psi_1}\right)\Bigg]\Bigg\}\Delta_{\rm UV}, \tag{5.18}$$

$$i\Big(\Pi^{\rm UV}_{Z_X B_Y}(0)\Big)^{\psi}_{B} \supset 2\sin^2\phi\left(\frac{g^2v^2}{4}\right)^2\left(-\frac{i}{8\pi^2}\right)\sum_{\substack{p,q=1\\ l,k=0}}^{\infty}\Bigg\{\left(\frac{7}{6}\right)\left[\frac{1}{2}-\frac{7}{6}\sin^2\phi\right]$$

$$\times\Bigg[-\frac{1}{2}\left(\mathcal{G}^{(\widetilde{p}\widetilde{q})_L}_{q=0}\widetilde{\mathcal{G}}^{(\widetilde{p}\widetilde{q})_L}_{q=0}+\mathcal{G}^{(\widetilde{\bar{p}}\widetilde{\bar{q}})_R}_{q=0}\widetilde{\mathcal{G}}^{(\widetilde{\bar{p}}\widetilde{\bar{q}})_R}_{q=0}\right)\left(\widetilde{m}^{(p)\,2}_{\psi_1}+\widetilde{m}^{(q)\,2}_{\psi_1}\right)$$

$$+\left(\mathcal{G}^{(\widetilde{p}\widetilde{q})_L}_{q=0}\widetilde{\mathcal{G}}^{(\widetilde{\bar{p}}\widetilde{\bar{q}})_R}_{q=0}+\mathcal{G}^{(\widetilde{\bar{p}}\widetilde{\bar{q}})_R}_{q=0}\widetilde{\mathcal{G}}^{(\widetilde{p}\widetilde{q})_L}_{q=0}\right)\times\left(\widetilde{m}^{(p)}_{\psi_1}\widetilde{m}^{(q)}_{\psi_1}\right)\Bigg]$$

$$+\left(\frac{1}{6}\right)\Big[-\frac{1}{2}-\frac{1}{6}\sin^2\phi\Big]\Bigg[-\frac{1}{2}\widetilde{\mathcal{G}}^{(lk)_L}_{q=0}\widetilde{\mathcal{G}}^{(lk)_L}_{q=0}\left(m^{(l)\,2}_{\psi_1}+m^{(k)\,2}_{\psi_1}\right)$$

$$-\frac{1}{2}\widetilde{\mathcal{G}}^{(\bar{p}\bar{q})_R}_{q=0}\widetilde{\mathcal{G}}^{(\bar{p}\bar{q})_R}_{q=0}\left(m^{(p)\,2}_{\psi_1}+m^{(q)\,2}_{\psi_1}\right)+\left(\mathcal{G}^{(pq)_L}_{q=0}\widetilde{\mathcal{G}}^{(\bar{p}\bar{q})_R}_{q=0}+\mathcal{G}^{(\bar{p}\bar{q})_R}_{q=0}\widetilde{\mathcal{G}}^{(pq)_L}_{q=0}\right)\left(m^{(p)}_{\psi_1}m^{(q)}_{\psi_1}\right)\Bigg]\Bigg\}\Delta_{\rm UV}. \tag{5.19}$$

Substituting expressions (5.16)-(5.19) into the definition of the T parameter we see that, contrary to the assumptions made in the literature, there is no cancellation of the $2/\epsilon$ terms for any of the individual KK contributions. This non-cancellation is a direct result of the dependence of the effective gauge-fermion couplings on the BCs of the gauge and fermionic fields and our use of BCs to break the gauged custodial symmetry of the model in both the gauge and fermionic sectors. This is most clearly highlighted by noting that the sought-after cancellation of UV divergent terms does indeed occur if simultaneously the $SU(2)_R$ gauge bosons have identical BCs and each fermionic multiplet is made up of fields with the same BCs.

It is also important to note that due to the presence of the fermionic bulk profiles in the effective gauge-fermion couplings the form of the divergent terms is different for each contribution rather than there being a common form across all modes. This appears to make the task of removing these terms more complicated still.

5.1.2 Renormalisation and Numerical Evaluation

In order for the UCRS model to be a useful phenomenological model, and consequently for us to be able to perform a numerical analysis of the fermionic one-loop contributions to T, we must now absorb the UV divergent terms proportional to Δ_{UV} identified in the previous section into its bare Lagrangian parameters. Although in the course of our investigation we have not been able to identify the form of the counterterm which would allow for the relevant divergent contributions to T to be removed we have decided, rather than stop our investigations at this stage, to assume that such a counterterm does indeed exit. Having made this assumption we are then able to use the $\overline{\mathrm{MS}}$ renormalisation scheme to remove the UV divergent parts from the relevant vacuum polarisations,

$$\Pi_{VV}^{\overline{\mathrm{MS}}}\left(q^2\right) = \Pi_{VV}\left(q^2\right) - \Pi_{VV}^{\mathrm{UV}}\left(q^2\right), \tag{5.20}$$

and subsequently proceed with our numerical analysis. It must be noted that if ultimately it is determined that no such counterterm exists the following analysis is no longer valid and indeed the validity of the UCRS model as a phenomenological model would be in question.

An important consequence of using the $\overline{\mathrm{MS}}$ scheme in the renormalisation of T is that all finite one-loop contributions now depend upon the arbitrary renormalisation scale μ. For the remainder of this work when discussing the GBM contributions to

T it is assumed that they have been evaluated at the scale of the Z boson mass, i.e. $\mu = m_Z$,

$$T^{\psi}_{B(T)} = T^{\psi}_{B(T)}\left(m_Z\right). \tag{5.21}$$

In related analytical expressions and plots we have explicitly stated the μ dependence of such contributions.

From the presence of the generally complicated overlap integrals in $\mathcal{G}^{(nm)}_{q=0}$ and $\widetilde{\mathcal{G}}^{(nm)}_{q=0}$ it can be assumed that it is necessary to use numerical methods to evaluate the individual contributions to T^{ψ}_{B}. In order to better understand the dependence of the contributions on the fundamental parameters of the theory, to more easily identify dominant contributions and also to be better able to make comparisons with other contributions, it would be useful to derive approximate analytical expressions for the individual KK contributions in much the same way as was done for the tree-level contributions. It is clear from our discussion of the form of fermionic bulk profiles that the relatively simple form of the fermionic zero mode profile, (2.47), will allow us to derive an approximate (again using the approximate form of the Higgs profile) analytical expression for the contribution arising from loops containing two zero mode fermions. In addition to these expressions, there is also a region of fermionic bulk mass parameter, c^{ψ}, space in which similar expressions can be obtained for the contributions from two $n = 1$ fermionic modes (or of course one $n = 1$ mode and one zero mode). We are able to obtain such expressions for contributions containing $n = 1$ modes because of the fact that in the region of parameter space $-0.5 \lesssim c_{\psi} \lesssim -0.3$ the mass of the $n = 1$ mode for fermionic fields with $(+,+)$ or $(-,+)$ BCs is less than the KK scale of the theory, i.e. $M_{KK} > m^{(1)}_{\psi}$. This property then allows for the Bessel functions which form the exact $n = 1$ profile, (2.48), to be Taylor expanded in the same manner as the Higgs profile in the previous section. This process leaves

us with the approximate expression

$$e^{ky/2} f^{(1)}_{L(R)}(y) \sim \sqrt{2kL(1+\alpha^{\psi}_{L(R)})} e^{-kL(1+\alpha^{\psi}_{L(R)})} e^{ky(1+\alpha^{\psi}_{L(R)})}, \tag{5.22}$$

which is now of a form which allows for the relevant overlap integrals to be performed analytically.

Utilising the above expression in conjunction with the approximate form of the Higgs profile, (4.16), and the fermionic zero mode profile, we are able to derive the following expressions for the relevant effective couplings

$$\widetilde{\mathcal{G}}^{(00)_{L^a(R)^a}}_{q=0} \simeq -\frac{kL}{2M^2_{KK}} \left[\frac{\left(1 \mp 2c^{\psi}_a\right)}{e^{\left(1\mp 2c^{\psi}_a\right)kL} - 1} \right] \frac{1}{3 \mp 2c^{\psi}_a} e^{\left(1\mp 2c^{\psi}_a\right)kL},$$

$$\mathcal{G}^{(00)_{L^a(R)^a}}_{q=0} \simeq \frac{1}{4M^2_{KK}} \Bigg\{ -\frac{1}{kL} + \frac{e^{(1\mp 2c^{\psi}_a)kL}}{e^{(1\mp 2c^{\psi}_a)kL} - 1} \left(\frac{1 \mp 2c^{\psi}_a}{3 \mp 2c^{\psi}_a} \right) (1 - 2kL) + \frac{(1+\nu)}{(2+\nu)}$$

$$+ \frac{(1+\nu)}{(2+\nu)^2} + \frac{e^{(1\mp 2c^{\psi}_a)kL}}{e^{(1\mp 2c^{\psi}_a)kL} - 1} \frac{2\left(1 \mp 2c^{\psi}_a\right)}{\left(3 \mp 2c^{\psi}_a\right)^2} \Bigg\}, \tag{5.23}$$

$$\widetilde{\mathcal{G}}^{(01)_{L^a(R)^a}}_{q=0} \simeq -\frac{kL}{2M^2_{KK}} \sqrt{\frac{2(1+\alpha^{\psi}_{L(R)})(1 \mp 2c^{\psi}_a)}{e^{(1\mp 2c^{\psi}_a)kL} - 1}} \frac{e^{(1/2\mp c^{\psi}_a)kL}}{(7/2 + \alpha^{\psi}_{L(R)} \mp c^{\psi}_a)},$$

$$\mathcal{G}^{(01)_{L^a(R)^a}}_{q=0} \simeq \frac{1}{4M^2_{KK}} \sqrt{\frac{2(1+\alpha^{\psi}_{L(R)})(1 \mp 2c^{\psi}_a)}{e^{(1\mp 2c^{\psi}_a)kL} - 1}} \Bigg\{ \frac{e^{\left(1/2\mp c^{\psi}_a\right)kL}}{(7/2 + \alpha^{\psi}_{L(R)} \mp c^{\psi}_a)} (1 - 2kL)$$

$$+ \frac{2e^{\left(1/2\mp c^{\psi}_a\right)kL}}{(7/2 + \alpha^{\psi}_{L(R)} \mp c^{\psi}_a)^2} \Bigg\}, \tag{5.24}$$

$$\widetilde{\mathcal{G}}^{(11)_{L^a(R)^a}}_{q=0} = -\frac{kL}{2M_{KK}^2}\frac{(1+\alpha^{\psi}_{L(R)})}{\left(2+\alpha^{\psi}_{L(R)}\right)},$$

$$\mathcal{G}^{(11)_{L^a(R)^a}}_{q=0} = \frac{1}{4M_{KK}^2}\Bigg\{ -\frac{1}{kL} + \frac{\left(1+\alpha^{\psi}_{L(R)}\right)}{\left(2+\alpha^{\psi}_{L(R)}\right)}(1-2kL) + \frac{(1+\nu)}{(2+\nu)} + \frac{(1+\nu)}{(2+\nu)^2}$$

$$+ \frac{\left(1+\alpha^{\psi}_{L(R)}\right)}{\left(2+\alpha^{\psi}_{L(R)}\right)^2}\Bigg\}. \tag{5.25}$$

From these expressions we are then able to derive approximate expressions for the three contributions to T_B^{ψ} containing $n = 1$ fermionic modes or lighter.

As each individual diagram is quadratic in effective couplings, we see from the above that the coefficient of the loop momentum integrals in the leading terms of the vacuum polarisations above must be of the order $(kL)^2/M_{KK}^4$. The question is now: to what degree does cancellation occur between the different vacuum polarisations? In order to more easily identify the origin of any cancellation which does occur, it is convenient to group together contributions to T_B^{ψ} which are proportional to the same QNs,

$$T_B^{\psi}(\mu) = \frac{4\pi}{s_W^2 c_W^2 m_Z^2}\Bigg[\left(\left(\Pi_{11}^{\overline{\rm MS}}(0)\right)^{\psi}_B - \left(\Pi_{T_R^3 T_R^3}^{\overline{\rm MS}}(0)\right)^{\psi}_B\right) - \sin^4\phi\left(\Pi_{YY}^{\overline{\rm MS}}(0)\right)^{\psi}_B$$

$$- 2\sin^2\phi\left(\Pi_{T_R^3 Y}^{\overline{\rm MS}}(0)\right)^{\psi}_B\Bigg], \tag{5.26}$$

where we define the new expressions

$$\left(\Pi_{11}^{\overline{\rm MS}}(q^2)\right)_B^{\psi} \supset \left(\frac{g^2v^2}{4}\right)^2 \sum_{\substack{p,q=1\\ l=0}}^{\infty} \Bigg\{ \Bigg[\left(\widetilde{\mathcal{G}}_q^{(\tilde{p}l)_L}\widetilde{\mathcal{G}}_q^{(\tilde{p}l)_L}\right)\left(L_{L^1L^1}^{\tilde{p}l}(q^2)\right)^{\overline{\rm MS}}$$

$$+ \left(\widetilde{\mathcal{G}}_q^{(\tilde{\bar{p}}\bar{q})_R}\widetilde{\mathcal{G}}_q^{(\tilde{\bar{p}}\bar{q})_R}\right)\left(L_{R^1R^1}^{\tilde{p}q}(q^2)\right)^{\overline{\rm MS}} + 2\left(\widetilde{\mathcal{G}}_q^{(\tilde{p}q)_L}\widetilde{\mathcal{G}}_q^{(\tilde{\bar{p}}\bar{q})_R}\right)\left(L_{L^1R^1}^{\tilde{p}q}(q^2)\right)^{\overline{\rm MS}}\Bigg]\Bigg\}, \tag{5.27}$$

$$\left(\Pi_{T_R^3T_R^3}^{\overline{\rm MS}}(q^2)\right)_B^{\psi} \supset \frac{1}{2}\left(\frac{g^2v^2}{4}\right)^2 \sum_{\substack{p,q=1\\ l,k=0}}^{\infty} \Bigg\{ \Bigg[\left(\widetilde{\mathcal{G}}_q^{(\widetilde{pq})_L}\widetilde{\mathcal{G}}_q^{(\widetilde{pq})_L}\right)\left(L_{L^1L^1}^{\widetilde{pq}}(q^2)\right)^{\overline{\rm MS}}$$

$$+ \left(\widetilde{\mathcal{G}}_q^{(\widetilde{\bar{p}\bar{q}})_R}\widetilde{\mathcal{G}}_q^{(\widetilde{\bar{p}\bar{q}})_R}\right)\left(L_{R^1R^1}^{\widetilde{pq}}(q^2)\right)^{\overline{\rm MS}} + 2\left(\widetilde{\mathcal{G}}_q^{(\widetilde{pq})_L}\widetilde{\mathcal{G}}_q^{(\widetilde{\bar{p}\bar{q}})_R}\right)\left(L_{L^1R^1}^{\widetilde{pq}}(q^2)\right)^{\overline{\rm MS}}\Bigg]$$

$$+ \Bigg[\left(\widetilde{\mathcal{G}}_q^{(lk)_L}\widetilde{\mathcal{G}}_q^{(lk)_L}\right)\left(L_{L^1L^1}^{lk}(q^2)\right)^{\overline{\rm MS}} + \left(\widetilde{\mathcal{G}}_q^{(\bar{p}\bar{q})_R}\widetilde{\mathcal{G}}_q^{(\bar{p}\bar{q})_R}\right)\left(L_{R^1R^1}^{pq}(q^2)\right)^{\overline{\rm MS}}$$

$$+ 2\left(\widetilde{\mathcal{G}}_q^{(pq)_L}\widetilde{\mathcal{G}}_q^{(\bar{p}\bar{q})_R}\right)\left(L_{L^1R^1}^{pq}(q^2)\right)^{\overline{\rm MS}}\Bigg]\Bigg\}, \tag{5.28}$$

$$\left(\Pi_{YY}^{\overline{\rm MS}}(q^2)\right)_B^{\psi} \supset 2\left(\frac{g^2v^2}{4}\right)^2 \sum_{\substack{p,q=1\\l,k=0}}^{\infty}\Bigg\{\left(\frac{7}{6}\right)^2$$

$$\times\Bigg[\left(\widetilde{\mathcal{G}}_q^{(\widetilde{pq})_L}\widetilde{\mathcal{G}}_q^{(\widetilde{pq})_L}+\mathcal{G}_q^{(\widetilde{pq})_L}\mathcal{G}_q^{(\widetilde{pq})_L}-2\widetilde{\mathcal{G}}_q^{(\widetilde{pq})_L}\mathcal{G}_q^{(\widetilde{pq})_L}\right)\left(L_{L^1L^1}^{\widetilde{pq}}(q^2)\right)^{\overline{\rm MS}}$$

$$+\left(\widetilde{\mathcal{G}}_q^{(\widetilde{pq})_R}\widetilde{\mathcal{G}}_q^{(\widetilde{pq})_L}+\mathcal{G}_q^{(\widetilde{pq})_R}\mathcal{G}_q^{(\widetilde{pq})_L}-2\widetilde{\mathcal{G}}_q^{(\widetilde{pq})_R}\mathcal{G}_q^{(\widetilde{pq})_L}\right)\left(L_{R^1L^1}^{\widetilde{pq}}(q^2)\right)^{\overline{\rm MS}}+L\leftrightarrow R\Bigg]$$

$$+\left(\frac{1}{6}\right)^2\Bigg[\left(\widetilde{\mathcal{G}}_q^{(kl)_L}\widetilde{\mathcal{G}}_q^{(kl)_L}+\mathcal{G}_q^{(kl)_L}\mathcal{G}_q^{(kl)_L}-2\widetilde{\mathcal{G}}_q^{(kl)_L}\mathcal{G}_q^{(kl)_L}\right)\left(L_{L^1L^1}^{kl}(q^2)\right)^{\overline{\rm MS}}$$

$$+\left(\widetilde{\mathcal{G}}_q^{(\bar{pq})_R}\widetilde{\mathcal{G}}_q^{(pq)_L}+\mathcal{G}_q^{(\bar{pq})_R}\mathcal{G}_q^{(pq)_L}-2\widetilde{\mathcal{G}}_q^{(\bar{pq})_R}\mathcal{G}_q^{(pq)_L}\right)\left(L_{R^1L^1}^{pq}(q^2)\right)^{\overline{\rm MS}}+L\leftrightarrow R\Bigg]\Bigg\}, \quad (5.29)$$

$$\left(\Pi^{\overline{\rm MS}}_{T^3_R Y}(q^2)\right)^{\psi}_{B} \supset 2\left(\frac{g^2v^2}{4}\right)^2 \sum_{\substack{p,q=1\\l,k=0}}^{\infty}\Bigg\{\left(\frac{1}{2}\right)$$

$$\times\left(\frac{7}{6}\right)\Bigg[\left(\widetilde{\mathcal{G}}_q^{(\widetilde{pq})_L}\mathcal{G}_q^{(\widetilde{pq})_L}-\widetilde{\mathcal{G}}_q^{(\widetilde{pq})_L}\widetilde{\mathcal{G}}_q^{(\widetilde{pq})_L}\right)\left(L^{\widetilde{pq}}_{L^1L^1}(q^2)\right)^{\overline{\rm MS}}$$

$$+\left(\widetilde{\mathcal{G}}_q^{(\widetilde{\bar{p}\bar{q}})_R}\mathcal{G}_q^{(\widetilde{pq})_L}-\widetilde{\mathcal{G}}_q^{(\widetilde{\bar{p}\bar{q}})_R}\widetilde{\mathcal{G}}_q^{(\widetilde{pq})_L}\right)\left(L^{\widetilde{pq}}_{R^1L^1}(q^2)\right)^{\overline{\rm MS}}+L\leftrightarrow R\Bigg]$$

$$-\left(\frac{1}{2}\right)\left(\frac{1}{6}\right)\Bigg[\left(\widetilde{\mathcal{G}}_q^{(kl)_L}\mathcal{G}_q^{(kl)_L}-\widetilde{\mathcal{G}}_q^{(kl)_L}\widetilde{\mathcal{G}}_q^{(kl)_L}\right)\left(L^{kl}_{L^1L^1}(q^2)\right)^{\overline{\rm MS}}$$

$$+\left(\widetilde{\mathcal{G}}_q^{(\bar{p}\bar{q})_R}\mathcal{G}_q^{(pq)_L}-\widetilde{\mathcal{G}}_q^{(\bar{p}\bar{q})_R}\widetilde{\mathcal{G}}_q^{(pq)_L}\right)\left(L^{pq}_{R^1L^1}(q^2)\right)^{\overline{\rm MS}}+L\leftrightarrow R\Bigg]\Bigg\} \tag{5.30}$$

and have used the superscript $\overline{\rm MS}$ as a shorthand for "all terms proportional to $\Delta_{\rm UV}$ removed".

Before discussing the approximate analytical form of the $n\leq 1$ contributions to T_B^{ψ} it is beneficial to first determine the leading order dependence on kL and M_{KK} of the vacuum polarisations appearing in (5.26). Assuming that following the trend of the expressions in (5.23)-(5.25) the leading order terms of all effective couplings have a common dependence on M_{KK} and kL, we are able to derive the following

relationships [1]

$$\left(\Pi_{11}^{\overline{\rm MS}}(0)\right)_B^{nm} \sim \left(\Pi_{T_R^3 T_R^3}^{\overline{\rm MS}}(0)\right)_B^{\psi} \sim \mathcal{O}\left((kL)^2/M_{KK}^4\right) \times \text{Loop integrals},$$

$$\left(\Pi_{YY}^{\overline{\rm MS}}(0)\right)_B^{nm} \sim \mathcal{O}\left(1/M_{KK}^4\right) \times \text{Loop integrals},$$

$$\left(\Pi_{T_R^3 Y}^{\overline{\rm MS}}(0)\right)_B^{nm} \sim \mathcal{O}\left(kL/M_{KK}^4\right) \times \text{Loop integrals}. \tag{5.31}$$

As regards how the $n \leq 1$ contributions depend upon the fundamental parameters of the theory, the expressions immediately above tell only part of the story. Specifically, although the vacuum polarisations dependending exclusively upon the QNs of the $SU(2)_R$ appear to be dominant, their importance to the contribution to T_B^{ψ} from a given KK level depends strongly upon the degree to which the custodial symmetry is broken at that fermionic level. For heavy KK modes, due to the aforementioned (section 2.2.3), numerically verified, approximate equality between the mass spectra for fermionic fields with $(+,+)$ and $(-,+)$ BCs, the custodial symmetry in the fermionic sector remains approximately *unbroken*, resulting in the approximate cancellation of the two $SU(2)_R$ vacuum polarisations,

$$\left(\Pi_{11}^{\overline{\rm MS}}(0)\right)_B^{nm} - \left(\Pi_{T_R^3 T_R^3}^{\overline{\rm MS}}(0)\right)_B^{nm} \simeq 0, \qquad\qquad n, m = 1, 2, 3 \ldots \tag{5.32}$$

The dominant terms in the contributions from heavy modes therefore arise from $\left(\Pi_{T_R^3 Y}^{\overline{\rm MS}}(0)\right)_B^{nm}$. At the $n = 0$ KK level however, there is no such residual custodial symmetry to protect T_B^{ψ}, broken as it is by the BC dependent existence of a fermionic zero mode. As a result, for diagrams containing at least one fermionic zero mode, T_B^{ψ} will be of the same order as the vacuum polarisations of the $SU(2)_R$ QNs, (5.31).

[1] Testing these relationships numerically we have found that it is fair to make this assumption regarding the kL and M_{KK} dependence of the effective couplings

The explicit forms, to leading order in the kL expansion, of the $n \leq 1$ contributions to T_B^{ψ} are as follows

$$T_B^{00}(\mu) \simeq \left(-\frac{\pi}{2s_W^2}\right)\left(\frac{g^2v^2}{4}\right)\frac{(kL)^2}{M_{KK}^4}\left\{\left(\frac{(1-2c_1^{\psi})}{e^{(1-2c_1^{\psi})kL}-1}\right)^2\frac{e^{2(1-2c_1^{\psi})kL}}{\left(3-2c_1^{\psi}\right)^2}+\mathcal{O}\left(\frac{1}{kL}\right)\right\}$$

$$\times\left(L^{00}_{L^1L^1}(0)\right)^{\overline{\text{MS}}}, \tag{5.33}$$

$$T_B^{10}(\mu) \simeq -T_B^{01}(\mu) \simeq \left(\frac{\pi}{s_W^2}\right)\left(\frac{g^2v^2}{4}\right)\frac{(kL)^2}{M_{KK}^4}\left\{\frac{\left(1+\alpha_L^{\psi}\right)\left(1-2c_1^{\psi}\right)}{e^{(1-2c_1^{\psi})kL}-1}\frac{e^{(1-2c_1^{\psi})kL}}{\left(7/2+\alpha_L^{\psi}-c_1^{\psi}\right)^2}\right.$$

$$\left.+\mathcal{O}\left(\frac{1}{kL}\right)\right\}\times\left(L^{10}_{L^1L^1}(0)\right)^{\overline{\text{MS}}}, \tag{5.34}$$

$$T_B^{11}(\mu) \simeq \left(-\frac{\pi\, c_W^2}{2s_W^4}\right)\left(\frac{g^2v^2}{4}\right)\frac{kL}{M_{KK}^4}\Bigg\{\Bigg[\left(\frac{\left(1+\alpha_L^\psi\right)}{\left(2+\alpha_L^\psi\right)}\right)^2+\frac{\left(1+\alpha_L^\psi\right)(1+\nu)}{\left(2+\alpha_L^\psi\right)(2+\nu)}$$

$$+\frac{\left(1+\alpha_L^\psi\right)(1+\nu)}{\left(2+\alpha_L^\psi\right)(2+\nu)^2}+\frac{\left(1+\alpha_L^\psi\right)(1+\nu)}{\left(2+\alpha_L^\psi\right)^3}+\mathcal{O}\left(\frac{1}{kL}\right)\Bigg]\left(L^{11}_{L^1L^1}(0)\right)^{\overline{\rm MS}}$$

$$+\Bigg[\left(\frac{\left(1+\alpha_L^\psi\right)}{\left(2+\alpha_L^\psi\right)}\right)\left(\frac{\left(1+\alpha_R^\psi\right)}{\left(2+\alpha_R^\psi\right)}\right)+\frac{\left(1+\alpha_L^\psi\right)(1+\nu)}{\left(2+\alpha_L^\psi\right)(2+\nu)}+\frac{\left(1+\alpha_L^\psi\right)(1+\nu)}{\left(2+\alpha_L^\psi\right)(2+\nu)^2}$$

$$+\frac{\left(1+\alpha_L^\psi\right)(1+\nu)}{\left(2+\alpha_R^\psi\right)^2\left(2+\alpha_L^\psi\right)}+\mathcal{O}\left(\frac{1}{kL}\right)\Bigg]\left(L^{11}_{L^1R^1}(0)\right)^{\overline{\rm MS}}+L\leftrightarrow R\Bigg\}, \tag{5.35}$$

where we have made the numerically backed assumption that $m_\psi^{(n)}=\widetilde{m}_\psi^{(n)}$. As can be seen from the above, the leading order terms of T_B^{10} and T_B^{01} are equal and opposite (a relationship which holds for all non-diagonal couplings involving a fermionic zero mode), with the result that these will cancel when summing all the individual contributions to T_B^ψ. It makes more sense, therefore, to think of these two non-diagonal contributions as a single contribution, the leading order term of which is given by

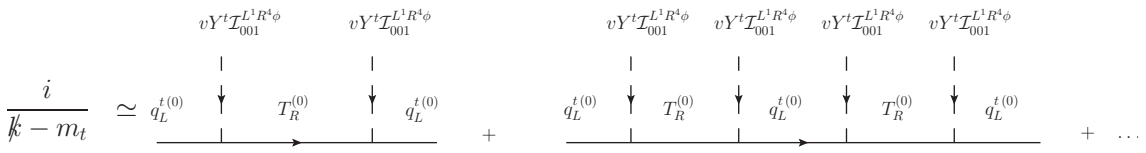

Figure 5.4: Definition of the zero mode top quark propagator used in the loop momentum integrals appearing in the contributions to T_B^{ψ}

the expression

$$T_B^{01}(\mu) + T_B^{10}(\mu) \simeq \left(-\frac{\pi c_W^2}{3s_W^4}\right)\left(\frac{g^2v^2}{4}\right)\frac{kL}{M_{KK}^4}\left\{\frac{\left(1+\alpha_L^{\psi}\right)\left(1-2c_1^{\psi}\right)}{e^{(1-2c_1^{\psi})kL}-1}\left[\frac{e^{(1-2c_1^{\psi})kL}}{\left(7/2+\alpha_L^{\psi}-c_1^{\psi}\right)^2}\right.\right.$$

$$\left.\left. + \frac{2e^{(1-2c_1^{\psi})kL}}{\left(7/2+\alpha_L^{\psi}-c_1^{\psi}\right)^3}\right] + \mathcal{O}\left(\frac{1}{kL}\right)\right\} \times \left(L^{10}_{L^1L^1}(0)\right)^{\overline{\text{MS}}}, \qquad (5.36)$$

where we have simplified the expression using the fact that the loop momentum integrals are symmetric in the two fermion masses.

A final, technical, detail which requires discussion is the evaluation of the loop momentum integrals containing fermionic zero modes. As in the KK basis these zero modes are by definition massless the loop momentum integrals in which they appear suffer from IR divergences in addition to the UV divergences common to all two fermion loop integrals. In order to regulate these IR divergences we replace the massless KK propagator with that obtained by summing all possible corrections from Yukawa mass insertions between two zero mode particles, figure 5.4. We note that on the left-hand side we have replaced the inserted Yukawa mass, $vY^t\mathcal{I}^{L^1R^4\phi}_{001}$, with the physical mass of the top quark, m_t. We are able to do this safely as again, the two quantities differ due to the mixing between zero and heavy KK modes caused by the SSB procedure and is therefore $\mathcal{O}(\varepsilon)$. As a similar replacement must be made for

bottom quark zero mode, we see that it is necessary when performing the numerical analysis for us to split up the loop integrals containing zero mode fermions into a top and bottom part, e.g.

$$\left(L^{00}_{L^1L^1}(0)\right)^{\overline{\rm MS}} = \frac{1}{2}\left[\left(L^{00}_{L^tL^t}(0)\right)^{\overline{\rm MS}} + \left(L^{00}_{L^bL^b}(0)\right)^{\overline{\rm MS}}\right]. \tag{5.37}$$

We conclude from this discussion that the loop momentum integrals containing only zero mode fermions are suppressed by a factor of at least ε (more in the case of the contributions from the zero mode bottom quarks) relative to the integrals containing at least one heavy KK mode. This suppression can be seen by making a rough estimation of the three loop integrals of interest,

$$\left(L^{0n}_{L(R)L(R)}(0)\right)^{\overline{\rm MS}} \sim \left(L^{nm}_{L(R)L(R)}(0)\right)^{\overline{\rm MS}} \sim M^2_{KK}\log M^2_{KK}/\mu^2,$$

$$\left(L^{00}_{L(R)L(R)}(0)\right)^{\overline{\rm MS}} \sim v^2\log v^2/\mu^2. \tag{5.38}$$

Taking all of this information into account, we see that although the coefficient of the loop integral is largest for T^{00}_B the enhancement of kL (relative to the other contributions considered) does not sufficiently compensate for the suppression caused by the smallness of the top quark mass relative to the KK scale of the theory (obviously for other fermions this effect is even larger). This means that in fact such contributions are subdominant to the contributions from those loops containing heavy fermionic modes. We would expect contributions containing at least one heavy mode (again treating the sum of the two non-diagonal contributions as a single contribution) to be of the same order of magnitude.

In order to put the magnitude of these contributions into some sort of overall context, it is useful to compare these individual GBM contributions with those tree-level contributions calculated in the previous chapter, as well as to a similarly estimated

individual KK Yukawa contribution containing four $n = 1$ fermionic modes. Comparing expressions (5.35) and (4.36) and using the estimate for the loop momentum integral stated in (5.38) we see that the individual bidoublet contributions containing heavy fermionic modes occur at the same order in the ε expansion, but two orders higher in the kL expansion. Although such an enhancement is $\mathcal{O}\left(10^3\right)$ the one-loop contributions have additional factors such as the small gauge coupling constant, as well as terms dependent upon the bidoublet bulk mass such as the loop momentum integrals, which must be considered when assessing the relative sizes of one-loop and tree-level contributions. A full assesment of the c^{ψ} dependence of the individual one-loop contributions is performed below but as a rough estimate we would predict that, dependening on the value of the bidoublet bulk mass parameter, c_1^{ψ}, the individual one-loop contributions to T_B^{ψ} are *at least* of the same order of magnitude as the tree-level contributions and possibly an order of magnitude larger.

In order to obtain an estimate for the contributions to T from a diagram containing no gauge boson mixing and four Yukawa mass insetions we must first evalute the overlap integrals associated with a single such mass insertion,

$$\mathcal{I}_{111}^{LR\phi} \simeq \sqrt{8(1+\alpha_L^{\psi})(1+\alpha_R^{\psi})\left(1+\nu\right)}\frac{(kL)^{1/2}}{\left(3+\alpha_L^{\psi}+\alpha_R^{\psi}+\nu\right)}. \tag{5.39}$$

Raising this expression to the fourth power, multiplying by v^4 and including an estimate of the size of the six fermion loop integral we find that the leading order term for such a contribution to T will be of the form

$$T_Y^{1111}\left(\mu\right) \sim \varepsilon^2 \left(kL\right)^2 \log M_{KK}^2/\mu^2, \tag{5.40}$$

where we have made a logical extension of the notation used for the GBM contributions to T. From this rough estimate we conclude that we would expect the bidoublet contributions to T from the GBM diagrams to be *subdominant* to those

from the Yukawa insertion diagrams featuring the third generation of quark due to those contributions being of a higher order in kL.

5.1.3 Numerical Analysis

In order to investigate the contributions to T_B^{ψ} from diagrams containing modes with $n > 1$, or indeed for values of the bulk mass parameter outside of the range for which our expansion of the $n = 1$ fermionic profile is valid, it is necessary to use numerical methods. The main initial concern is whether the infinite sum of individual contributions converges: a question which essentially boils down to whether the decrease in effective couplings caused by the increasingly oscillatory fermionic profiles dominates over the simultaneous increase in loop momentum integrals. As we were unable to find an analytical solution for the summation of all KK levels we must instead investigate the convergence of these contributions numerically, i.e. sum up contributions to T_B^{ψ} from an increasingly large number of KK modes. In order to represent this sum (and the equivalent sum involving the contributions from the triplet modes) we define the functions

$$T_{B(T)}^{sum}\left(N_{max}\right) = \sum_{n=0}^{N_{max}} \sum_{m=0}^{N_{max}} T_{B(T)}^{(nm)}\left(m_Z\right). \tag{5.41}$$

Performing such a study we obtain figure 5.6, from which we observe that the contributions to T from the fermionic bidoublets do not converge.

Faced with this lack of convergence we are restricted for the remainder of this thesis to investigating numerically the functional dependence of individual contributions on a selection of the fundamental parameters of the theory. In order to perform such an investigation it is first necessary to decide upon a "benchmark" set of parameters which can be used to fix the parameters not under investigation in

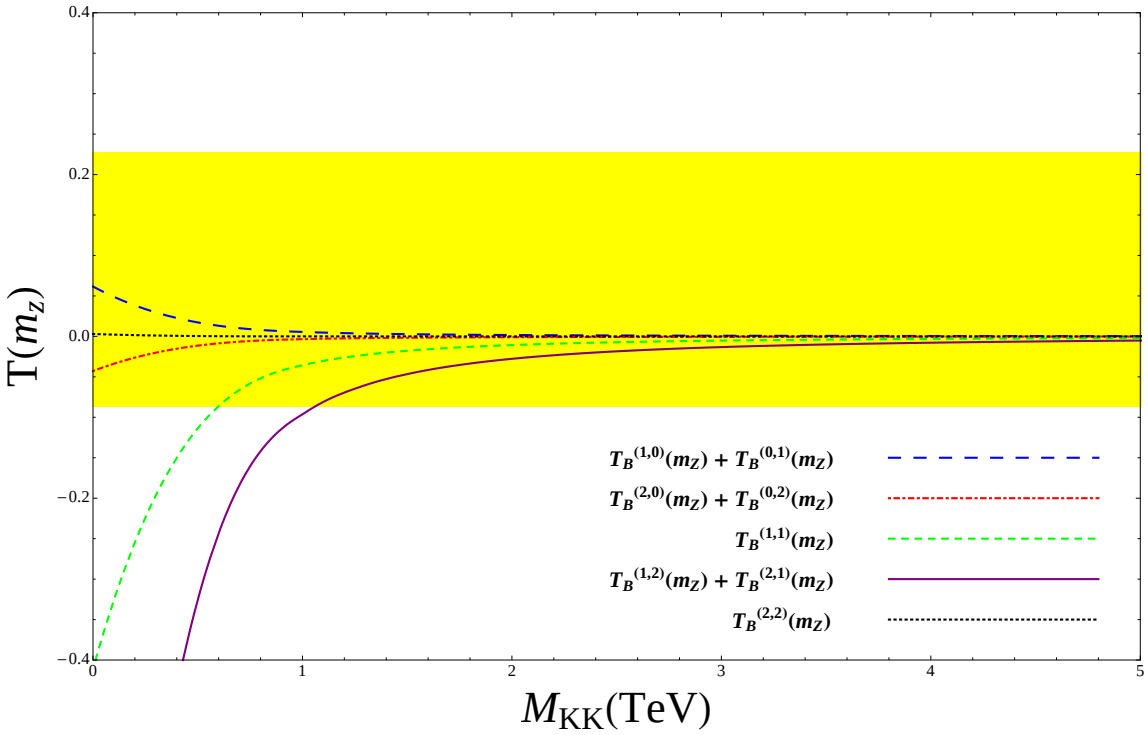

Figure 5.5: The dependence on the KK scale of the theory, $M_{KK} = ke^{-kL}$, of the contributions to T_B^{ψ} arising from diagrams containing $n = 2$ fermionic modes or lower calculated within the framework of the standard UCRS model. In calculating these contributions we have assumed $m_{\psi}^{(n)} = \widetilde{m}_{\psi}^{(n)}$ and have used the benchmark choice for the bidoublet bulk mass parameter, $c_1^{\psi} = 0.45$. Due to the high level of suppression relative to the other contributions we omit $T_B^{(0,0)}$ from the above. The yellow band gives the current experimental limit on the T parameter at the 95% confidence level obtained using a Higgs mass of $m_h = 117\,GeV$ [56].

any particular study. For all plots, unless explicitly stated otherwise, the following set of parameters are assumed to be correct,

$$c_1^{\psi} = 0.45, \qquad c_4^{\psi} = -0.58, \qquad kL = 36.8, \qquad M_{KK} \simeq 1.5\,TeV. \tag{5.42}$$

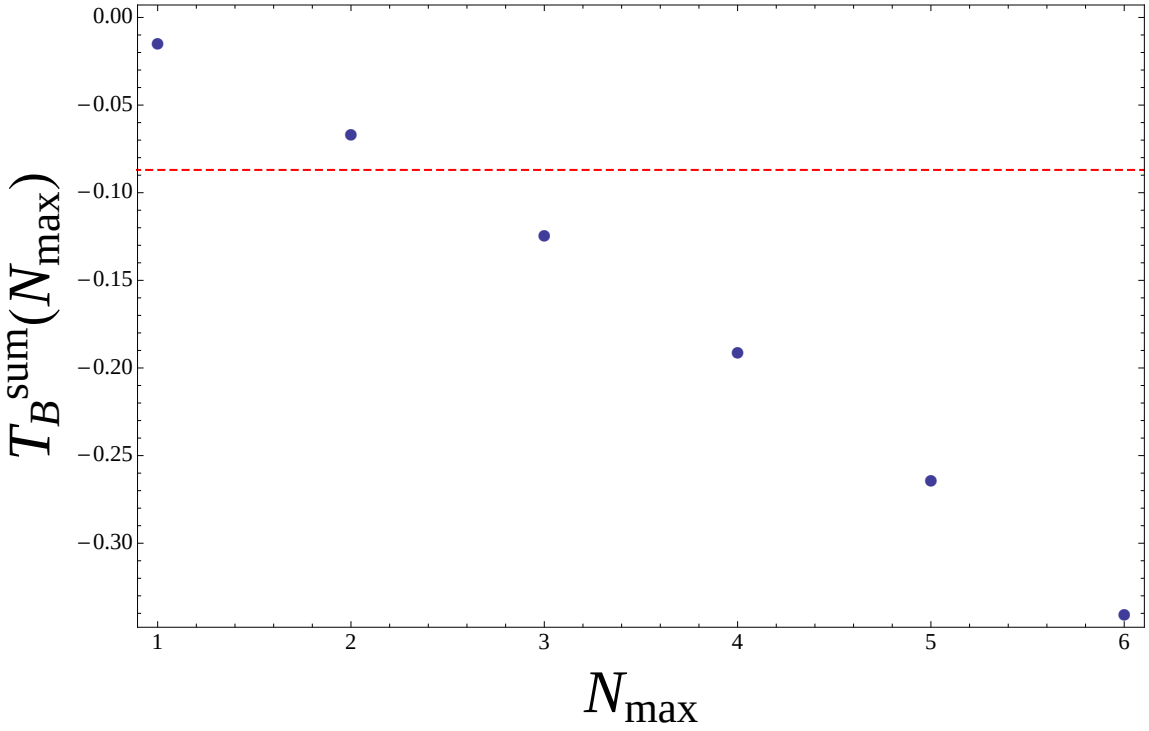

Figure 5.6: The sum of individual contributions to T_B^{ψ} from modes up to and including N_{max}, $T_B^{sum}(N_{max}) = \sum_{n=0}^{N_{max}} \sum_{m=0}^{N_{max}} T_B^{(nm)}(m_Z)$, calculated within the framework of the standard UCRS model. For this calculation it was assumed that $M_{KK} \simeq 1.5\,TeV$ $(kL = 36.8)$ and $c_1^{\psi} = 0.45$. The dashed red line indicates the current lower experimental limit on the T parameter at the 95% confidence level obtained using a Higgs mass of $m_h = 117\,GeV$ [56].

The value of the bidoublet and triplet bulk mass parameters, c_1^ψ and c_4^ψ respectively, were chosen such that with a dimensionless Yukawa coupling $\mathcal{O}(1)$ it was possible to reproduce the observed bottom mass, $m_b = 4.4\,GeV$, without having a phenomenologically troublesome (due to the anomalous Zb_Lb_L coupling) IR localised right-handed SM bottom quark. Clearly there are other choices of these parameters which meet this simple criterion, however, as this choice exhibits the two salient features of all such choices (an IR localised left-handed SM top and bottom with a UV localised right-handed bottom) we decided that this choice is as good as any for the current analysis.

Our chief concern in performing this analysis is again to determine the strength of the phenomenological constraints from the T parameter on M_{KK}. As well as showing the non-convergence of the infinite sum over all individual KK contributions to T_B^ψ our numerical analysis has shown the first few individual contributions to be at least the same order of magnitude as the contributions coming from the higher KK levels; in the majority of cases they are larger. In figure 5.5 we have therefore investigated the M_{KK} dependence of all contributions from diagrams containing fermionic modes of KK level $n = 2$ and lower. As can be seen from this figure, the dominant contribution of those considered is that associated with diagrams containing $n = 1$ and $n = 2$ (and no zero) modes. Comparing figures 4.6 and 5.5 we see that the constraint applied to M_{KK} from these individual contributions is of a similar level to that coming from the tree-level contributions to the S parameter and is considerably more stringent than that arising from the tree-level contributions to T.

Due to the large hierarchy amongst SM fermionic masses, the bidoublet bulk mass parameter values required to reproduce the SM fermionic mass spectrum could be anywhere in the range $-1 < c_1^\psi < 1$ [6]. As a result of this broad range it is useful to investigate the constraints on M_{KK} from the bidoublet contributions to T across

the whole range of the plausible c_1^ψ range and not just for the "benchmark" top quark value used in figure 5.5. Such an investigation also allows for us to determine the relative importance of the contributions to T_B^ψ from the different generations of quarks and leptons. To this end we have considered in figure 5.7 the c_1^ψ dependence of the same five contributions as in figure 5.5 for a KK scale of $M_{KK} \sim 1.5\,TeV$ ($kL = 36.8$).

From this plot we see that across the whole of the c_1^ψ parameter range the $(1,1)$ contribution is the dominant contribution of those considered and, more generally, that all contributions have a relatively complicated dependence on the bulk mass parameter. This complicated dependence is a direct result of the Bessel function-like nature of the mass equations from which the mass spectra of the fermionic fields are derived. This connection is shown particularly clearly at $c_1^\psi = -0.5$ where a discontinuity in the c_1^ψ dependence of those contributions containing the $n = 1$ mode is the result of a similar feature in the c_1^ψ dependence of the $n = 1$ mass spectrum. In addition to this complicated c_1^ψ dependence we also see the increase of those contributions containing at least one zero mode for regions of c_1^ψ relating to IR localisation simply associated with the well known exponential nature of the fermionic zero mode profiles.

The main conclusion which can be drawn from figure 5.7 with regards to the constraints on M_{KK} is that for the majority of the parameter space the constraint coming from the $(1,1)$ contributions are of a similar strength to those arising from S_{tree}, but in a region of parameter space around $c_1^\psi \sim -0.5$ the $(1,1)$ contributions to T_B^ψ could possibly become more important. This fact, in addition to the non-convergence of the KK sum, clearly indicates the failure of the gauged custodial symmetry to protect the T parameter from large quantum corrections. Given the complicated nature of the c_1^ψ dependence exhibited in 5.7 there are not too many

conclusions which can be drawn with regards to the relevant importance of contributions to T_B^{ψ} from the remaining fermionic flavours. We can, however, see the expected increase in the contributions from diagrams containing zero modes for values of c_1^{ψ} associated with the IR localisation of left-handed zero modes ($c_1^{\psi} < -0.5$).

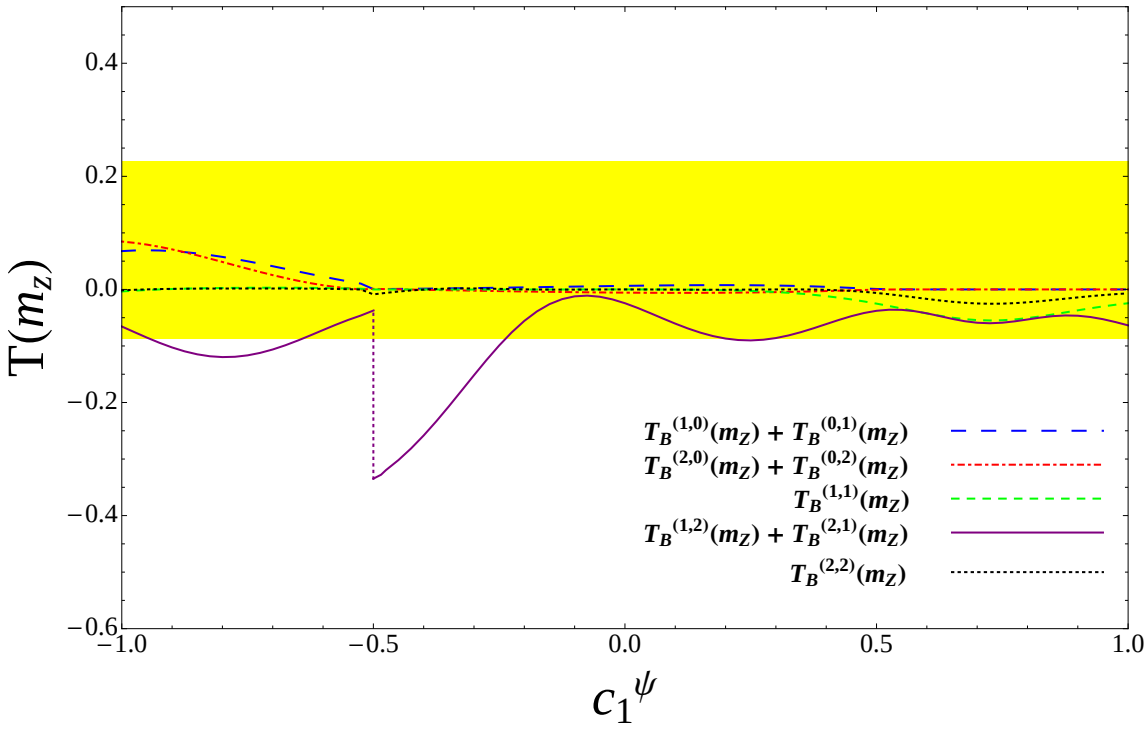

Figure 5.7: The dependence on the bidoublet bulk mass parameter, c_1^{ψ}, of the contributions to T_B^{ψ} arising from diagrams containing $n = 2$ fermionic modes or lower calculated within the framework of the standard UCRS model. It has been assumed during this calculation that $m_{\psi}^{(n)} = \widetilde{m}_{\psi}^{(n)}$ and that $M_{KK} \simeq 1.5\,TeV$ $(kL = 36.8)$. Due to the high level of suppression relative to the other contributions we omit $T_B^{(0,0)}$ from the above. The from The yellow band is the current experimental limit on the T parameter at the 95% confidence level obtained using a Higgs mass of $m_h = 117\,GeV$ [56], while the dotted purple line indicates a discontinuity.

5.1.4 The LRS Model

We now wish to investigate whether the potentially severe constraints on M_{KK} from bidoublet contributions to T discussed above can be ameliorated somewhat using an LRS variant of the UCRS model. As discussed briefly in the Introduction, the difference between the "Little RS model" [23] and the standard RS model is the fact that the goal of solving the full gauge hierarchy probelm, so important to the motivation of the RS model, is dropped in the LRS model in favour of solving the smaller hierarchy between the weak scale and that required to adequently suppress higher-dimensional flavour violation operators, $\mathcal{O}\left(10^3\, TeV\right)$. In order to implement such a change of focus we must make the following change in the fundamental parameters of the theory,

$$(M_*)_{LRS} \sim k_{LRS} = 10^3\, TeV. \tag{5.43}$$

In order to maintain the same value for our benchmark KK scale ($M_{KK} \simeq 1.5\, TeV$) we must simultaneously make the following change to the benchmark parameters shown in (5.42),

$$kL = 6.1. \tag{5.44}$$

Considering the dependence on kL of the approximate analytical expressions for the contributions to T_B^ψ derived so far, it is clear to see how such a change in the benchmark parameters may bring about a loosening of the constraints on M_{KK} from the fermionic loop contributions to T_B^ψ. All other benchmark parameters will remain the same for the numerical analysis to follow.

Repeating the convergence test for the sum over all individual KK contributions to T_B^ψ we obtain figure 5.8 from which we again observe the lack of convergence of

the sum over all KK contributions to T_B^ψ. It is important to note however that in the case of the LRS variant of the UCRS model after 6 KK levels have been included in the summation, the lower experimental bound on T shown in figure 5.6 is yet to be reached. Extrapolating from the points shown in figure 5.8 we estimate that 11 KK levels would have to be included in our sum for the experimental limit to be surpassed. This is a considerable weakening of the constraint on M_{KK} compared to the standard UCRS model.

In figure 5.9 is shown the KK scale dependence of the contributions to T_B^ψ from diagrams containing $n = 2$ modes or lower using the LRS benchmark value for kL ($kL = 6.1$). Comparing this figure with figure 5.5 we see that although the relationship between the different contributions is the same for both parameter choices the expected reduction in the absolute values of the contributions in the LRS model relative to the standard UCRS model is clearly observed. The same pattern is observed in the c_1^ψ dependence of the contributions. Comparing figures 5.7 and 5.10 we see that the dependence of all contributions is the same in both the standard and LRS varieties of the UCRS model but the absolute values of the LRS case are approximately two orders of magnitude lower than in the standard case.

We can conclude therefore that the constraints on M_{KK} from the individual bidoublet contributions to T can be weakened greatly through the use of a LRS style framework. As the tree-level contributions to the S parameter are to leading order independent of the parameter combination kL the constraint on M_{KK} from this source remains the same and will therefore dominate over all individual contributions to T. Of course as the sum of all individual contributions to T is still divergent, the constraint on M_{KK} arising from the total bidoublet contribution to T, although weaker than in the standard UCRS case, will still be the dominant constraint. Without a proper regularisation we are unable to evaluate this numerically.

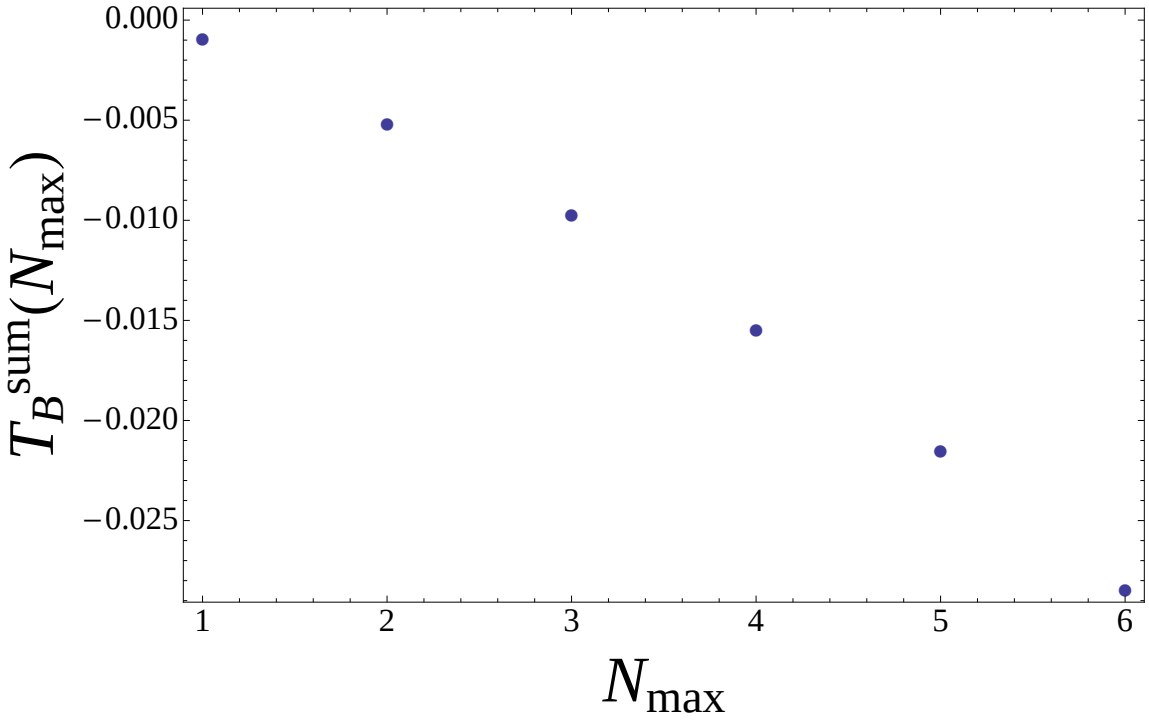

Figure 5.8: The sum of individual contributions to T_B^{ψ} from modes up to and including N_{max}, $T_B^{sum}(m_Z, N_{max}) = \sum_{n=0}^{N_{max}} \sum_{m=0}^{N_{max}} T_B^{(nm)}(m_Z)$, calculated within the framework of an LRS variant of the UCRS model. For this calculation it was assumed that $k_{LRS} = 10^3\, TeV$, $M_{KK} \simeq 1.5\, TeV$ $(kL = 6.1)$ and $c_1^{\psi} = 0.45$.

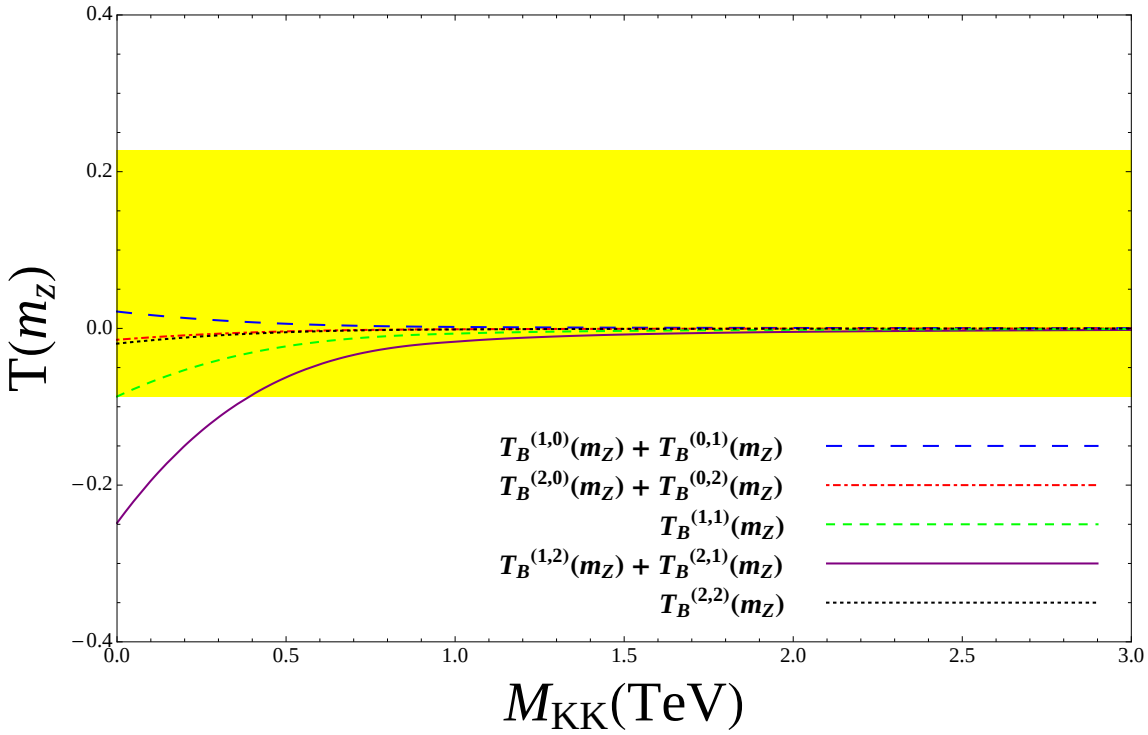

Figure 5.9: The dependence on the KK scale of the theory, $M_{KK} = ke^{-kL}$, of the contributions to T_B^{ψ} arising from diagrams containing $n = 2$ fermionic modes or lower calculated within the framework of an LRS variant of the UCRS model. In calculating these contributions we have assumed $m_{\psi}^{(n)} = \widetilde{m}_{\psi}^{(n)}$, $k_{LRS} = 10^3\, TeV$ and have used the benchmark choice for the bidoublet bulk mass parameter, $c_1^{\psi} = 0.45$. Due to the high level of suppression relative to the other contributions we omit $T_B^{(0,0)}$ from the above. The yellow band gives the current experimental limit on the T parameter at the 95% confidence level obtained using a Higgs mass of $m_h = 117\, GeV$ [56].

5.2 Triplet Contributions

In addition to the contributions arising from the fermionic bidoublets discussed in detail in the previous section, the UCRS model also contains similar contributions

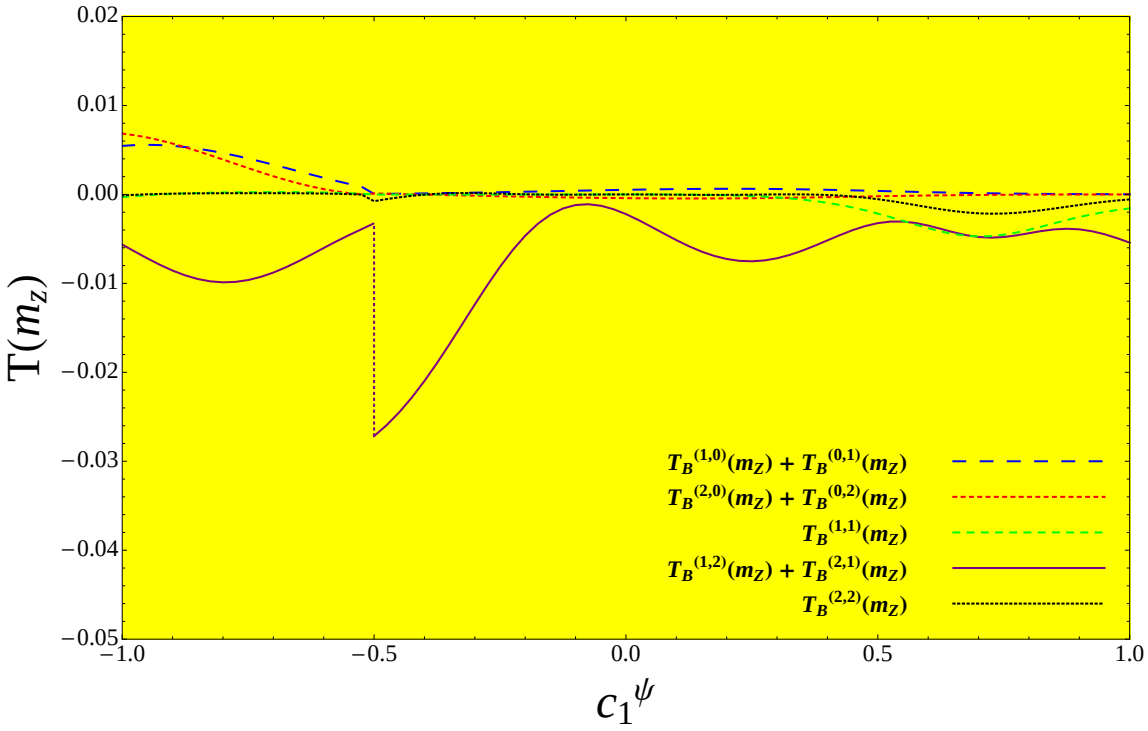

Figure 5.10: The dependence on the bidoublet bulk mass parameter, c_1^{ψ}, of the contributions to T_B^{ψ} arising from diagrams containing $n = 2$ fermionic modes or lower calculated within the framework of an LRS variant of the UCRS model. It has been assumed during this calculation that $m_{\psi}^{(n)} = \widetilde{m}_{\psi}^{(n)}$, $k_{LRS} = 10^3\,TeV$ and that $M_{KK} \simeq 1.5\,TeV$ $(kL = 6.1)$. Due to the high level of suppression relative to the other contributions we omit $T_B^{(0,0)}$ from the above. The yellow band is the current experimental limit on the T parameter at the 95% confidence level obtained using a Higgs mass of $m_h = 117\,GeV$ [56], while the dotted purple line indicates a discontinuity.

from the right-handed fermionic triplets in which the right-handed, down-type SM fermions are embedded, (3.26). Although these contributions (see the lower halves of figures 5.1 and 5.2) have broadly the same structure as those involving the bidoublet fields the triplet nature of the multiplet does result in some important differences and it is therefore necessary to state separately the form of the relevant vacuum polarisation contributions

$$\begin{aligned}\left(\Pi_{11}^{\overline{\rm MS}}(q^2)\right)_T^{\psi} \supset \left(\frac{g_4^2 v^2}{4}\right)^2 \sum_{\substack{p,q=1\\ l=0}}^{\infty} \Bigg\{ \Bigg[& \left(\widetilde{\mathcal{G}}_q^{(\tilde{\bar{p}}\tilde{q})_L}\widetilde{\mathcal{G}}_q^{(\tilde{p}\tilde{q})_L}\right)\left(L_{L^4L^4}^{\tilde{\bar{p}}\tilde{q}}(q^2)\right)^{\overline{\rm MS}} \\ & + \left(\widetilde{\mathcal{G}}_q^{(\tilde{p}l)_R}\widetilde{\mathcal{G}}_q^{(\tilde{p}l)_R}\right)\left(L_{R^4R^4}^{\tilde{\bar{l}}\bar{l}}(q^2)\right)^{\overline{\rm MS}} + 2\left(\widetilde{\mathcal{G}}_q^{(\tilde{p}q)_R}\widetilde{\mathcal{G}}_q^{(\tilde{\bar{p}}\tilde{q})_L}\right)\left(L_{L^4R^4}^{\tilde{\bar{p}}\tilde{q}}(q^2)\right)^{\overline{\rm MS}}\Bigg] \\ & + \Bigg[\left(\widetilde{\mathcal{G}}_q^{(\tilde{\bar{p}}\tilde{\bar{q}})_L}\widetilde{\mathcal{G}}_q^{(\tilde{\bar{p}}\tilde{\bar{q}})_L}\right)\left(L_{L^4L^4}^{\tilde{\bar{p}}\tilde{\bar{q}}}(q^2)\right)^{\overline{\rm MS}} + \left(\widetilde{\mathcal{G}}_q^{(\tilde{p}\tilde{q})_R}\widetilde{\mathcal{G}}_q^{(\tilde{p}\tilde{q})_R}\right)\left(L_{R^4R^4}^{\tilde{\bar{p}}\tilde{\bar{q}}}(q^2)\right)^{\overline{\rm MS}} \\ & + 2\left(\widetilde{\mathcal{G}}_q^{(\tilde{p}\tilde{q})_R}\widetilde{\mathcal{G}}_q^{(\tilde{\bar{p}}\tilde{\bar{q}})_L}\right)\left(L_{L^4R^4}^{\tilde{\bar{p}}\bar{l}}(q^2)\right)^{\overline{\rm MS}}\Bigg]\Bigg\},\end{aligned} \tag{5.45}$$

$$\Big(\Pi^{\overline{\rm MS}}_{T_R^3T_R^3}(q^2)\Big)^{\psi}_{T} \supset \left(\frac{g_4^2v^2}{4}\right)^2 \sum_{\substack{p,q=1\\l,k=0}}^{\infty}\Bigg\{\Bigg[\Big(\widetilde{\mathcal{G}}_q^{(\widetilde{p}\widetilde{q})_R}\widetilde{\mathcal{G}}_q^{(\widetilde{p}\widetilde{q})_R}\Big)\Big(L^{\widetilde{\bar{p}}\widetilde{\bar{q}}}_{R^4R^4}(q^2)\Big)^{\overline{\rm MS}}$$

$$+\Big(\widetilde{\mathcal{G}}_q^{(\widetilde{\bar{p}}\widetilde{\bar{q}})_L}\widetilde{\mathcal{G}}_q^{(\widetilde{\bar{p}}\widetilde{\bar{q}})_L}\Big)\Big(L^{\widetilde{\bar{p}}\widetilde{\bar{q}}}_{L^4L^4}(q^2)\Big)^{\overline{\rm MS}}+2\Big(\widetilde{\mathcal{G}}_q^{(\widetilde{p}\widetilde{q})_R}\widetilde{\mathcal{G}}_q^{(\widetilde{\bar{p}}\widetilde{\bar{q}})_L}\Big)\Big(L^{\widetilde{\bar{p}}\widetilde{\bar{q}}}_{L^4R^4}(q^2)\Big)^{\overline{\rm MS}}\Bigg]$$

$$+\Bigg[\Big(\widetilde{\mathcal{G}}_q^{(lk)_R}\widetilde{\mathcal{G}}_q^{(lk)_R}\Big)\Big(L^{\overline{l}\overline{k}}_{R^4R^4}(q^2)\Big)^{\overline{\rm MS}}+\Big(\widetilde{\mathcal{G}}_q^{(\bar{p}\bar{q})_L}\widetilde{\mathcal{G}}_q^{(\bar{p}\bar{q})_L}\Big)\Big(L^{\bar{p}\bar{q}}_{L^4L^4}(q^2)\Big)^{\overline{\rm MS}}$$

$$+2\Big(\widetilde{\mathcal{G}}_q^{(pq)_R}\widetilde{\mathcal{G}}_q^{(\bar{p}\bar{q})_L}\Big)\Big(L^{\bar{p}\bar{q}}_{L^4R^4}(q^2)\Big)^{\overline{\rm MS}}\Bigg]\Bigg\}, \tag{5.46}$$

$$\Big(\Pi^{\overline{\rm MS}}_{YY}(q^2)\Big)^{\psi}_{T} \supset \left(\frac{g^2v^2}{4}\right)^2 \sum_{\substack{p,q=1\\l,k=0}}^{\infty}\Bigg\{\left(\frac{5}{3}\right)^2\Bigg[\Big(\widetilde{\mathcal{G}}_q^{(\widetilde{p}\widetilde{q})_R}\widetilde{\mathcal{G}}_q^{(\widetilde{p}\widetilde{q})_R}+\mathcal{G}_q^{(\widetilde{p}\widetilde{q})_R}\mathcal{G}_q^{(\widetilde{p}\widetilde{q})_R}-2\widetilde{\mathcal{G}}_q^{(\widetilde{p}\widetilde{q})_R}\mathcal{G}_q^{(\widetilde{p}\widetilde{q})_R}\Big)$$

$$\times\Big(L^{\widetilde{\bar{p}}\widetilde{\bar{q}}}_{R^4R^4}(q^2)\Big)^{\overline{\rm MS}}$$

$$+\Big(\widetilde{\mathcal{G}}_q^{(\widetilde{p}\widetilde{q})_R}\widetilde{\mathcal{G}}_q^{\left(\widetilde{\bar{p}}\widetilde{\bar{q}}\right)_L}+\mathcal{G}_q^{(\widetilde{p}\widetilde{q})_R}\mathcal{G}_q^{\left(\widetilde{\bar{p}}\widetilde{\bar{q}}\right)_L}-2\widetilde{\mathcal{G}}_q^{(\widetilde{p}\widetilde{q})_R}\mathcal{G}_q^{\left(\widetilde{\bar{p}}\widetilde{\bar{q}}\right)_L}\Big)\Big(L^{\widetilde{\bar{p}}\widetilde{\bar{q}}}_{R^4L^4}(q^2)\Big)^{\overline{\rm MS}}+L\leftrightarrow R\Bigg]$$

$$+\left(\frac{1}{3}\right)^2\Bigg[\Big(\widetilde{\mathcal{G}}_q^{(lk)_R}\widetilde{\mathcal{G}}_q^{(lk)_R}+\mathcal{G}_q^{(lk)_R}\mathcal{G}_q^{(lk)_R}-2\widetilde{\mathcal{G}}_q^{(lk)_R}\mathcal{G}_q^{(lk)_R}\Big)\Big(L^{\overline{l}\overline{k}}_{R^4R^4}(q^2)\Big)^{\overline{\rm MS}}$$

$$\Big(\widetilde{\mathcal{G}}_q^{(pq)_R}\widetilde{\mathcal{G}}_q^{(\bar{p}\bar{q})_L}+\mathcal{G}_q^{(pq)_R}\mathcal{G}_q^{(\bar{p}\bar{q})_L}-2\widetilde{\mathcal{G}}_q^{(pq)_R}\mathcal{G}_q^{(\bar{p}\bar{q})_L}\Big)\Big(L^{\bar{p}\bar{q}}_{R^4L^4}(q^2)\Big)^{\overline{\rm MS}}+L\leftrightarrow R\Bigg]\Bigg\}, \tag{5.47}$$

$$\left(\Pi^{\overline{\rm MS}}_{T^3_R Y}(q^2)\right)^{\psi}_{T} \supset \left(\frac{g^2v^2}{4}\right)^2 \sum_{\substack{p,q=1\\l,k=0}}^{\infty} \Bigg\{ \left(\frac{5}{3}\right) \Bigg[\left(\widetilde{\mathcal{G}}^{(\widetilde{p}\widetilde{q})_R}_q \mathcal{G}^{(\widetilde{p}\widetilde{q})_R}_q - \widetilde{\mathcal{G}}^{(\widetilde{p}\widetilde{q})_R}_q \widetilde{\mathcal{G}}^{(\widetilde{p}\widetilde{q})_R}_q\right) \left(L^{\bar{\tilde{p}}\bar{\tilde{q}}}_{R^4R^4}(q^2)\right)^{\overline{\rm MS}}$$

$$+ \left(\widetilde{\mathcal{G}}^{(\widetilde{p}\widetilde{q})_R}_q \mathcal{G}^{\left(\bar{\tilde{p}}\bar{\tilde{q}}\right)_L}_q - \widetilde{\mathcal{G}}^{(\widetilde{p}\widetilde{q})_R}_q \widetilde{\mathcal{G}}^{\left(\bar{\tilde{p}}\bar{\tilde{q}}\right)_L}_q\right) \left(L^{\widetilde{p}\widetilde{q}}_{R^4L^4}(q^2)\right)^{\overline{\rm MS}} + L \leftrightarrow R \Bigg]$$

$$+ \left(-\frac{1}{3}\right) \Bigg[\left(\widetilde{\mathcal{G}}^{(kl)_R}_q \mathcal{G}^{(kl)_R}_q - \widetilde{\mathcal{G}}^{(kl)_R}_q \widetilde{\mathcal{G}}^{(kl)_R}_q\right) \left(L^{\bar{k}\bar{l}}_{R^4R^4}(q^2)\right)^{\overline{\rm MS}}$$

$$+ \left(\widetilde{\mathcal{G}}^{(pq)_R}_q \mathcal{G}^{(\bar{p}\bar{q})_L}_q - \widetilde{\mathcal{G}}^{(pq)_R}_q \widetilde{\mathcal{G}}^{(\bar{p}\bar{q})_L}_q\right) \left(L^{\bar{p}\bar{q}}_{R^4L^4}(q^2)\right)^{\overline{\rm MS}} + L \leftrightarrow R \Bigg] \Bigg\}. \tag{5.48}$$

From these expressions we see that the contributions from the bidoublet fields and those from the triplet fields share a common structure, the difference between the two sets of contributions arising from the different sets of QNs and BCs of the constituent fermionic fields. In general, and again assuming the equality of the two distinct mass spectra which are present ($\bar{m}^{(n)}_{\psi} = \bar{\tilde{m}}^{(n)}_{\psi}$), the dependence on the fundamental parameters of the theory of an individual triplet contribution will be the same as that for the equivalent bidoublet contribution. The exceptions to this rule of thumb are the non-diagonal contributions containing a zero mode field, the two combinations of which are no longer equal and opposite to first order in the kL expansion,

$$T^{0n}_T \sim \mathcal{O}\left((kL)^2/M^4_{KK}\right) \times \text{Loop integrals},$$

$$T^{n0}_T \sim \mathcal{O}(kL/M^4_{KK}) \times \text{Loop integrals}. \tag{5.49}$$

Unlike the case of the contributions from loops containing two bidoublet zero modes, the leading order non-diagonal contribution is not suppressed relative to the higher contributions by the size of the loop integral by which it is multiplied, however, due to the necessarily UV localised (in order to correctly reproduce the SM fermionic mass spectrum) nature of the triplet zero modes it will in fact be exponentially suppressed and will again be subdominant. We must again conclude that the leading order GBM contributions are those from diagrams containing two heavy modes and that as such they are subdominant to Yukawa insertion contributions from diagrams containing similar KK modes. For completeness we again utilise the expressions (5.23)-(5.25) to state the approximate analytical expressions for the contributions to T_T^{ψ} from $n \leq 1$ modes

$$T_T^{00}(\mu) \simeq \left(-\frac{\pi}{s_W^2}\right)\left(\frac{g^2v^2}{4}\right)\frac{(kL)^2}{M_{KK}^4}\left\{\left(\frac{(1+2c_4^{\psi})}{e^{(1+2c_4^{\psi})kL}-1}\right)^2\frac{e^{2(1+2c_4^{\psi})kL}}{\left(3+2c_4^{\psi}\right)^2}+\mathcal{O}\left(\frac{1}{kL}\right)\right\}$$

$$\times\left(L^{00}_{R^4R^4}(0)\right)^{\overline{\text{MS}}}, \tag{5.50}$$

$$T_T^{01}(\mu) \simeq \left(-\frac{2\pi}{s_W^2}\right)\left(\frac{g^2v^2}{4}\right)\frac{(kL)^2}{M_{KK}^4}\left\{\frac{\left(1+\alpha_R^{\psi}\right)\left(1+2c_4^{\psi}\right)}{e^{(1+2c_4^{\psi})kL}-1}\frac{e^{(1+2c_4^{\psi})kL}}{\left(7/2+\alpha_R^{\psi}+c_4^{\psi}\right)^2}\right.$$

$$\left.+\mathcal{O}\left(\frac{1}{kL}\right)\right\}\times\left(L^{\bar{1}0}_{R^4R^4}(0)\right)^{\overline{\text{MS}}}, \tag{5.51}$$

$$T_T^{10}(\mu) \simeq \left(-\frac{\pi c_W^2}{3s_W^4}\right)\left(\frac{g^2v^2}{4}\right)\frac{kL}{M_{KK}^4}\left\{\frac{\left(1+\alpha_R^\psi\right)\left(1+2c_4^\psi\right)}{e^{(1+2c_4^\psi)kL}-1}\left[\frac{e^{(1+2c_4^\psi)kL}}{\left(7/2+\alpha_R^\psi+c_4^\psi\right)^2}\right.\right.$$

$$\left.\left.+\frac{2e^{(1+2c_4^\psi)kL}}{\left(7/2+\alpha_R^\psi+c_4^\psi\right)^3}\right]+\mathcal{O}\left(\frac{1}{kL}\right)\right\}\times\left(L^{\bar{1}0}_{R^4R^4}(0)\right)^{\overline{\rm MS}}, \tag{5.52}$$

$$T_T^{11}(\mu) \simeq \left(-\frac{2\pi c_W^2}{s_W^4}\right)\left(\frac{g^2v^2}{4}\right)\frac{kL}{M_{KK}^4}\left\{\left[\left(\frac{\left(1+\alpha_L^\psi\right)}{\left(2+\alpha_L^\psi\right)}\right)^2+\frac{\left(1+\alpha_L^\psi\right)(1+\nu)}{\left(2+\alpha_L^\psi\right)(2+\nu)}\right.\right.$$

$$+\frac{\left(1+\alpha_L^\psi\right)(1+\nu)}{\left(2+\alpha_L^\psi\right)(2+\nu)^2}+\frac{\left(1+\alpha_L^\psi\right)(1+\nu)}{\left(2+\alpha_L^\psi\right)^3}+\mathcal{O}\left(\frac{1}{kL}\right)\left.\right]\left(L^{\bar{1}\bar{1}}_{L^4L^4}(0)\right)^{\overline{\rm MS}}$$

$$+\left[\left(\frac{\left(1+\alpha_L^\psi\right)}{\left(2+\alpha_L^\psi\right)}\right)\left(\frac{\left(1+\alpha_R^\psi\right)}{\left(2+\alpha_R^\psi\right)}\right)+\frac{\left(1+\alpha_L^\psi\right)(1+\nu)}{\left(2+\alpha_L^\psi\right)(2+\nu)}+\frac{\left(1+\alpha_L^\psi\right)(1+\nu)}{\left(2+\alpha_L^\psi\right)(2+\nu)^2}\right.$$

$$\left.\left.+\frac{\left(1+\alpha_L^\psi\right)(1+\nu)}{\left(2+\alpha_R^\psi\right)^2\left(2+\alpha_L^\psi\right)}+\mathcal{O}\left(\frac{1}{kL}\right)\right]\left(L^{\bar{1}\bar{1}}_{L^4R^4}(0)\right)^{\overline{\rm MS}}+L\leftrightarrow R\right\}. \tag{5.53}$$

To make the difference between the two separate sources of contributions manifest, we repeat the numerical analysis performed in the previous section for the case of contributions from the triplet modes. We have first tested numerically the convergence of the contributions and found that, just as was the case for bidoublet contributions, they appear to diverge, figure 5.11.

In figure 5.12 is shown the KK scale dependence of the contributions arising from

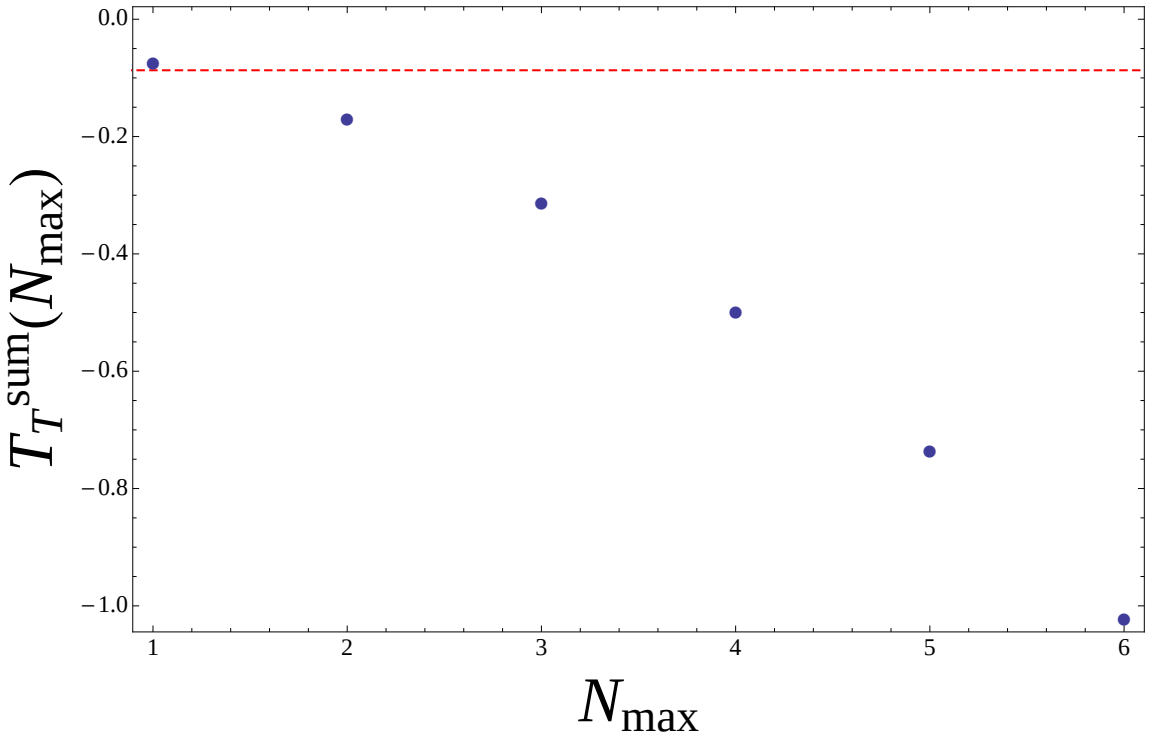

Figure 5.11: The sum of individual contributions to T_T^{ψ} from modes up to and including N_{max}, $T_T^{sum}(N_{max}) = \sum_{n=0}^{N_{max}} \sum_{m=0}^{N_{max}} T_T^{(nm)}(m_Z)$. For this calculation it was assumed that $M_{KK} \simeq 1.5\,TeV$ $(kL = 36.8)$ and $c_4^{\psi} = -0.58$. The dashed red line indicates the current lower experimental limit on the T parameter at the 95% confidence level obtained using a Higgs mass of $m_h = 117\,GeV$ [56].

diagrams containing only $n = 2$ fermionic modes or lighter for $c_4^\psi = -0.58$. It can be seen from this figure that the general form of the KK scale dependence for the triplet contributions is very similar to that for the bidoublet contributions, with the largest contributions providing constraints on M_{KK} of a similar order to that arising from S_{tree}. The one noticeable difference between the two cases is the smallness of the triplet contributions containing zero modes. This is simply due to their UV brane localisation for the value of c_4^ψ taken as our benchmark.

Figure 5.13 shows the dependence of the same individual contributions to T_T^ψ on the bulk mass parameter c_4^ψ. This has a very different form to the equivalent plot for the individual bidoublet contributions (figure 5.7). The most noteworthy difference between the two cases is the large range of c_4^ψ values for which the constraint placed on M_{KK} is clearly more stringent than that from S_{tree}; this feature follows directly from the aforementioned lack of custodial protection for such contributions. Although it might be suspected that such a feature would be problematic for model builders, the exponential UV brane localisation required in order to reproduce the mass spectrum of the SM down-type fermions means that in practice $c_4^\psi \not\gtrsim -0.5$ therefore neatly avoiding any potential problems for all generations of down-type fermion.

We can conclude that for a value of c_4^ψ which correctly reproduces the SM fermionic mass spectrum, the individual contributions to T from the fermionic triplet modes impose constraints on M_{KK} at a similar level to those arising from the fermionic bidoublet modes and also that arising from S_{tree}. It is noted, however, that for a larger region of c_4^ψ parameter space the constraints arising from the individual triplet contributions are in fact more stringent than that associated with S_{tree}. Again, a more severe constraint on M_{KK} arises from the non-convergence of the sum over all individual contributions.

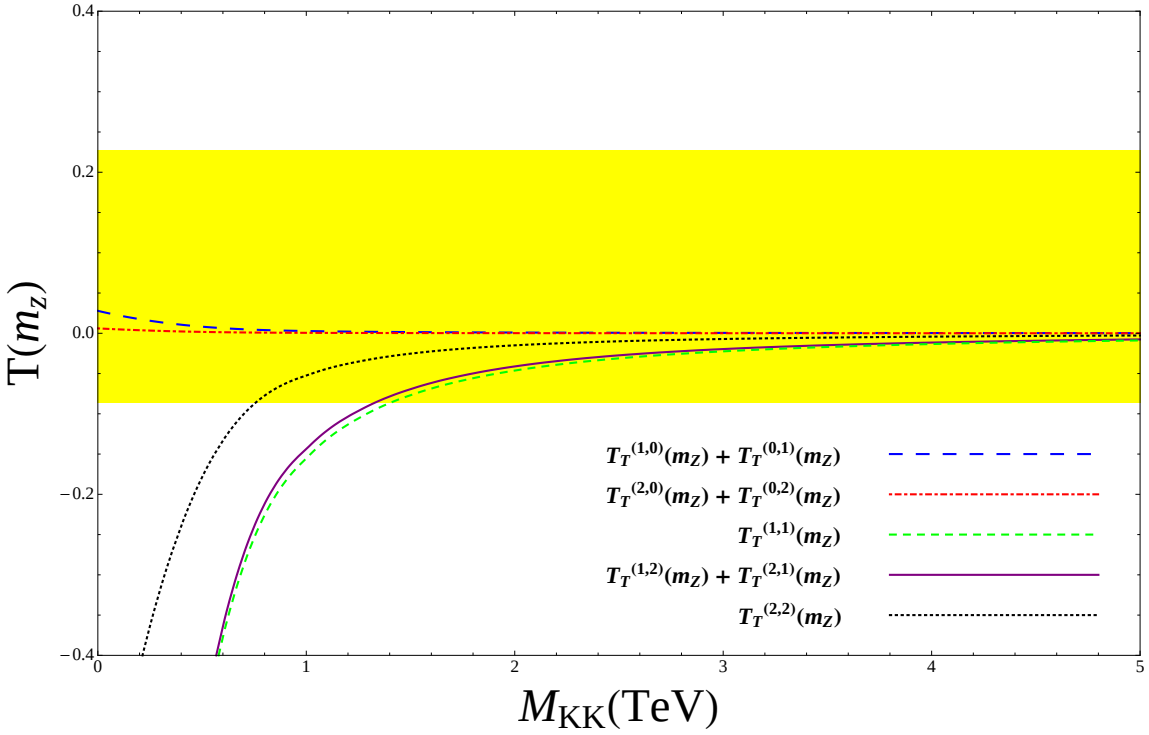

Figure 5.12: The dependence on the KK scale of the theory, $M_{KK} = ke^{-kL}$, of the contributions to T_T^{ψ} arising from diagrams containing $n = 2$ fermionic modes or lower calculated within the framework of the standard UCRS model. In calculating these contributions we have assumed $\bar{m}_{\psi}^{(n)} = \tilde{\bar{m}}_{\psi}^{(n)}$ and have used the benchmark choice for the triplet bulk mass parameter, $c_4^{\psi} = -0.58$. Due to the high level of suppression relative to the other contributions we omit $T_T^{(0,0)}$ from the above. The yellow band gives the current experimental limit on the T parameter at the 95% confidence level obtained using a Higgs mass of $m_h = 117\,GeV$ [56].

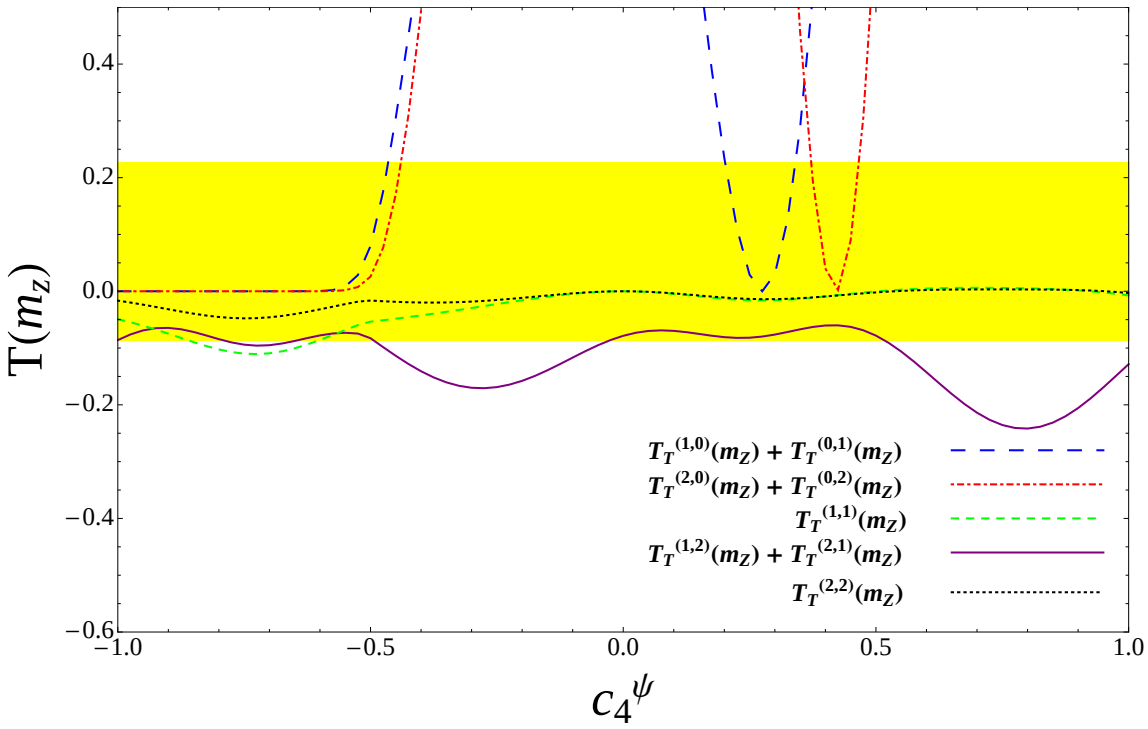

Figure 5.13: The dependence on the triplet bulk mass parameter, c_4^{ψ}, of the contributions to T_T^{ψ} arising from diagrams containing $n = 2$ fermionic modes or lower calculated within the framework of the standard UCRS model. It has been assumed during this calculation that $\bar{m}_{\psi}^{(n)} = \tilde{\bar{m}}_{\psi}^{(n)}$ and that $M_{KK} \simeq 1.5\,TeV$ $(kL = 36.8)$. Due to the high level of suppression relative to the other contributions we omit $T_T^{(0,0)}$ from the above. The yellow band is the current experimental limit on the T parameter at the 95% confidence level obtained using a Higgs mass of $m_h = 117\,GeV$ [56].

5.2.1 The LRS Model

Repeating the LRS analysis for the triplet contributions we again obtain plots for their dependence on M_{KK}, figure 5.15, and c_4^ψ, figure 5.16. In the case of the c_4^ψ dependence plot we observe the same relationship between the LRS plot and the standard plot as was seen for the bidoublet contributions, namely that the dependence of all contributions on c_4^ψ remains the same but the magnitude of the contributions is approximately an order of magnitude smaller in the LRS case.

In the case of the M_{KK} dependence plot there is a new feature which requires explaining. Due to the fact that for our benchmark value of c_4^ψ the right-handed triplet zero mode is UV localised, contributions from diagrams containing both heavy and zero mode fermions are exponentially suppressed (see (5.34)). For such contributions a reduction in kL results in a reduction in the degree of exponential suppression and therefore an increase relative to the standard case. The behaviour of the remaining contributions in the face of the kL reduction is the same as for the bidoublet case.

In summary, we again see the potential of the LRS framework to weaken the constraints on M_{KK} from the individual contributions to T. We also find again that the constraint arising from the sum of individual contributions is weakened slightly relative to the standard case with 7 KK levels needing to be included in the sum for the lower experimental limit at 95% level to be surpassed, figure 5.14; the non-convergent sum remains the dominant constraint on M_{KK}.

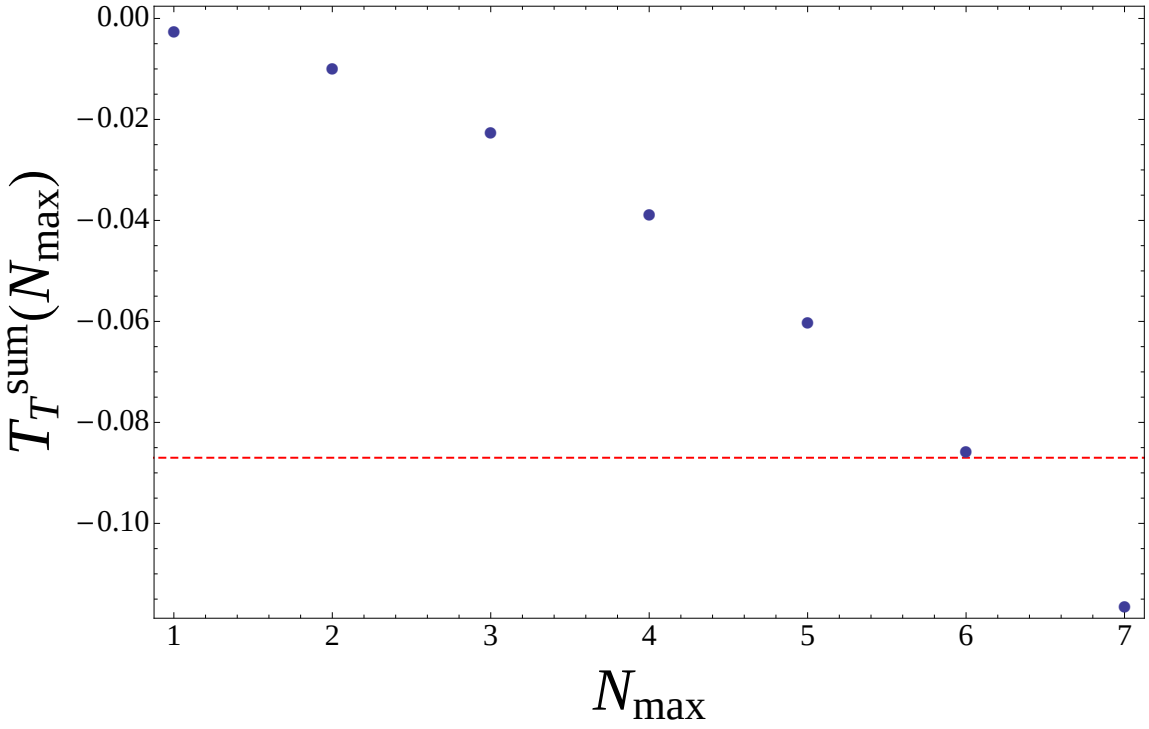

Figure 5.14: The sum of individual contributions to T_B^{ψ} from modes up to and including N_{max}, $T_T^{sum}(N_{max}) = \sum_{n=0}^{N_{max}} \sum_{m=0}^{N_{max}} T_T^{(nm)}(m_Z)$, calculated within the framework of an LRS variant of the UCRS model. For this calculation it was assumed that $k_{LRS} = 10^3\,TeV$, $M_{KK} \simeq 1.5\,TeV$ ($kL = 6.1$) and $c_4^{\psi} = -0.58$. The dashed red line indicates the current lower experimental limit on the T parameter at the 95% confidence level obtained using a Higgs mass of $m_h = 117\,GeV$ [56].

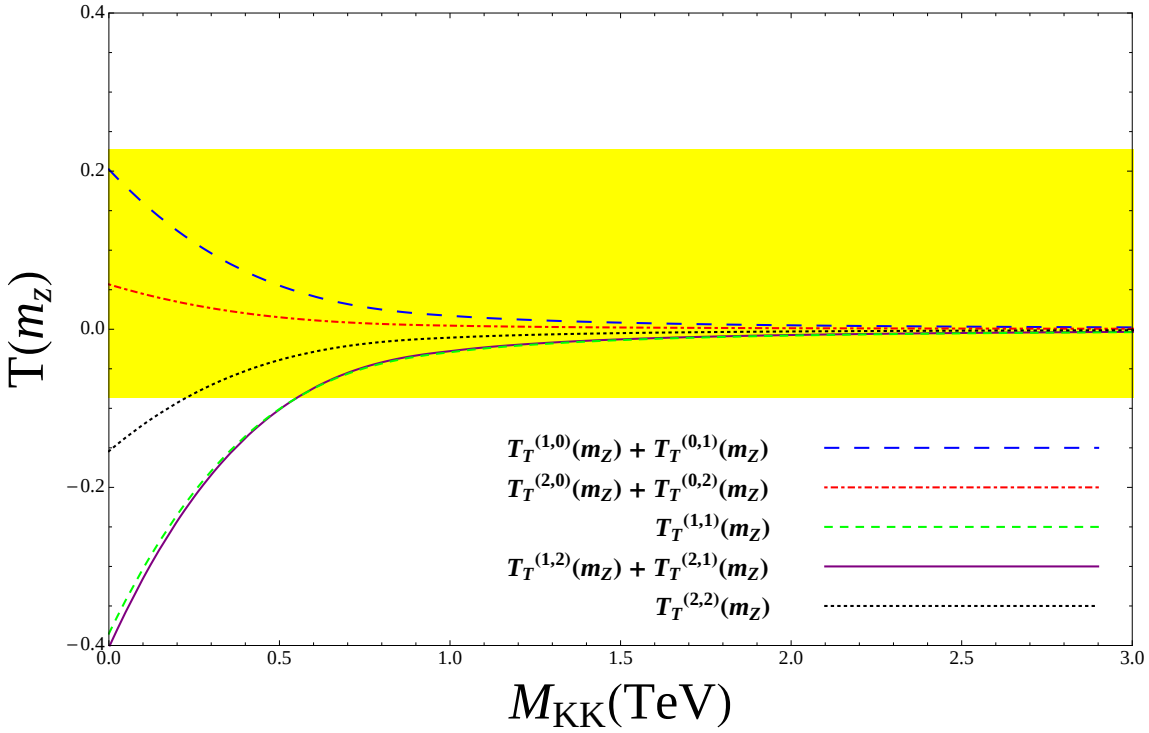

Figure 5.15: The dependence on the KK scale of the theory, $M_{KK} = ke^{-kL}$, of the contributions to T_T^{ψ} arising from diagrams containing $n = 2$ fermionic modes or lower calculated within the framework of an LRS variant of the UCRS model. In calculating these contributions we have assumed $\bar{m}_{\psi}^{(n)} = \tilde{\bar{m}}_{\psi}^{(n)}$, $k_{LRS} = 10^3\, TeV$ and have used the benchmark choice for the triplet bulk mass parameter, $c_4^{\psi} = -0.58$. Due to the high level of suppression relative to the other contributions we omit $T_T^{(0,0)}$ from the above. The yellow band gives the current experimental limit on the T parameter at the 95% confidence level obtained using a Higgs mass of $m_h = 117\, GeV$ [56].

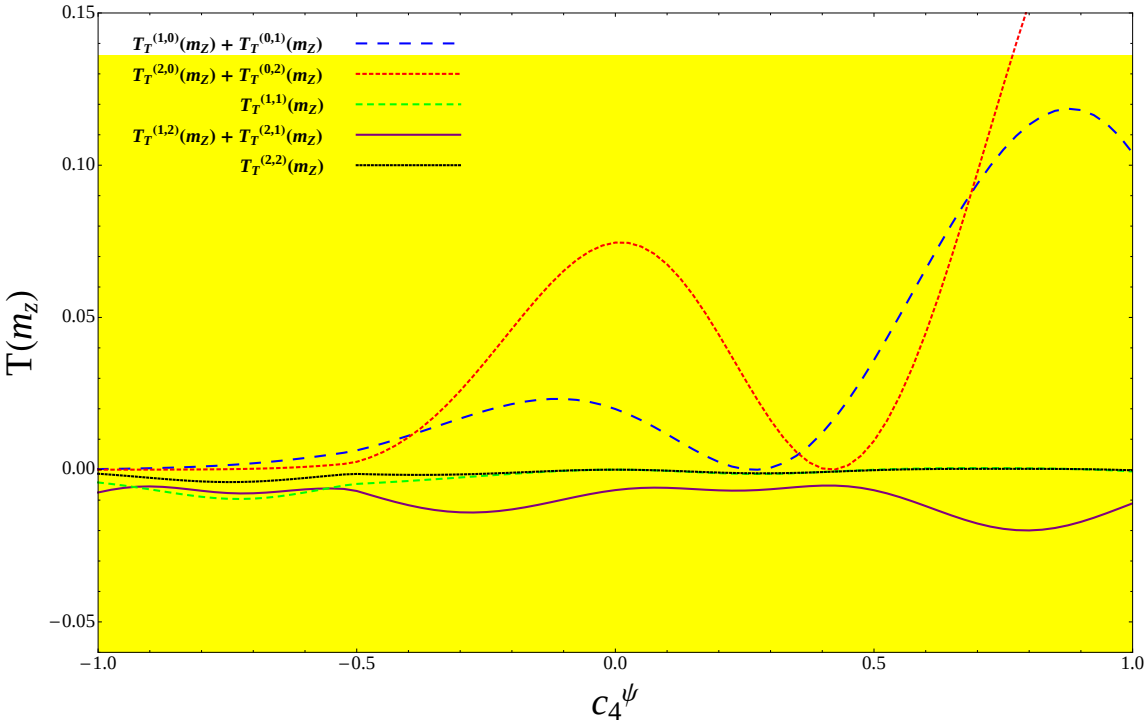

Figure 5.16: The dependence on the triplet bulk mass parameter, c_4^{ψ}, of the contributions to T_T^{ψ} arising from diagrams containing $n = 2$ fermionic modes or lower calculated within the framework of an LRS variant of the UCRS model. It has been assumed during this calculation that $\bar{m}_{\psi}^{(n)} = \tilde{\bar{m}}_{\psi}^{(n)}$, $k_{LRS} = 10^3\,TeV$ and that $M_{KK} \simeq 1.5\,TeV$ $(kL = 6.1)$. Due to the high level of suppression relative to the other contributions we omit $T_T^{(0,0)}$ from the above. The yellow band is the current experimental limit on the T parameter at the 95% confidence level obtained using a Higgs mass of $m_h = 117\,GeV$ [56].

Chapter 6

Summary and Outlook

In this thesis we have have considered the tree-level and fermionic one-loop contributions to the S and T oblique parameters within the framework of the Universal Custodial Randall-Sundrum (UCRS) model. In chapter 2 we have introduced the basic principles of the standard RS model: namely that it is a 5D model containing an additional compact spatial dimension with exponential warping along its length and two three-branes at its boundaries. This warped geometry leads to the property that the 4D effective mass scale depends exponentially on the position along the extra dimension. If the model is to solve the Hierarchy Problem, as was its original motivation, one end of the compact dimension must have an effective scale the same as the 5D mass scale (set to be of the same order as the 4D Planck scale) while the other has an effective scale $\mathcal{O}(TeV)$.

In chapter 3 the UCRS model is introduced in detail with particular attention paid to the description of the breaking of the extended, custodial, gauge symmetry of the model. Also discussed in detail is the multiplet structure of the fermionic sector and the changes in the gauge fixing Lagrangian needed if the analogue of the SM

R_ξ gauges are to be implemented in a model with the additional scalar degrees of freedom associated with a bulk Higgs field. We have additionally derived the form of the Feynman rules and mass matrices for all of the scalar degrees of freedom in the model.

In chapter 4 we have considered the contributions to the S and T parameters at tree-level in the UCRS. The particular focus of our investigation has been to determine whether the T parameter receives the same protection from the custodial gauge symmetry at tree-level as in the non-universal custodial RS models previously considered in the literature. To this end, approximate analytical expressions for the contributions to the S and T parameter were derived and their dependence on M_{KK} plotted. From these plots we were able to determine that at tree-level the T parameter does indeed receive the same protection from the gauged custodial symmetry as in the non-universal case and therefore the S parameter is responsible for the most stringent constraint on the KK scale of the theory.

In chapter 5 we have extended our consideration of the contributions to the T parameter to those arising from fermionic one-loop sources, and specifically those contributions arising from diagrams which contain mixing between right and left-handed gauge boson modes but no Yukawa mass insertions. Contrary to the assumptions made in the literature we have found that the individual KK contributions from fermionic bidoublet and triplet modes are in fact UV divergent and that the sum over all such KK contributions is also divergent. Although these divergent sums clearly place very stringent constraints on M_{KK}, without an adequate approach to their regularisation we were unable to evaluate these numerically. For the remainder of the chapter we were therefore limited to investigating the constraints on M_{KK} found from consideration of the individual KK contributions to T and were able to compare their relative importance to the constraint arising from S_{tree}. These investi-

gations showed that for both the bidoublet and triplet cases individual contributions from diagrams containing modes of $n = 2$ or lighter could impose constraints on M_{KK} or a similar strength to S_{tree}. In certain regions of the bulk fermionic mass parameter space the constraints from the individual loop contributions were in fact much stronger. These results lead us to the conclusion that the gauged custodial symmetry does not protect the T parameter from large quantum corrections.

With regards to the possible direction of future work following on from this thesis, the key question regarding the UCRS model which we have left unanswered is: does a counterterm (or set of counterterms) exist which is able to absorb the UV divergent terms we have shown to be present within the KK fermionic loop contributions to T? If the answer is no then it would raise serious questions as to the validity of the UCRS model, as stated in this thesis, as a quantum field theory and would suggest the investigation of alternative methods of breaking the extended gauge symmetry of the UCRS model down to that of the SM as an interesting area of future study.

On the other hand, if the answer is yes then (after determing the form of such a counterterm) it would be interesting to further investigate the degree to which the protection of the T parameter provided by the gauged custodial symmetry at tree-level is broken at the one-loop level. The first step in such an investigation would be to find a suitable regularisation for the divergent KK sum over the individual fermionic loop contributions to T, thereby allowing the associated constraint on M_{KK} to be calculated. It would also be of interest to calculate the contributions to T arising from loop diagrams containing the additional physical scalar DOFs discussed in chapter 3 as well as to complete a detailed investigation of those contributions from loops containing gauge boson modes briefly discussed in reference [31].

Appendix A

Overlap Integrals

A.1 Definition

In order to efficiently and clearly express both the mass matrices and Feynman rules of the scalar sector of the UCRS model it is necessary to define a general overlap integral involving the bulk profiles of all fields. The general approach used is that the type of field appearing in the integral is listed in the superscript of the shorthand while the index associated with that field is listed directly below it as a subscript. The tilde notation already introduced in chapter 2 can then be used to show the specific BCs of the fields appearing. The labels used for each of the five varieties of field in our model are all fairly transparent, however we find it convenient to list

them here as way of a reference:

$$\begin{aligned} f_H^{(n)}(y) &\rightarrow \phi, \\ f_R^{(n)}(y) &\rightarrow R^a, \\ f_L^{(n)}(y) &\rightarrow L^a, \\ f_V^{(n)}(y) &\rightarrow V, \\ f_S^{(n)}(y) &\rightarrow S. \end{aligned} \tag{A.1}$$

As an example of this notation at work we give as an example the overlap integral featuring in the Feynman rule for the interaction between two right-handed top quark modes and a heavy mode of the gauge scalar $Z_{X\,5}$,

$$\mathcal{I}^{R^1 R^1 S}_{\bar{l}\bar{m}\tilde{\bar{n}}} = \frac{1}{L}\int_0^L dy \left(e^{ky/2}\bar{f}^{(l)}_{R^1}(y)\right)\left(e^{ky/2}\bar{f}^{(m)}_{R^1}(y)\right)\left(e^{-ky}\tilde{\bar{f}}^{(n)}_{S}\right) \tag{A.2}$$

There are three features of this integral, and these overlap integrals in general, which should be stated explicitly:

- It is the normalised bulk profile of the field labeled, found from its orthonormality condition, which appears in the integrand not simply the form found by solving the relevant equation of motion.

- The range of integral is always over the whole of the extra dimension and is always accompanied by a factor of $1/L$.

- The superscript of the fermionic field label indicates the multiplet from which it originates (see (3.25) and (3.26)) and therefore the bulk mass parameter, c^a, on which the bulk profile depends.

Appendix B

Feynman Rules

B.1 Propagators

As we have decided to treat the weak scale masses arising from the SSB procedure as perturbations to the KK reduced theory, the propagators associated with each variety of internal line are defined as follows

$\psi^{(n)}$:

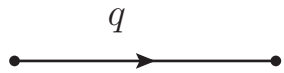

$$= \quad \frac{i}{\not{q} - M_{\psi}^{(n)}} \tag{B.1}$$

where $M_{\psi}^{(n)}$ is the KK mass associated with the n^{th} mode of the fermionic field, $\Psi(x, y)$. Note that $M_{\psi}^{(0)} = 0$.

The propagators of the vector boson modes, in the R_{ξ} gauges, are defined as

$V_{\mu}^{(n)}$:

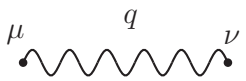

$$= \quad \frac{-i}{q^2 - M_V^{(n)\,2}} \left(g_{\mu\nu} - \frac{q_\mu q_\nu}{q^2 - \xi_V M_V^{(n)\,2}} \left(1 - \xi_V\right) \right) \tag{B.2}$$

where $M_V^{(n)}$ is the mass of the n^{th} KK mode of the 4D vector field $V_\mu(x,y)$. In the case of the vector propagators $n = 0, 1, 2\ldots$ and $M_V^{(0)\,2} = 0$. We note that as the S, T and U parameters are defined only in terms of the transverse parts of the gauge boson propagators the obvious gauge choice in which to work is the Feynman-t'Hooft gauge, $\xi_V = 1$. Another consequence of the transverse nature of the oblique parameters is that it is not necessary to include Faddeev-Popov ghosts in their calculation and hence the omission of their Feynman rules from this section.

The propagators of the gauge scalar modes are defined as

$V_5^{(n)}$:

$$= \frac{i}{q^2 - \xi_V M_V^{(n)\,2}} \tag{B.3}$$

where M_V^2 are the same masses as defined above but where now the index is $n = 1, 2, \ldots$

The propagators of the WGB modes are defined as

$\phi^{i\,(n)}$:

$$= \frac{i}{q^2 - \xi^i M_H^{(n)\,2}} \tag{B.4}$$

where we define the mass terms

$$M_H^{(1)\,2} = 0,$$

$$M_H^{(n)\,2} = m_H^{(n)\,2} \qquad (n = 2, 3, \ldots) \tag{B.5}$$

and we note that using these mass conventions the $n = 1$ mode is massless. ξ^i is the gauge fixing parameter appropriate for the WGB ϕ^i.

The propagators of the physical Higgs modes are defined as

$h^{(n)}$: 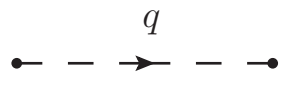 $= \dfrac{i}{q^2 - M_H^{(n)\,2}}$ (B.6)

B.2 Gauge Scalar Couplings to Fermions

In tables B.2-B.8 we list the vertex factors for the interactions between gauge scalar and quark modes. We find it convenient to define the effective couplings [40]

$$g_Z(\Psi) = \frac{g_5}{\sqrt{L}\cos\psi}\left(T_L^3(\Psi) - \sin^2\psi\, Q_{EM}(\Psi)\right)$$

$$g_{Z_X}(\Psi) = \frac{g_5}{\sqrt{L}\cos\phi}\left(T_R^3(\Psi) - \left(T_R^3(\Psi) + Q_X(\Psi)\right)\sin^2\phi\right) \tag{B.7}$$

$$e = \frac{g_5\,\sin\psi}{\sqrt{L}} \tag{B.8}$$

We have not explicitly stated the vertex factors associated with the interactions of the scalar gluon modes as they can easily be obtained from those of the scalar photon modes by introducing a factor of the $SU\,(3)$ group generators t^a and replacing the factors of $eQ_{EM}\,(\psi)$ with the 4D strong coupling constant g_s

Couplings of 2 zero mode quarks to neutral gauge scalar modes	
$A_5^{(k)}$ **couplings**	
$\bar{q}_L^{d\,(0)} q_L^{d\,(0)} A_5^{(k)}$	$-\gamma^5 e\, Q_{EM}(q^d)\, \mathcal{I}_{00\bar{k}}^{L^1 L^1 S}$
$\bar{q}_L^{u\,(0)} q_L^{u\,(0)} A_5^{(k)}$	$-\gamma^5 e\, Q_{EM}(q^u)\, \mathcal{I}_{00\bar{k}}^{L^1 L^1 S}$
$\bar{D}_R^{(0)} D_R^{(0)} A_5^{(k)}$	$-\gamma^5 e\, Q_{EM}(D)\, \mathcal{I}_{00\bar{k}}^{R^3 R^3 S}$
$\bar{u}_R^{(0)} u_R^{(0)} A_5^{(k)}$	$-\gamma^5 e\, Q_{EM}(u)\, \mathcal{I}_{00\bar{k}}^{R^2 R^2 S}$
$Z_5^{(k)}$ **couplings**	
$\bar{q}_L^{d\,(0)} q_L^{d\,(0)} Z_5^{(k)}$	$-\gamma^5\, g_{Z_X}(q^d)\, \mathcal{I}_{00\bar{k}}^{L^1 L^1 S}$
$\bar{q}_L^{u\,(0)} q_L^{u\,(0)} Z_5^{(k)}$	$-\gamma^5 g_{Z_X}(q^u)\, \mathcal{I}_{00\bar{k}}^{L^1 L^1 S}$
$\bar{D}_R^{(0)} D_R^{(0)} Z_5^{(k)}$	$-\gamma^5 g_{Z_X}(D)\, \mathcal{I}_{00\bar{k}}^{R^3 R^3 S}$
$\bar{u}_R^{(0)} u_R^{(0)} Z_5^{(k)}$	$-\gamma^5 g_{Z_X}(u)\, \mathcal{I}_{00\bar{k}}^{R^2 R^2 S}$
$Z_{X\,5}^{(k)}$ **couplings**	
$\bar{q}_L^{d\,(0)} q_L^{d\,(0)} Z_{X\,5}^{(k)}$	$-\gamma^5\, g_{Z_X}\left(q^d\right)\, \mathcal{I}_{00\tilde{\bar{k}}}^{L^1 L^1 S}$
$\bar{q}_L^{u\,(0)} q_L^{u\,(0)} Z_{X\,5}^{(k)}$	$-\gamma^5\, g_{Z_X}\left(q^u\right)\, \mathcal{I}_{00\tilde{\bar{k}}}^{L^1 L^1 S}$
$\bar{D}_R^{(0)} D_R^{(0)} Z_{X\,5}^{(k)}$	$-\gamma^5\, g_{Z_X}\left(D\right)\, \mathcal{I}_{00\tilde{\bar{k}}}^{R^3 R^3 S}$
$\bar{u}_R^{(0)} u_R^{(0)} Z_{X\,5}^{(k)}$	$-\gamma^5\, g_{Z_X}\left(u\right)\, \mathcal{I}_{00\tilde{\bar{k}}}^{R^2 R^2 S}$

Table B.1: A list of the vertex factors for interactions between neutral gauge scalar KK modes and two quark zero modes.

Couplings of 1 zero mode and 1 heavy quark to neutral gauge scalar modes	
$A_5^{(k)}$ **couplings**	
$\bar{q}_L^{d\,(n)} q_L^{d\,(0)} A_5^{(k)}$	$-\gamma^5 e\, Q_{EM}(q^d)\, \mathcal{I}_{n0\bar{k}}^{L^1 L^1 S}$
$\bar{q}_L^{u\,(n)} q_L^{u\,(0)} A_5^{(k)}$	$-\gamma^5 e\, Q_{EM}(q^u)\, \mathcal{I}_{n0\bar{k}}^{L^1 L^1 S}$
$\bar{D}_R^{(n)} D_R^{(0)} A_5^{(k)}$	$-\gamma^5 e\, Q_{EM}(D)\, \mathcal{I}_{n0\bar{k}}^{R^3 R^3 S}$
$\bar{u}_R^{(n)} u_R^{(0)} A_5^{(k)}$	$-\gamma^5 e\, Q_{EM}(u)\, \mathcal{I}_{n0\bar{k}}^{R^2 R^2 S}$
$Z_5^{(k)}$ **couplings**	
$\bar{q}_L^{d\,(n)} q_L^{d\,(0)} Z_5^{(k)}$	$-\gamma^5\, g_{Z_X}(q^d)\, \mathcal{I}_{n0\bar{k}}^{L^1 L^1 S}$
$\bar{q}_L^{u\,(n)} q_L^{u\,(0)} Z_5^{(k)}$	$-\gamma^5 g_{Z_X}(q^u)\, \mathcal{I}_{n0\bar{k}}^{L^1 L^1 S}$
$\bar{D}_R^{(n)} D_R^{(0)} Z_5^{(k)}$	$-\gamma^5 g_{Z_X}(D)\, \mathcal{I}_{n0\bar{k}}^{R^3 R^3 S}$
$\bar{u}_R^{(n)} u_R^{(0)} Z_5^{(k)}$	$-\gamma^5 g_{Z_X}(u)\, \mathcal{I}_{n0\bar{k}}^{R^2 R^2 S}$

$Z_{X\,5}^{(k)}$ **couplings**	
$\bar{q}_L^{d\,(n)} q_L^{d\,(0)} Z_{X\,5}^{(k)}$	$-\gamma^5\, g_{Z_X}\left(q^d\right)\ \mathcal{I}_{n0\tilde{\tilde{k}}}^{L^1 L^1 S}$
$\bar{q}_L^{u\,(n)} q_L^{u\,(0)} Z_{X\,5}^{(k)}$	$-\gamma^5\, g_{Z_X}\left(q^u\right)\ \mathcal{I}_{n0\tilde{\tilde{k}}}^{L^1 L^1 S}$
$\bar{D}_R^{(n)} D_R^{(0)} Z_{X\,5}^{(k)}$	$-\gamma^5\, g_{Z_X}\left(D\right)\ \mathcal{I}_{n0\tilde{\tilde{k}}}^{R^3 R^3 S}$
$\bar{u}_R^{(n)} u_R^{(0)} Z_{X\,5}^{(k)}$	$-\gamma^5\, g_{Z_X}\left(u\right)\ \mathcal{I}_{n0\tilde{\tilde{k}}}^{R^2 R^2 S}$

Table B.2: A list of the vertex factors for interactions between a neutral gauge scalar mode, a heavy quark mode and a single zero mode quark.

Couplings of 2 heavy left-handed quarks to $A_5^{(k)}$	
$Q_{EM} = 5/3$ **quark couplings**	
$\bar{\chi}_L^{u\,(n)} \chi_L^{u\,(m)} A_5^{(k)}$	$-\gamma^5 e\, Q_{EM}(\chi^u)\, \mathcal{I}^{L^1 L^1 S}_{\tilde{n}\tilde{m}\bar{k}}$
$\bar{\psi}_L^{'\,(n)} \psi_L^{'\,(m)} A_5^{(k)}$	$-\gamma^5\, e\, Q_{EM}(\psi')\, \mathcal{I}^{L^3 L^3 S}_{\tilde{n}\tilde{m}\bar{k}}$
$\bar{\psi}_L^{''\,(n)} \psi_L^{''\,(m)} A_5^{(k)}$	$-\gamma^5\, e\, Q_{EM}(\psi'')\, \mathcal{I}^{L^3 L^3 S}_{\tilde{n}\tilde{m}\bar{k}}$
$Q_{EM} = 2/3$ **quark couplings**	
$\bar{q}_L^{u\,(n)} q_L^{u\,(m)} A_5^{(k)}$	$-\gamma^5\, e\, Q_{EM}(q^u)\, \mathcal{I}^{L^1 L^1 S}_{nm\bar{k}}$
$\bar{\chi}_L^{d\,(n)} \chi_L^{d\,(m)} A_5^{(k)}$	$-\gamma^5 e\, Q_{EM}(\chi^d)\, \mathcal{I}^{L^1 L^1 S}_{\tilde{n}\tilde{m}\bar{k}}$
$\bar{u}_L^{(n)} u_L^{(m)} A_5^{(k)}$	$-\gamma^5\, e\, Q_{EM}(u)\, \mathcal{I}^{L^2 L^2 S}_{\bar{n}\bar{m}\bar{k}}$
$\bar{U}_L^{'\,(n)} U_L^{'\,(m)} A_5^{(k)}$	$-\gamma^5\, e\, Q_{EM}(U')\, \mathcal{I}^{L^3 L^3 S}_{\tilde{n}\tilde{m}\bar{k}}$
$\bar{U}_L^{''\,(n)} U_L^{''\,(m)} A_5^{(k)}$	$-\gamma^5\, e\, Q_{EM}(U'')\, \mathcal{I}^{L^3 L^3 S}_{\tilde{n}\tilde{m}\bar{k}}$
$Q_{EM} = -1/3$ **quark couplings**	
$\bar{q}_L^{d\,(n)} q_L^{d\,(m)} A_5^{(k)}$	$-\gamma^5\, e\, Q_{EM}(q^d)\, \mathcal{I}^{L^1 L^1 S}_{nm\bar{k}}$
$\bar{D}_L^{(n)} D_L^{(m)} A_5^{(k)}$	$-\gamma^5\, e\, Q_{EM}(D)\, \mathcal{I}^{L^3 L^3 S}_{\tilde{n}\tilde{m}\bar{k}}$
$\bar{D}_L^{'\,(n)} D_L^{'\,(m)} A_5^{(k)}$	$-\gamma^5\, e\, Q_{EM}(D')\, \mathcal{I}^{L^3 L^3 S}_{\tilde{n}\tilde{m}\bar{k}}$

Table B.3: A list of the vertex factors for interactions between the $A_5^{(k)}$ modes and two left-handed heavy quarks.

Couplings of 2 heavy left-handed quarks to $Z_5^{(k)}$	
$Q_{EM} = 5/3$ **quark couplings**	
$\bar{\chi}_L^{u\,(n)} \chi_L^{u\,(m)} Z_5^{(k)}$	$-\gamma^5\, g_{Z_X}(\chi^u)\, \mathcal{I}^{L^1 L^1 S}_{\tilde{n}\tilde{m}\bar{k}}$
$\bar{\psi}_L^{'\,(n)} \psi_L^{'\,(m)} Z_5^{(k)}$	$-\gamma^5\, g_{Z_X}(\psi')\, \mathcal{I}^{L^3 L^3 S}_{\tilde{n}\tilde{m}\bar{k}}$
$\bar{\psi}_L^{''\,(n)} \psi_L^{''\,(m)} Z_5^{(k)}$	$-\gamma^5\, g_{Z_X}(\psi'')\, \mathcal{I}^{L^3 L^3 S}_{\tilde{n}\tilde{m}\bar{k}}$
$Q_{EM} = 2/3$ **quark couplings**	
$\bar{q}_L^{u\,(n)} q_L^{u\,(m)} Z_5^{(k)}$	$-\gamma^5\, g_{Z_X}(q^u)\, \mathcal{I}^{L^1 L^1 S}_{nm\bar{k}}$
$\bar{\chi}_L^{d\,(n)} \chi_L^{d\,(m)} Z_5^{(k)}$	$-\gamma^5\, g_{Z_X}(\chi^d)\, \mathcal{I}^{L^1 L^1 S}_{\tilde{n}\tilde{m}\bar{k}}$
$\bar{u}_L^{(n)} u_L^{(m)} Z_5^{(k)}$	$-\gamma^5\, g_{Z_X}(u)\, \mathcal{I}^{L^2 L^2 S}_{\bar{n}\bar{m}\bar{k}}$
$\bar{U}_L^{'\,(n)} U_L^{'\,(m)} Z_5^{(k)}$	$-\gamma^5\, g_{Z_X}(U')\, \mathcal{I}^{L^3 L^3 S}_{\tilde{n}\tilde{m}\bar{k}}$
$\bar{U}_L^{''\,(n)} U_L^{''\,(m)} Z_5^{(k)}$	$-\gamma^5\, g_{Z_X}(U'')\, \mathcal{I}^{L^3 L^3 S}_{\tilde{n}\tilde{m}\bar{k}}$
$Q_{EM} = -1/3$ **quark couplings**	
$\bar{q}_L^{d\,(n)} q_L^{d\,(m)} Z_5^{(k)}$	$-\gamma^5\, g_{Z_X}(q^d)\, \mathcal{I}^{L^1 L^1 S}_{nm\bar{k}}$
$\bar{D}_L^{'\,(n)} D_L^{'\,(m)} Z_5^{(k)}$	$-\gamma^5\, g_{Z_X}(D')\, \mathcal{I}^{L^3 L^3 S}_{\tilde{n}\tilde{m}\bar{k}}$
$\bar{D}_L^{(n)} D_L^{(m)} Z_5^{(k)}$	$-\gamma^5\, g_{Z_X}(D)\, \mathcal{I}^{L^3 L^3 S}_{\tilde{n}\tilde{m}\bar{k}}$

Table B.4: A list of the vertex factors for interactions between the $Z_5^{(k)}$ modes and two left-handed heavy quarks.

Couplings of 2 heavy left-handed quarks to $Z^{(k)}_{X\,5}$	
$Q_{EM} = 5/3$ **quark couplings**	
$\bar{\chi}^{u\,(n)}_L \chi^{u\,(m)}_L Z^{(k)}_{X\,5}$	$-\gamma^5\, g_{Z_X}(\chi^u)\, \mathcal{I}^{L^1 L^1 S}_{\tilde{n}\tilde{m}\tilde{k}}$
$\bar{\psi}^{'\,(n)}_L \psi^{'\,(m)}_L Z^{(k)}_{X\,5}$	$-\gamma^5\, g_{Z_X}(\psi')\, \mathcal{I}^{L^3 L^3 S}_{\tilde{n}\tilde{m}\tilde{k}}$
$\bar{\psi}^{''\,(n)}_L \psi^{''\,(m)}_L Z^{(k)}_{X\,5}$	$-\gamma^5\, g_{Z_X}(\psi'')\, \mathcal{I}^{L^3 L^3 S}_{\tilde{n}\tilde{m}\tilde{k}}$
$Q_{EM} = 2/3$ **quark couplings**	
$\bar{q}^{u\,(n)}_L q^{u\,(m)}_L Z^{(k)}_{X\,5}$	$-\gamma^5\, g_{Z_X}(q^u)\, \mathcal{I}^{L^1 L^1 S}_{n m \tilde{k}}$
$\bar{\chi}^{d\,(n)}_L \chi^{d\,(m)}_L Z^{(k)}_{X\,5}$	$-\gamma^5\, g_{Z_X}(\chi^d)\, \mathcal{I}^{L^1 L^1 S}_{\tilde{n}\tilde{m}\tilde{k}}$
$\bar{u}^{(n)}_L u^{(m)}_L Z^{(k)}_{X\,5}$	$-\gamma^5\, g_{Z_X}(u)\, \mathcal{I}^{L^2 L^2 S}_{\bar{n}\bar{m}\tilde{k}}$
$\bar{U}^{'\,(n)}_L U^{'\,(m)}_L Z^{(k)}_{X\,5}$	$-\gamma^5\, g_{Z_X}(U')\, \mathcal{I}^{L^3 L^3 S}_{\tilde{n}\tilde{m}\tilde{k}}$
$\bar{U}^{''\,(n)}_L U^{''\,(m)}_L Z^{(k)}_{X\,5}$	$-\gamma^5\, g_{Z_X}(U'')\, \mathcal{I}^{L^3 L^3 S}_{\tilde{n}\tilde{m}\tilde{k}}$
$Q_{EM} = -1/3$ **quark couplings**	
$\bar{q}^{d\,(n)}_L q^{d\,(m)}_L Z^{(k)}_{X\,5}$	$-\gamma^5\, g_{Z_X}(q^d)\, \mathcal{I}^{L^1 L^1 S}_{n m \tilde{k}}$
$\bar{D}^{(n)}_L D^{(m)}_L Z^{(k)}_{X\,5}$	$-\gamma^5\, g_{Z_X}(D)\, \mathcal{I}^{L^3 L^3 S}_{\bar{n}\bar{m}\tilde{k}}$
$\bar{D}^{'\,(n)}_L D^{'\,(m)}_L Z^{(k)}_{X\,5}$	$-\gamma^5\, g_{Z_X}(D')\, \mathcal{I}^{L^3 L^3 S}_{\tilde{n}\tilde{m}\tilde{k}}$

Table B.5: A list of the vertex factors for interactions between the $Z^{(k)}_{X\,5}$ modes and two left-handed heavy quarks.

Couplings of 2 zero mode quarks to $W_{L\,5}^{+\,(k)}$	
$\bar{q}_L^{u\,(0)} q_L^{d\,(0)} W_{L\,5}^{+\,(k)}$	$-\gamma^5 \dfrac{g}{\sqrt{2}} \mathcal{I}_{00\bar{k}}^{L^1 L^1 S}$

Table B.6: The vertex factor for the single interaction involving two *zero mode quarks and a positively charged gauge boson. The vertex factors for the equivalent $W_{L\,5}^{-\,(k)}$ interactions are identical.*

Couplings of 1 zero mode and 1 heavy quark to positive gauge scalar modes	
$W_{L\,5}^{+\,(k)}$ **couplings**	
$\bar{q}_L^{u\,(n)} q_L^{d\,(0)} W_{L\,5}^{+\,(k)}$	$-\gamma^5 \dfrac{g}{\sqrt{2}} \mathcal{I}_{n0\bar{k}}^{L^1 L^1 S}$
$W_{R\,5}^{+\,(k)}$ **couplings**	
$\bar{\chi}_L^{u\,(n)} q_L^{u\,(0)} W_{R\,5}^{+\,(k)}$	$-\gamma^5 \dfrac{g}{\sqrt{2}} \mathcal{I}_{\tilde{n}0\tilde{\bar{k}}}^{L^1 L^1 S}$
$\bar{\chi}_L^{d\,(n)} q_L^{d\,(0)} W_{R\,5}^{+\,(k)}$	$-\gamma^5 \dfrac{g}{\sqrt{2}} \mathcal{I}_{\tilde{n}0\tilde{\bar{k}}}^{L^1 L^1 S}$

Table B.7: A list of the vertex factors for the interactions between positively charged gauge scalar modes and a single zero mode quark. The vertex factors for the equivalent negative gauge scalar interactions are identical.

Couplings of 2 heavy quarks to positive charged gauge scalar modes	
$W^{+\,(k)}_{L\,5}$ **Couplings**	
$\bar{q}^{u\,(n)}_{L} q^{d\,(m)}_{L} W^{+\,(k)}_{L\,5}$	$-\gamma^5 \, \dfrac{g}{\sqrt{2}} \, \mathcal{I}^{L^1 L^1 S}_{nm\tilde{k}}$
$\bar{\chi}^{u\,(n)}_{L} \chi^{d\,(m)}_{L} W^{+\,(k)}_{L\,5}$	$-\gamma^5 \, \dfrac{g}{\sqrt{2}} \, \mathcal{I}^{L^1 L^1 S}_{\tilde{n}\tilde{m}\tilde{k}}$
$\bar{U}^{\prime\,(n)}_{L} D^{\prime\,(m)}_{L} W^{+\,(k)}_{L\,5}$	$-\gamma^5 \, g \, \mathcal{I}^{L^3 L^3 S}_{\tilde{n}\tilde{m}\tilde{k}}$
$\bar{\psi}^{\prime\,(n)}_{L} U^{\prime\,(m)}_{L} W^{+\,(k)}_{L\,5}$	$\gamma^5 \, g \, \mathcal{I}^{L^3 L^3 S}_{\tilde{n}\tilde{m}\tilde{k}}$
$W^{+\,(k)}_{R\,5}$ **Couplings**	
$\bar{\chi}^{u\,(n)}_{L} q^{u\,(m)}_{L} W^{+\,(k)}_{R\,5}$	$-\gamma^5 \, \dfrac{g}{\sqrt{2}} \, \mathcal{I}^{L^1 L^1 S}_{\tilde{n}m\tilde{\tilde{k}}}$
$\bar{\chi}^{d\,(n)}_{L} q^{d\,(m)}_{L} W^{+\,(k)}_{R\,5}$	$-\gamma^5 \, \dfrac{g}{\sqrt{2}} \, \mathcal{I}^{L^1 L^1 S}_{\tilde{n}m\tilde{\tilde{k}}}$
$\bar{U}^{\prime\prime\,(n)}_{L} D^{(m)}_{L} W^{+\,(k)}_{R\,5}$	$-\gamma^5 \, g \, \mathcal{I}^{L^3 L^3 S}_{\tilde{n}\tilde{m}\tilde{\tilde{k}}}$
$\bar{\psi}^{\prime\prime\,(n)}_{L} U^{\prime\prime\,(m)}_{L} W^{+\,(k)}_{R\,5}$	$\gamma^5 \, g \, \mathcal{I}^{L^3 L^3 S}_{\tilde{n}\tilde{m}\tilde{\tilde{k}}}$

Table B.8: A list of vertex factors for the interactions between positively charged gauge scalar modes and two heavy quarks. The vertex factors for the equivalent negative gauge scalar interactions are identical.

B.3 Higgs Sector Scalar Couplings to Fermions

In tables B.9-B.18 we list the vertex factors for the interactions between the scalar DOFs originating from the Higgs bidoublet (WGB and physical Higgs field) and quark modes. We refer to these scalar DOFs as a group as the Higgs sector scalars (HSS).

It is also necessary to define the dimensionless 4D effective Yukawa couplings

$$Y^{u,\,d} = \frac{Y^{u,\,d}_{5D}}{\sqrt{L}} \tag{B.9}$$

Couplings of 2 zero mode quarks to WGB modes	
$\phi^{0\,(k)}$ **couplings**	
$\bar{q}_L^{u\,(0)} u_R^{(0)} \phi^{0\,(k)}$	$-Y^u\, \mathcal{I}_{00k}^{L^1R^2\phi}$
$\bar{q}_L^{d\,(0)} D_R^{(0)} \phi^{0\,(k)}$	$Y^d\, \mathcal{I}_{00k}^{L^1R^3\phi}$
$\phi^{-\,(k)}$ **coupling**	
$\bar{q}_L^{d\,(0)} u_R^{(0)} \phi^{-\,(k)}$	$-\sqrt{2}Y^u\, \mathcal{I}_{00k}^{L^1R^2\phi}$
$\phi^{+\,(k)}$ **coupling**	
$\bar{q}_L^{u\,(0)} D_R^{(0)} \phi^{+\,(k)}$	$-\sqrt{2}Y^d\, \mathcal{I}_{00k}^{L^1R^3\phi}$

Table B.9: A list of vertex factors for interactions between WGB modes and two zero mode quarks.

Couplings of $\phi^{0\,(k)}$ to 1 zero mode and 1 heavy quark	
$\xi_1 \to \xi_2$ **transitions**	
$\bar{q}_L^{u\,(0)} u_R^{(m)} \phi^{0\,(k)}$	$-Y^u\ \mathcal{I}_{0mk}^{L^1R^2\phi}$
$\bar{\chi}_L^{d\,(n)} u_R^{(0)} \phi^{0\,(k)}$	$-Y^u\ \mathcal{I}_{\tilde{n}0k}^{L^1R^2\phi}$
$\xi_1 \to T_3$ **transitions**	
$\bar{q}_L^{d\,(0)} D_R^{'(m)} \phi^{0\,(k)}$	$Y^d\ \mathcal{I}_{0\tilde{\tilde{m}}k}^{L^1R^3\phi}$
$\bar{q}_L^{u\,(0)} U_R^{'(m)} \phi^{0\,(k)}$	$\frac{1}{\sqrt{2}} Y^d\ \mathcal{I}_{0\tilde{\tilde{m}}k}^{L^1R^3\phi}$
$\xi_1 \to T_4$ **transitions**	
$\bar{q}_L^{d\,(0} D_R^{(m)} \phi^{0\,(k)}$	$Y^d\ \mathcal{I}_{0mk}^{L^1R^3\phi}$
$\bar{q}_L^{u\,(0)} U_R^{''(m)} \phi^{0\,(k)}$	$\frac{1}{\sqrt{2}} Y^d\ \mathcal{I}_{0\tilde{\tilde{m}}k}^{L^1R^3\phi}$

Table B.10: A list of vertex factors for interactions involving $\phi^{0\,(k)}$, a zero mode and a heavy quark.

Couplings of $\phi^{+\,(k)}$ to 1 zero mode and 1 heavy quark	
$\xi_1 \to \xi_2$ **transitions**	
$\bar{\chi}_L^{u\,(n)} u_R^{(0)} \phi^{+\,(k)}$	$\sqrt{2} Y^u \, \mathcal{I}_{\widetilde{n}0k}^{L^1 R^2 \phi}$
$\xi_1 \to T_4$ **transitions**	
$\bar{q}_L^{u\,(0)} D_R^{(m)} \phi^{+\,(k)}$	$-\sqrt{2} Y^d \, \mathcal{I}_{0mk}^{L^1 R^3 \phi}$

Table B.11: A list of vertex factors for interactions between $\phi^{+\,(k)}$, a zero mode and a heavy quark.

Couplings of $\phi^{-\,(k)}$ to 1 zero mode and 1 heavy quark	
$\xi_1 \to \xi_2$ **transitions**	
$\bar{q}_L^{d\,(0)} u_R^{(m)} \phi^{-\,(k)}$	$-\sqrt{2} Y^u \; \mathcal{I}_{0mk}^{L^1 R^2 \phi}$
$\xi_1 \to T_3$ **transitions**	
$\bar{q}_L^{d\,(0)} U_R^{'\,(m)} \phi^{-\,(k)}$	$-\sqrt{2} Y^u \; \mathcal{I}_{0\tilde{\bar{m}}k}^{L^1 R^3 \phi}$
$\bar{q}_L^{u\,(0)} \psi_R^{'\,(m)} \phi^{-\,(k)}$	$\sqrt{2} Y^d \; \mathcal{I}_{0\tilde{\bar{m}}k}^{L^1 R^3 \phi}$
$\xi_1 \to T_4$ **transitions**	
$\bar{q}_L^{d\,(0)} U_R^{''\,(m)} \phi^{-\,(k)}$	$-\sqrt{2} Y^u \; \mathcal{I}_{0\tilde{\bar{m}}k}^{L^1 R^3 \phi}$

Table B.12: A list of vertex factors for interactions between negatively charged WGB modes and a single zero mode quark.

Couplings of $\phi^{0\,(k)}$ to 2 heavy quarks	
$\xi_1 \to \xi_2$ **transitions**	
$\bar{q}_L^{u\,(n)} u_R^{(m)} \phi^{0\,(k)}$	$-Y^u\ \mathcal{I}^{L^1R^2\phi}_{nmk}$
$\bar{\chi}_L^{u\,(n)} u_R^{(m)} \phi^{0\,(k)}$	$-Y^u\ \mathcal{I}^{L^1R^2\phi}_{\tilde{n}mk}$
$\xi_1 \to T_3$ **transitions**	
$\bar{q}_L^{d\,(n)} D_R^{'\,(m)} \phi^{0\,(k)}$	$Y^d\ \mathcal{I}^{L^1R^3\phi}_{n\tilde{\tilde{m}}k}$
$\bar{q}_L^{u\,(n)} U_R^{'\,(m)} \phi^{0\,(k)}$	$\frac{1}{\sqrt{2}} Y^d\ \mathcal{I}^{L^1R^3\phi}_{n\tilde{\tilde{m}}k}$
$\bar{\chi}_L^{d\,(n)} U_R^{'\,(m)} \phi^{0\,(k)}$	$\frac{-1}{\sqrt{2}} Y^d\ \mathcal{I}^{L^1R^3\phi}_{\tilde{n}\tilde{\tilde{m}}k}$
$\bar{\chi}_L^{u\,(n)} \psi_R^{'\,(m)} \phi^{0\,(k)}$	$Y^d\ \mathcal{I}^{L^1R^3\phi}_{\tilde{n}\tilde{\tilde{m}}k}$
$\xi_1 \to T_4$ **transitions**	
$\bar{q}_L^{d\,(n)} D_R^{(m)} \phi^{0\,(k)}$	$Y^d\ \mathcal{I}^{L^1R^3\phi}_{nmk}$
$\bar{q}_L^{u\,(n)} U_R^{''\,(m)} \phi^{0\,(k)}$	$-\frac{1}{\sqrt{2}} Y^d\ \mathcal{I}^{L^1R^3\phi}_{n\tilde{\tilde{m}}k}$
$\bar{\chi}_L^{u\,(n)} U_R^{''\,(m)} \phi^{0\,(k)}$	$\frac{1}{\sqrt{2}} Y^d\ \mathcal{I}^{L^1R^3\phi}_{\tilde{n}\tilde{\tilde{m}}k}$
$\bar{\chi}_L^{u\,(n)} \psi_R^{''\,(m)} \phi^{0\,(k)}$	$Y^d\ \mathcal{I}^{L^1R^3\phi}_{\tilde{n}\tilde{\tilde{m}}k}$

Table B.13: A list of vertex factors for the interactions between $\phi^{0\,(k)}$ and two heavy quarks.

Couplings of $\phi^{+\,(k)}$ to 2 heavy quarks	
$\xi_1 \to \xi_2$ **transitions**	
$\bar{\chi}_L^{u\,(n)} u_R^{(m)} \phi^{+\,(k)}$	$\sqrt{2} Y^u \, \mathcal{I}^{L^1 R^2 \phi}_{\tilde{n} m k}$
$\xi_1 \to T_3$ **transitions**	
$\bar{\chi}_L^{d\,(n)} D_R^{'\,(m)} \phi^{+\,(k)}$	$-\sqrt{2} Y^d \, \mathcal{I}^{L^1 R^3 \phi}_{\tilde{n}\tilde{\tilde{m}} k}$
$\bar{\chi}_L^{u\,(n)} U_R^{'\,(m)} \phi^{+\,(k)}$	$-Y^d \, \mathcal{I}^{L^1 R^3 \phi}_{\tilde{n}\tilde{\tilde{m}} k}$
$\xi_1 \to T_4$ **transitions**	
$\bar{q}_L^{u\,(n)} D_R^{(m)} \phi^{+\,(k)}$	$-\sqrt{2} Y^d \, \mathcal{I}^{L^1 R^3 \phi}_{n m k}$
$\bar{\chi}_L^{u\,(n)} U_R^{''\,(m)} \phi^{+\,(k)}$	$-Y^d \, \mathcal{I}^{L^1 R^3 \phi}_{\tilde{n}\tilde{\tilde{m}} k}$

Table B.14: A list of vertex factors for the interactions between $\phi^{+\,(k)}$ and two heavy quarks.

Couplings of $\phi^{-\,(k)}$ to 2 heavy quarks	
$\xi_1 \to \xi_2$ **transitions**	
$\bar{q}_L^{d\,(n)} u_R^{(m)} \phi^{-\,(k)}$	$-\sqrt{2} Y^u \, \mathcal{I}^{L^1 R^2 \phi}_{nmk}$
$\xi_1 \to T_3$ **transitions**	
$\bar{q}_L^{d\,(n)} U_R^{'\,(m)} \phi^{-\,(k)}$	$-Y^u \, \mathcal{I}^{L^1 R^3 \phi}_{n\tilde{\tilde{m}}k}$
$\bar{q}_L^{u\,(n)} \psi_R^{'\,(m)} \phi^{-\,(k)}$	$\sqrt{2} Y^d \, \mathcal{I}^{L^1 R^3 \phi}_{n\tilde{\tilde{m}}k}$
$\xi_1 \to T_4$ **transitions**	
$\bar{q}_L^{d\,(n)} U_R^{''\,(m)} \phi^{-\,(k)}$	$-Y^u \, \mathcal{I}^{L^1 R^3 \phi}_{n\tilde{\tilde{m}}k}$
$\bar{\chi}_L^{d\,(n)} \psi_R^{''\,(m)} \phi^{-\,(k)}$	$\sqrt{2} Y^d \, \mathcal{I}^{L^1 R^3 \phi}_{\tilde{n}\tilde{\tilde{m}}k}$

Table B.15: A list of vertex factors for the interactions between $\phi^{-\,(k)}$ and two heavy quarks.

Couplings of $h^{(k)}$ to 2 zero mode quarks	
$\bar{q}_L^{u\,(0)} u_R^{(0)} h^{(k)}$	$-iY^u \, \mathcal{I}^{L^1 R^2 \phi}_{00k}$
$\bar{q}_L^{d\,(0)} D_R^{(0)} h^{(k)}$	$-iY^d \, \mathcal{I}^{L^1 R^2 \phi}_{00k}$

Table B.16: A list of vertex factors for the interactions between $h^{(k)}$ and two zero mode quarks.

Couplings of $h^{(k)}$ to 1 zero mode and 1 heavy quark	
$\xi_1 \to \xi_2$ **transitions**	
$\bar{\chi}_L^{d\,(n)} u_R^{(0)} h^{(k)}$	$iY^u\ \mathcal{I}^{L^1R^2\phi}_{\tilde{n}0k}$
$\bar{q}_L^{u\,(0)} u_R^{(m)} h^{(k)}$	$-iY^u\ \mathcal{I}^{L^1R^2\phi}_{0mk}$
$\xi_1 \to T_3$ **transitions**	
$\bar{q}_L^{d\,(0)} D_R^{'\,(m)} h^{(k)}$	$-iY^d\ \mathcal{I}^{L^1R^3\phi}_{0\tilde{\bar{m}}k}$
$\bar{q}_L^{u\,(0)} U_R^{'\,(m)} h^{(k)}$	$\frac{i}{\sqrt{2}} Y^d\ \mathcal{I}^{L^1R^3\phi}_{0\tilde{\bar{m}}k}$
$\xi_1 \to T_4$ **transitions**	
$\bar{q}_L^{d\,(0)} D_R^{(m)} h^{(k)}$	$-iY^u\ \mathcal{I}^{L^1R^3\phi}_{0mk}$
$\bar{q}_L^{u\,(0)} U_R^{''\,(m)} h^{(k)}$	$-\frac{i}{\sqrt{2}} Y^d\ \mathcal{I}^{L^1R^3\phi}_{0\tilde{\bar{m}}k}$

Table B.17: A list of vertex factors for the interactions between $h^{(k)}$, one zero mode and one heavy quark.

Couplings of $h^{(k)}$ to 2 heavy quarks	
$\xi_1 \to \xi_2$ **transitions**	
$\bar{\chi}_L^{d\,(n)} u_R^{(m)} h^{(k)}$	$iY^u\ \mathcal{I}^{L^1R^2\phi}_{\widetilde{n}mk}$
$\bar{q}_L^{u\,(n)} u_R^{(m)} h^{(k)}$	$-iY^u\ \mathcal{I}^{L^1R^2\phi}_{nmk}$
$\xi_1 \to T_3$ **transitions**	
$\bar{q}_L^{d\,(n)} D_R^{'(m)} h^{(k)}$	$iY^d\ \mathcal{I}^{L^1R^3\phi}_{n\widetilde{\widetilde{m}}k}$
$\bar{q}_L^{u\,(n)} U_R^{'(m)} h^{(k)}$	$\frac{i}{\sqrt{2}} Y^d\ \mathcal{I}^{L^1R^3\phi}_{n\widetilde{\widetilde{m}}k}$
$\bar{\chi}_L^{d\,(n)} U_R^{'(m)} h^{(k)}$	$\frac{i}{\sqrt{2}} Y^d\ \mathcal{I}^{L^1R^3\phi}_{\widetilde{n}\widetilde{\widetilde{m}}k}$
$\bar{\chi}_L^{u\,(n)} \psi_R^{'(m)} h^{(k)}$	$-iY^d\ \mathcal{I}^{L^1R^3\phi}_{\widetilde{n}\widetilde{\widetilde{m}}k}$
$\xi_1 \to T_4$ **transitions**	
$\bar{q}_L^{d\,(n)} D_R^{(m)} h^{(k)}$	$-iY^u\ \mathcal{I}^{L^1R^3\phi}_{nmk}$
$\bar{q}_L^{u\,(n)} U_R^{''(m)} h^{(k)}$	$-\frac{i}{\sqrt{2}} Y^d\ \mathcal{I}^{L^1R^3\phi}_{n\widetilde{\widetilde{m}}k}$
$\bar{\chi}_L^{d\,(n)} U_R^{''(m)} h^{(k)}$	$-\frac{i}{\sqrt{2}} Y^d\ \mathcal{I}^{L^1R^3\phi}_{\widetilde{n}\widetilde{\widetilde{m}}k}$
$\bar{\chi}_L^{u\,(n)} \psi_R^{''(m)} h^{(k)}$	$iY^d\ \mathcal{I}^{L^1R^3\phi}_{\widetilde{n}\widetilde{\widetilde{m}}k}$

Table B.18: A list of vertex factors for interactions between $h^{(k)}$ and two heavy quarks.

B.4 Couplings of 2 Gauge Scalars to 1 Vector Boson

In tables B.19-B.23 we list the vertex factors for interactions between two gauge scalar and one gauge vector modes.

Couplings of the zero mode photon to 2 gauge scalar modes	
$W_{L\,5}^{-\,(n)} W_{L\,5}^{+\,(n)} A^{(0)\,\mu}$	$e\left(q^- - q^+\right)_\mu$
$W_{R\,5}^{-\,(n)} W_{R\,5}^{+\,(n)} A^{(0)\,\mu}$	$e\left(q^- - q^+\right)_\mu$

Table B.19: A list of vertex factors for interactions involving the zero mode photon and two gauge scalar modes.

Couplings of the zero mode Z boson to 2 gauge scalar modes	
$W_{L\,5}^{-\,(n)} W_{L\,5}^{+\,(n)} Z^{(0)\,\mu}$	$g\cos\psi\left(q^- - q^+\right)_\mu$
$W_{R\,5}^{-\,(n)} W_{R\,5}^{+\,(n)} Z^{(0)\,\mu}$	$-g\dfrac{\sin^2\psi}{\cos\psi}\left(q^- - q^+\right)_\mu$

Table B.20: A list of vertex factors for interactions involving the zero mode Z vector boson and two gauge scalar modes.

Couplings of the zero mode $W_L^{\pm}$ boson to 2 gauge scalar modes	
$W_{L\,5}^{\pm\,(n)} A_5^{(n)} W_L^{\mp\,(0)\,\mu}$	$\mp e \left(q^{\pm} - q^{\gamma}\right)_{\mu}$
$W_{L\,5}^{\pm\,(n)} Z_5^{(n)} W_L^{\mp\,(0)\,\mu}$	$\mp g \cos\psi \left(q^{\pm} - q^{Z}\right)_{\mu}$

Table B.21: A list of vertex factors for interactions involving the zero mode $W_L^{\pm}$ bosons and two gauge scalar modes.

Couplings of a heavy neutral vector boson mode and 2 gauge scalar modes	
$A^{(k)\,\mu}$ **couplings**	
$W_{L\,5}^{-\,(n)} W_{L\,5}^{+\,(m)} A^{(k)\,\mu}$	$e \left(q^{-} - q^{+}\right)_{\mu} \mathcal{I}^{SSV}_{\tilde{n}\tilde{m}k}$
$W_{R\,5}^{-\,(n)} W_{R\,5}^{+\,(m)} A^{(k)\,\mu}$	$e \left(q^{-} - q^{+}\right)_{\mu} \mathcal{I}^{SSV}_{\tilde{\tilde{n}}\tilde{\tilde{m}}k}$
$Z^{(k)\,\mu}$ **couplings**	
$W_{L\,5}^{-\,(n)} W_{L\,5}^{+\,(m)} Z^{(k)\,\mu}$	$g \cos\psi \left(q^{-} - q^{+}\right)_{\mu} \mathcal{I}^{SSV}_{\tilde{n}\tilde{m}k}$
$W_{R\,5}^{-\,(n)} W_{R\,5}^{+\,(m)} Z^{(k)\,\mu}$	$-g \dfrac{\sin^2\psi}{\cos\psi} \left(q^{-} - q^{+}\right)_{\mu} \mathcal{I}^{SSV}_{\tilde{\tilde{n}}\tilde{\tilde{m}}k}$
$Z_X^{(k)\,\mu}$ **couplings**	
$W_{R\,5}^{-\,(n)} W_{R\,5}^{+\,(m)} Z_X^{(k)\,\mu}$	$g \cos\phi \left(q^{-} - q^{+}\right)_{\mu} \mathcal{I}^{SSV}_{\tilde{\tilde{n}}\tilde{\tilde{m}}\tilde{k}}$

Table B.22: A list of vertex factors for interactions involving a heavy neutral vector boson mode and two charged gauge scalar modes.

Couplings of a heavy, positive vector boson mode and 2 gauge scalar modes	
$W_L^{+\,(k)\,\mu}$ **couplings**	
$W_{L\,5}^{-\,(n)} A_5^{(m)} W_L^{+\,(k)\,\mu}$	$e\ \left(q^- - q^\gamma\right)_\mu\ \mathcal{I}^{SSV}_{\tilde{n}\tilde{m}k}$
$W_{L\,5}^{-\,(n)} Z_5^{(m)} W_L^{+\,(k)\,\mu}$	$g\cos\psi\ \left(q^- - q^Z\right)_\mu\ \mathcal{I}^{SSV}_{\tilde{n}\tilde{m}k}$
$W_L^{+\,(k)\,\mu}$ **couplings**	
$W_{R\,5}^{-\,(n)} A_5^{(m)} W_R^{+\,(k)\,\mu}$	$e\ \left(q^- - q^\gamma\right)_\mu\ \mathcal{I}^{SSV}_{\tilde{n}\tilde{m}\tilde{k}}$
$W_{R\,5}^{-\,(n)} Z_5^{(m)} W_R^{+\,(k)\,\mu}$	$-g\dfrac{\sin^2\psi}{\cos\psi}\ \left(q^- - q^Z\right)_\mu\ \mathcal{I}^{SSV}_{\tilde{n}\tilde{m}\tilde{k}}$
$W_{R\,5}^{-\,(n)} Z_{X\,5}^{(m)} W_R^{+\,(k)\,\mu}$	$g\cos\phi\ \left(q^- - q^{Z_X}\right)_\mu\ \mathcal{I}^{SSV}_{\tilde{\tilde{n}}\tilde{\tilde{m}}\tilde{k}}$

Table B.23: A list of the vertex factors for interactions involving a heavy, positively charged vector boson mode and two gauge scalar modes. The vertex factors for the equivalent interactions involving negatively charged vector bosons are the same up to a relative minus sign.

B.5 Couplings of 2 Higgs Sector Scalars to 1 Vector Boson

In tables B.24-B.26 we list the vertex factors associated with the interactions between scalar DOFs from the Higgs bidoublet and vector boson modes.

Couplings of zero mode vector bosons to HSS modes	
$A^{(0)\,\mu}$ **coupling**	
$\phi^{+\,(n)}\phi^{-\,(n)}A^{(0)\,\mu}$	$-e\left(q^{-}-q^{+}\right)_{\mu}$
$Z^{(0)\,\mu}$ **couplings**	
$\phi^{+\,(n)}\phi^{-\,(n)}Z^{(0)\,\mu}$	$\frac{-g}{2}\left(\frac{1-2\sin^{2}\psi}{\cos\psi}\right)\left(q^{-}-q^{+}\right)_{\mu}$
$W_{L}^{+\,(0)\,\mu}$ **couplings**	
$\phi^{0\,(n)}h^{(n)}Z^{(0)\,\mu}$	$\frac{ig}{2\cos\psi}\left(q^{h}-q^{0}\right)$
$\phi^{+\,(n)}\phi^{0\,(n)}W_{L}^{-\,(0)\,\mu}$	$\frac{-g}{2}\left(q^{+}-q^{0}\right)_{\mu}$
$\phi^{-\,(n)}\phi^{0\,(n)}W_{L}^{+\,(0)\,\mu}$	$\frac{-g}{2}\left(q^{0}-q^{-}\right)_{\mu}$
$\phi^{+\,(n)}h^{(n)}W_{L}^{-\,(0)\,\mu}$	$\frac{-ig}{2}\left(q^{+}-q^{h}\right)_{\mu}$
$\phi^{-\,(n)}h^{(n)}W_{L}^{+\,(0)\,\mu}$	$\frac{-ig}{2}\left(q^{-}-q^{h}\right)_{\mu}$

Table B.24: A list of vertex factors for interactions involving zero mode vector bosons and two HSS modes.

Couplings of a heavy, neutral vector boson mode to 2 HSS modes	
$A^{(0)\,\mu}$ **couplings**	
$\phi^{+\,(n)}\phi^{-\,(m)}A^{(k)\,\mu}$	$-e\ \ (q^- - q^+)_\mu\ \mathcal{I}^{\phi\phi V}_{nmk}$
$Z^{(k)\,\mu}$ **couplings**	
$\phi^{+\,(n)}\phi^{-\,(m)}Z^{(k)\,\mu}$	$\dfrac{-g}{2}\left(\dfrac{1-2\sin^2\psi}{\cos\psi}\right)\ (q^- - q^+)_\mu\ \mathcal{I}^{\phi\phi V}_{nmk}$
$\phi^{0\,(n)}h^{(m)}Z^{(k)\,\mu}$	$\dfrac{ig}{2\cos\psi}\ \left(q^h - q^0\right)_\mu\ \mathcal{I}^{\phi\phi V}_{nmk}$
$Z_X^{(0)\,\mu}$ **couplings**	
$\phi^{+\,(n)}\phi^{-\,(m)}Z_X^{(k)\,\mu}$	$\dfrac{-g}{2}\cos\phi\ (q^- - q^+)_\mu\ \mathcal{I}^{\phi\phi V}_{nm\tilde{k}}$
$\phi^{0\,(n)}h^{(m)}Z_X^{(k)\,\mu}$	$\dfrac{-ig}{2}\cos\phi\ \left(q^h - q^0\right)_\mu\ \mathcal{I}^{\phi\phi V}_{nm\tilde{k}}$

Table B.25: A list of vertex factors for interactions involving a heavy, neutral vector boson mode and two HSS modes.

Couplings of a heavy, positive vector boson mode to 2 HSS modes	
$\phi^{-\,(n)}\phi^{0\,(m)}W_L^{+\,(k)\,\mu}$	$\dfrac{-g}{2}\,\left(q^0-q^-\right)_\mu\,\mathcal{I}^{\phi\phi V}_{nmk}$
$\phi^{-\,(n)}\phi^{0\,(m)}W_R^{+\,(k)\,\mu}$	$\dfrac{-g}{2}\,\left(q^0-q^-\right)_\mu\,\mathcal{I}^{\phi\phi V}_{nm\widetilde{k}}$

Table B.26: A list of vertex factors for interactions involving a heavy, positively charged vector boson mode and two HSS modes. The vertex factors for the equivalent interactions involving negative vector boson modes are the same up to a relative minus sign.

B.6 Couplings of 1 Gauge Scalar to 2 Vector Bosons

In tables B.28- B.31 we list the vertex factors for interactions between two gauge vector modes and a single gauge scalar mode. Simply decomposing the gauge fields and dimensionally reducing our theory as normal, the couplings of interest contain the following, dimensionful, overlap integral factor

$$\mathcal{I}^{V'VS}_{nmk} = \frac{1}{L}\int_0^L dy\, e^{-2ky}\left(\partial_5 f^{(n)}_{\mu}\right) f^{(m)}_{\mu} f^{(k)}_{5}. \tag{B.10}$$

It is preferable however to write couplings in terms of dimensionless overlap integrals and so we use the gauge field profile identity (derived using the usual Bessel function identity 2.40),

$$\partial_5 f^{(n)}_{V}(y) = m^{(n)}_{V} f^{(n)}_{S}, \tag{B.11}$$

to rewrite our overlap integral in the form

$$\mathcal{I}^{V'VS}_{nmk} = m^{(n)}_{V}\,\mathcal{I}^{SVS}_{nmk} = \frac{m^{(n)}_{V}}{L}\int_0^L dy\, e^{-2ky} f^{(n)}_{S}(y) f^{(m)}_{V}(y) f^{(k)}_{S}(y). \tag{B.12}$$

An important feature to note about the couplings between two gauge vector modes and a gauge scalar mode is that, with the exception of those couplings given in table B.31, there are no couplings between vector fields of the same KK mode (diagonal couplings). Due to the small difference in the masses and bulk profiles associated with the different BCs the size of these diagonal couplings are much smaller than that of the non-diagonal coupling proportional as they to the mass difference between different KK modes.

Couplings of a negative gauge scalar mode to 1 zero mode and 1 heavy vector boson	
$W_{R\,5}^{-\,(k)}$ **couplings**	
$W_R^{+\,(n)\,\mu} A^{(0)\,\nu} W_{R\,5}^{-\,(k)}$	$-e\,\widetilde{m}_V^{(n)}\;\mathcal{I}^{SVS}_{\tilde{\bar{n}}0\tilde{\bar{k}}}$
$W_R^{+\,(n)\,\mu} Z^{(0)\,\nu} W_{R\,5}^{-\,(k)}$	$g\dfrac{\sin^2\psi}{\cos\psi}\,\widetilde{m}_V^{(n)}\;\mathcal{I}^{SVS}_{\tilde{\bar{n}}0\tilde{\bar{k}}}$
$W_{L\,5}^{-\,(k)}$ **couplings**	
$W_L^{+\,(0)\,\mu} A^{(m)\,\nu} W_{L\,5}^{-\,(k)}$	$e\,m_V^{(m)}\;\mathcal{I}^{SVS}_{\bar{m}0\bar{k}}$
$W_L^{+\,(n)\,\mu} A^{(0)\,\nu} W_{L\,5}^{-\,(k)}$	$-e\,m_V^{(n)}\;\mathcal{I}^{SVS}_{\bar{n}0\bar{k}}$
$W_L^{+\,(0)\,\mu} Z^{(m)\,\nu} W_{L\,5}^{-\,(k)}$	$g\cos\psi\,m_V^{(m)}\;\mathcal{I}^{SVS}_{\bar{m}0\bar{k}}$
$W_L^{+\,(n)\,\mu} Z^{(0)\,\nu} W_{L\,5}^{-\,(k)}$	$-g\cos\psi\,m_V^{(n)}\;\mathcal{I}^{SVS}_{\bar{m}0\bar{k}}$

Table B.27: A list of vertex factors for interactions involving a negatively charged gauge scalar mode, one zero mode and one heavy vector boson. The vertex factors associated with the equivalent interactions involving positive gauge scalar modes are the same up to a relative minus sign.

Couplings of neutral gauge scalar modes to 1 zero mode and 1 heavy vector boson	
$W_L^{+\,(0)\,\mu} W_L^{-\,(m)\,\nu} A_5^{(k)}$	$-e\, m_V^{(m)}\ \mathcal{I}^{SVS}_{\bar{m}0\bar{k}}$
$W_L^{+\,(n)\,\mu} W_L^{-\,(0)\,\nu} A_5^{(k)}$	$e\, m_V^{(m)}\ \mathcal{I}^{SVS}_{\bar{0}n\bar{k}}$
$W_L^{+\,(0)\,\mu} W_L^{-\,(m)\,\nu} Z_5^{(k)}$	$-g\cos\psi\, m_V^{(m)}\ \mathcal{I}^{SVS}_{\bar{m}0\bar{k}}$
$W_L^{+\,(n)\,\mu} W_L^{-\,(0)\,\nu} Z_5^{(k)}$	$g\cos\psi\, m_V^{(m)}\ \mathcal{I}^{SVS}_{\bar{0}n\bar{k}}$

Table B.28: A list of vertex factors for interactions involving a neutral gauge scalar mode, one zero mode and one heavy vector boson.

Non-diagonal couplings of a negative gauge scalar mode to 2 heavy vector bosons	
$W_{R\,5}^{-\,(k)}$ **couplings**	
$W_R^{+\,(n)\,\mu} A^{(m)\,\nu} W_{R\,5}^{-\,(k)}$	$-e\left(\widetilde{m}_V^{(n)}\,\mathcal{I}^{SVS}_{\tilde{\tilde{n}}\tilde{m}\tilde{\tilde{k}}} - m_V^{(m)}\,\mathcal{I}^{SVS}_{m\tilde{n}\tilde{\tilde{k}}}\right)$
$W_R^{+\,(n)\,\mu} Z^{(m)\,\nu} W_{R\,5}^{-\,(k)}$	$g\dfrac{\sin^2\psi}{\cos\psi}\left(\widetilde{m}_V^{(n)}\,\mathcal{I}^{SVS}_{\tilde{\tilde{n}}\tilde{m}\tilde{\tilde{k}}} - m_V^{(m)}\,\mathcal{I}^{SVS}_{m\tilde{n}\tilde{\tilde{k}}}\right)$
$W_R^{+\,(n)\,\mu} Z_X^{(m)\,\nu} W_{R\,5}^{-\,(k)}$	$-g\cos\phi\left(\widetilde{m}_V^{(n)}\,\mathcal{I}^{SVS}_{\tilde{n}\tilde{m}\tilde{\tilde{k}}} - \widetilde{m}_V^{(m)}\,\mathcal{I}^{SVS}_{\tilde{\tilde{m}}\tilde{n}\tilde{\tilde{k}}}\right)$
$W_{L\,5}^{-\,(k)}$ **couplings**	
$W_L^{+\,(n)\,\mu} A^{(m)\,\nu} W_{L\,5}^{-\,(k)}$	$-e\left(m_V^{(n)}\,\mathcal{I}^{SVS}_{\bar{n}m\tilde{\tilde{k}}} - m_V^{(m)}\,\mathcal{I}^{SVS}_{mn\tilde{\tilde{k}}}\right)$
$W_L^{+\,(n)\,\mu} Z^{(m)\,\nu} W_{L\,5}^{-\,(k)}$	$-g\cos\psi\left(m_V^{(n)}\,\mathcal{I}^{SVS}_{\bar{n}m\tilde{\tilde{k}}} - m_V^{(m)}\,\mathcal{I}^{SVS}_{mn\tilde{\tilde{k}}}\right)$

Table B.29: A list of vertex factors for the interactions between a negative gauge scalar mode and two heavy vector bosons. The vertex factors associated with the equivalent interactions involving positive gauge scalar modes are the same up to a relative minus sign.

Non-diagonal couplings of a neutral gauge scalar mode to 2 heavy vector bosons	
$W_L^{+\,(n)\,\mu}$ **couplings**	
$W_L^{+\,(n)\,\mu} W_L^{-\,(m)\,\nu} A_5^{(k)}$	$e\left(m_V^{(n)}\,\mathcal{I}^{SVS}_{\bar{n}m\bar{k}} - m_V^{(m)}\,\mathcal{I}^{SVS}_{\bar{m}n\bar{k}}\right)$
$W_L^{+\,(n)\,\mu} W_L^{-\,(m)\,\nu} Z_5^{(k)}$	$g\cos\psi\left(m_V^{(n)}\,\mathcal{I}^{SVS}_{\bar{n}m\bar{k}} - m_V^{(m)}\,\mathcal{I}^{SVS}_{\bar{m}n\bar{k}}\right)$
$W_R^{+\,(n)\,\mu}$ **couplings**	
$W_R^{+\,(n)\,\mu} W_R^{-\,(m)\,\nu} A_5^{(k)}$	$e\left(\widetilde{m}_V^{(n)}\,\mathcal{I}^{SVS}_{\tilde{\bar{n}}\tilde{m}\bar{k}} - \widetilde{m}_V^{(m)}\,\mathcal{I}^{SVS}_{\tilde{\bar{m}}\tilde{n}\bar{k}}\right)$
$W_R^{+\,(n)\,\mu} W_R^{-\,(m)\,\nu} Z_5^{(k)}$	$-g\dfrac{\sin^2\psi}{\cos\psi}\left(\widetilde{m}_V^{(n)}\,\mathcal{I}^{SVS}_{\tilde{\bar{n}}\tilde{m}\bar{k}} - \widetilde{m}_V^{(m)}\,\mathcal{I}^{SVS}_{\tilde{\bar{m}}\tilde{n}\bar{k}}\right)$
$W_R^{+\,(n)\,\mu} W_R^{-\,(m)\,\nu} Z_{X\,5}^{(k)}$	$g\cos\phi\left(\widetilde{m}_V^{(n)}\,\mathcal{I}^{SVS}_{\tilde{\bar{n}}\tilde{m}\tilde{\bar{k}}} - \widetilde{m}_V^{(m)}\,\mathcal{I}^{SVS}_{\tilde{\bar{m}}\tilde{n}\tilde{\bar{k}}}\right)$

Table B.30: A list of vertex factors for the interactions between a neutral gauge scalar mode and two heavy vector bosons.

Diagonal couplings of a gauge scalar mode and 2 heavy vector bosons	
$W_R^{+\,(n)\,\mu} A^{(n)\,\nu} W_{R\,5}^{-\,(k)}$	$-e\left(\widetilde{m}_V^{(n)}\,\mathcal{I}^{SVS}_{\tilde{\bar{n}}n\tilde{\bar{k}}} - m_V^{(n)}\,\mathcal{I}^{SVS}_{\bar{n}\tilde{n}\tilde{\bar{k}}}\right)$
$W_R^{+\,(n)\,\mu} Z^{(n)\,\nu} W_{R\,5}^{-\,(k)}$	$g\dfrac{\sin^2\phi}{\cos\psi}\left(\widetilde{m}_V^{(n)}\,\mathcal{I}^{SVS}_{\tilde{\bar{n}}n\tilde{\bar{k}}} - m_V^{(n)}\,\mathcal{I}^{SVS}_{\bar{n}\tilde{n}\tilde{\bar{k}}}\right)$

Table B.31: A list of vertex factors for interactions involving one gauge scalar and two heavy vector bosons of the same KK level. The vertex factors associated with the equivalent interactions involving positive gauge scalar modes are the same up to a relative minus sign.

B.7 Couplings of 1 Higgs Sector Scalar to 2 Vector Bosons

In tables B.32-B.35 we list the vertex factors associated with the interactions involving two vector boson modes and a single HSS mode.

Couplings of 1 HSS to 2 zero mode vector bosons	
$W_L^{+\,(0)\,\mu} W_L^{-\,(0)\,\nu} h^{(1)}$	$\dfrac{ivg^2}{2}\, g_{\mu\nu}$
$Z^{(0)\,\mu} Z^{(0)\,\nu} h^{(1)}$	$\dfrac{ivg^2}{2\cos^2\psi}\, g_{\mu\nu}$
$Z^{(0)\,\mu} W_L^{\pm\,(0)\,\nu} \phi^{\mp\,(1)}$	$vg^2 \dfrac{\sin^2\psi}{2\cos\psi}\, g_{\mu\nu}$
$A^{(0)\,\mu} W_L^{\pm\,(0)\,\nu} \phi^{\mp\,(1)}$	$-ve\dfrac{g}{2}\, g_{\mu\nu}$

Table B.32: A list of vertex factors for the zero mode interactions between two zero mode vector bosons and a single zero mode HSS.

Couplings of neutral HSS to 1 heavy and 1 zero mode vector boson	
$h^{(k)}$ **couplings**	
$W_L^{+\,(0)\,\mu} W_L^{-\,(m)\,\nu} h^{(k)}$	$\dfrac{ivg^2}{2}\, g_{\mu\nu}\, \mathcal{I}^{VV\phi\phi}_{0m1k}$
$W_R^{\pm\,(n)\,\mu} W_L^{\mp\,(0)\,\nu} h^{(k)}$	$-i\dfrac{vg^2}{2}\, g_{\mu\nu}\, \mathcal{I}^{VV\phi\phi}_{\tilde{n}01k}$
$Z^{(0)\,\mu} Z^{(m)\,\nu} h^{(k)}$	$\dfrac{ivg^2}{4\cos^2\psi}\, g_{\mu\nu}\, \mathcal{I}^{VV\phi\phi}_{n01k}$
$Z^{(0)\,\mu} Z_X^{(m)\,\nu} h^{(k)}$	$-i\dfrac{vg^2}{2}\dfrac{\cos\phi}{\cos\psi}\, g_{\mu\nu}\, \mathcal{I}^{VV\phi\phi}_{0\tilde{m}1k}$
$\phi^{0\,(k)}$ **couplings**	
$W_R^{+\,(n)\,\mu} W_L^{-\,(0)\,\nu} \phi^{0\,(k)}$	$-\dfrac{vg^2}{2}\, g_{\mu\nu}\, \mathcal{I}^{VV\phi\phi}_{\tilde{n}01k}$
$W_L^{+\,(0)\,\mu} W_R^{-\,(m)\,\nu} \phi^{0\,(k)}$	$\dfrac{vg^2}{2}\, g_{\mu\nu}\, \mathcal{I}^{VV\phi\phi}_{0\tilde{m}1k}$

Table B.33: A list of vertex factors for interactions between a neutral HSS mode, a zero mode and a heavy vector boson and a neutral HSS.

Couplings of $\phi^{-\,(k)}$ to 1 heavy and 1 zero mode vector boson	
$W_L^{+\,(m)\,\nu}$ **couplings**	
$A^{(0)\,\mu} W_L^{+\,(m)\,\nu} \phi^{-\,(k)}$	$-ve\dfrac{g}{2}\, g_{\mu\nu}\, \mathcal{I}^{VV\phi\phi}_{0m1k}$
$Z^{(0)\,\mu} W_L^{+\,(m)\,\nu} \phi^{-\,(k)}$	$vg^2 \dfrac{\sin^2\psi}{2\cos\psi}\, g_{\mu\nu}\, \mathcal{I}^{VV\phi\phi}_{0m1k}$
$Z_X^{(n)\,\mu} W_L^{+\,(0)\,\nu} \phi^{-\,(k)}$	$-\dfrac{vg^2}{2}\cos\phi\, g_{\mu\nu}\, \mathcal{I}^{VV\phi\phi}_{\tilde{n}01k}$
$W_R^{+\,(m)\,\nu}$ **couplings**	
$Z^{(0)\,\mu} W_R^{+\,(m)\,\nu} \phi^{-\,(k)}$	$vg^2 \cos\psi\, g_{\mu\nu}\, \mathcal{I}^{VV\phi\phi}_{0\tilde{m}1k}$
$A^{(0)\,\mu} W_R^{+\,(m)\,\nu} \phi^{-\,(k)}$	$ve\dfrac{g}{2}\, g_{\mu\nu}\, \mathcal{I}^{VV\phi\phi}_{0\tilde{m}1k}$

Table B.34: A list of vertex factors for interactions between a negatively charged HSS mode, a heavy and a zero mode vector boson. The vertex factors associated with the equivalent interactions involving positive HSS modes are the same up to a relative minus sign.

Couplings of a neutral HSS to 2 heavy vector bosons	
$h^{(k)}$ **couplings**	
$W_L^{+\,(n)\,\mu} W_L^{-\,(m)\,\nu} h^{(k)}$	$\dfrac{ivg^2}{2}\, g_{\mu\nu}\, \mathcal{I}^{VV\phi\phi}_{nm1k}$
$W_R^{\pm\,(n)\,\mu} W_L^{\mp\,(m)\,\nu} h^{(k)}$	$-i\dfrac{vg^2}{2}\, g_{\mu\nu}\, \mathcal{I}^{VV\phi\phi}_{\tilde{n}m1k}$
$Z^{(n)\,\mu} Z^{(m)\,\nu} h^{(k)}$	$\dfrac{ivg^2}{4\cos^2\psi}\, g_{\mu\nu}\, \mathcal{I}^{VV\phi\phi}_{nm1k}$
$Z^{(n)\,\mu} Z_X^{(m)\,\nu} h^{(k)}$	$-i\dfrac{vg^2}{2}\dfrac{\cos\phi}{\cos\psi}\, g_{\mu\nu}\, \mathcal{I}^{VV\phi\phi}_{n\tilde{m}1k}$
$W_R^{+\,(n)\,\mu} W_R^{-\,(m)\,\nu} h^{(k)}$	$i\dfrac{vg^2}{2}\, g_{\mu\nu}\, \mathcal{I}^{VV\phi\phi}_{\tilde{n}\tilde{m}1k}$
$Z_X^{(n)\,\mu} Z_X^{(m)\,\nu} h^{(k)}$	$i(2)\cos\phi\dfrac{vg^2}{4}\, g_{\mu\nu}\, \mathcal{I}^{VV\phi\phi}_{\tilde{n}\tilde{m}1k}$
$\phi^{0\,(k)}$ **couplings**	
$W_R^{+\,(n)\,\mu} W_L^{-\,(0)\,\nu} \phi^{0\,(k)}$	$-\dfrac{vg^2}{2}\, g_{\mu\nu}\, \mathcal{I}^{VV\phi\phi}_{\tilde{n}01k}$
$W_L^{+\,(0)\,\mu} W_R^{-\,(m)\,\nu} \phi^{0\,(k)}$	$\dfrac{vg^2}{2}\, g_{\mu\nu}\, \mathcal{I}^{VV\phi\phi}_{0\tilde{m}1k}$

Table B.35: A list of vertex factors for interactions between a single HSS mode and two heavy vector bosons.

Couplings of $\phi^{-\,(k)}$ to 2 heavy vector bosons	
$W_L^{+\,(m)\,\nu}$ **couplings**	
$A^{(n)\,\mu} W_L^{+\,(m)\,\nu} \phi^{-\,(k)}$	$-ve\dfrac{g}{2}\, g_{\mu\nu}\, \mathcal{I}^{VV\phi\phi}_{nm1k}$
$Z^{(n)\,\mu} W_L^{+\,(m)\,\nu} \phi^{-\,(k)}$	$vg^2 \dfrac{\sin^2\psi}{2\cos\psi}\, g_{\mu\nu}\, \mathcal{I}^{VV\phi\phi}_{nm1k}$
$Z_X^{(n)\,\mu} W_L^{+\,(m)\,\nu} \phi^{-\,(k)}$	$-\dfrac{vg^2}{2}\cos\phi\, g_{\mu\nu}\, \mathcal{I}^{VV\phi\phi}_{\tilde{n}m1k}$
$W_R^{+\,(m)\,\nu}$ **couplings**	
$Z^{(n)\,\mu} W_R^{+\,(m)\,\nu} \phi^{-\,(k)}$	$vg^2 \cos\psi\, g_{\mu\nu}\, \mathcal{I}^{VV\phi\phi}_{n\tilde{m}1k}$
$A^{(n)\,\mu} W_R^{+\,(m)\,\nu} \phi^{-\,(k)}$	$ve\dfrac{g}{2}\, g_{\mu\nu}\, \mathcal{I}^{VV\phi\phi}_{n\tilde{m}1k}$

Table B.36: A list of vertex factors for interactions between a negatively charged HSS mode and two heavy vector bosons. The vertex factors associated with the equivalent interactions involving positive HSS modes are the same up to a relative minus sign.

B.8 Couplings of 2 Higgs Sector Scalars to 2 Vector Bosons

In tables B.37-B.45 we list the vertex factors the interactions involving two vector boson modes and two HSS modes

Couplings of 2 charged WGB modes to 2 zero mode vector Bosons	
Charged vector bosons	
$W_L^{+\,(0)\,\mu} W_L^{-\,(0)\,\nu} \phi^{+\,(k)} \phi^{-\,(k)}$	$\dfrac{ig^2}{2}\, g_{\mu\nu}$
Neutral vector bosons	
$Z^{(0)\,\mu} Z^{(0)\,\nu} \phi^{-\,(k)} \phi^{+\,(k)}$	$\dfrac{ig^2}{2} \dfrac{\left(1 - 2\sin^2\psi\right)^2}{\cos^2\psi}\, g_{\mu\nu}$
$A^{(0)\,\mu} A^{(0)\,\nu} \phi^{-\,(k)} \phi^{+\,(k)}$	$2ie^2 g_{\mu\nu}$
$Z^{(0)\,\mu} A^{(0)\,\nu} \phi^{-\,(k)} \phi^{+\,(k)}$	$ige \dfrac{\left(1 - 2\sin^2\psi\right)}{\cos\psi}\, g_{\mu\nu}$

Table B.37: A list of vertex factors for interactions involving two charged HSS modes and two zero mode vector bosons.

Couplings of 2 neutral HSS modes and 2 zero mode vector bosons	
Charged vector bosons	
$W_L^{+\,(0)\,\mu} W_L^{-\,(0)\,\nu} h^{(k)} h^{(k)}$	$\dfrac{ig}{2}\, g_{\mu\nu}$
$W_L^{+\,(0)\,\mu} W_L^{-\,(0)\,\nu} \phi^{0\,(k)} \phi^{0\,(k)}$	$\dfrac{ig}{2}\, g_{\mu\nu}$
Neutral vector bosons	
$Z^{(0)\,\mu} Z^{(0)\,\nu} \phi^{0\,(k)} \phi^{0\,(k)}$	$\dfrac{ig^2}{2\cos^2\psi}\, g_{\mu\nu}$
$Z^{(0)\,\mu} Z^{(0)\,\nu} h^{(k)} h^{(k)}$	$\dfrac{ig^2}{2\cos^2\psi}\, g_{\mu\nu}$

Table B.38: A list of vertex factors for interactions involving two neutral HSS modes and two zero mode vector bosons.

Couplings of 1 charged and 1 neutral HSS mode to 2 zero mode vector bosons	
$Z^{(0)\,\mu} W_L^{\pm\,(0)\,\nu} \phi^{\mp\,(k)} h^{(k)}$	$\pm\dfrac{ge}{2}\tan\psi\, g_{\mu\nu}$
$Z^{(0)\,\mu} W_L^{\pm\,(0)\,\nu} \phi^{\mp\,(k)} \phi^{0\,(k)}$	$i\dfrac{ge}{2}\tan\psi\, g_{\mu\nu}$
$A^{(0)\,\mu} W_L^{\pm\,(0)\,\nu} \phi^{\mp\,(k)} h^{(k)}$	$\mp\dfrac{ge}{2}\, g_{\mu\nu}$
$A^{(0)\,\mu} W_L^{\pm\,(0)\,\nu} \phi^{\mp\,(k)} \phi^{0\,(k)}$	$-i\dfrac{ge}{2}\, g_{\mu\nu}$

Table B.39: A list of vertex factors for interactions involving a charged HSS, a neutral HSS and two zero mode vector bosons.

Couplings of 2 charged WGB modes to 1 zero mode and 1 heavy vector boson	
Charged vector bosons	
$W_L^{+\,(n)} W_L^{-\,(0)\,\nu} \phi^{+\,(k)} \phi^{-\,((l))}$	$\frac{ig^2}{2}\, g_{\mu\nu}\, \mathcal{I}^{VV\phi\phi}_{n0kl}$
$W_R^{-\,(n)\,\mu} W_L^{-\,(0)\,\nu} \phi^{+\,(k)} \phi^{+\,(l)}$	$-\frac{ig^2}{2}\, g_{\mu\nu}\, \mathcal{I}^{VV\phi\phi}_{\widetilde{n}0kl}$
$W_R^{+\,(n)\,\mu} W_L^{+\,(0)\,\nu} \phi^{-\,(k)} \phi^{-\,(l)}$	$-\frac{ig^2}{2}\, g_{\mu\nu}\, \mathcal{I}^{VV\phi\phi}_{\widetilde{n}0kl}$
Neutral vector bosons	
$A^{(n)\,\mu} A^{(0)\,\nu} \phi^{-\,(k)} \phi^{+\,(l)}$	$ie^2\, g_{\mu\nu}\, \mathcal{I}^{VV\phi\phi}_{n0kl}$
$Z^{(n)\,\mu} Z^{(0)\,\nu} \phi^{-\,(k)} \phi^{+\,(l)}$	$\frac{ig^2}{4} \frac{\left(1-2\sin^2\psi\right)^2}{\cos^2\psi}\, g_{\mu\nu}\, \mathcal{I}^{VV\phi\phi}_{n0kl}$
$Z^{(n)\,\mu} A^{(0)\,\nu} \phi^{-\,(k)} \phi^{+\,(l)}$	$ige \frac{\left(1-2\sin^2\psi\right)}{\cos\psi}\, g_{\mu\nu}\, \mathcal{I}^{VV\phi\phi}_{n0kl}$
$Z_X^{(n)\,\mu} A^{(0)\,\nu} \phi^{-\,(k)} \phi^{+\,(l)}$	$ige\, \cos\phi\, g_{\mu\nu}\, \mathcal{I}^{VV\phi\phi}_{\widetilde{n}0kl}$
$Z_X^{(n)\,\mu} Z^{(0)\,\nu} \phi^{-\,(k)} \phi^{+\,(l)}$	$\frac{ig^2\cos\phi}{2} \frac{\left(1-2\sin^2\psi\right)}{\cos\psi}\, g_{\mu\nu}\, \mathcal{I}^{VV\phi\phi}_{\widetilde{n}0kl}$

Table B.40: A list of vertex factors for interactions involving two charged HSS modes, one zero mode and one heavy vector boson.

Couplings of 2 neutral HSS modes to 1 zero mode and 1 heavy vector boson	
Charged vector bosons	
$W_L^{+\,(n)\,\mu} W_L^{-\,(0)\,\nu} h^{(k)} h^{(l)}$	$(2)\dfrac{ig}{4}\, g_{\mu\nu}\, \mathcal{I}^{VV\phi\phi}_{n0kl}$
$W_L^{+\,(n)\,\mu} W_L^{-\,(0)\,\nu} \phi^{0\,(k)} \phi^{0\,(l)}$	$(2)\dfrac{ig}{4}\, g_{\mu\nu}\, \mathcal{I}^{VV\phi\phi}_{n0kl}$
$W_R^{\pm\,(n)\,\mu} W_L^{\mp\,(0)\,\nu} h^{(k)} h^{(l)}$	$-(2)\dfrac{ig^2}{4}\, g_{\mu\nu}\, \mathcal{I}^{VV\phi\phi}_{\widetilde{n}0kl}$
$W_R^{\pm\,(n)\,\mu} W_L^{\mp\,(0)\,\nu} \phi^{0\,(k)} \phi^{0\,(l)}$	$-(2)\dfrac{ig^2}{4}\, g_{\mu\nu}\, \mathcal{I}^{VV\phi\phi}_{\widetilde{n}0kl}$
$W_R^{\pm\,(n)\,\mu} W_L^{\mp\,(0)\,\nu} \phi^{0\,(k)} h^{(l)}$	$\mp\dfrac{g^2}{2}\, g_{\mu\nu}\, \mathcal{I}^{VV\phi\phi}_{\widetilde{n}0kl}$
Neutral vector bosons	
$Z^{(n)\,\mu} Z^{(0)\,\nu} \phi^{0\,(k)} \phi^{0\,(l)}$	$(2)\dfrac{ig^2}{8\cos^2\psi}\, g_{\mu\nu}\, \mathcal{I}^{VV\phi\phi}_{n0kl}$
$Z_X^{(n)\,\mu} Z^{(0)\,\nu} \phi^{0\,(k)} \phi^{0\,(l)}$	$-(2)\dfrac{ig^2}{4}\dfrac{\cos\phi}{\cos\psi}\, g_{\mu\nu}\, \mathcal{I}^{VV\phi\phi}_{\widetilde{n}0kl}$
$Z^{(n)\,\mu} Z^{(0)\,\nu} h^{(k)} h^{(l)}$	$(2)\dfrac{ig^2}{8\cos^2\psi}\, g_{\mu\nu}\, \mathcal{I}^{VV\phi\phi}_{n0kl}$
$Z_X^{(n)\,\mu} Z^{(0)\,\nu} h^{(k)} h^{(l)}$	$-(2)\dfrac{ig^2}{4}\dfrac{\cos\phi}{\cos\psi}\, g_{\mu\nu}\, \mathcal{I}^{VV\phi\phi}_{\widetilde{n}0kl}$

Table B.41: A list of vertex factors for interactions involving two neutral HSS modes, one zero mode and one heavy vector boson.

Couplings of 1 charged and 1 neutral HSS mode to 1 zero mode and 1 heavy vector boson	
$h^{(l)}$ **couplings**	
$W_R^{\pm\,(n)\,\mu} Z^{(0)\,\nu} \phi^{\mp\,(k)} h^{(l)}$	$\pm\dfrac{g^2}{2}\cos\psi\, g_{\mu\nu}\, \mathcal{I}^{VV\phi\phi}_{\widetilde{n}0kl}$
$W_R^{\pm\,(n)\,\mu} A^{(0)\,\nu} \phi^{\mp\,(k)} h^{(l)}$	$\pm\dfrac{eg}{2}\, g_{\mu\nu}\, \mathcal{I}^{VV\phi\phi}_{\widetilde{n}0kl}$
$Z_X^{(n)\,\mu} W_L^{\pm\,(0)\,\nu} \phi^{\mp\,(k)} h^{(l)}$	$\mp\dfrac{g^2}{2}\cos\phi\, g_{\mu\nu}\, \mathcal{I}^{VV\phi\phi}_{\widetilde{n}0kl}$
$\phi^{0\,(l)}$ **couplings**	
$W_R^{\pm\,(n)\,\mu} A^{(0)\,\nu} \phi^{\mp\,(k)} \phi^{0\,(l)}$	$\dfrac{-ieg}{2}\, g_{\mu\nu}\, \mathcal{I}^{VV\phi\phi}_{\widetilde{n}0kl}$
$W_R^{\pm\,(n)\,\mu} Z^{(0)\,\nu} \phi^{\mp\,(k)} \phi^{0\,(l)}$	$\dfrac{-ig^2}{2}\cos\psi\, g_{\mu\nu}\, \mathcal{I}^{VV\phi\phi}_{\widetilde{n}0kl}$
$Z_X^{(n)\,\mu} W_L^{\pm\,(0)\,\nu} \phi^{\mp\,(k)} \phi^{0\,(l)}$	$-\dfrac{g^2}{2}\cos\phi\, g_{\mu\nu}\, \mathcal{I}^{VV\phi\phi}_{\widetilde{n}0kl}$

Table B.42: A list of vertex factors for interactions involving one charged and one neutral HSS mode and one zero mode and one heavy vector boson.

Couplings of 2 charged WGB modes to 2 heavy vector bosons	
Charged vector bosons	
$W_L^{+\,(n)} W_L^{-\,(m)\,\nu} \phi^{+\,(k)} \phi^{-\,((l))}$	$\dfrac{ig^2}{2}\, g_{\mu\nu}\, \mathcal{I}^{VV\phi\phi}_{nmkl}$
$W_R^{\pm\,(n)\,\mu} W_L^{\pm\,(m)\,\nu} \phi^{\mp\,(k)} \phi^{\mp\,(l)}$	$-\dfrac{ig^2}{2}\, g_{\mu\nu}\, \mathcal{I}^{VV\phi\phi}_{\widetilde{n}mkl}$
$W_R^{+\,(n)\,\mu} W_R^{-\,(m)\,\nu} \phi^{-\,(k)} \phi^{+\,(l)}$	$\dfrac{ig^2}{2}\, g_{\mu\nu}\, \mathcal{I}^{VV\phi\phi}_{\widetilde{n}\widetilde{m}kl}$
Neutral vector bosons	
$A^{(n)\,\mu} A^{(m)\,\nu} \phi^{-\,(k)} \phi^{+\,(k)}$	$(2)\, ie^2\, g_{\mu\nu}\, \mathcal{I}^{VV\phi\phi}_{nmkl}$
$Z^{(n)\,\mu} Z^{(m)\,\nu} \phi^{-\,(k)} \phi^{+\,(k)}$	$\dfrac{(2)\, ig^2}{4} \dfrac{\left(1 - 2\sin^2\psi\right)^2}{\cos^2\psi}\, g_{\mu\nu}\, \mathcal{I}^{VV\phi\phi}_{nmkl}$
$Z^{(n)\,\mu} A^{(m)\,\nu} \phi^{-\,(k)} \phi^{+\,(k)}$	$\dfrac{ige}{2} \dfrac{\left(1 - 2\sin^2\psi\right)}{\cos\psi}\, g_{\mu\nu}\, \mathcal{I}^{VV\phi\phi}_{nmkl}$
$Z_X^{(n)\,\mu} A^{(m)\,\nu} \phi^{-\,(k)} \phi^{+\,(l)}$	$\dfrac{ige}{2} \cos\phi\, g_{\mu\nu}\, \mathcal{I}^{VV\phi\phi}_{\widetilde{n}mkl}$
$Z_X^{(n)\,\mu} Z^{(m)\,\nu} \phi^{-\,(k)} \phi^{+\,(l)}$	$\dfrac{ig^2 \cos\phi}{2} \dfrac{\left(1 - 2\sin^2\psi\right)}{\cos\psi}\, g_{\mu\nu}\, \mathcal{I}^{VV\phi\phi}_{\widetilde{n}mkl}$
$Z_X^{(n)\,\mu} Z_X^{(m)\,\nu} \phi^{-\,(k)} \phi^{+\,(l)}$	$\dfrac{(2) ig_2^2}{4} \cos^2\phi\, g_{\mu\nu}\, \mathcal{I}^{VV\phi\phi}_{\widetilde{n}\widetilde{m}kl}$

Table B.43: A list of vertex factors for interactions involving two charged HSS modes and two heavy vector bosons.

Couplings of 2 neutral HSS modes to 2 heavy vector bosons	
Charged vector bosons	
$W_L^{+\,(n)\,\mu} W_L^{-\,(m)\,\nu} \phi^{0\,(k)} \phi^{0\,(k)}$	$(2)\dfrac{ig}{4}\, g_{\mu\nu}\, \mathcal{I}^{VV\phi\phi}_{nmkl}$
$W_L^{+\,(n)\,\mu} W_L^{-\,(m)\,\nu} h^{(k)} h^{(l)}$	$(2)\dfrac{ig}{4}\, g_{\mu\nu}\, \mathcal{I}^{VV\phi\phi}_{nmkl}$
$W_R^{\pm\,(n)\,\mu} W_L^{\mp\,(m)\,\nu} h^{(k)} h^{(l)}$	$-(2)\dfrac{ig^2}{4}\, g_{\mu\nu}\, \mathcal{I}^{VV\phi\phi}_{\widetilde{n}mkl}$
$W_R^{\pm\,(n)\,\mu} W_L^{\mp\,(m)\,\nu} \phi^{0\,(k)} \phi^{0\,(l)}$	$-(2)\dfrac{ig^2}{4}\, g_{\mu\nu}\, \mathcal{I}^{VV\phi\phi}_{\widetilde{n}mkl}$
$W_R^{\pm\,(n)\,\mu} W_L^{\mp\,(m)\,\nu} \phi^{0\,(k)} h^{(l)}$	$\mp\dfrac{g^2}{2}\, g_{\mu\nu}\, \mathcal{I}^{VV\phi\phi}_{\widetilde{n}mkl}$
$W_R^{+\,(n)\,\mu} W_R^{-\,(m)\,\nu} \phi^{0\,(k)} \phi^{0\,(l)}$	$(2)\dfrac{ig^2}{4}\, g_{\mu\nu}\, \mathcal{I}^{VV\phi\phi}_{\widetilde{n}\widetilde{m}kl}$
$W_R^{+\,(n)\,\mu} W_R^{-\,(m)\,\nu} h^{(k)} h^{(l)}$	$(2)\dfrac{ig^2}{4}\, g_{\mu\nu}\, \mathcal{I}^{VV\phi\phi}_{\widetilde{n}\widetilde{m}kl}$
Neutral vector bosons	
$Z^{(n)\,\mu} Z^{(m)\,\nu} \phi^{0\,(k)} \phi^{0\,(l)}$	$(2)(2)\dfrac{ig^2}{8\cos^2\psi}\, g_{\mu\nu}\, \mathcal{I}^{VV\phi\phi}_{nmkl}$
$Z^{(n)\,\mu} Z^{(m)\,\nu} h^{(k)} h^{(l)}$	$(2)(2)\dfrac{ig^2}{8\cos^2\psi}\, g_{\mu\nu}\, \mathcal{I}^{VV\phi\phi}_{nmkl}$
$Z_X^{(n)\,\mu} Z^{(m)\,\nu} \phi^{0\,(k)} \phi^{0\,(l)}$	$-(2)\dfrac{ig^2}{4}\dfrac{\cos\phi}{\cos\psi}\, g_{\mu\nu}\, \mathcal{I}^{VV\phi\phi}_{\widetilde{n}mkl}$
$Z_X^{(n)\,\mu} Z^{(m)\,\nu} h^{(k)} h^{(l)}$	$-(2)\dfrac{ig^2}{4}\dfrac{\cos\phi}{\cos\psi}\, g_{\mu\nu}\, \mathcal{I}^{VV\phi\phi}_{\widetilde{n}mkl}$
$Z_X^{(n)\,\mu} Z_X^{(m)\,\nu} \phi^{0\,(k)} \phi^{0\,(l)}$	$(2)(2)\dfrac{ig_2^2}{8}\cos^2\phi\, g_{\mu\nu}\, \mathcal{I}^{VV\phi\phi}_{\widetilde{n}\widetilde{m}kl}$
$Z_X^{(n)\,\mu} Z_X^{(m)\,\nu} h^{(k)} h^{(l)}$	$(2)(2)\dfrac{ig_2^2}{8}\cos^2\phi\, g_{\mu\nu}\, \mathcal{I}^{VV\phi\phi}_{\widetilde{n}\widetilde{m}kl}$

Table B.44: A list of vertex factors for interactions involving two neutral HSS modes two heavy vector bosons.

Couplings of 1 charged and 1 neutral HSS mode to 2 heavy vector bosons	
$h^{(l)}$ **couplings**	
$W_R^{\pm\,(n)\,\mu} Z^{(m)\,\nu} \phi^{\mp\,(k)} h^{(l)}$	$\pm\frac{g^2}{2}\cos\psi\, g_{\mu\nu}\, \mathcal{I}^{VV\phi\phi}_{\tilde{n}mkl}$
$W_L^{\pm\,(n)\,\mu} Z^{(m)\,\nu} \phi^{\mp\,(k)} h^{(l)}$	$\pm\frac{g^2}{2}\cos\psi\, g_{\mu\nu}\, \mathcal{I}^{VV\phi\phi}_{nmkl}$
$W_R^{\pm\,(n)\,\mu} A^{(m)\,\nu} \phi^{\mp\,(k)} h^{(l)}$	$\pm\frac{eg}{2}\, g_{\mu\nu}\, \mathcal{I}^{VV\phi\phi}_{\tilde{n}mkl}$
$W_L^{\pm\,(n)\,\mu} A^{(m)\,\nu} \phi^{\mp\,(k)} h^{(l)}$	$\mp\frac{eg}{2}\, g_{\mu\nu}\, \mathcal{I}^{VV\phi\phi}_{nmkl}$
$Z_X^{(n)\,\mu} W_L^{\pm\,(m)\,\nu} \phi^{\mp\,(k)} h^{(l)}$	$\mp\frac{g^2}{2}\cos\phi\, g_{\mu\nu}\, \mathcal{I}^{VV\phi\phi}_{\tilde{n}mkl}$
$\phi^{0\,(l)}$ **couplings**	
$W_R^{\pm\,(n)\,\mu} A^{(m)\,\nu} \phi^{\mp\,(k)} \phi^{0\,(l)}$	$\frac{-ieg}{2}\, g_{\mu\nu}\, \mathcal{I}^{VV\phi\phi}_{\tilde{n}mkl}$
$W_L^{\pm\,(n)\,\mu} A^{(m)\,\nu} \phi^{\mp\,(k)} \phi^{0\,(l)}$	$\frac{-ieg}{2}\, g_{\mu\nu}\, \mathcal{I}^{VV\phi\phi}_{nmkl}$
$W_R^{\pm\,(n)\,\mu} Z^{(m)\,\nu} \phi^{\mp\,(k)} \phi^{0\,(l)}$	$\frac{-ig^2}{2}\cos\psi\, g_{\mu\nu}\, \mathcal{I}^{VV\phi\phi}_{\tilde{n}mkl}$
$W_L^{\pm\,(n)\,\mu} Z^{(m)\,\nu} \phi^{\mp\,(k)} \phi^{0\,(l)}$	$\frac{ig^2}{2}\cos\psi\, g_{\mu\nu}\, \mathcal{I}^{VV\phi\phi}_{nmkl}$
$Z_X^{(n)\,\mu} W_L^{\pm\,(m)\,\nu} \phi^{\mp\,(k)} \phi^{0\,(l)}$	$-\frac{ig^2}{2}\cos\phi\, g_{\mu\nu}\, \mathcal{I}^{VV\phi\phi}_{\tilde{n}mkl}$

Table B.45: A list of vertex factors for interactions involving one charged and one neutral HSS mode and two heavy vector bosons.

B.9 Couplings of 2 Gauge Scalars to 2 Vector Bosons

In tables B.46-B.54 we list the vertex factors for the interactions between two gauge scalar modes and two vector boson modes.

Couplings of 2 charged zero mode vector bosons to 2 gauge scalar modes	
Charged gauge scalars	
$W_L^{+\,(0)\,\mu} W_L^{-\,(0)\,\nu} W_{L\,5}^{+\,(k)} W_{L\,5}^{-\,(k)}$	$2ig^2\, g_{\mu\nu}$
Neutral gauge scalars	
$W_L^{+\,(0)\,\mu} W_L^{-\,(0)\,\nu} Z_5^{(k)} Z_5^{(k)}$	$2ig^2 4\cos^2\psi g_{\mu\nu}$
$W_L^{+\,(0)\,\mu} W_L^{-\,(0)\,\nu} A_5^{(k)} A_5^{(k)}$	$2ie^2 g_{\mu\nu}$
$W_L^{+\,(0)\,\mu} W_L^{-\,(0)\,\nu} A_5^{(k)} Z_5^{(k)}$	$2ieg\cos\psi g_{\mu\nu}$

Table B.46: A list of vertex factors for all interactions involving two charged zero mode vector bosons and two gauge scalar modes.

Couplings of 2 neutral zero mode vector bosons to 2 gauge scalar modes	
$W_{L\,5}^{+\,(k)}$ **couplings**	
$Z^{(0)\,\mu} Z^{(0)\,\nu} W_{L\,5}^{+\,(k)} W_{L\,5}^{-\,(k)}$	$2ig^2 \cos^2\psi \, g_{\mu\nu}$
$A^{(0)\,\mu} A^{(0)\,\nu} W_{L\,5}^{+\,(k)} W_{L\,5}^{-\,(k)}$	$2ie^2 \, g_{\mu\nu}$
$Z^{(0)\,\mu} A^{(0)\,\nu} W_{L\,5}^{+\,(k)} W_{L\,5}^{-\,(k)}$	$2ieg \cos\psi \, g_{\mu\nu}$
$W_{R\,5}^{+\,(k)}$ **couplings**	
$Z^{(0)\,\mu} Z^{(0)\,\nu} W_{R\,5}^{+\,(k)} W_{R\,5}^{-\,(k)}$	$2ie^2 \sin^2\phi \, g_{\mu\nu}$
$A^{(0)\,\mu} A^{(0)\,\nu} W_{R\,5}^{+\,(k)} W_{R\,5}^{-\,(k)}$	$2ie^2 \, g_{\mu\nu}$
$Z^{(0)\,\mu} A^{(0)\,\nu} W_{R\,5}^{+\,(k)} W_{R\,5}^{-\,(k)}$	$-2ie^2 \sin\phi \, g_{\mu\nu}$

Table B.47: A list of vertex factors for all interactions involving two neutral zero mode vector bosons and 2 gauge scalar modes.

Couplings of 1 neutral and 1 positive zero mode vector boson to 2 gauge scalar modes	
$Z_5^{(k)}$ **couplings**	
$W_L^{+\,(0)\,\mu} Z^{(0)\,\nu} W_{L\,5}^{-\,(k)} Z_5^{(k)}$	$-ig^2 \cos^2\psi \, g_{\mu\nu}$
$W_L^{+\,(0)\,\mu} A^{(0)\,\nu} W_{L\,5}^{-\,(k)} Z_5^{(k)}$	$-ige \cos\psi \, g_{\mu\nu}$
$A_5^{(k)}$ **couplings**	
$W_L^{+\,(0)\,\mu} A^{(0)\,\nu} W_{L\,5}^{-\,(k)} A_5^{(k)}$	$-ie^2 \, g_{\mu\nu}$
$W_L^{+\,(0)\,\mu} Z^{(0)\,\nu} W_{L\,5}^{-\,(k)} A_5^{(k)}$	$-ige \cos\psi \, g_{\mu\nu}$

Table B.48: A list of vertex factors for interactions involving one positive and one neutral zero mode vector boson and two gauge scalar modes. The equivalent interactions involving negative vector boson modes have identical vertex factors.

Couplings of 1 zero mode and 1 heavy charged vector boson to 2 gauge scalar modes	
Charged gauge scalars	
$W_L^{+\,(n)\,\mu} W_L^{-\,(0)\,\nu} W_{L\,5}^{+\,(k)} W_{L\,5}^{-\,(l)}$	$2ig^2\, g_{\mu\nu}\, \mathcal{I}^{VVSS}_{n0\bar{k}\bar{l}}$
Neutral gauge scalars	
$W_L^{+\,(n)\,\mu} W_L^{-\,(0)\,\nu} Z_5^{(k)} Z_5^{(l)}$	$(2)ig^2 \cos^2\psi\, g_{\mu\nu}\, \mathcal{I}^{VVSS}_{n0\bar{k}\bar{l}}$
$W_L^{+\,(n)\,\mu} W_L^{-\,(0)\,\nu} A_5^{(k)} A_5^{(l)}$	$(2)ie^2\, g_{\mu\nu}\, \mathcal{I}^{VVSS}_{n0\bar{k}\bar{l}}$
$W_L^{+\,(n)\,\mu} W_L^{-\,(0)\,\nu} A_5^{(k)} Z_5^{(l)}$	$2ig^2 \cos\psi \sin\psi\, g_{\mu\nu}\, \mathcal{I}^{VVSS}_{n0\bar{k}\bar{l}}$

Table B.49: A list of vertex factors for interactions involving one charged zero mode vector boson, one charged heavy vector boson and two gauge scalar fields.

Couplings of 1 zero mode and 1 heavy neutral vector boson to two gauge scalar modes	
$W_{L\,5}^{-\,(l)}$ **couplings**	
$Z^{(n)\,\mu} Z^{(0)\,\nu} W_{L\,5}^{+\,(k)} W_{L\,5}^{-\,(l)}$	$ig^2 \cos^2\psi \, g_{\mu\nu} \, \mathcal{I}^{VVSS}_{n0\bar{k}\bar{l}}$
$A^{(n)\,\mu} A^{(0)\,\nu} W_{L\,5}^{+\,(k)} W_{L\,5}^{-\,(l)}$	$ie^2 \, g_{\mu\nu} \, \mathcal{I}^{VVSS}_{n0\bar{k}\bar{l}}$
$Z^{(n)\,\mu} A^{(0)\,\nu} W_{L\,5}^{+\,(k)} W_{L\,5}^{-\,(l)}$	$2ieg \cos\psi \, g_{\mu\nu} \, \mathcal{I}^{VVSS}_{n0\bar{k}\bar{l}}$
$W_{R\,5}^{-\,(l)}$ **couplings**	
$Z^{(n)\,\mu} Z^{(0)\,\nu} W_{R\,5}^{+\,(k)} W_{R\,5}^{-\,(l)}$	$ie^2 \sin^2\phi \, g_{\mu\nu} \, \mathcal{I}^{VVSS}_{n0\tilde{k}\tilde{l}}$
$A^{(n)\,\mu} A^{(0)\,\nu} W_{R\,5}^{+\,(k)} W_{R\,5}^{-\,(l)}$	$ie^2 \, g_{\mu\nu} \, \mathcal{I}^{VVSS}_{n0\tilde{k}\tilde{l}}$
$Z^{(n)\,\mu} A^{(0)\,\nu} W_{R\,5}^{+\,(k)} W_{R\,5}^{-\,(l)}$	$-2ieg \sin\phi \sin\psi \, g_{\mu\nu} \, \mathcal{I}^{VVSS}_{n0\tilde{k}\tilde{l}}$
$Z_X^{(n)\,\mu} A^{(0)\,\nu} W_{R\,5}^{+\,(k)} W_{R\,5}^{-\,(l)}$	$2ig^2 \cos\phi \cos\psi \, g_{\mu\nu} \, \mathcal{I}^{VVSS}_{\tilde{n}0\tilde{k}\tilde{l}}$
$Z_X^{(n)\,\mu} Z^{(0)\,\nu} W_{R\,5}^{+\,(k)} W_{R\,5}^{-\,(l)}$	$-2ige \cos\phi \, g_{\mu\nu} \, \mathcal{I}^{VVSS}_{\tilde{n}0\tilde{k}\tilde{l}}$

Table B.50: A list of vertex factors for interactions involving one neutral zero mode vector boson, one neutral heavy vector boson and 2 gauge scalar modes.

Couplings of 1 heavy positive and 1 zero mode neutral vector boson to 2 gauge scalar modes	
$Z_5^{(l)}$ **couplings**	
$W_L^{+\,(n)\,\mu} Z^{(0)\,\nu} W_{L\,5}^{-\,(k)} Z_5^{(l)}$	$-ig^2 \cos^2\psi \, g_{\mu\nu} \, \mathcal{I}^{VVSS}_{n0\bar{k}\bar{l}}$
$W_L^{+\,(n)\,\mu} A^{(0)\,\nu} W_{L\,5}^{-\,(k)} Z_5^{(l)}$	$-ige \cos\psi \, g_{\mu\nu} \, \mathcal{I}^{VVSS}_{n0\tilde{\bar{k}}\bar{l}}$
$W_R^{+\,(n)\,\mu} A^{(0)\,\nu} W_{R\,5}^{-\,(k)} Z_5^{(l)}$	$ie \sin\phi \, g_{\mu\nu} \, \mathcal{I}^{VVSS}_{\tilde{n}0\tilde{\bar{k}}\bar{l}}$
$W_R^{+\,(n)\,\mu} Z^{(0)\,\nu} W_{R\,5}^{-\,(k)} Z_5^{(l)}$	$-ie^2 \sin^2\phi \, g_{\mu\nu} \, \mathcal{I}^{VVSS}_{\tilde{n}0\tilde{\bar{k}}\bar{l}}$
$A_5^{(l)}$ **couplings**	
$W_L^{+\,(n)\,\mu} A^{(0)\,\nu} W_{L\,5}^{-\,(k)} A_5^{(l)}$	$-ie^2 \, g_{\mu\nu} \, \mathcal{I}^{VVSS}_{n0\bar{k}\bar{l}}$
$W_L^{+\,(n)\,\mu} Z^{(0)\,\nu} W_{L\,5}^{-\,(k)} A_5^{(l)}$	$-ige \cos\psi \, g_{\mu\nu} \, \mathcal{I}^{VVSS}_{n0\bar{k}\bar{l}}$
$W_R^{+\,(n)\,\mu} A^{(0)\,\nu} W_{R\,5}^{-\,(k)} A_5^{(l)}$	$-ie^2 \, g_{\mu\nu} \, \mathcal{I}^{VVSS}_{\tilde{n}0\tilde{\bar{k}}\bar{l}}$
$W_R^{+\,(n)\,\mu} Z^{(0)\,\nu} W_{R\,5}^{-\,(k)} A_5^{(l)}$	$ie \sin\phi \, g_{\mu\nu} \, \mathcal{I}^{VVSS}_{\tilde{n}0\tilde{\bar{k}}\bar{l}}$
$Z_{X\,5}^{(l)}$ **couplings**	
$W_R^{+\,(n)\,\mu} A^{(0)\,\nu} W_{R\,5}^{-\,(k)} Z_{X\,5}^{(l)}$	$-ig^2 \cos\phi \cos\psi \, g_{\mu\nu} \, \mathcal{I}^{VVSS}_{\tilde{n}0\tilde{\bar{k}}\bar{l}}$
$W_R^{+\,(n)\,\mu} Z^{(0)\,\nu} W_{R\,5}^{-\,(k)} Z_{X\,5}^{(l)}$	$ig^2 \cos\phi \cos\phi \, g_{\mu\nu} \, \mathcal{I}^{VVSS}_{\tilde{n}0\tilde{\bar{k}}\bar{l}}$

Table B.51: A list of vertex factors for interactions involving one positive heavy vector boson, one neutral zero mode vector bosons and two gauge scalar modes. The vertex factors of the equivalent interactions involving negative vector bosons are identical.

Couplings of 2 heavy charged vector bosons to 2 gauge scalar modes	
$W_L^{+\,(n)\,\mu}$ **couplings**	
$W_L^{+\,(n)\,\mu} W_L^{-\,(m)\,\nu} W_{L\,5}^{+\,(k)} W_{L\,5}^{-\,(l)}$	$2ig^2\, g_{\mu\nu}\, \mathcal{I}^{VVSS}_{nm\bar{k}\bar{l}}$
$W_L^{+\,(n)\,\mu} W_L^{-\,(m)\,\nu} Z_5^{(k)} Z_5^{(l)}$	$(2)ig^2 \cos^2\psi\, g_{\mu\nu}\, \mathcal{I}^{VVSS}_{nm\bar{k}\bar{l}}$
$W_L^{+\,(n)\,\mu} W_L^{-\,(m)\,\nu} A_5^{(k)} A_5^{(l)}$	$(2)ie^2\, g_{\mu\nu}\, \mathcal{I}^{VVSS}_{nm\bar{k}\bar{l}}$
$W_L^{+\,(n)\,\mu} W_L^{-\,(m)\,\nu} A_5^{(k)} Z_5^{(l)}$	$2ig^2 \cos\psi \sin\psi\, g_{\mu\nu}\, \mathcal{I}^{VVSS}_{nm\bar{k}\bar{l}}$
$W_R^{+\,(n)\,\mu}$ **couplings**	
$W_R^{+\,(n)\,\mu} W_R^{-\,(m)\,\nu} A_5^{(k)} A_5^{(l)}$	$(2)ie^2\, g_{\mu\nu}\, \mathcal{I}^{VVSS}_{\tilde{n}\tilde{m}\bar{k}\bar{l}}$
$W_R^{+\,(n)\,\mu} W_R^{-\,(m)\,\nu} Z_5^{(k)} Z_5^{(l)}$	$(2)ie^2 \sin^2\phi\, g_{\mu\nu}\, \mathcal{I}^{VVSS}_{\tilde{n}\tilde{m}\bar{k}\bar{l}}$
$W_R^{+\,(n)\,\mu} W_R^{-\,(m)\,\nu} A_5^{(k)} Z_5^{(l)}$	$ie^2 \sin\phi\, g_{\mu\nu}\, \mathcal{I}^{VVSS}_{\tilde{n}\tilde{m}\bar{k}\bar{l}}$
$W_R^{+\,(n)\,\mu} W_R^{-\,(m)\,\nu} Z_{X\,5}^{(k)} Z_5^{(l)}$	$ieg \cos\phi \sin\phi\, g_{\mu\nu}\, \mathcal{I}^{VVSS}_{\tilde{n}\tilde{m}\tilde{\bar{k}}\bar{l}}$
$W_R^{+\,(n)\,\mu} W_R^{-\,(m)\,\nu} Z_{X\,5}^{(k)} A_5^{(l)}$	$ieg \cos\phi\, g_{\mu\nu}\, \mathcal{I}^{VVSS}_{\tilde{n}\tilde{m}\tilde{\bar{k}}\bar{l}}$
$W_R^{+\,(n)\,\mu} W_R^{-\,(m)\,\nu} Z_{X\,5}^{(k)} Z_{X\,5}^{(l)}$	$(2)ig^2 \cos^2\phi\, g_{\mu\nu}\, \mathcal{I}^{VVSS}_{\tilde{n}\tilde{m}\tilde{\bar{k}}\tilde{\bar{l}}}$

Table B.52: A list of vertex factors for interactions involving 2 charged heavy vector bosons and two gauge scalar fields.

Couplings 2 heavy neutral vector bosons to two gauge scalar modes	
$W_{L\,5}^{-\,(l)}$ **couplings**	
$Z^{(n)\,\mu} Z^{(m)\,\nu} W_{L\,5}^{+\,(k)} W_{L\,5}^{-\,(l)}$	$ig^2 \cos^2\psi \, g_{\mu\nu} \, \mathcal{I}^{VVSS}_{nm\bar{k}\bar{l}}$
$A^{(n)\,\mu} A^{(m)\,\nu} W_{L\,5}^{+\,(k)} W_{L\,5}^{-\,(l)}$	$ie^2 \, g_{\mu\nu} \, \mathcal{I}^{VVSS}_{nm\bar{k}\bar{l}}$
$Z^{(n)\,\mu} A^{(m)\,\nu} W_{L\,5}^{+\,(k)} W_{L\,5}^{-\,(l)}$	$2ieg \cos\psi \, g_{\mu\nu} \, \mathcal{I}^{VVSS}_{nm\bar{k}\bar{l}}$
$W_{R\,5}^{-\,(l)}$ **couplings**	
$Z^{(n)\,\mu} Z^{(m)\,\nu} W_{R\,5}^{+\,(k)} W_{R\,5}^{-\,(l)}$	$ie^2 \sin^2\phi \, g_{\mu\nu} \, \mathcal{I}^{VVSS}_{nm\tilde{k}\tilde{l}}$
$A^{(n)\,\mu} A^{(m)\,\nu} W_{R\,5}^{+\,(k)} W_{R\,5}^{-\,(l)}$	$ie^2 \, g_{\mu\nu} \, \mathcal{I}^{VVSS}_{nm\tilde{\tilde{k}}\tilde{\tilde{l}}}$
$Z^{(n)\,\mu} A^{(m)\,\nu} W_{R\,5}^{+\,(k)} W_{R\,5}^{-\,(l)}$	$-2ieg \sin\phi \sin\psi \, g_{\mu\nu} \, \mathcal{I}^{VVSS}_{nm\tilde{\tilde{k}}\tilde{\tilde{l}}}$
$Z_X^{(n)\,\mu} A^{(m)\,\nu} W_{R\,5}^{+\,(k)} W_{R\,5}^{-\,(l)}$	$2ig^2 \cos\phi \cos\psi \, g_{\mu\nu} \, \mathcal{I}^{VVSS}_{nm\tilde{\tilde{k}}\tilde{\tilde{l}}}$
$Z_X^{(n)\,\mu} Z^{(m)\,\nu} W_{R\,5}^{+\,(k)} W_{R\,5}^{-\,(l)}$	$-2ige \cos\phi \, g_{\mu\nu} \, \mathcal{I}^{VVSS}_{nm\tilde{\tilde{k}}\tilde{\tilde{l}}}$
$Z_X^{(n)\,\mu} Z_X^{(m)\,\nu} W_{R\,5}^{+\,(k)} W_{R\,5}^{-\,(l)}$	$(2)ig^2 \cos^2\phi \, g_{\mu\nu} \, \mathcal{I}^{VVSS}_{\tilde{n}\tilde{m}\tilde{\tilde{k}}\tilde{\tilde{l}}}$

Table B.53: A list of vertex factors for interactions involving two neutral neutral heavy vector bosons and 2 gauge scalar modes.

Couplings of 1 positive and 1 neutral heavy vector boson to 2 gauge scalar modes	
$Z_5^{(l)}$ **couplings**	
$W_L^{+\,(n)\,\mu} Z^{(m)\,\nu} W_{L\,5}^{-\,(k)} Z_5^{(l)}$	$-ig^2 \cos^2\psi \, g_{\mu\nu} \, \mathcal{I}^{VVSS}_{nm\bar{k}\bar{l}}$
$W_L^{+\,(n)\,\mu} A^{(m)\,\nu} W_{L\,5}^{-\,(k)} Z_5^{(l)}$	$-ige \cos\psi \, g_{\mu\nu} \, \mathcal{I}^{VVSS}_{nm\tilde{\bar{k}}\bar{l}}$
$W_R^{+\,(n)\,\mu} A^{(m)\,\nu} W_{R\,5}^{-\,(k)} Z_5^{(l)}$	$ie \sin\phi \, g_{\mu\nu} \, \mathcal{I}^{VVSS}_{\tilde{n}m\tilde{\bar{k}}\bar{l}}$
$W_R^{+\,(n)\,\mu} Z^{(m)\,\nu} W_{R\,5}^{-\,(k)} Z_5^{(l)}$	$-ie^2 \sin^2\phi \, g_{\mu\nu} \, \mathcal{I}^{VVSS}_{\tilde{n}m\tilde{\bar{k}}\bar{l}}$
$W_R^{+\,(n)\,\mu} Z_X^{(m)\,\nu} W_{R\,5}^{-\,(k)} Z_5^{(l)}$	$ig^2 \cos\phi \cos\psi \, g_{\mu\nu} \, \mathcal{I}^{VVSS}_{\tilde{n}\tilde{m}\tilde{\bar{k}}\bar{l}}$
$A_5^{(l)}$ **couplings**	
$W_L^{+\,(n)\,\mu} A^{(m)\,\nu} W_{L\,5}^{-\,(k)} A_5^{(l)}$	$-ie^2 \, g_{\mu\nu} \, \mathcal{I}^{VVSS}_{nm\bar{k}\bar{l}}$
$W_L^{+\,(n)\,\mu} Z^{(m)\,\nu} W_{L\,5}^{-\,(k)} A_5^{(l)}$	$-ige \cos\psi \, g_{\mu\nu} \, \mathcal{I}^{VVSS}_{nm\tilde{\bar{k}}\bar{l}}$
$W_R^{+\,(n)\,\mu} A^{(m)\,\nu} W_{R\,5}^{-\,(k)} A_5^{(l)}$	$-ie^2 \, g_{\mu\nu} \, \mathcal{I}^{VVSS}_{\tilde{n}m\tilde{\bar{k}}\bar{l}}$
$W_R^{+\,(n)\,\mu} Z^{(m)\,\nu} W_{R\,5}^{-\,(k)} A_5^{(l)}$	$ie \sin\phi \, g_{\mu\nu} \, \mathcal{I}^{VVSS}_{\tilde{n}m\tilde{\bar{k}}\bar{l}}$
$W_R^{+\,(n)\,\mu} Z_X^{(m)\,\nu} W_{R\,5}^{-\,(k)} A_5^{(l)}$	$-ig^2 \cos\phi \cos\psi \, g_{\mu\nu} \, \mathcal{I}^{VVSS}_{\tilde{n}\tilde{m}\tilde{\bar{k}}\bar{l}}$

$Z_{X\,5}^{(l)}$ **couplings**	
$W_R^{+\,(n)\,\mu} A^{(m)\,\nu} W_{R\,5}^{-\,(k)} Z_{X\,5}^{(l)}$	$-ig^2 \cos\phi \cos\psi \, g_{\mu\nu} \, \mathcal{I}^{VVSS}_{\tilde{n}mkl}$
$W_R^{+\,(n)\,\mu} Z^{(m)\,\nu} W_{R\,5}^{-\,(k)} Z_{X\,5}^{(l)}$	$ig^2 \cos\phi \cos\phi \, g_{\mu\nu} \, \mathcal{I}^{VVSS}_{\tilde{n}m\tilde{k}\tilde{l}}$
$W_R^{+\,(n)\,\mu} Z_X^{(m)\,\nu} W_{R\,5}^{-\,(k)} Z_{X\,5}^{(l)}$	$-ig^2 \cos^2\phi \, g_{\mu\nu} \, \mathcal{I}^{VVSS}_{\tilde{n}\tilde{m}kl}$

Table B.54: A list of vertex factors for interactions involving one positive heavy vector boson, one neutral heavy vector bosons and two gauge scalar modes. The vertex factors of the equivalent interactions involving negative vector bosons are identical.

Appendix C

Mixed Propagator Derivation

C.1 (+,+) Propagator

In order to calculate the analytical form of the mixed coordinate propagator we must return to the bilinear part of the 5D gauge field Lagrangian which, after gauge fixing, is of the form

$$\mathcal{L}_{gauge} \supset A_\mu \left[\partial^2 \eta^{\mu\nu} - \partial_5 \left(e^{-2ky} \partial_5 \right) \eta^{\mu\nu} - \left(1 - \frac{1}{\xi} \right) \partial^\mu \partial^\nu \right] A_\nu. \tag{C.1}$$

Moving to 4D momentum space, we see that the operator for which we are interested in finding the Green's function is

$$\mathcal{O}^{\mu\nu} = \left[q^2 \eta^{\mu\nu} - \partial_5 \left(e^{-2ky} \partial_5 \right) \eta^{\mu\nu} - \left(1 - \frac{1}{\xi} \right) q^\mu q^\nu \right]. \tag{C.2}$$

Our task is therefore to find the function $\triangle_{\mu\nu}(y, y')$ which obeys the following relation

$$\mathcal{O}^{\mu\nu} \triangle_{\mu\lambda}(y, y') = \delta^\nu_\lambda \delta(y - y'). \tag{C.3}$$

As usual we are now able to express the 5D propagator as a sum of four-dimensionally transverse and parallel components,

$$\triangle_{\mu\nu}(y,y') = -iG_p(y,y')\left(\eta^{\mu\nu} - \frac{q^\mu q^\nu}{q^2}\right) - iG_{q/\sqrt{\xi}}(y,y')\left(\frac{q^\mu q^\nu}{q^2}\right), \tag{C.4}$$

where the 4D Lorentz scalar function $G_p(y,y')$ obeys the condition [1]

$$\left[\partial_5\left(e^{-2ky}\partial_5\right) - q^2\right] G_q(y,y') = \delta(y-y'). \tag{C.5}$$

We are now able to use the standard continuity method to solve this equation. First we solve the homogeneous equation for the situations $y < y'$ and $y > y'$

$$G_{q<}(y,y') = N^1 e^{ky}\left[AJ_1(\epsilon e^{ky}) - BY_1(\epsilon e^{ky})\right], \tag{C.6}$$

$$G_{q>}(y,y') = N^2 e^{ky}\left[CJ_1(\epsilon e^{ky}) - DY_1\left(\epsilon e^{ky}\right)\right], \tag{C.7}$$

where $J_1(x)$ and $Y_1(x)$ are the usual Bessel functions of order 1, $\epsilon = q/k$ and all other previously undefined terms are constants to be determined from boundary conditions. The first of these conditions are from the BCs obeyed by the gauge field which is under investigation. Due to the regions of validity of the expressions above $G_{q<}(G_{q>})$ must obey the BC at the Planck (TeV) brane. Considering the $(+,+)$ case this enables us to determine that

$$A = Y_0(\epsilon), \qquad C = Y_0(\epsilon e^{kL}),$$

$$B = J_0(\epsilon), \qquad D = J_0(\epsilon e^{kL}). \tag{C.8}$$

In order to determine the remaining two constants we need to apply the conditions of continuity and derivative discontinuity at the point $y = y'$. Integrating (C.5) a

[1] We can see that this is the case by substituting the above general form into C.3

small distance either side of $y = y'$ we find that the two conditions are

$$N^1(y')\left[AJ_1(\epsilon e^{ky'}) - BY_1(\epsilon e^{ky'})\right] = N^2(y')\left[CJ_1(\epsilon e^{ky'}) - DY_1(\epsilon e^{ky'})\right], \tag{C.9}$$

$$\begin{aligned} &N^2(y')\left[(CJ_1(x) - DY_1(x)) + x\left(C\partial_x J_1(x)\right) - D\partial_x Y_1(x)\right] \\ &- N^1(y')\left[(AJ_1(x) - BY_1(x)) + x\left(A\partial_x J_1(x) - B\partial_x Y_1(x)\right)\right] = \frac{e^{ky'}}{k}, \end{aligned} \tag{C.10}$$

where $x = \epsilon e^{ky'}$. We are able to solve for one of the two unknown constants using the Wronskian identity,

$$J_1(x)\frac{dY_1(x)}{dx} - Y_1(x)\frac{dJ_1(x)}{dx} = \frac{2}{\pi x}. \tag{C.11}$$

We finally find that

$$G_p(y, y') = -\frac{\pi e^{k(y+y')}}{2k\left(AD - BC\right)}\left[AJ_1(\epsilon e^{ky_<}) - BY_1(\epsilon e^{ky_<})\right]\left[CJ_1(\epsilon e^{ky_>}) - DY_1(\epsilon e^{ky_>})\right], \tag{C.12}$$

where $y_<(y_>)$ is the smaller (larger) of the two coordinates y and y'

The final step to enable us to obtain an relatively simple explicit expression for the KK mixing contributions to the tree-level T parameter is to expand (C.12) in terms of the small parameter ϵ. We can then take the limit that $q \to 0$ and, in the case of gauge fields with the $(+,+)$ BC, remove the zero mode contribution. Using

the series expansions (for $x \ll 1$):

$$Y_0(x) = \frac{2}{\pi}\left[\gamma_E + \ln\left(\frac{x}{2}\right)\right] - \frac{x^2}{2\pi} - \frac{1}{2\pi}\left[\gamma_E + \ln\left(\frac{x}{2}\right)\right] x^2 + \mathcal{O}(x^4), \tag{C.13}$$

$$J_0(x) = 1 - \frac{x^2}{4} + \mathcal{O}(x^4), \tag{C.14}$$

$$Y_1(x) = -\frac{2}{\pi x} - \frac{x}{2\pi} + \frac{1}{\pi}\ln\left(\frac{x}{2}\right) x + \frac{5}{32\pi}x^3 + \frac{1}{8}\ln\left(\frac{x}{2}\right) x^3 + \mathcal{O}(x^5), \tag{C.15}$$

$$J_1(x) = \frac{x}{2} - \frac{x^3}{16} + \mathcal{O}(x^5), \tag{C.16}$$

we find that, up to $\mathcal{O}(\epsilon)$, (C.12) takes the form

$$G_q^{++}(y,y') = \frac{1}{Lq^2} + \frac{1}{4k\,(kL)}\left\{\frac{1-e^{2kL}}{kL} + e^{2ky_<}\left(1-2ky_<\right) + e^{2ky_>}\left[1+2k\left(L-y_>\right)\right]\right\}. \tag{C.17}$$

We immediately see that the first, divergent, term is exactly of the form of the zero-mode propagator and so will be subtracted from the propagator used in our expression for the T parameter,

$$\bar{G}_{q=0}^{++}(y,y') = \frac{1}{4k\,(kL)}\left\{\frac{1-e^{2kL}}{kL} + e^{2ky_<}\left(1-2ky_<\right) + e^{2ky_>}\left[1+2k\left(L-y_>\right)\right]\right\} \tag{C.18}$$

C.2 (-,+) Propagator

The exact expression for the $(-+)$ mixed propagator can be found from (C.12) with the replacements

$$A = Y_1(\epsilon), \qquad C = Y_0(\epsilon e^{kL})$$

$$B = J_1(\epsilon), \qquad D = J_0(\epsilon e^{kL}) \tag{C.19}$$

Expanding this expression in exactly the same way as was done for the $(++)$ propagator we obtain the $q = 0$ limit

$$\bar{G}^{-+}_{q=0}(y, y') = -\frac{1}{2k}\left[e^{2ky_<} - 1\right] \tag{C.20}$$

Appendix D

Veltman-Passarino Functions

D.1 Definitions

For the Veltman-Passarino functions we have used the following conventions

$$16\pi^2\mu^\epsilon \int \frac{d^n k}{i\,(2\pi)^n} \frac{1}{k^2 - m^2} = A_0\left(m^2\right),$$

$$16\pi^2\mu^\epsilon \int \frac{d^n k}{i\,(2\pi)^n} \frac{1}{\left[k^2 - m_1^2\right]\left[(k-q)^2 - m_2^2\right]} = B_0\left(q^2, m_1^2, m_2^2\right),$$

$$16\pi^2\mu^\epsilon \int \frac{d^n k}{i\,(2\pi)^n} \frac{k_\mu}{\left[k^2 - m_1^2\right]\left[(k-q)^2 - m_2^2\right]} = q_\mu B_1\left(q^2, m_1^2, m_2^2\right),$$

$$16\pi^2\mu^\epsilon \int \frac{d^n k}{i\,(2\pi)^n} \frac{k_\mu k_\nu}{\left[k^2 - m_1^2\right]\left[(k-q)^2 - m_2^2\right]} = q_\mu q_\nu B_{21}\left(q^2, m_1^2, m_2^2\right)$$

$$+ g_{\mu\nu} B_{22}\left(q^2, m_1^2, m_2^2\right). \qquad \text{(D.1)}$$

where $n = 4 - 2\epsilon$ is the number of dimensions in which the loop momentum integral is to be performed. As the explicit forms of these functions are only required for numerical analysis we decide not to present them in full here, instead we direct the reader towards the appendices of reference [58] for details.

D.2 UV Behaviour

We now separate the UV divergent parts of those VP functions defined above from their finite parts, represented using lower case letters (a notation used in reference [59])

$$A_0\left(m^2\right) = m^2\Delta + a_0\left(m^2\right)$$

$$B_0\left(q^2, m_1^2, m_2^2\right) = \Delta + b_0\left(q^2, m_1^2, m^2{}_{,2}\right)$$

$$B_1\left(q^2, m_1^2, m_2^2\right) = \frac{1}{2}\Delta + b_1\left(q^2, m_1^2, m^2{}_{,2}\right)$$

$$B_{21}\left(q^2, m_1^2, m_2^2\right) = \frac{1}{3}\Delta + b_{21}\left(q^2, m_1^2, m^2{}_{,2}\right)$$

$$B_{22}\left(q^2, m_1^2, m_2^2\right) = \left(\frac{m_1^2 + m_2^2}{4} - \frac{q^2}{12}\right)\Delta b_{22}\left(q^2, m_1^2, m_2^2\right) \tag{D.2}$$

where again we define Δ as the terms which are removed in a $\overline{\text{MS}}$ renormalisation procedure,

$$\Delta = \frac{2}{\epsilon} - \gamma_E + \ln 4\pi \tag{D.3}$$

where γ_E is the Euler-Mascheroni constant.

Bibliography

[1] H.-C. Cheng and I. Low, "TeV symmetry and the little hierarchy problem," *JHEP* **09** (2003) 051, arXiv:hep-ph/0308199.

[2] S. P. Martin, "A Supersymmetry Primer," arXiv:hep-ph/9709356. M. E. Peskin, "Supersymmetry in Elementary Particle Physics," arXiv:0801.1928 [hep-ph].

[3] N. Arkani-Hamed, S. Dimopoulos, and G. R. Dvali, "The hierarchy problem and new dimensions at a millimeter," *Phys. Lett.* **B429** (1998) 263–272, arXiv:hep-ph/9803315.

[4] L. Randall and R. Sundrum, "A large mass hierarchy from a small extra dimension," *Phys. Rev. Lett.* **83** (1999) 3370–3373, arXiv:hep-ph/9905221.

[5] T. Gherghetta and A. Pomarol, "Bulk fields and supersymmetry in a slice of AdS," *Nucl. Phys.* **B586** (2000) 141–162, arXiv:hep-ph/0003129.

[6] S. J. Huber and Q. Shafi, "Fermion Masses, Mixings and Proton Decay in a Randall- Sundrum Model," *Phys. Lett.* **B498** (2001) 256–262, arXiv:hep-ph/0010195.

[7] M. E. Peskin and T. Takeuchi, "Estimation of oblique electroweak corrections," *Phys. Rev.* **D46** (1992) 381–409.

[8] H. Davoudiasl, J. L. Hewett, and T. G. Rizzo, "Bulk gauge fields in the Randall-Sundrum model," *Phys. Lett.* **B473** (2000) 43–49, arXiv:hep-ph/9911262.

[9] C. Csaki, J. Erlich, and J. Terning, "The effective Lagrangian in the Randall-Sundrum model and electroweak physics," *Phys. Rev.* **D66** (2002) 064021, arXiv:hep-ph/0203034.

[10] A. Delgado and A. Falkowski, "Electroweak observables in a general 5D background," *JHEP* **05** (2007) 097, arXiv:hep-ph/0702234.

[11] S. Casagrande, F. Goertz, U. Haisch, M. Neubert, and T. Pfoh, "Flavor Physics in the Randall-Sundrum Model: I. Theoretical Setup and Electroweak Precision Tests," *JHEP* **10** (2008) 094, arXiv:0807.4937 [hep-ph].

[12] H. Davoudiasl, J. L. Hewett, and T. G. Rizzo, "Experimental probes of localized gravity: On and off the wall," *Phys. Rev.* **D63** (2001) 075004, arXiv:hep-ph/0006041.

[13] A. Pomarol, "Gauge bosons in a five-dimensional theory with localized gravity," *Phys. Lett.* **B486** (2000) 153–157, arXiv:hep-ph/9911294.

[14] Y. Grossman and M. Neubert, "Neutrino masses and mixings in non-factorizable geometry," *Phys. Lett.* **B474** (2000) 361–371, arXiv:hep-ph/9912408.

[15] S. J. Huber and Q. Shafi, "Higgs mechanism and bulk gauge boson masses in the Randall-Sundrum model," *Phys. Rev.* **D63** (2001) 045010, arXiv:hep-ph/0005286.

[16] S. J. Huber, C.-A. Lee, and Q. Shafi, "Kaluza-Klein excitations of W and Z at the LHC?," *Phys. Lett.* **B531** (2002) 112–118, arXiv:hep-ph/0111465.

[17] S. J. Huber, "Flavor violation and warped geometry," *Nucl. Phys.* **B666** (2003) 269–288, arXiv:hep-ph/0303183.

[18] K. Agashe, G. Perez, and A. Soni, "Flavor structure of warped extra dimension models," *Phys. Rev.* **D71** (2005) 016002, arXiv:hep-ph/0408134.

[19] J. L. Hewett, F. J. Petriello, and T. G. Rizzo, "Precision measurements and fermion geography in the Randall-Sundrum model revisited," *JHEP* **09** (2002) 030, arXiv:hep-ph/0203091.

[20] K. Agashe and R. Contino, "The minimal composite Higgs model and electroweak precision tests," *Nucl. Phys.* **B742** (2006) 59–85, arXiv:hep-ph/0510164.

[21] K. Agashe, R. Contino, L. Da Rold, and A. Pomarol, "A custodial symmetry for Z b anti-b," *Phys. Lett.* **B641** (2006) 62–66, arXiv:hep-ph/0605341.

[22] M. Blanke, A. J. Buras, B. Duling, S. Gori, and A. Weiler, "Delta F=2 Observables and Fine-Tuning in a Warped Extra Dimension with Custodial Protection," *JHEP* **03** (2009) 001, arXiv:0809.1073 [hep-ph].

[23] H. Davoudiasl, G. Perez, and A. Soni, "The Little Randall-Sundrum Model at the Large Hadron Collider," *Phys. Lett.* **B665** (2008) 67–71, arXiv:0802.0203 [hep-ph].

[24] M. Schmaltz and D. Tucker-Smith, "Little Higgs Review," *Ann. Rev. Nucl. Part. Sci.* **55** (2005) 229–270, arXiv:hep-ph/0502182. I. Antoniadis, "The physics of extra dimensions," *Lect. Notes Phys.* **720** (2007) 293–321, arXiv:hep-ph/0512182.

[25] K. Agashe, R. Contino, and A. Pomarol, "The Minimal Composite Higgs Model," *Nucl. Phys.* **B719** (2005) 165–187, arXiv:hep-ph/0412089.

[26] M. S. Carena, E. Ponton, J. Santiago, and C. E. M. Wagner, "Light Kaluza-Klein states in Randall-Sundrum models with custodial SU(2)," *Nucl. Phys.* **B759** (2006) 202–227, arXiv:hep-ph/0607106.

[27] M. S. Carena, E. Ponton, J. Santiago, and C. E. M. Wagner, "Electroweak constraints on warped models with custodial symmetry," *Phys. Rev.* **D76** (2007) 035006, arXiv:hep-ph/0701055.

[28] S. Chang, J. Hisano, H. Nakano, N. Okada, and M. Yamaguchi, "Bulk standard model in the Randall-Sundrum background," *Phys. Rev.* **D62** (2000) 084025, arXiv:hep-ph/9912498.

[29] H. Davoudiasl, B. Lillie, and T. G. Rizzo, "Off-the-Wall Higgs in the Universal Randall-Sundrum Model," *JHEP* **08** (2006) 042, arXiv:hep-ph/0508279.

[30] G. Cacciapaglia, C. Csaki, G. Marandella, and J. Terning, "The gaugephobic Higgs," *JHEP* **02** (2007) 036, arXiv:hep-ph/0611358.

[31] K. Agashe, A. Delgado, M. J. May, and R. Sundrum, "RS1, custodial isospin and precision tests," *JHEP* **08** (2003) 050, arXiv:hep-ph/0308036.

[32] G. Cacciapaglia, C. Csaki, G. Marandella, and J. Terning, "A New Custodian for a Realistic Higgsless Model," *Phys. Rev.* **D75** (2007) 015003,

arXiv:hep-ph/0607146. R. Contino, L. Da Rold, and A. Pomarol, "Light custodians in natural composite Higgs models," *Phys. Rev.* **D75** (2007) 055014, arXiv:hep-ph/0612048.

[33] H. Davoudiasl and T. G. Rizzo, "New Dimensions for Randall-Sundrum Phenomenology," *JHEP* **11** (2008) 013, arXiv:0809.4440 [hep-ph].

[34] L. Randall and R. Sundrum, "An alternative to compactification," *Phys. Rev. Lett.* **83** (1999) 4690–4693, arXiv:hep-th/9906064.

[35] J. M. Maldacena, "The large N limit of superconformal field theories and supergravity," *Adv. Theor. Math. Phys.* **2** (1998) 231–252, arXiv:hep-th/9711200.

[36] R. Contino, Y. Nomura, and A. Pomarol, "Higgs as a holographic pseudo-Goldstone boson," *Nucl. Phys.* **B671** (2003) 148–174, arXiv:hep-ph/0306259.

[37] W. D. Goldberger and M. B. Wise, "Modulus stabilization with bulk fields," *Phys. Rev. Lett.* **83** (1999) 4922–4925, arXiv:hep-ph/9907447.

[38] T. Kaluza, "On the Problem of Unity in Physics," *Sitzungsber.Preuss.Akad.Wiss.Berlin (Math.Phys.)* **1921** (1921) 966–972.
O. Klein, "Quantum Theory and Five-Dimensional Theory of Relativity.," *Z.Phys.* **37** (1926) 895–906.

[39] W. D. Goldberger and M. B. Wise, "Bulk fields in the Randall-Sundrum compactification scenario," *Phys. Rev.* **D60** (1999) 107505, arXiv:hep-ph/9907218.

[40] M. E. Albrecht, M. Blanke, A. J. Buras, B. Duling, and K. Gemmler, "Electroweak and Flavour Structure of a Warped Extra Dimension with Custodial Protection," *JHEP* **09** (2009) 064, arXiv:0903.2415 [hep-ph].

[41] C. Csaki, C. Grojean, H. Murayama, L. Pilo, and J. Terning, "Gauge theories on an interval: Unitarity without a Higgs," *Phys. Rev.* **D69** (2004) 055006, arXiv:hep-ph/0305237.

[42] C. Csaki, J. Hubisz, and P. Meade, "Electroweak symmetry breaking from extra dimensions," arXiv:hep-ph/0510275.

[43] N. Arkani-Hamed and M. Schmaltz, "Hierarchies without symmetries from extra dimensions," *Phys. Rev.* **D61** (2000) 033005, arXiv:hep-ph/9903417.

[44] G. R. Dvali and M. A. Shifman, "Families as neighbors in extra dimension," *Phys. Lett.* **B475** (2000) 295–302, arXiv:hep-ph/0001072.

[45] N. Arkani-Hamed, L. J. Hall, D. Tucker-Smith, and N. Weiner, "Flavor at the TeV scale with extra dimensions," *Phys. Rev.* **D61** (2000) 116003, arXiv:hep-ph/9909326.

[46] S. Glashow, J. Iliopoulos, and L. Maiani, "Weak Interactions with Lepton-Hadron Symmetry," *Phys.Rev.* **D2** (1970) 1285–1292.

[47] M. Quiros, "New ideas in symmetry breaking," arXiv:hep-ph/0302189.
C. Biggio, "Symmetry breaking in extra dimensions," arXiv:hep-ph/0312209.

[48] L. J. Hall and Y. Nomura, "Gauge unification in higher dimensions," *Phys. Rev.* **D64** (2001) 055003, arXiv:hep-ph/0103125.

[49] A. Muck, A. Pilaftsis, and R. Ruckl, "Minimal Higher-Dimensional Extensions of the Standard Model and Electroweak Observables," *Phys. Rev.* **D65** (2002) 085037, arXiv:hep-ph/0110391.

[50] L. Randall and M. D. Schwartz, "Quantum field theory and unification in AdS5," *JHEP* **11** (2001) 003, arXiv:hep-th/0108114.

[51] F. Goertz and T. Pfoh, "On the Perturbative Approach in the Randall-Sundrum Model," *JHEP* **10** (2008) 035, arXiv:0809.1378 [hep-ph].

[52] S. Casagrande, F. Goertz, U. Haisch, M. Neubert, and T. Pfoh, "The Custodial Randall-Sundrum Model: From Precision Tests to Higgs Physics," *JHEP* **09** (2010) 014, arXiv:1005.4315 [hep-ph].

[53] M. S. Carena, A. Delgado, E. Ponton, T. M. P. Tait, and C. E. M. Wagner, "Precision electroweak data and unification of couplings in warped extra dimensions," *Phys. Rev.* **D68** (2003) 035010, arXiv:hep-ph/0305188.

[54] M. S. Carena, E. Ponton, T. M. P. Tait, and C. E. M. Wagner, "Opaque branes in warped backgrounds," *Phys. Rev.* **D67** (2003) 096006, arXiv:hep-ph/0212307.

[55] C. Burgess and G. D. Moore, *The Standard Model: A Primer*. Cambridge University Press, 2007.

[56] **Particle Data Group** Collaboration, K. Nakamura *et al.*, "Review of particle physics," *J.Phys.G* **G37** (2010) 075021.

[57] G. Passarino and M. Veltman, "One Loop Corrections for e+ e- Annihilation Into mu+ mu- in the Weinberg Model," *Nucl.Phys.* **B160** (1979) 151.

[58] S. Pokorski, *Gauge Field Theories*. Cambridge Monographs on Mathematical Physics. Cambridge University Press, 2nd ed., 2000.

[59] J. D. Wells, "TASI lecture notes: Introduction to precision electroweak analysis," `arXiv:hep-ph/0512342`.